ORIGINAL ARTICLE

Association between time to treatment failure and peripheral eosinophils in patients with non–small cell lung cancer treated with immune checkpoint inhibitors

Hajime Osawa[1], Toshihiro Shiozawa[1], Shinichiro Okauchi[2], Kunihiko Miyazaki[3], Takahide Kodama[3], Katsunori Kagohashi[2], Ryota Nakamura[4], Hiroaki Satoh[2], Nobuyuki Hizawa[1]

1 Division of Respiratory Medicine, Faculty of Medicine, University of Tsukuba, Tsukuba, Japan
2 Division of Respiratory Medicine, Mito Medical Center, University of Tsukuba–Mito Kyodo General Hospital, Mito, Japan
3 Division of Respiratory Medicine, Ryugasaki Saiseikai Hospital, Ryugasaki, Japan
4 Division of Surgery, National Hospital Organization Mito Medical Center, Mito, Japan

KEY WORDS

eosinophils, immune checkpoint inhibitor, non–small cell lung cancer, time to treatment failure

EDITORIAL

by Ramos-Casals et al

ABSTRACT

INTRODUCTION There is an unmet clinical need to identify biomarkers predicting which patients with non–small cell lung cancer (NSCLC) would benefit from treatment with immune checkpoint inhibitors (ICPIs).

OBJECTIVES The purpose of this study was to draw a detailed time to treatment failure (TTF) curve with information on the changes in peripheral eosinophil expression during ICPI treatment for NSCLC, and to clarify whether eosinophil expression can predict prolonged TTF.

PATIENTS AND METHODS In 259 patients with NSCLC treated with ICPI therapy, peripheral eosinophil counts and percentages at the time of each ICPI administration were evaluated from the beginning of ICPI treatment up to TTF. Univariable and multivariable analyses were performed to identify clinical factors associated with TTF.

RESULTS Patients receiving ICPI monotherapy (n = 180) were divided into 3 groups (TTF ≤6 weeks, TTF >6 weeks and ≤24 weeks, and TTF >24 weeks) and the number of patients with an eosinophil percentage of 5% or more within 6 weeks of ICPI therapy initiation was significantly different among these groups. In univariable and multivariable analyses, performance status of 0 to 1, immune-related adverse event not requiring ICPI discontinuation as well as an eosinophil percentage of 5% or more and an eosinophil count of 330/μ or more within 6 weeks of ICPI therapy initiation were significant favorable factors for prolonged TTF. In patients treated with combination therapy of ICPI and chemotherapy (n = 79), the number of patients with an eosinophil percentage of 5% or more within 12 weeks of therapy initiation was significantly different between patients with a TTF of up to 12 weeks and those with a more prolonged TTF. However, the only significant favorable factor for TTF was female sex.

CONCLUSIONS In NSCLC patients treated with ICPI therapy, particularly ICPI monotherapy, eosinophil measurements during treatment might be useful for predicting prolonged TTF.

Correspondence to:
Hiroaki Satoh, MD, PhD,
Division of Respiratory Medicine,
Mito Medical Center, University
of Tsukuba–Mito Kyodo General
Hospital, 3-2-7 Miya-machi,
Mito, Ibaraki 310–0105, Japan,
phone: +81 29 231 2371,
email: hirosato@md.tsukuba.ac.jp
Received: May 18, 2021.
Revision accepted: June 20, 2021.
Published online: June 28, 2021.
Pol Arch Intern Med. 2021;
131 (10): 16049
doi:10.20452/pamw.16049

INTRODUCTION Immune checkpoint inhibitors (ICPIs) have significantly changed the treatment of advanced non–small cell lung cancer (NSCLC).[1,2] In particular, the long plateau in the tail of the survival curve of patients treated with ICPI therapy is impressive, and the number of patients with advanced NSCLC who can be cured is astonishing.[1,2] However, not every patient will benefit from ICPI and be cured. When the results of progression-free survival in clinical trials of ICPI monotherapy were examined in detail, patients could be divided into 3 groups: no response group, short-term response group, and long-term response group.[3-8] However, in clinical

WHAT'S NEW?

With the advent of immune checkpoint inhibitors (ICPIs), the treatment of many carcinomas has made great strides. However, it is currently difficult to identify patients who would benefit from treatment with ICPIs. As a biomarker for ICPI therapy, programmed cell death ligand 1 (PD-L1) expression has been utilized. However, PD-L1 may show different immunostaining levels depending on where it was collected. In this study, we found that an eosinophil percentage of 5% or more as well as an eosinophil count of 330/μl or more within 6 weeks of ICPI therapy initiation were significant favorable factors associated with time to treatment failure in patients receiving ICPI monotherapy. In patients treated with combination therapy of ICPI and chemotherapy, eosinophil variability was further complicated by myelosuppression by antitumor drugs. However, fluctuations in the levels of peripheral eosinophils have been observed, and detailed analysis of this phenomenon might reveal the usefulness of eosinophils as biomarkers. Our study suggests that there is a possibility to predict response to ICPI therapy based on peripheral eosinophil expression.

trials of combination therapy involving ICPI and chemotherapy, the proportion of individuals included in the no response group was found to be very small, leaving 2 primary groups of patients with short- and long-term response.[9,10]

In ICPI therapy, programmed death ligand 1 (PD-L1) is considered the most common biomarker predicting the response to treatment.[11,12] However, the expression of PD-L1 relies on immunostaining of pathological specimens, and the biopsy site may not fully represent the entire lung cancer.[12] What is more, the results of PD-L1 expression may differ depending on the place where the surgically excised specimen is stained and evaluated.[12] Therefore, better biomarkers are needed in the clinical setting. A biomarker that does not require a complicated system or costly equipment but, rather, is easy and inexpensive to evaluate, and, if possible, derived from standard clinical data, would be highly useful clinically. These factors are driving the search for new biomarkers other than PD--L1.[13-31] Studies have been investigating whether neutrophils, lymphocytes, and eosinophils could be useful in this regard.[18-31] Although the detailed biological mechanism, either direct or indirect, is unknown, it seems that changes in peripheral blood cell counts are associated with ICPI treatment, and this phenomenon has been the focus of several studies.[18,20,22,23,29,31] To the best of our knowledge, however, no investigation has been performed of the detailed changes of eosinophils during the clinical course of individual patients.

Recently, we reported the importance of eosinophil variability after the initiation of ICPI therapy.[32] Our study found that time to treatment failure (TTF) of ICPI therapy was longer in patients with a maximum eosinophil percentage greater than 5% and a maximum eosinophil count of 330/μl or more at 5 weeks since the initiation of therapy.[32] However, we did not separately analyze peripheral eosinophil expression in patients treated with ICPI monotherapy and those treated with combination therapy of ICPI and chemotherapy, although there were no significant differences in patient backgrounds between these 2 groups. Moreover, it was not possible to show in detail the changes in eosinophil expression during the clinical courses of individual patients. We believed that these data are important, and that an analysis visualizing detailed TTF including this information is absolutely necessary; therefore, we conducted the present study.

The purpose was to investigate whether peripheral eosinophil expression, as a convenient and inexpensive biomarker, could help predict whether or not ICPI treatment should be continued. In particular, we focused on findings that would be useful for selecting patients who could be treated with ICPIs for a long period of time, and for those who should switch from ICPIs to other therapeutic agents.

PATIENTS AND METHODS **Patients** We analyzed the medical records of all patients diagnosed with NSCLC in 3 tertiary hospitals in Japan (Mito Medical Center, University of Tsukuba–Mito Kyodo General Hospital, Ryugasaki Saiseikai Hospital, and Tsukuba University Hospital) between February 2016 and March 2021. All patients with NSCLC treated with ICPI monotherapy or combination therapy of ICPI and chemotherapy during this period were included. NSCLC was diagnosed based on the World Health Organization classification. Tumor node metastasis staging (TNM Classification, 8th Edition) using computed tomography or magnetic resonance imaging of the head, bone scans, and ultrasonography and/or computed tomography of the abdomen was performed in all patients prior to ICPI therapy initiation. Patients with the following comorbidities or a history of treatment for these conditions were excluded: parasitic infestations, allergic diseases, autoimmune diseases, and hematologic malignancies. Patients with chronic obstructive pulmonary disease and those with bronchial asthma and chronic obstructive pulmonary disease overlap requiring systemic steroid use were also excluded. Particular attention was paid to adrenal insufficiency as an immune-related adverse event (irAE). Patients who developed eosinophilia associated with adrenal insufficiency as an irAE were excluded from this study. Demographic data of the patients, including age, sex, Eastern Cooperative Oncology Group score for performance status (PS), histopathology, disease stage, PD-L1 expression, objective tumor response, and survival, were obtained from the patients' medical records. Tumor response was evaluated as complete response, partial response, stable disease, or progressive disease according to the Response Evaluation Criteria in Solid Tumors (Version 1.1).

Measurement of peripheral eosinophil count and percentage Eosinophil counts and percentages were measured at the same time as complete

blood count before and during ICPI therapy. Results were obtained from the medical records of each patient. Counts for leukocyte subpopulations were measured by routine clinical laboratory analysis using a Sysmex XN 3000 analyzer (Sysmex Co, Ltd, Kobe, Japan).

Measurements of eosinophils In a previous study, we established that an eosinophil percentage of 5% or more and an eosinophil count of 330/μl or more 5 weeks following the initiation of ICPI therapy were the optimal cutoff values for patients with controlled disease.[32] However, current administration methods for ICPIs are every 2, 3, and 6 weeks.[3-10] Therefore, in the present study, we used the thresholds of an eosinophil percentage of 5% or more and an eosinophil count of 330/μl or more within 6 weeks after the initiation of treatment in patients treated with ICPI monotherapy. In patients treated with combination therapy of ICPI and chemotherapy, we adopted the same cutoff values noted within 12 weeks after the initiation of treatment.

Time to treatment failure and changes in eosinophil levels during immune checkpoint inhibitor therapy Peripheral eosinophils were measured after each ICPI administration. Regarding the eosinophil percentage, a TTF curve was drawn by color-coding the period until the next administration according to whether the eosinophil percentage of 5% or more was reached or not. Similarly, for the peripheral eosinophil count, a TTF curve was created by color-coding the period until the next administration depending on the presence or absence of an eosinophil count of 330/μl or more. Next, we compared the groups, based on whether the threshold of an eosinophil percentage of 5% or more or the eosinophil count of 330/μl or more was reached or not, either within 6 or 12 weeks following the initiation of treatment (in patients treated with ICPI monotherapy and those treated with ICPI combination therapy of ICPI and chemotherapy, respectively).

For the purpose of determining the characteristics of individuals with long-term therapeutic efficacy of ICPI treatment, we also investigated data on changes in eosinophil expression in patients with a TTF of 120 weeks or longer (for patients treated with ICPI monotherapy) or 60 weeks or longer (for those treated with combination therapy of ICPI and chemotherapy).

Univariable and multivariable analyses We performed a univariable analysis to investigate the association between characteristics of the patients (sex, PS, age, pathology, cancer stage, driver genes, PD-L1 expression, and irAEs) and TTF. In patients treated with ICPI monotherapy, we looked for the association between TTF and an eosinophil rate of 5% or more and eosinophil count of 330/μl or more within 6 weeks of the start of treatment. Similarly, in patients treated with combination therapy of ICPI and chemotherapy, the association between TTF and an eosinophil rate of 5% or more and eosinophil count of 330/μl or more within 12 weeks of treatment initiation was examined. Factors that were statistically significant in a univariable analysis were entered into the multivariable model. The analyses were performed separately for patients receiving ICPIs alone and those receiving the ICPI and chemotherapy combination.

Statistical analysis The χ^2 test was used to compare nominal variables and the nonparametric Mann–Whitney test was used to compare values with unknown population variance. We adopted the definition of TTF that is commonly used in cancer treatment; that is, the interval from initiation of therapy with ICPIs to treatment discontinuation or the last follow-up visit. Time to treatment failure was estimated by the Kaplan–Meier method and compared using the log-rank test. We used the Cox proportional hazards model and forward-backward stepwise method to determine the independent variables used in the final model. In this study, multivariable analyses were performed using only the variables with a *P* value of less than 0.1 in a univariable analysis. Time to treatment failure was the dependent variable in that model. All statistical analyses were conducted using SPSS, version 23 (IBM Corporation, Armonk, New York, United States). A *P* value of less than 0.05 was considered significant.

Ethics This study conformed to the Ethical Guidelines for Clinical Studies issued by the Ministry of Health, Labor, and Welfare of Japan. Written informed consent for participation in a noninterventional retrospective study was obtained from each patient. The analysis of the medical records of patients with lung cancer was approved by the ethics committee of Mito Medical Center–University of Tsukuba Hospital (No. 20–57).

RESULTS

Patient characteristics We analyzed the clinical characteristics of 259 patients who met all inclusion criteria within the study period. Detailed data of the study patients are shown in TABLE 1. Of those 259 patients enrolled, 180 were treated with ICPI monotherapy and 79 were treated with combination therapy of ICPI and chemotherapy.

In the former group, the median TTF was 12 weeks (range, 3–217 weeks; 20 patients had ongoing treatment). A total of 71 patients (39.4%) had an eosinophil rate of 5% or more, with a median rate of 7.9% (range, 5%–53%). Eighty-five patients (47.2%) had an eosinophil count of 330/μl or more, with a median count of 598/μl (range, 330–6413/μl). Among the 180 patients treated with ICPI monotherapy, 8 had a TTF of 120 weeks or more, including 7 individuals with an eosinophil rate of 5% or more achieved several times over the course of treatment.

In the group of patients treated with combination therapy of ICPI and chemotherapy, the median TTF was 23 weeks (range, 9–93 weeks; 25

TABLE 1 Characteristics of patients with non–small cell lung cancer treated with immune checkpoint inhibitor monotherapy and combination therapy including immune checkpoint inhibitors and chemotherapy

Parameter		ICPI monotherapy (n = 180)	Combination therapy of ICPI and chemotherapy (n = 79)
Age, y, median (range)		69 (29–87)	69 (29–80)
Sex	Male	39	20
	Female	141	59
PS (ECOG)	0–1	152	77
	≥2	28	2
Pathology	Adenocarcinoma	114	49
	Other	66	30
Cancer stage	IIIA–C	49	15
	IVA–B	131	64
Driver genes	Absent	161	5
	Present	19	74
PD-L1 expression	≥25%	71	19
	<25%	109	60
ICPI	Pembrolizumab	55	61
	Atezolizumab	23	11
	Nivolumab	102	0
	Durvalumab	0	6
	Nivolumab + Ipilimumab	0	1
Response	Complete response	5	0
	Partial response	53	48
	Stable disease	66	25
	Progressive disease	55	6
irAE (not requiring discontinuation of ICPI)	Present	24	11
	Absent	156	68
TTF, w, median (range)		12 (3–217)	23 (9–93)
Ongoing treatment		20	25

Abbreviations: ECOG, Eastern Cooperative Oncology Group; ICPI, immune checkpoint inhibitor; irAE, immune-related adverse event; PD-L1, programmed death ligand 1; PS, performance status; TTF, time to treatment failure

patients had ongoing treatment). Thirty-seven patients (46.8%) had an eosinophil percentage of at least 5%, with a median rate of 8.2% (range, 5.2%–33%), whereas 33 individuals (41.8%) had an eosinophil count of 330/μl or more, with a median count of 616/μl (range, 381–5742/μl). Seven of the 79 patients in this group had a TTF of 60 weeks or more, with 4 of these individuals achieving an eosinophil rate of 5% or more several times.

Time to treatment failure curves and patient grouping by information on peripheral eosinophils The TTF curves of 180 patients who received ICPI monotherapy are shown in FIGURE 1A and 1B. Based on these curves, the patients were divided into 3 groups: no response group (group I: TTF ≤6 weeks), short-term response group (group II: TTF >6 weeks and ≤24 weeks), and long-term response group (group III: TTF >24 weeks). Characteristics of the patients (sex, PS, age, pathology, cancer stage, driver genes, and PD-L1 expression) were not different between these groups (TABLES 2 and 3).

The same analysis was performed for individuals treated with combination therapy of ICPI and chemotherapy. The TTF curves of these patients are shown in FIGURE 2A and 2B. On this basis, the patients were divided into 2 groups of short-term and long-term response (group IV: TTF ≤12 weeks and group V: TTF >12 weeks, respectively). No differences in patient characteristics were found between these groups (TABLES 2 and 3).

Data on peripheral eosinophils in particular groups are summarized in TABLE 4. In patients treated with ICPI monotherapy, the number of patients with an eosinophil rate of 5% or more within 6 weeks of treatment initiation was significantly different among the 3 groups ($P = 0.003$). A separate analysis was performed with an eosinophil count of 330/μl adopted as the cutoff, but there was no significant difference in the ratio of patients between the groups

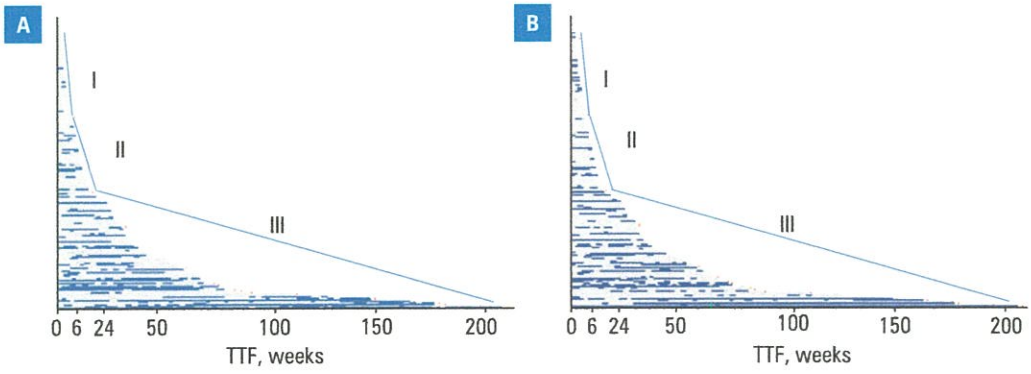

FIGURE 1 Time to treatment failure (TTF) curves of patients treated with immune checkpoint inhibitor monotherapy (n = 180); A – TTF curve with a cutoff peripheral blood eosinophil percentage of 5%; B – TTF curve with a cutoff eosinophil count of 330/μl. The curves were drawn by color-coding the period until the next administration of immune checkpoint inhibitor according to whether the specified cutoff values were achieved (dark blue) or not (gray). Patients were divided into 3 groups: no response group (group I, TTF ≤6 weeks), short-term response group (group II, TTF >6 weeks and ≤24 weeks), and long-term response group (group III, TTF >24 weeks).

TABLE 2 Comparison of patient characteristics by patient group[a]

Parameter		Patients treated with ICPI monotherapy (n = 180)				Patients treated with combination therapy of ICPI and chemotherapy (n = 79)		
		Group I (n = 58)	Group II (n = 54)	Group III (n = 68)	*P* value	Group IV (n = 19)	Group V (n = 60)	*P* value
Sex	Female	16	13	10	0.19	6	14	0.47
	Male	42	41	58		13	46	
PS (ECOG)	0–1	45	47	60	0.21	18	59	0.38
	≥2	13	7	8		1	1	
Age, y	<70	32	27	40	0.62	9	35	0.4
	≥70	26	27	28		10	25	
Pathology	Adenocarcinoma	43	31	41	0.14	11	38	0.67
	Other	15	23	27		8	22	
Cancer stage	IIIA–C	15	14	20	0.88	2	13	0.29
	IVA–B	43	40	48		17	47	
Driver genes	Absent	48	51	62	0.11	17	57	0.39
	Present	10	3	6		2	3	
PD-L1 expression	≥25%	20	18	33	0.15	7	12	0.13
	<25%	38	36	35		12	48	

a Stratification based on the therapeutic efficacy reflected by TTF: group I, TTF ≤6 weeks; group II, TTF >6 weeks and ≤24 weeks; group III, TTF >24 weeks; group IV, TTF ≤12 weeks; group V, TTF >12 weeks

Abbreviations: see TABLE 1

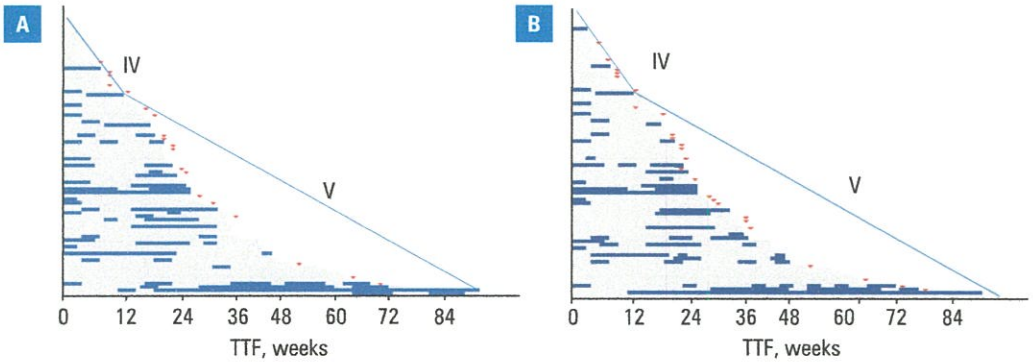

FIGURE 2 Time to treatment failure (TTF) curves of patients treated with combination therapy of immune checkpoint inhibitors and chemotherapy (n = 79); **A** – TTF curve with a cutoff peripheral blood eosinophil percentage of 5%; **B** – TTF curve with a cutoff eosinophil count of 330/μl. The curves were drawn by color-coding the period until the next administration of immune checkpoint inhibitor according to whether the specified cutoff values were achieved (dark blue) or not (gray). Patients were divided into 2 groups: short-term response group (group IV, TTF ≤12 weeks) and long-term response group (group V, TTF >12 weeks).

(P = 0.099). Similarly, in patients treated with combination therapy of ICPI and chemotherapy, the number of patients with an eosinophil rate of 5% or more within 12 weeks of the start of treatment was significantly different between the 2 groups (P = 0.023). With regard to the number of patients with an eosinophil count of 330/μl, there was no difference between the groups (P = 0.268).

Univariable and multivariable analyses As mentioned earlier, the groups did not differ in terms of patient characteristics (TABLES 2 and 3). The results of univariable and multivariable analyses are shown in TABLE 5. In patients treated with ICPI monotherapy, PS of 0 to 1, IrAE not requiring ICPI discontinuation, and an eosinophil percentage of 5% or more within 6 weeks of treatment initiation were significant favorable factors for prolonged therapeutic efficacy in a multivariable analysis. An eosinophil count of 330/μl or more within 6 weeks of ICPI therapy initiation was associated with a prolonged TTF in both univariable and multivariable analyses, whereas a PD-L1 expression exceeding 25% was not.

In patients treated with combination therapy of ICPI and chemotherapy, female sex was the only significant favorable factor for prolonged therapeutic efficacy in a univariable analysis (P = 0.019).

TABLE 3 Comparison of patient characteristics by peripheral eosinophil expression

Parameter		Patients treated with ICPI monotherapy (n = 180)			Patients treated with combination therapy of ICPI and chemotherapy (n = 79)		
		Eo ≥5% within 6 weeks			Eo ≥5% within 12 weeks		
		Present (n = 40)	Absent (n = 140)	*P* value	Present (n = 25)	Absent (n = 54)	*P* value
Sex	Female	8	31	0.77	4	16	0.2
	Male	32	109		21	38	
PS (ECOG)	0–1	36	116	0.27	25	52	0.99
	≥2	4	24		0	2	
Age, y	<70	25	74	0.28	15	29	0.63
	70≥	15	66		10	25	
Pathology	Adenocarcinoma	21	94	0.09	14	35	0.47
	Other	19	46		11	19	
Cancer stage	IIIA–C	11	38	0.96	6	9	0.54
	IVA–B	29	102		19	45	
Driver genes	Present	3	16	0.48	0	5	0.17
	Absent	37	124		25	49	
PD-L1 expression	≥25%	18	53	0.42	8	11	0.27
	<25%	22	87		17	43	
irAE (not requiring discontinuation of ICPI)	Present	7	17	0.38	2	9	0.3
	Absent	33	123		23	45	
Parameter		Eo ≥330/μl within 6 weeks			Eo ≥330/μl within 12 weeks		
		Present (n = 53)	Absent (n = 127)	*P* value	Present (n = 23)	Absent (n = 56)	*P* value
Sex	Female	8	31	0.23	3	17	0.11
	Male	45	96		20	39	
PS (ECOG)	0–1	45	107	0.99	23	51	0.99
	≥2	8	20		0	2	
Age, y	<70	35	64	0.06	13	31	0.99
	≥70	18	63		10	25	
Pathology	Adenocarcinoma	31	84	0.33	13	36	0.61
	Others	22	43		10	20	
Stage	IIIA-C	12	37	0.46	5	10	0.76
	IVA-B	41	90		18	46	
Driver genes	Present	3	16	0.2	0	5	0.31
	Absent	50	111		23	51	
PD-L1 expression	≥25%	24	47	0.32	9	10	0.08
	<25%	29	80		14	46	
irAE (not requiring discontinuation of ICPI)	Present	9	15	0.35	3	8	0.85
	Absent	44	112		20	48	

Abbreviations: Eo, eosinophils; others, see TABLE 1

DISCUSSION Based on the Kaplan–Meier curves of progression-free survival in several clinical trials of ICPI monotherapy for NSCLC, patients could be stratified into 3 groups: no response group, short-term response group, and long-term response group.[3-8] On the other hand, patients who received combination therapy of ICPI and chemotherapy could be divided into 2 groups of short-term and long-term response.[9, 10] On the basis of these stratifications, the relationship between the count and percentage of peripheral eosinophils and TTF was investigated. First, we created the Kaplan–Meier curves for TTF with eosinophil expression measured at the time of each ICPI administration during the clinical course of every patient. These data showed that the 3 groups of patients treated with ICPI monotherapy (group I: TTF ≤6 weeks; group II: TTF >6 weeks and ≤24 weeks; group III: TTF >24 weeks) differed significantly in terms of the number of patients with an eosinophil percentage of 5% or more achieved within 6 weeks of therapy initiation. In both univariable and multivariable analyses, not only a PS of 0 to 1 and IrAEs not

TABLE 4 Peripheral eosinophil expression in groups of patients with different time to treatment failure[a]

Parameter[b]		Patients treated with ICPI monotherapy (n = 180)				Patients treated with combination therapy of ICPI and chemotherapy (n = 79)		
		Group I (n = 58)	Group II (n = 54)	Group III (n = 68)	*P* value	Group IV (n = 19)	Group V (n = 60)	*P* value
Eosinophil percentage ≥5%	Present	4	15	21	0.003	2	23	0.023
	Absent	54	39	47		17	37	
Eosinophil count ≥330/μl	Present	12	15	26	0.099	3	20	0.268
	Absent	46	39	42		16	40	

a Stratification based on the therapeutic efficacy reflected by TTF: group I, TTF ≤6 weeks; group II, TTF >6 weeks and ≤24 weeks; group III, TTF >24 weeks; group IV, TTF ≤12 weeks; group V, TTF >12 weeks

b Threshold for achieving the specified counts and percentages of eosinophils was set at 6 weeks for patients treated with ICPI monotherapy and 12 weeks for those treated with combination therapy of ICPI and chemotherapy.

Abbreviations: see TABLE 1

requiring ICPI discontinuation, but also an eosinophil percentage of 5% or more and an eosinophil count of 330/μl or more within 6 weeks of ICPI treatment initiation were significant favorable factors for prolonged therapeutic efficacy. In patients treated with combination therapy of ICPI and chemotherapy, the number of patients with an eosinophil percentage of 5% or more within 12 weeks of therapy initiation was significantly different between groups IV and V ($P = 0.0231$). However, in a univariable analysis, the only significant favorable factor for prolonged TTF was female sex. Therefore, in this study, factors predicting a prolonged therapeutic efficacy in patients treated with combination therapy of ICPI and chemotherapy could not be determined.

We adopted cutoffs of 6 and 12 weeks for achieving an eosinophil percentage of 5% or more and an eosinophil count of 330/μl or more for patients receiving ICPI monotherapy and combination therapy of ICPI and chemotherapy, respectively. This was to reflect as much patient information as possible in terms of the therapeutic efficacy of ICPI treatment, but it remains arguable whether these grouping thresholds were optimal.

A few reports suggested the involvement of eosinophils in cancer immunity.[33-38] However, it is unlikely that the increased number of eosinophils in the peripheral blood directly reflects the immune status of cancerous lesions. Indeed, some study patients in the long-term response group had an increase in the absolute eosinophil count up to 1000/μl and a high percentage of eosinophils, exceeding 20%. However, in the majority of patients, no such high eosinophil count or percentage was observed. Based on these results, the relative variability of eosinophil count in peripheral blood linked to the fluctuation of other blood cells might be more important. It might also be consistent with the observation that the percentage of eosinophils was a more useful prognostic factor than the absolute eosinophil count.

Elucidation of the biological role of eosinophils in cancer immunity is likely to be an area of future research. At the same time, our understanding of the changes in peripheral blood cells during ICPI therapy will increase. Such advances will clarify the role of eosinophil expression as a biomarker for response to ICPI therapy. In this study, we did not find a clear association between eosinophil variability and TTF in patients treated with combination therapy of ICPI and chemotherapy. Myelosuppression by antitumor drugs causes neutropenia, which is presumed to further complicate the movement of peripheral blood cells. As such, this area will also benefit from future research.

This study has several limitations. Firstly, we did not elucidate the relationship between changes in eosinophils following ICPI therapy and the biological role of eosinophils. Secondly, it was a retrospective study that included patients with various baseline characteristics. Thirdly, it involved a limited number of patients with a short follow-up period, and the number of patients required was not prespecified based on the power calculation. Among the 79 patients treated with combination therapy of ICPI and chemotherapy, 25 were on treatment during the study, and this might have influenced the results. Fourthly, we focused on the indications for patients who should switch from ICPI to other treatment and those who can continue ICPI therapy for a long period of time. Therefore, the analysis was conducted with the intention of providing useful information as to whether the treatment could be continued at 2 to 3 courses of ICPI monotherapy and at 3 to 4 courses of combination therapy of ICPI and chemotherapy.

Although the contribution of ICPI therapy to prolonging survival in many patients with carcinoma is significant, ICPIs can cause irAEs in different organs throughout the body, and these irAEs range from controllable to life-threatening.[39] Therefore, as clinicians, we should be on the alert for the onset of irAEs. On the other hand, however, an association between controllable irAEs and prolonged survival has been reported.[40,41] Therefore, in the event of an irAE, it should first be determined whether it is controllable. Subsequently, the decision

TABLE 5 Results of univariable and multivariable analyses in patients treated with immune checkpoint inhibitor monotherapy

Parameter	Univariable analysis		Multivariable analysis	
	P value	Hazard ratio	95% CI	*P* value
Eosinophil percentage ≥5% within 6 weeks				
Female sex	0.17	–	–	–
PS (ECOG), 0–1	0.077	1.559	1.007–2.412	0.047
Age, ≤70 years	0.56	–	–	–
Pathology, adenocarcinoma	0.42	–	–	–
Cancer stage, IIIA–C	0.41	–	–	–
Driver genes, absent	0.12	–	–	–
PD-L1 expression, ≥25%	0.043	1.234	0.930–1.831	0.12
irAE not requiring ICPI discontinuation, present	<0.001	2.826	1.680–4.754	<0.001
Eosinophil percentage ≥5% within 6 weeks of ICPI therapy initiation, present	0.003	1.837	1.242–2.717	0.002
Eosinophil count ≥330/μl within 6 weeks				
Female sex	0.17	–	–	–
PS (ECOG), 0–1	0.077	1.722	1.115–2.660	0.014
Age, ≤70 years	0.56	–	–	–
Pathology, adenocarcinoma	0.42	–	–	–
Cancer stage, IIIA–C	0.41	–	–	–
Driver genes, absent	0.12	–	–	–
PD-L1 expression, ≥25%	0.04	1.303	0.929–1.826	0.125
irAE not requiring ICPI discontinuation, present	<0.001	2.784	1.653–4.690	<0.001
Eosinophil count ≥330/μl within 6 weeks of ICPI therapy initiation, present	0.061	1.471	1.038–2.085	0.03

Abbreviations: see **TABLE 1**

whether to continue ICPI therapy can be made in consideration of the changes in peripheral eosinophils associated with ICPI treatment.

ARTICLE INFORMATION

ACKNOWLEDGMENTS *The authors wish to express special thanks to* Yuika Sasatani, MD, Gen Ohara, MD, and Shinya Sato, MD for their help in data collection and valuable advice on this study.

CONTRIBUTION STATEMENT HO and HS designed the study. SO, TS, KM, YS, GO, KK, SS, TK, and HS collected the data. HO, SO, KN, RN, HS, and NH analyzed the data and prepared the manuscript. All authors approved the final version of the article.

CONFLICT OF INTEREST None declared.

HOW TO CITE Osawa H, Shiozawa T, Okauchi S, et al. Association between time to treatment failure and peripheral eosinophils in patients with non–small cell lung cancer treated with immune checkpoint inhibitors. Pol Arch Intern Med. 2021; 131: 16049. doi:10.20452/pamw.16049

REFERENCES

1 Remon J, Passiglia F, Ahn MJ, et al. Immune checkpoint inhibitors in thoracic malignancies: review of the existing evidence by an IASLC Expert Panel and recommendations. J Thorac Oncol. 2020; 15: 914-947.

2 Qiu Z, Chen Z, Zhang C, Zhong W. Achievements and futures of immune checkpoint inhibitors in non-small cell lung cancer. Exp Hematol Oncol. 2019; 8: 19.

3 Rizvi NA, Mazières J, Planchard D, et al. Activity and safety of nivolumab, an anti-PD-1 immune checkpoint inhibitor, for patients with advanced, refractory squamous non-small-cell lung cancer (CheckMate 063): a phase 2, single-arm trial. Lancet Oncol. 2015; 16: 257-265.

4 Brahmer J, Reckamp KL, Baas P, et al. Nivolumab versus docetaxel in advanced squamous-cell non-small-cell lung cancer. N Engl J Med. 2015; 373: 123-135.

5 Borghaei H, Paz-Ares L, Horn L, et al. Nivolumab versus docetaxel in advanced nonsquamous non-small-cell lung cancer. N Engl J Med. 2015; 373: 1627-1639.

6 Garon EB, Rizvi NA, Hui R, et al. Pembrolizumab for the treatment of non-small-cell lung cancer. N Engl J Med. 2015; 372: 2018-2028.

7 Herbst RS, Baas P, Kim DW, et al. Pembrolizumab versus docetaxel for previously treated, PD-L1-positive, advanced non-small-cell lung cancer (KEYNOTE-010): a randomised controlled trial. Lancet. 2016; 387: 1540-1550.

8 Fehrenbacher L, Spira A, Ballinger M, et al. Atezolizumab versus docetaxel for patients with previously treated non-small-cell lung cancer (POPLAR): a multicentre, open-label, phase 2 randomised controlled trial. Lancet. 2016; 387: 1837-1846.

9 Gandhi L, Rodríguez-Abreu D, Gadgeel S, et al. Pembrolizumab plus chemotherapy in metastatic non-small-cell lung cancer. N Engl J Med. 2018; 378: 2078-2092.

10 West H, McCleod M, Hussein M, et al. Atezolizumab in combination with carboplatin plus nab-paclitaxel chemotherapy compared with chemotherapy alone as first-line treatment for metastatic non-squamous non-small-cell lung cancer (IMpower130): a multicentre, randomised, open-label, phase 3 trial. Lancet Oncol. 2019; 20: 924-937.

11 Lantuejoul S, Sound-Tsao M, Cooper WA, et al. PD-L1 testing for lung cancer in 2019: perspective from the IASLC pathology committee. J Thorac Oncol. 2020; 15: 499-519.

12 Williams JB, Li S, Higgs EF, et al. Tumor heterogeneity and clonal cooperation influence the immune selection of IFN-γ-signaling mutant cancer cells. Nat Commun. 2020; 11: 602.

13 Simon SCS, Hu X, Panten J, et al. Eosinophil accumulation predicts response to melanoma treatment with immune checkpoint inhibitors. Oncoimmunology. 2020; 9: 1727116.

14 Rigoni A, Colombo MP, Pucillo C. Mast cells, basophils and eosinophils: from allergy to cancer. Semin Immunol. 2018; 35: 29-34.

15 Simon SCS, Utikal J, Umansky V. Opposing roles of eosinophils in cancer. Cancer Immunol Immunother. 2019; 68: 823-833.

16 Wang X, Zhang B, Chen X, et al. Lactate dehydrogenase and baseline markers associated with clinical outcomes of advanced esophageal squamous cell carcinoma patients treated with camrelizumab (SHR-1210), a novel anti-PD-1 antibody. Thorac Cancer. 2019; 10: 1395-1401.

17 Benitez JC, Recondo G, Rassy E, Mezquita L. The LIPI score and inflammatory biomarkers for selection of patients with solid tumors treated with checkpoint inhibitors. Q J Nucl Med Mol Imaging. 2020; 64: 162-174.

18 Delyon J, Mateus C, Lefeuvre D, et al. Experience in daily practice with ipilimumab for the treatment of patients with metastatic melanoma: an early increase in lymphocyte and eosinophil counts is associated with improved survival. Ann Oncol. 2013; 24: 1697-1703.

19 Umansky V, Utikal J, Gebhardt C. Predictive immune markers in advanced melanoma patients treated with ipilimumab. Oncoimmunology. 2016; 5: e1158901.

20 Moreira A, Leisgang W, Schuler G, Heinzerling L. Eosinophilic count as a biomarker for prognosis of melanoma patients and its importance in the response to immunotherapy. Immunotherapy. 2017; 9: 115-121.

21 Buder-Bakhaya K, Hassel JC. Biomarkers for clinical benefit of immune checkpoint inhibitor treatment – a review from the melanoma perspective and beyond. Front Immunol. 2018; 9: 1474.

22 Simon SCS, Hu X, Panten J, et al. Eosinophil accumulation predicts response to melanoma treatment with immune checkpoint inhibitors. Oncoimmunology. 2020; 9: 1727116.

23 Tanizaki J, Haratani K, Hayashi H, et al. Peripheral blood biomarkers associated with clinical outcome in non-small cell lung cancer patients treated with nivolumab. J Thorac Oncol. 2018; 13: 97-105.

24 Facchinetti F, Veneziani M, Buti S, et al. Clinical and hematologic parameters address the outcomes of non-small-cell lung cancer patients treated with nivolumab. Immunotherapy. 2018; 10: 681-694.

25 Fujimoto S, Fujita A, Minato K, et al. Complete response of a patient with lung squamous cell carcinoma after only three administrations of nivolumab [in Japanese]. Jpn J Lung Cancer (Haigan). 2018; 58: 292-297.

26 Inomata M, Kado T, Okazawa S, et al. Peripheral PD1-positive CD4 T-lymphocyte count can predict progression-free survival in patients with non-small cell lung cancer receiving immune checkpoint inhibitor. Anticancer Res. 2019; 39: 6887-6893.

27 Soda H, Ogawara D, Fukuda Y, et al. Dynamics of blood neutrophil--related indices during nivolumab treatment may be associated with response to salvage chemotherapy for non-small cell lung cancer: a hypothesis-generating study. Thorac Cancer. 2019; 10: 341-346.

28 Lou Y, Marin-Acevedo JA, Vishnu P, et al. Hypereosinophilia in a patient with metastatic non-small-cell lung cancer treated with antiprogrammed cell death 1 (anti-PD-1) therapy. Immunotherapy. 2019; 11: 577-584.

29 Alves A, Sucena I, Dias M, et al. Eosinophilia in lung cancer patients treated with immunotherapy. Eur Respir J. 2019; 54 (suppl 63): PA4664.

30 Singh N, Lubana SS, Constantinou G, Leaf AN. Immunocheckpoint inhibitor- (Nivolumab-) associated hypereosinophilia in non-small-cell lung carcinoma. Case Rep Oncol Med. 2020; 2020: 7492634.

31 Hude I, Sasse S, Bröckelmann PJ, et al. Leucocyte and eosinophil counts predict progression-free survival in relapsed or refractory classical Hodgkin lymphoma patients treated with PD1 inhibition. Br J Haematol. 2018; 181: 837-840.

32 Okauchi S, Shiozawa T, Miyazaki K, et al. Association between peripheral eosinophils and clinical outcomes in patients with non-small cell lung cancer treated with immune checkpoint inhibitors. Pol Arch Intern Med. 2021; 131: 152-160.

33 Sawyers CL, Golde DW, Quan S, Nimer SD. Production of granulocyte--macrophage colony-stimulating factor in two patients with lung cancer, leukocytosis, and eosinophilia. Cancer. 1992; 69: 1342-1346.

34 Matsumoto S, Tamai T, Yanagisawa K, et al. Lung cancer with eosinophilia in the peripheral blood and the pleural fluid. Intern Med. 1992; 31: 525-529.

35 Pandit R, Scholnik A, Wulfekuhler L, Dimitrov N. Non-small-cell lung cancer associated with excessive eosinophilia and secretion of interleukin-5 as a paraneoplastic syndrome. Am J Hematol. 2007; 82: 234-237.

36 El-Osta H, El-Haddad P, Nabbout N. Lung carcinoma associated with excessive eosinophilia. J Clin Oncol. 2008; 26: 3456-3457.

37 Rigoni A, Colombo MP, Pucillo C. Mast cells, basophils and eosinophils: from allergy to cancer. Semin Immunol. 2018; 35: 29-34.

38 Simon SCS, Utikal J, Umansky V. Opposing roles of eosinophils in cancer. Cancer Immunol Immunother. 2019; 68: 823-833.

39 Domagała-Kulawik J, Leszek P, Owczarek W, et al. Immunotherapy of solid tumors: safety of treatment. Pol Arch Intern Med. 2020; 130: 766-778.

40 Fan Y, Xie W, Huang H, et al. Association of immune related adverse events with efficacy of immune checkpoint inhibitors and overall survival in cancers: a systemic review and meta-analysis. Front Oncol. 2021; 11: 633032.

41 Corsello SM, Barnabei A, Marchetti P, et al. Endocrine side effects induced by immune checkpoint inhibitors. J Clin Endocrinol Metab. 2013; 98: 1361-1375.

Surgery Today (2022) 52:763–773
https://doi.org/10.1007/s00595-021-02388-1

ORIGINAL ARTICLE

National survey on deceased donor organ transplantation during the COVID-19 pandemic in Japan

Taihei Ito[1] · Takashi Kenmochi[1] · Atsuhiko Ota[2] · Kaori Kuramitsu[3] · Akihiko Soyama[4] · Osamu Kinoshita[5] · Susumu Eguchi[4] · Kenji Yuzawa[6] · Hiroto Egawa[7]

Received: 9 June 2021 / Accepted: 11 August 2021 / Published online: 23 October 2021

Abstract

Purpose We investigated the status of deceased organ donation and transplantation through a questionnaire distributed to transplant centers in Japan during the COVID-19 pandemic.

Methods The questionnaire was distributed electronically to 206 transplant centers for heart ($n=11$), lung ($n=10$), liver ($n=25$), kidney ($n=130$), pancreas ($n=18$), and small intestine ($n=12$) transplantation. Organ donations and organ transplantation data were extracted from the Japan Organ Transplant Network website.

Results We received questionnaire responses from 177 centers (response rate, 86%). In 2020, the number of brain-dead donors (BDDs) decreased to 68 (69% of the year-on-year average) and the number of donors after cardiac death (DCDs) decreased to 9 (32% of the year-on-year average). Eighty-five (48%) transplant centers (heart, $n=0$; lung, $n=0$; liver, $n=4$; kidney, $n=78$; pancreas, $n=22$; and small intestine, $n=0$) suspended transplant surgeries in response to the COVID-19 pandemic. Consequently, the number of organ transplantations from deceased donors was significantly lower in 2020 than in 2019.

Conclusion Although the COVID-19 pandemic has had less impact in Japan than in other countries, it has affected transplantation activity significantly, suspending transplantation surgeries in 48% of the transplantation centers, including 78% of the kidney transplantation centers, and reducing the number of organ donations to 61% of the year-on-year average.

Keywords COVID-19 · Brain-dead donors · Donors after cardiac death · Solid organ transplantation

✉ Taihei Ito
i-taihei@fujita-hu.ac.jp

1 Department of Transplantation and Regenerative Medicine, Fujita Health University, School of Medicine, Dengakugakubo 1-98, Kutsukakecho, Toyoake, Aichi 470-1192, Japan

2 Department of Public Health, Fujita Health University School of Medicine, Toyoake, Aichi, Japan

3 Division of Hepato-Biliary-Pancreatic Surgery, Kobe University Graduate School of Medicine, Kobe, Hyogo, Japan

4 Department of Surgery, Nagasaki University Graduate School of Biomedical Sciences, Nagasaki, Nagasaki, Japan

5 Department of Cardiac Surgery, Graduate School of Medicine, The University of Tokyo, Bunkyo, Tokyo, Japan

6 Department of Transplantation Surgery, National Hospital Organization Mito Medical Center, Mito, Ibaraki, Japan

7 Department of Surgery, Institute of Gastroenterology, Tokyo Women's Medical University, Shinjuku, Tokyo, Japan

Introduction

In the first 10 years after the establishment of the Brain Death Organ Transplant Act in 1997, the annual number of brain-dead donors (BDDs) in Japan was less than 10. This low number at the time was attributed to the fact that brain death referred only to human death in cases of donation for organ transplantation, and brain-dead donors (BDDs) were required to have made their intention clear before brain death. The law was revised in 2009 to state that even if the donor's intention to donate organs was unknown, organ donation from BDDs was able to be approved with the consent of the family. The law was enforced in 2010, resulting in increased numbers of organ donations from BDDs [1]. This had a positive impact on patients awaiting solid organ transplantation (SOT) for organ failure [2–6].

The COVID-19 pandemic has ravaged the globe since early 2020 [7–11]. While the numbers of patients with COVID-19 and related deaths in Japan have been relatively

low in comparison with other countries [12, 13], the treatment of COVID-19 patients in emergency medical care and the intensive-care unit (ICU) has been difficult, raising concern about the decline of general medical practices [14–16].

In transplant medical care, essential immunosuppressive therapy after transplantation has a negative impact on mortality from this new viral infection. The COVID-19-related mortality rate in SOT recipients has been reported to range from 18 to 34% [17–19]. Moreover, COVID-19 is a serious life-threatening infectious disease for individuals with organ failure who are awaiting transplantation, and the decline in transplant activity also impacts the prognosis of these patients. For example, the COVID-19-related mortality rate in patients awaiting kidney transplantation who required dialysis was reported to range from 20 to 32% [18, 20–32].

In response to the impact of the COVID-19 pandemic on transplant activity, on March 6, 2020, the Japan Society for Transplantation published the first edition of the basic guidelines for transplantation medicine for new coronavirus infection (COVID-19). The guidelines have been updated according to the outbreak situation in Japan, with the latest edition, version 4.1 released on February 4, 2021 [33]. In the first edition, the recommendation for the implementation of SOT was as follows: "If possible, waiting for organ transplantation until the situation of the COVID-19 pandemic improves is recommended in order to avoid the risk of infection from donors or community-acquired infection under immunosuppression after transplantation". However, the recommendation in the latest version (version 4.1) is as follows: "In the implementation of solid organ transplantation, the risk of the COVID-19 infection from the donor and the risk of the aggravation of COVID-19 infection under immunosuppression after transplantation must be properly explained to obtain sufficient informed consent about…". Thus, although the COVID-19 pandemic may influence organ donation and transplant activity in Japan remarkably, no report has clarified the real situation.

We investigated the status of deceased organ donation and organ transplantation in Japan during the COVID-19 pandemic, using a questionnaire that was distributed to transplant centers, to clarify the current status of transplantation activity in Japan during the COVID-19 pandemic.

Methods

A questionnaire survey was conducted as part of a welfare and labor science special research project entitled, "Survey research for organ transplantation from BDDs and donors after cardiac death (DCDs) during the pandemic of COVID-19". The questionnaire, including 23 questions on the medical system, the SOT policy, and the implementation status in each center during the COVID-19 pandemic, was distributed electronically to 206 transplant centers in Japan (heart centers, $n=11$; lung centers, $n=10$; liver centers, $n=25$; kidney centers, $n=130$; pancreas centers, $n=18$; and small-intestine centers, $n=12$) from December, 2020 to January, 2021 during the third wave of the COVID-19 pandemic, with the development of a website entrusted to Tokai Kyodo Printing. The representatives of each center registered their answers. The numbers of deceased organ donations and SOTs were counted by searching the Japan Organ Transplant Network website (https://www.jotnw.or.jp/). The number of COVID-19-positive patients in Japan was estimated based on announcements made by the Ministry of Health, Labor and Welfare (https://www.mhlw.go.jp/stf/covid-19/kokunainohasseijoukyou.html).

The Microsoft Excel software program (Microsoft, USA) was used to summarize the data. Categorical data are shown as frequencies and percentages.

Results

Changes in the number of COVID-19-positive patients and organ donations in Japan

Figure 1 shows the changes in the number of BDDs and DCDs in Japan. In 1997, the law on organ transplantation was enacted, with organ donations from BDDs (black solid bars) implemented. Despite this legislation, there was no marked increase in organ donations from BDDs. The law was revised in 2009 and enforced in 2010, after which the number of brain-dead organ donations began to steadily increase, reaching a record high of 98 in 2019. In contrast, the number of DCDs (white solid bars) has decreased since the revision of the law, to about 30 in recent years. In early 2020, the first cases of COVID-19 were detected in Japan, and in 2020, the number of BDDs and DCDs decreased to 68 and 9, respectively.

Figure 2 shows the changes in the number of COVID-19-positive patients (gray solid bar) and the monthly number of organ donations (BDDs, black solid bars; DCDs, white solid bars) from January, 2020. The first case of COVID-19 in Japan was confirmed in February, 2020, with the number peaking in April, 2020 in the first wave of the COVID-19 pandemic. This was followed by a second wave in August, 2020, and a third wave in February, 2021. By the time of writing, at the end of March 2021, the third wave had begun to converge. By March 20, 2021, the total number of COVID-19 positive patients in Japan had reached 451,830, with 8788 COVID-19-related deaths.

In contrast, the number of BDDs at the beginning of 2020 did not decrease significantly from that in 2019. However, since the autumn of 2020, when the third wave of the COVID-19 pandemic started, the number of organ donations

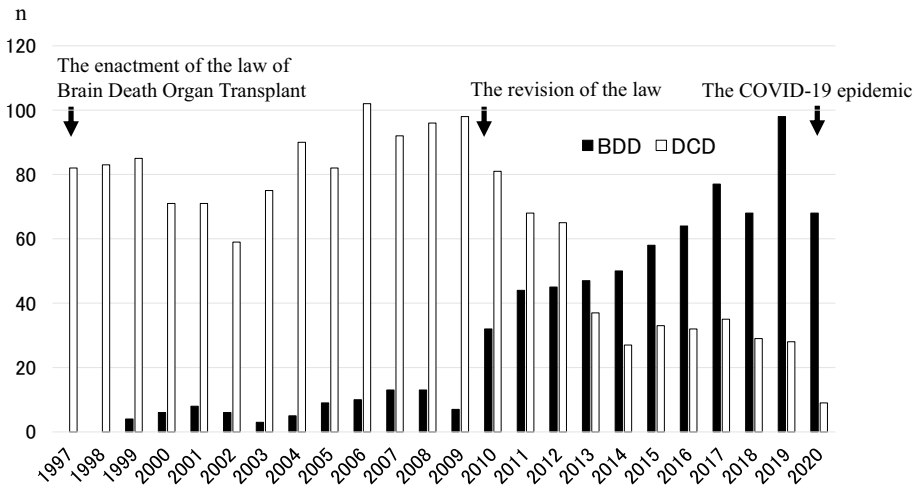

Fig. 1 Annual numbers of deceased organ donations in Japan. Organ donations from brain-dead donors (BDDs) (black solid bars) began in 1997, when the law on organ transplantation was enacted. When the law was revised in 2009, the number of brain-dead organ donations increased steadily, reaching a record high of 98 cases in 2019. In contrast, the number of donors after cardiac death (DCDs) (white solid bars) has decreased since the revision of the law, falling to approximately 30 in recent years. In 2020, after detection of the first COVID-19-positive patients in Japan, the number of BDDs and DCDs decreased to 68 and 9, respectively

has decreased, with no organ donations in December, 2020. It is noteworthy that the number of DCDs, which require a long waiting period for transplant doctors, has dropped significantly since early 2020, to only nine cases in 2020. This represents the first single-digit figure in the records, and highlights the significant impact of the COVID-19 pandemic on organ donation in Japan (Fig. 2).

As a result, the annual number of SOTs from deceased donors decreased significantly in 2020 compared with the number in 2019, with the exception of small-intestine transplants (Fig. 3). There were 84 cases of heart transplantation in 2019 vs. 54 in 2020 (64% of the year-on-year average) and 79 cases of lung transplantation in 2019 vs. 58 in 2020 (73% of the year-on-year average). Regarding abdominal organ transplantation, there were 88 cases of liver transplantation in 2019 vs. 63 in 2020 (72% of the year-on-year average) and 176 cases of kidney transplantation, including 46 cases of simultaneous pancreas transplantation (SPK) and 6 cases of simultaneous liver transplantation (SLK), in 2019 vs. 124 in 2020 (SPK, $n=24$; SLK, $n=5$; 71% of the

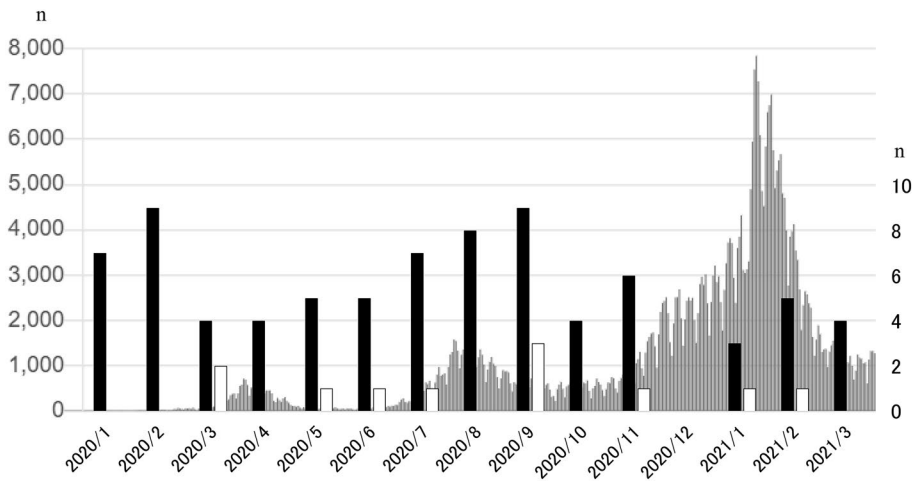

Fig. 2 Numbers of COVID-19-positive patients and deceased donors in 2020. The change in the number of COVID-19-positive patients is displayed as solid gray bars, and the monthly numbers of organ donations from BDDs and DCDs since January 2020 are shown as solid black bars and solid white bars, respectively. Since the autumn of 2020, when the third wave of the COVID-19 pandemic started, the number of organ donations has decreased. In December 2020, there were no organ donations. It is noteworthy that the number of DCDs, which require a long waiting period for transplant doctors, has dropped significantly since early 2020

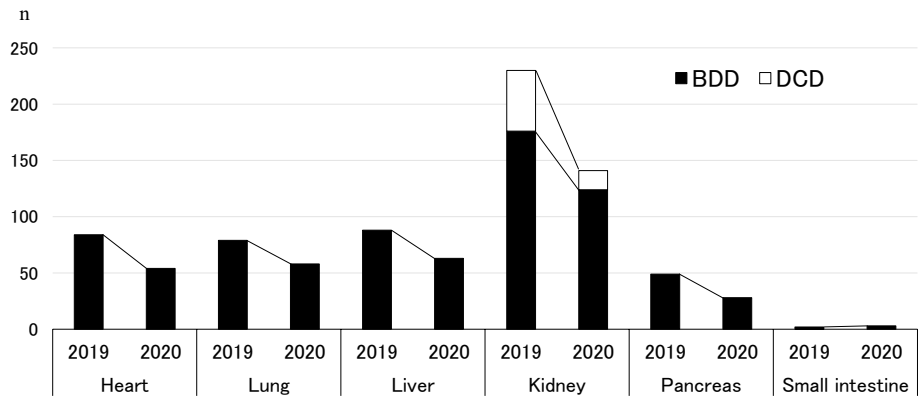

Fig. 3 Annual numbers of transplantations from deceased donors in 2019 and 2020 in Japan. There were 84 cases of heart transplantation in 2019 vs. 54 in 2020 (64% of the year-on-year average) and 79 cases of lung transplantation in 2019 vs. 58 in 2020 (73% of the year-on-year average). For abdominal organ transplantation, there were 88 cases of liver transplantation in 2019 vs. 63 in 2020 (72% of the year-on-year average) and 176 cases of kidney transplantation, including 46 of simultaneous pancreas transplantation (SPK) and 6 of simultaneous liver transplantation (SLK), in 2019 vs. 124 (SPK, $n=24$; SLK, $n=5$; 71% of the year-on-year average) in 2020. Pancreas transplants also decreased from 49 cases in 2019 to 28 in 2020 (57% of the year-on-year average). Small-intestine transplants increased slightly from two cases in 2019 to three in 2020

year-on-year average). Pancreas transplants also decreased from 49 cases in 2019 to 28 in 2020 (57% of the year-on-year average), whereas small-intestine transplants increased slightly from 2 cases in 2019 to 3 in 2020.

Current status of transplant medical care at transplant centers in Japan

We received questionnaire responses from 177 of the 206 centers, representing a response rate of 86% (heart centers, 100%; lung centers, 90%; liver centers, 100%; kidney centers, 79%; pancreas centers, 100%; small-intestine centers, 92%).

Table 1 summarizes the medical care for COVID-19 (other than transplants) that was provided in transplant centers. Among the responding centers, 98 (55%) were designated hospitals for infection (Q1), and 155 (88%), including those other than designated hospitals for infection, had wards dedicated to the treatment of COVID-19-positive patients (Q3). ICUs were set up in-hospital at 172 centers (97%) (Q4), and patients with severe COVID-19 sequelae were treated in the ICU at 144 centers (81%) (Q5). Regarding in-hospital tests for COVID-19, PCR testing was performed at 169 centers (95%) (Q6), antigen tests were performed at 151 centers (85%) (Q7), and antibody tests were performed at 90 centers (51%) (Q8). A total of 161 centers (90%) had established rules on surgical treatment (including surgery other than transplantation) during the COVID-19 pandemic (Q9).

Table 2 summarizes the results of the questionnaire on the status of transplant programs at transplant centers in Japan during the COVID-19 pandemic. Regarding the continuation of providing transplant medical care, following discussions held at 151 centers (85%) (Q10), 85 centers (48%) suspended transplant medical care because of the COVID-19 pandemic (Q12). While no center discontinued its transplant surgery for heart and lung transplants, one center (4%) suspended liver transplants, 80 (78%) suspended kidney transplants, and 4 (22%) suspended pancreas transplants (Fig. 4a). In 41 centers (23%), this discussion involved a single department, in 57 (32%) it involved multiple departments concerned with SOT, and in 44 (25%) it involved the whole hospital (Q11). The reasons for suspending transplant surgeries (Q13) were as follows: there were COVID-19-positive patients in the hospital ($n=12$; 7%), there were COVID-19-positive patients in the prefecture ($n=26$; 15%), the in-hospital medical care system or examination system was inadequate for assessing COVID-19 ($n=34$; 19%), all surgical treatment (including transplantation) was restricted ($n=33$; 19%), and transplant surgery was suspended in accordance with the guidelines of the Japan Society for Transplantation ($n=57$; 32%) (Fig. 4b). Fifty-six centers (31%) suspended all transplants, including both deceased and living donor transplantation, 25 (14%) suspended only living donor transplantation, and 1 (1%) suspended only deceased donor transplantation (Fig. 4c) (Q14).

During the period of the questionnaire (December, 2020–January, 2021), transplant surgery was still suspended at seven centers (4%), all of which were kidney transplant programs. The reasons for resuming transplant surgeries (Q15) were as follows: reduction in the number of COVID-19 infections at the hospital ($n=9$; 5%), lack of spread of COVID-19 infection confirmed in the hospital ($n=11$; 6%), reduction in the number of COVID-19 infections in the local area ($n=29$; 16%), establishment of an in-hospital medical

Table 1 Medical care for COVID-19 in transplant centers

		Answer	Overall (%) $n=177$	Heart $n=11$	Lung $n=9$	Liver $n=25$	Kidney $n=103$	Pancreas $n=18$	Small intestine $n=11$
Q1	Is your center an infectious disease designated hospital?	Yes	98 (55)	2 (18)	6 (67)	18 (72)	52 (50)	12 (67)	8 (73)
		No	79 (45)	9 (82)	3 (33)	7 (28)	51 (50)	6 (33)	3 (27)
Q2	Do you have a special outpatient clinic that provides care for patients with fever in your hospital?	Yes	127 (72)	5 (45)	6 (67)	18 (72)	79 (77)	12 (67)	7 (64)
		No	49 (28)	6 (55)	3 (33)	7 (28)	23 (22)	6 (33)	4 (36)
Q3	Do you have a ward dedicated to treating COVID-19 infected patients in your hospital?	Yes	155 (88)	11 (100)	9 (100)	20 (80)	90 (87)	17 (94)	8 (73)
		No	22 (12)	0 (0)	0 (0)	5 (20)	13 (13)	1 (6)	3 (27)
Q4	Do you have an ICU in your hospital?	Yes	172 (97)	11 (100)	9 (100)	25 (100)	98 (95)	18 (100)	11 (100)
		No	5 (3)	0 (0)	0 (0)	0 (0)	5 (5)	0 (0)	0 (0)
Q5	Does the ICU accept treatment for patients infected with COVID-19?	Yes	144 (81)	11 (100)	9 (100)	23 (92)	76 (74)	15 (83)	10 (91)
		No	32 (19)	0 (0)	0 (0)	2 (8)	26 (25)	3 (17)	1 (9)
Q6	Is it possible to perform PCR tests in-hospital for COVID-19 in your center?	Yes	169 (95)	11 (100)	9 (100)	25 (100)	95 (92)	18 (100)	11 (100)
		No	7 (4)	0 (0)	0 (0)	0 (0)	7 (7)	0 (0)	0 (0)
Q7	Is it possible to perform antigen tests in-hospital for COVID-19 in your center?	Yes	151 (85)	9 (82)	8 (89)	20 (80)	90 (87)	16 (89)	8 (73)
		No	21 (12)	0 (0)	1 (11)	3 (12)	13 (13)	2 (11)	2 (18)
Q8	Is it possible to perform antibody tests in-hospital for COVID-19 in your center?	Yes	90 (51)	8 (73)	6 (67)	14 (56)	46 (45)	10 (56)	6 (55)
		No	78 (44)	2 (18)	3 (33)	9 (36)	54 (52)	7 (39)	3 (27)
Q9	Do you have any rules related to COVID-19 concerning the performance of surgical treatment (including surgery other than transplantation) in your center?	Yes	161 (90)	9 (82)	9 (100)	23 (92)	94 (91)	17 (94)	9 (82)
		No	12 (7)	0 (0)	0 (0)	1 (4)	8 (8)	1 (6)	2 (18)

care system and testing for COVID-19 ($n=51$; 29%), restrictions on surgeries other than transplantation ($n=28$; 16%), and surgeries re-established in accordance with the guidelines of the Japan Society for Transplantation ($n=34$; 19%).

Of the centers with ongoing transplant surgery at the time of the questionnaire, 112 (63%) were providing transplant medical care without special restrictions, while 34 (19%) were limiting transplant surgery to cases considered difficult to postpone (Fig. 4d) (Q16). Depending on the future spread of the COVID-19 pandemic, only 30 centers (17%) answered that they would continue to provide transplant medical care without any restrictions, while 92 (52%) answered that they would consider suspending their transplant surgeries depending on the presence of COVID-19 in the ICU or hospital. Thirty-four centers answered that they would discontinue transplant surgeries in the event of nosocomial COVID-19 infection (Q17).

During the COVID-19 pandemic, 21 centers (12%) answered that they had been restricted from dispatching to organ recovery (Q18), and 14 centers (8%) answered that they had abandoned organ recovery efforts because of the COVID-19 pandemic (Q19). Even when organ recovery was possible, 12 centers (7%) reported that they had abandoned transplant surgery because of the COVID-19 pandemic (Q20).

Before any transplant surgery, 161 institutions (90%) performed a preoperative COVID-19 screening test of SOT recipients (Q21). A total of 112 centers (63%) answered that the post-transplant follow-up systems had changed in accordance with the COVID-19 pandemic (Q22), and most (123 centers, 69%) answered that follow-up outpatient visits after transplantation were set at longer intervals (Q23).

Discussion

The findings of this study confirmed that the COVID-19 pandemic reduced the number of organ donations, especially from DCDs. In Japan, organ donation from DCDs was performed without the withdrawal of life-support including respiration, which sometimes forces the organ recovery team to wait a long time in the donor's hospital. This was considered why DCDs were so markedly reduced by the COVID-19 pandemic. Our questionnaire survey revealed the organ donation situation in Japan. In addition to a reduction in the number of organ donations, half of the transplant centers suspended transplant surgery, particularly abdominal organ transplant surgeries, because of the COVID-19 pandemic. While transplant surgeries were resuming in most institutions when the questionnaire was distributed, approximately 20% of the transplant centers limited SOT surgery to those patients whose prognosis would have been severely affected by postponing surgery, and about 10% of centers indicated that it was necessary to abandon organ recovery or SOT in

Table 2 Results of the questionnaire on the status of transplant programs

		Answer	Overall (%) $n=177$	Heart $n=11$	Lung $n=9$	Liver $n=25$	Kidney $n=103$	Pancreas $n=18$	Small intestine $n=11$
Q10	Have you ever discussed the continuation of the transplant surgeries in the hospital during the COVID-19 pandemic?	Yes	151 (85)	8 (73)	6 (67)	20 (80)	94 (91)	15 (83)	8 (73)
		No	26 (15)	3 (27)	3 (33)	5 (20)	9 (9)	3 (17)	3 (27)
Q11	To what extent did that discussion take place?	Single department	41 (23)	0 (0)	1 (17)	5 (25)	30 (32)	3 (20)	2 (25)
		Multiple department	57 (32)	5 (63)	0 (0)	9 (45)	31 (33)	8 (53)	4 (50)
		All over hospital	44 (25)	3 (38)	5 (83)	5 (25)	25 (27)	4 (27)	2 (25)
		Others	7 (4)	0 (0)	0 (0)	1 (5)	6 (6)	0 (0)	0 (0)
Q12	Have the organ transplant surgeries in your hospital been stopped due to the COVID-19 pandemic?	Yes	85 (48)	0 (0)	0 (0)	1 (4)	80 (78)	4 (22)	0 (0)
		No	92 (52)	11 (100)	9 (100)	24 (96)	23 (22)	14 (78)	11 (100)
Q13	What was the reason for the decision to suspend the organ transplant surgeries? (Multiple answers allowed)	Presence of COVID-19-positive patients after transplantation in the hospital	0 (0)	N/A	N/A	0 (0)	0 (0)	0 (0)	N/A
		Presence of COVID-19-positive patients in the hospital	12 (7)	N/A	N/A	1 (100)	11 (14)	0 (0)	N/A
		Presence of COVID-19-positive patients in the area (prefecture)	26 (15)	N/A	N/A	0 (0)	26 (33)	0 (0)	N/A
		In-hospital medical care system or examination system inadequate for assessing COVID-19	34 (19)	N/A	N/A	1 (100)	33 (41)	0 (0)	N/A
		All surgical treatments restricted, including transplantation	33 (19)	N/A	N/A	1 (100)	30 (38)	2 (50)	N/A
		Following the guidelines of the Japan Society for Transplantation	57 (32)	N/A	N/A	0 (0)	54 (68)	3 (75)	N/A
		Others	16 (9)	N/A	N/A	0 (0)	15 (19)	1 (25)	N/A
Q14	What kind of organ transplants were suspended?	Both deceased donor transplants and living donor transplantation	56 (31)	N/A	N/A	1 (100)	51 (64)	4 (100)	N/A
		Only living donor transplantation	25 (14)	N/A	N/A	0 (0)	25 (31)	0 (0)	N/A
		Only high-risk transplantation including ABO incompatible cases	0 (0)	N/A	N/A	0 (0)	0 (0)	0 (0)	N/A
		Deceased donor transplantation	1 (1)	N/A	N/A	0 (0)	1 (1)	0 (0)	N/A
		Others	3 (2)	N/A	N/A	0 (0)	3 (4)	0 (0)	N/A

Table 2 (continued)

		Answer	Overall (%) $n=177$	Heart $n=11$	Lung $n=9$	Liver $n=25$	Kidney $n=103$	Pancreas $n=18$	Small intestine $n=11$
Q15	What was the reason for resuming the organ transplant surgeries? (Multiple answers allowed)	Reduction in numbers of COVID-19 infections in the hospital	9 (5)	N/A	N/A	0 (0)	8 (11)	1 (25)	N/A
		A lack of spread of COVID-19 infection confirmed in the hospital	11 (6)	N/A	N/A	1 (100)	8 (11)	2 (50)	N/A
		Reduction in numbers of COVID-19 infections in the local area	29 (16)	N/A	N/A	0 (0)	27 (36)	2 (50)	N/A
		Establishment of an in-hospital medical care system and examination system for COVID-19	51 (29)	N/A	N/A	1 (100)	48 (64)	2 (50)	N/A
		Restrictions on surgeries other than transplantation lifted	28 (16)	N/A	N/A	1 (100)	25 (33)	2 (50)	N/A
		Following the guidelines of the Japan Society for Transplantation	34 (19)	N/A	N/A	0 (0)	32 (43)	2 (50)	N/A
		Others	8 (4)	N/A	N/A	0 (0)	8 (11)	0 (0)	N/A
Q16	What kind of organ transplants are being performed if the program is ongoing?	Without any particular restrictions	112 (63)	11 (100)	6 (67)	14 (56)	66 (69)	9 (50)	6 (55)
		Limited to cases considering being difficult to postpone	34 (19)	0 (0)	1 (11)	9 (36)	15 (16)	5 (28)	4 (36)
		Others	18 (10)	0 (0)	1 (11)	2 (8)	10 (10)	4 (22)	1 (9)
Q17	If the COVID-19 epidemic expands more in the near future, how do you think that organ transplants be carried out in your hospital?	Without any particular restrictions	30 (17)	5 (45)	1 (11)	4 (16)	13 (14)	4 (22)	3 (27)
		Considering discontinuing their transplant surgeries depending on the presence of COVID-19 patients in the ICU	60 (34)	5 (45)	7 (78)	15 (60)	20 (21)	6 (33)	7 (64)
		Considering discontinuing their transplant surgeries depending on the presence of COVID-19 patients in the hospital	32 (18)	1 (9)	0 (0)	6 (24)	19 (20)	3 (17)	3 (27)
		Discontinue the transplant surgeries should nosocomial COVID-19 infection be observed	34 (19)	1 (9)	0 (0)	2 (8)	30 (31)	0 (0)	1 (9)
		Not decided, yet	24 (13)	2 (18)	1 (11)	2 (8)	15 (16)	4 (22)	0 (0)
		Others	23 (13)	0 (0)	0 (0)	3 (12)	16 (17)	4 (22)	0 (0)
Q18	Have you placed any restrictions on the dispatch of organ recovery from your center during the COVID-19 pandemic?	Yes	21 (12)	0 (0)	0 (0)	1 (4)	18 (17)	1 (6)	1 (9)
		No	148	11 (100)	9 (100)	22 (88)	79 (77)	17 (94)	10 (91)
Q19	Have you experienced any cases in which organ recovery was abandoned due to a COVID-19 infection?	Yes	14 (8)	3 (27)	0 (0)	0 (0)	8 (8)	3 (17)	0 (0)
		No	156 (88)	8 (73)	9 (100)	23 (92)	90 (87)	15 (83)	11 (100)

Table 2 (continued)

		Answer	Overall (%) $n=177$	Heart $n=11$	Lung $n=9$	Liver $n=25$	Kidney $n=103$	Pancreas $n=18$	Small intestine $n=11$
Q20	Have you experienced any cases in which organ transplantation was abandoned due to a COVID-19 infection even though organ recovery was possible?	Yes	12 (7)	1 (9)	1 (11)	0 (0)	9 (9)	1 (6)	0 (0)
		No	158 (89)	10 (91)	8 (89)	23 (92)	89 (86)	17 (94)	11 (100)
Q21	How do you handle patients who are candidates for organ transplantation during the COVID-19 pandemic? (Multiple answers allowed)	Be sure to perform chest CT	125 (70)	8 (73)	6 (67)	11 (44)	85 (83)	13 (72)	2 (18)
		Perform chest CT if the patient has some symptoms	16 (9)	1 (9)	0 (0)	5 (20)	3 (3)	3 (17)	4 (36)
		Be sure to screen for COVID-19 (PCR test, antigen test, etc.)	161 (90)	9 (82)	9 (100)	22 (88)	93 (90)	18 (100)	10 (91)
		Screen for COVID-19 (PCR test, antigen test, etc.), if there are chest CT findings or the patient has some symptoms	6 (3)	1 (9)	0 (0)	2 (8)	2 (2)	0 (0)	1 (9)
		Others	6 (3)	1 (9)	0 (0)	0 (0)	5 (5)	0 (0)	0 (0)
Q22	Have there been any changes in the post-transplant follow-up systems during the COVID-19 pandemic in your hospital?	No change	65 (37)	6 (55)	3 (33)	9 (36)	37 (36)	6 (33)	4 (36)
		The system has changed a little	80 (45)	5 (45)	6 (67)	11 (44)	45 (44)	9 (50)	4 (36)
		The system has changed considerably	29 (16)	0 (0)	0 (0)	5 (20)	18 (17)	3 (17)	3 (27)
		The system has all changed	3 (2)	0 (0)	0 (0)	0 (0)	3 (3)	0 (0)	0 (0)
Q23	If you answered "yes" to Q22, please explain how the post-transplant follow-up systems have changed. (Multiple answers allowed)	Outpatient visits for patients after transplantation were set to be performed at longer intervals	123 (69)	6 (100)	4 (80)	16 (76)	77 (94)	12 (92)	8 (89)
		Try to give more medicine than usual	66 (37)	4 (67)	3 (60)	9 (43)	44 (54)	4 (31)	2 (22)
		Examination are limited as much as possible	14 (8)	0 (0)	1 (20)	2 (10)	9 (11)	2 (15)	0 (0)
		Try to patients stay in the out-patients clinic as short as possible	51 (29)	2 (33)	3 (60)	5 (24)	35 (43)	4 (31)	2 (22)
		Try to make each other patients avoid contact	36 (20)	3 (50)	2 (40)	5 (24)	21 (26)	2 (15)	3 (33)
		Others	21 (12)	2 (33)	3 (60)	5 (24)	8 (10)	1 (8)	2 (22)

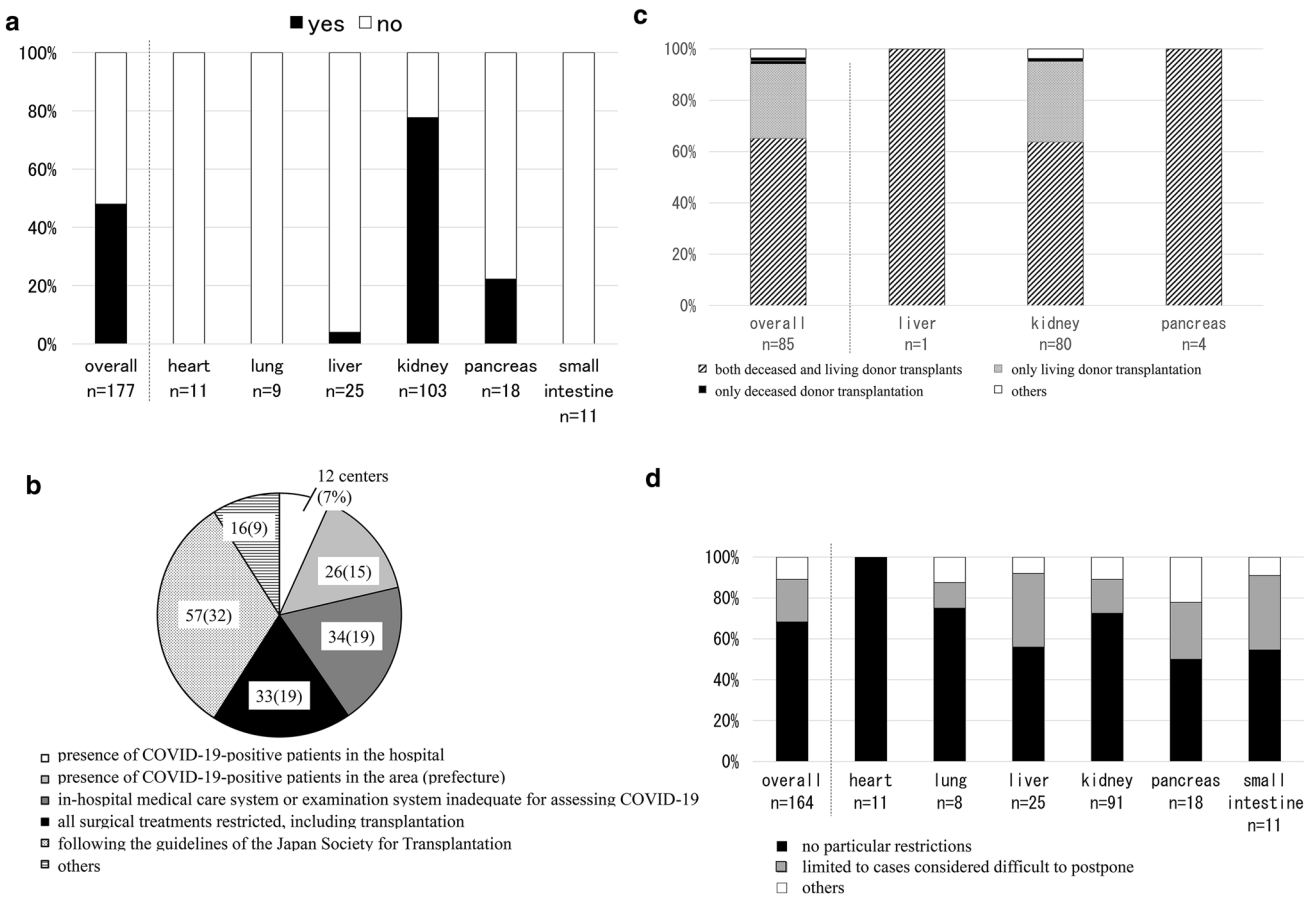

Fig. 4 Answers to questions about porting program continuation. Q12: Have organ transplant surgeries in your hospital been stopped due to the COVID-19 pandemic? (**a**), Q13: What was the reason for the decision to suspend organ transplant surgeries? (Multiple answers allowed) (**b**), Q14: What kind of organ transplants were suspended? (**c**), Q16: What kind of organ transplants are being performed if transplant surgery is ongoing? (**d**). Response summaries: Q12: While no center discontinued its transplant surgeries for heart and lung transplants, one center (4%) suspended its transplant surgeries for liver transplants, 80 (78%) suspended their transplant surgeries for kidney transplants, and 4 (22%) suspended their transplant surgeries for pancreas transplants (**a**). Q13: The reasons for discontinuing transplantation were as follows: COVID-19-positive patients in the hospital ($n=12$; 7%), COVID-19-positive patients in the prefecture ($n=26$; 15%), in-hospital medical care system or examination system inadequate for assessing COVID-19 ($n=34$; 19%), all surgical treatment (including transplantation) restricted ($n=33$; 19%), and suspended in accordance with guidelines of the Japan Society for Transplantation ($n=57$; 32%) (**b**). Q14: Fifty-six centers (31%) discontinued all transplants, including both deceased and living donor transplantation, 25 (14%) discontinued only living donor transplantation, and 1 (1%) discontinued only deceased donor transplantation (**c**). Q16: Of the centers with an ongoing transplant surgeries at the time of the questionnaire, 112 (63%) were providing transplant medical care without any specific restrictions, while 34 (19%) were limiting transplant surgery to cases when it was considered difficult to postpone (**d**)

some cases because of the COVID-19 pandemic. The present study confirmed that the COVID-19 pandemic has had a significantly negative impact on both organ donation and the performance of SOT.

In the United States, the number of patients registered as waiting for SOT and transplant surgery in April, 2020, was reported to have decreased in all United Network for Organ Sharing regions, and the mortality rate of these waiting patients had increased in more than half of the regions [34]. It was also reported that in March and April, 2020, when the COVID-19 pandemic began, the number of new wait-list patient enrollments, deceased-donor kidney transplants, and living-donor kidney transplants, fell below expectations by 18%, 24%, and 87%, respectively [35]. In Europe, the COVID-19 pandemic was reported to have had a similarly severe impact on transplant medical care, with the number of referrals of potential donors decreasing by 39% in the United Kingdom [36] and the number of potential deceased organ donors decreasing by 16% in comparison with previous years in France [37]. Conversely, in South Korea, (as in Japan), where the COVID-19 pandemic manifested relatively early with a less impact than in the United States and Europe, there was no significant change reported in the number of liver transplantations or kidney transplantations as of March and April, 2020 [38, 39], respectively, from the previous year, for both living donor transplants and BDD

transplants. These findings showed that the ability to perform organ transplantation is dependent on the severity of the spread of COVID-19 in a given country; however, as these reports relate to the situation in spring 2020, subsequent reports on the overall situation of organ transplantation in 2020 are awaited.

Unfortunately, during the severe COVID-19 pandemic at the present time, in many countries, including Japan, available medical resources are likely to be assigned to countermeasures against the COVID-19 pandemic, necessitating a reduction in transplantation activity. In several countries, newly developed vaccines are improving the impact of the COVID-19 pandemic [40–45], and facilitating the rebuilding of a normal lifestyle. It is thought that the acquisition of herd immunity through vaccination will improve the survival of patients with organ failure who are awaiting transplantation and promote transplant medical care.

The present study had several limitations. The overall response rate to the questionnaire was 86%, which may be considered relatively high; however, the response rate of the kidney transplant centers was approximately 80%, which is slightly low. The questionnaire survey in this study was conducted from December, 2020 to January, 2021, when the background of the COVID-19 pandemic in Japan was in a state of flux. In particular, the number of COVID-19-positive patients in the third wave increased rapidly, and from January 2021, a state of emergency was declared in some cities, including Tokyo. The movement of people was greatly restricted and the situation was changing, which may have affected organ recovery; thus, the answers to our questionnaire survey might have varied greatly depending on the time of the response. Furthermore, the number of living donor organ transplantations was not mentioned in this paper, as the effects of the COVID-19 pandemic on the state of living transplantation in Japan is being investigated in another study.

Conclusion

At the end of March, 2021, the number of patients infected with COVID-19 in the third wave of the pandemic began to decline. Although the COVID-19 pandemic in Japan is less severe than in other countries, it has had a large impact on the overall transplantation activity, suspending transplantation surgeries in 48% of the transplantation centers, including 78% of the kidney transplantation centers, and reducing the number of organ donations to 61% of the year-on-year average. This situation should be monitored closely.

Acknowledgements We like to thank the 177 transplant centers that responded to the questionnaire during the national COVID-19 pandemic crisis.

Funding This research was funded by Health, Labour and Welfare Policy Research Grants.

Declarations

Conflict of interest We have no conflicts of interest to declare in association with this study.

References

1. Soyama A, Eguchi S. The current status and future perspectives of organ donation in Japan: learning from the systems in other countries. Surg Today. 2016;46(4):387–92.
2. Soyama A, Eguchi S, Egawa H. Liver transplantation in Japan. Liver Transpl. 2016;22(10):1401–7.
3. Fukushima N, Ono M, Saito S, Saiki Y, Kubota S, Tanoue Y, et al. Heart donation in Japan before and after the revision of the Japanese Transplantation Act. Transpl Proc. 2014;46(6):2050–3.
4. Egawa H, Tanabe K, Fukushima N, Date H, Sugitani A, Haga H. Current status of organ transplantation in Japan. Am J Transpl. 2012;12(3):523–30.
5. Fukushima N, Ono M, Saiki Y, Sawa Y, Nunoda S, Isobe M. Registry report on heart transplantation in Japan (June 2016). Circ J. 2017;81(3):298–303.
6. Ito T, Kenmochi T, Aida N, Kurihara K, Tomimaru Y, Ito T. Impact of the revision of the law on pancreatic transplants in Japan—an analysis of the Japanese Pancreas Transplants Registry. J Hepatobiliary Pancreat Sci. 2021;28(4):353-64.
7. Liu X, Huang J, Li C, Zhao Y, Wang D, Huang Z, et al. The role of seasonality in the spread of COVID-19 pandemic. Environ Res. 2021;195:110874.
8. Gholizadeh P, Sanogo M, Oumarou A, Mohamed MN, Cissoko Y, Saliou Sow M, et al. Fighting COVID-19 in the West Africa after experiencing the Ebola epidemic. Health Promot Perspect. 2021;11(1):5–11.
9. Kliem F. ASEAN and the EU amidst COVID-19: overcoming the self-fulfilling prophecy of realism. Asia Eur J. 2021;13:1–19.
10. Chowell G, Mizumoto K. The COVID-19 pandemic in the USA: what might we expect? Lancet. 2020;395(10230):1093–4.
11. Novelli G, Biancolella M, Mehrian-Shai R, Erickson C, Godri Pollitt KJ, Vasiliou V, et al. COVID-19 update: the first 6 months of the pandemic. Hum Genom. 2020;14(1):48.
12. Furuse Y, Ko YK, Saito M, Shobugawa Y, Jindai K, Saito T, et al. Epidemiology of COVID-19 outbreak in Japan, from January-March 2020. Jpn J Infect Dis. 2020;73(5):391–3.
13. Amengual O, Atsumi T. COVID-19 pandemic in Japan. Rheumatol Int. 2021;41(1):1–5.
14. Hayakawa S, Komine-Aizawa S, Mor GG. COVID-19 pandemic and pregnancy. J Obstet Gynaecol Res. 2020;46(10):1958–66.

15. Mori M, Ikeda N, Taketomi A, Asahi Y, Takesue Y, Orimo T, et al. COVID-19: clinical issues from the Japan Surgical Society. Surg Today. 2020;50(8):794–808.
16. Suka M, Yamauchi T, Yanagisawa H. Changes in health status, workload, and lifestyle after starting the COVID-19 pandemic: a web-based survey of Japanese men and women. Environ Health Prev Med. 2021;26(1):37.
17. Fava A, Cucchiari D, Montero N, Toapanta N, Centellas FJ, Vila-Santandreu A, et al. Clinical characteristics and risk factors for severe COVID-19 in hospitalized kidney transplant recipients: a multicentric cohort study. Am J Transpl. 2020;20(11):3030–41.
18. Sanchez-Alvarez JE, Perez Fontan M, Jimenez Martin C, Blasco Pelicano M, Cabezas Reina CJ, Sevillano Prieto AM, et al. SARS-CoV-2 infection in patients on renal replacement therapy Report of the COVID-19. Registry of the Spanish Society of Nephrology (SEN). Nefrologia. 2020;40(3):272–8.
19. Cravedi P, Suraj SM, Azzi Y, Haverly M, Farouk S, Perez-Saez MJ, et al. COVID-19 and kidney transplantation: results from the TANGO International Transplant Consortium. Am J Transpl. 2020;20(11):3140-8.
20. Alberici F, Delbarba E, Manenti C, Econimo L, Valerio F, Pola A, et al. A report from the Brescia Renal COVID Task Force on the clinical characteristics and short-term outcome of hemodialysis patients with SARS-CoV-2 infection. Kidney Int. 2020;98(1):20–6.
21. Tortonese S, Scriabine I, Anjou L, Loens C, Michon A, Benabdelhak M, et al. COVID-19 in patients on maintenance dialysis in the Paris region. Kidney Int Rep. 2020;5(9):1535–44.
22. Keller N, Chantrel F, Krummel T, Bazin-Kara D, Faller AL, Muller C, et al. Impact of first-wave COronaVIrus disease 2019 infection in patients on haemoDIALysis in Alsace: the observational COVIDIAL study. Nephrol Dial Transpl. 2020;35(8):1338–411.
23. Corbett RW, Blakey S, Nitsch D, Loucaidou M, McLean A, Duncan N, et al. Epidemiology of COVID-19 in an Urban Dialysis Center. J Am Soc Nephrol. 2020;31(8):1815–23.
24. Valeri AM, Robbins-Juarez SY, Stevens JS, Ahn W, Rao MK, Radhakrishnan J, et al. Presentation and outcomes of patients with ESKD and COVID-19. J Am Soc Nephrol. 2020;31(7):1409–15.
25. Ng JH, Hirsch JS, Wanchoo R, Sachdeva M, Sakhiya V, Hong S, et al. Outcomes of patients with end-stage kidney disease hospitalized with COVID-19. Kidney Int. 2020;98(6):1530–9.
26. Caillard S, Anglicheau D, Matignon M, Durrbach A, Greze C, Frimat L, et al. An initial report from the French SOT COVID Registry suggests high mortality due to COVID-19 in recipients of kidney transplants. Kidney Int. 2020;98(6):1549–58.
27. Webb GJ, Marjot T, Cook JA, Aloman C, Armstrong MJ, Brenner EJ, et al. Outcomes following SARS-CoV-2 infection in liver transplant recipients: an international registry study. Lancet Gastroenterol Hepatol. 2020;5(11):1008–16.
28. Colmenero J, Rodriguez-Peralvarez M, Salcedo M, Arias-Milla A, Munoz-Serrano A, Graus J, et al. Epidemiological pattern, incidence, and outcomes of COVID-19 in liver transplant patients. J Hepatol. 2021;74(1):148–55.
29. Ketcham SW, Adie SK, Malliett A, Abdul-Aziz AA, Bitar A, Grafton G, et al. Coronavirus disease-2019 in heart transplant recipients in Southeastern Michigan: a case series. J Card Fail. 2020;26(6):457–61.
30. Rivinius R, Kaya Z, Schramm R, Boeken U, Provaznik Z, Heim C, et al. COVID-19 among heart transplant recipients in Germany: a multicenter survey. Clin Res Cardiol. 2020;109(12):1531–9.
31. Iacovoni A, Boffini M, Pidello S, Simonato E, Barbero C, Sebastiani R, et al. A case series of novel coronavirus infection in heart transplantation from 2 centers in the pandemic area in the North of Italy. J Heart Lung Transpl. 2020;39(10):1081–8.
32. Aversa M, Benvenuto L, Anderson M, Shah L, Robbins H, Pereira M, et al. COVID-19 in lung transplant recipients: a single center case series from New York City. Am J Transpl. 2020;20(11):3072–80.
33. Ortiz-Brizuela E, Leal-Vega F, Cuellar-Rodriguez J, Bobadilla-Del-Valle M, Ponce-de-Leon A. Vaccine-derived varicella zoster infection in a kidney transplant recipient after zoster vaccine live administration. Vaccine. 2019;37(27):3576–9.
34. Cholankeril G, Podboy A, Alshuwaykh OS, Kim D, Kanwal F, Esquivel CO, et al. Early impact of COVID-19 on solid organ transplantation in the United States. Transplantation. 2020;104(11):2221–4.
35. Boyarsky BJ, Werbel WA, Durand CM, Avery RK, Jackson KR, Kernodle AB, et al. Early national and center-level changes to kidney transplantation in the United States during the COVID-19 epidemic. Am J Transpl. 2020;20(11):3131–9.
36. Manara AR, Mumford L, Callaghan CJ, Ravanan R, Gardiner D. Donation and transplantation activity in the UK during the COVID-19 lockdown. Lancet. 2020;396(10249):465–6.
37. Legeai C, Malaquin G, Lamotte C, Antoine C, Averland B, Jasseron C, et al. Impact of coronavirus disease 2019 on organ donation and transplantation in France. Transpl Int. 2021;34(1):204–6.
38. Lee JM. Effect of COVID-19 on liver transplantation in Korea. Transpl Infect Dis. 2020;22(5):e13384.
39. Lee J, Huh KH. Kidney transplantation trends in South Korea during the COVID-19 pandemic. Kidney Int. 2020;98(2):512–3.
40. Hall VJ, Foulkes S, Saei A, Andrews N, Oguti B, Charlett A, et al. COVID-19 vaccine coverage in health-care workers in England and effectiveness of BNT162b2 mRNA vaccine against infection (SIREN): a prospective, multicentre, cohort study. Lancet. 2021;397(10286):1725–35.
41. Abu-Raddad LJ, Chemaitelly H, Yassine HM, Benslimane FM, Al Khatib HA, Tang P, et al. Pfizer-BioNTech mRNA BNT162b2 COVID-19 vaccine protection against variants of concern after one versus two doses. J Travel Med. 2021. https://doi.org/10.1093/jtm/taab083.
42. Voysey M, Costa Clemens SA, Madhi SA, Weckx LY, Folegatti PM, Aleyet PK, et al. Single-dose administration and the influence of the timing of the booster dose on immunogenicity and efficacy of ChAdOx1 nCoV-19 (AZD1222) vaccine: a pooled analysis of four randomised trials. Lancet. 2021;397(10277):881–91.
43. Abu-Raddad LJ, Chemaitelly H, Butt AA. Effectiveness of the BNT162b2 COVID-19 vaccine against the B.1.1.7 and B.1.351 variants. N Engl J Med. 2021;385(2):187–9.
44. Baden LR, El Sahly HM, Essink B, Kotloff K, Frey S, Novak R, et al. Efficacy and safety of the mRNA-1273 SARS-CoV-2 vaccine. N Engl J Med. 2021;384(5):403–16.
45. Chemaitelly H, Yassine HM, Benslimane FM, Al Khatib HA, Tang P, Hasan MR, et al. mRNA-1273 COVID-19 vaccine effectiveness against the B.1.1.7 and B.1.351 variants and severe COVID-19 disease in Qatar. Nat Med. 2021. https://doi.org/10.1038/s41591-021-01446-y.

Surgery Today (2022) 52:763–773
https://doi.org/10.1007/s00595-021-02388-1

ORIGINAL ARTICLE

National survey on deceased donor organ transplantation during the COVID-19 pandemic in Japan

Taihei Ito[1] · Takashi Kenmochi[1] · Atsuhiko Ota[2] · Kaori Kuramitsu[3] · Akihiko Soyama[4] · Osamu Kinoshita[5] · Susumu Eguchi[4] · Kenji Yuzawa[6] · Hiroto Egawa[7]

Received: 9 June 2021 / Accepted: 11 August 2021 / Published online: 23 October 2021

Abstract

Purpose We investigated the status of deceased organ donation and transplantation through a questionnaire distributed to transplant centers in Japan during the COVID-19 pandemic.

Methods The questionnaire was distributed electronically to 206 transplant centers for heart ($n=11$), lung ($n=10$), liver ($n=25$), kidney ($n=130$), pancreas ($n=18$), and small intestine ($n=12$) transplantation. Organ donations and organ transplantation data were extracted from the Japan Organ Transplant Network website.

Results We received questionnaire responses from 177 centers (response rate, 86%). In 2020, the number of brain-dead donors (BDDs) decreased to 68 (69% of the year-on-year average) and the number of donors after cardiac death (DCDs) decreased to 9 (32% of the year-on-year average). Eighty-five (48%) transplant centers (heart, $n=0$; lung, $n=0$; liver, $n=4$; kidney, $n=78$; pancreas, $n=22$; and small intestine, $n=0$) suspended transplant surgeries in response to the COVID-19 pandemic. Consequently, the number of organ transplantations from deceased donors was significantly lower in 2020 than in 2019.

Conclusion Although the COVID-19 pandemic has had less impact in Japan than in other countries, it has affected transplantation activity significantly, suspending transplantation surgeries in 48% of the transplantation centers, including 78% of the kidney transplantation centers, and reducing the number of organ donations to 61% of the year-on-year average.

Keywords COVID-19 · Brain-dead donors · Donors after cardiac death · Solid organ transplantation

✉ Taihei Ito
i-taihei@fujita-hu.ac.jp

1 Department of Transplantation and Regenerative Medicine, Fujita Health University, School of Medicine, Dengakugakubo 1-98, Kutsukakecho, Toyoake, Aichi 470-1192, Japan

2 Department of Public Health, Fujita Health University School of Medicine, Toyoake, Aichi, Japan

3 Division of Hepato-Biliary-Pancreatic Surgery, Kobe University Graduate School of Medicine, Kobe, Hyogo, Japan

4 Department of Surgery, Nagasaki University Graduate School of Biomedical Sciences, Nagasaki, Nagasaki, Japan

5 Department of Cardiac Surgery, Graduate School of Medicine, The University of Tokyo, Bunkyo, Tokyo, Japan

6 Department of Transplantation Surgery, National Hospital Organization Mito Medical Center, Mito, Ibaraki, Japan

7 Department of Surgery, Institute of Gastroenterology, Tokyo Women's Medical University, Shinjuku, Tokyo, Japan

Introduction

In the first 10 years after the establishment of the Brain Death Organ Transplant Act in 1997, the annual number of brain-dead donors (BDDs) in Japan was less than 10. This low number at the time was attributed to the fact that brain death referred only to human death in cases of donation for organ transplantation, and brain-dead donors (BDDs) were required to have made their intention clear before brain death. The law was revised in 2009 to state that even if the donor's intention to donate organs was unknown, organ donation from BDDs was able to be approved with the consent of the family. The law was enforced in 2010, resulting in increased numbers of organ donations from BDDs [1]. This had a positive impact on patients awaiting solid organ transplantation (SOT) for organ failure [2–6].

The COVID-19 pandemic has ravaged the globe since early 2020 [7–11]. While the numbers of patients with COVID-19 and related deaths in Japan have been relatively

low in comparison with other countries [12, 13], the treatment of COVID-19 patients in emergency medical care and the intensive-care unit (ICU) has been difficult, raising concern about the decline of general medical practices [14–16].

In transplant medical care, essential immunosuppressive therapy after transplantation has a negative impact on mortality from this new viral infection. The COVID-19-related mortality rate in SOT recipients has been reported to range from 18 to 34% [17–19]. Moreover, COVID-19 is a serious life-threatening infectious disease for individuals with organ failure who are awaiting transplantation, and the decline in transplant activity also impacts the prognosis of these patients. For example, the COVID-19-related mortality rate in patients awaiting kidney transplantation who required dialysis was reported to range from 20 to 32% [18, 20–32].

In response to the impact of the COVID-19 pandemic on transplant activity, on March 6, 2020, the Japan Society for Transplantation published the first edition of the basic guidelines for transplantation medicine for new coronavirus infection (COVID-19). The guidelines have been updated according to the outbreak situation in Japan, with the latest edition, version 4.1 released on February 4, 2021 [33]. In the first edition, the recommendation for the implementation of SOT was as follows: "If possible, waiting for organ transplantation until the situation of the COVID-19 pandemic improves is recommended in order to avoid the risk of infection from donors or community-acquired infection under immunosuppression after transplantation". However, the recommendation in the latest version (version 4.1) is as follows: "In the implementation of solid organ transplantation, the risk of the COVID-19 infection from the donor and the risk of the aggravation of COVID-19 infection under immunosuppression after transplantation must be properly explained to obtain sufficient informed consent about…". Thus, although the COVID-19 pandemic may influence organ donation and transplant activity in Japan remarkably, no report has clarified the real situation.

We investigated the status of deceased organ donation and organ transplantation in Japan during the COVID-19 pandemic, using a questionnaire that was distributed to transplant centers, to clarify the current status of transplantation activity in Japan during the COVID-19 pandemic.

Methods

A questionnaire survey was conducted as part of a welfare and labor science special research project entitled, "Survey research for organ transplantation from BDDs and donors after cardiac death (DCDs) during the pandemic of COVID-19". The questionnaire, including 23 questions on the medical system, the SOT policy, and the implementation status in each center during the COVID-19 pandemic, was distributed electronically to 206 transplant centers in Japan (heart centers, $n=11$; lung centers, $n=10$; liver centers, $n=25$; kidney centers, $n=130$; pancreas centers, $n=18$; and small-intestine centers, $n=12$) from December, 2020 to January, 2021 during the third wave of the COVID-19 pandemic, with the development of a website entrusted to Tokai Kyodo Printing. The representatives of each center registered their answers. The numbers of deceased organ donations and SOTs were counted by searching the Japan Organ Transplant Network website (https://www.jotnw.or.jp/). The number of COVID-19-positive patients in Japan was estimated based on announcements made by the Ministry of Health, Labor and Welfare (https://www.mhlw.go.jp/stf/covid-19/kokunainohasseijoukyou.html).

The Microsoft Excel software program (Microsoft, USA) was used to summarize the data. Categorical data are shown as frequencies and percentages.

Results

Changes in the number of COVID-19-positive patients and organ donations in Japan

Figure 1 shows the changes in the number of BDDs and DCDs in Japan. In 1997, the law on organ transplantation was enacted, with organ donations from BDDs (black solid bars) implemented. Despite this legislation, there was no marked increase in organ donations from BDDs. The law was revised in 2009 and enforced in 2010, after which the number of brain-dead organ donations began to steadily increase, reaching a record high of 98 in 2019. In contrast, the number of DCDs (white solid bars) has decreased since the revision of the law, to about 30 in recent years. In early 2020, the first cases of COVID-19 were detected in Japan, and in 2020, the number of BDDs and DCDs decreased to 68 and 9, respectively.

Figure 2 shows the changes in the number of COVID-19-positive patients (gray solid bar) and the monthly number of organ donations (BDDs, black solid bars; DCDs, white solid bars) from January, 2020. The first case of COVID-19 in Japan was confirmed in February, 2020, with the number peaking in April, 2020 in the first wave of the COVID-19 pandemic. This was followed by a second wave in August, 2020, and a third wave in February, 2021. By the time of writing, at the end of March 2021, the third wave had begun to converge. By March 20, 2021, the total number of COVID-19 positive patients in Japan had reached 451,830, with 8788 COVID-19-related deaths.

In contrast, the number of BDDs at the beginning of 2020 did not decrease significantly from that in 2019. However, since the autumn of 2020, when the third wave of the COVID-19 pandemic started, the number of organ donations

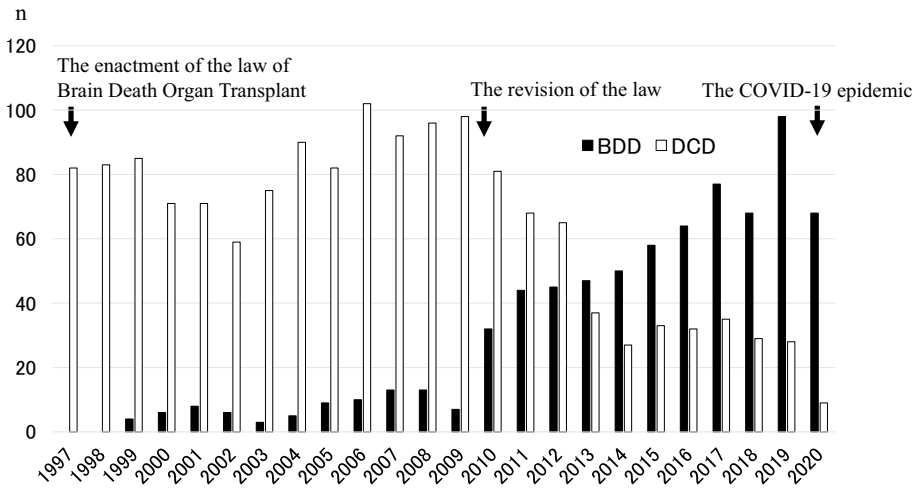

Fig. 1 Annual numbers of deceased organ donations in Japan. Organ donations from brain-dead donors (BDDs) (black solid bars) began in 1997, when the law on organ transplantation was enacted. When the law was revised in 2009, the number of brain-dead organ donations increased steadily, reaching a record high of 98 cases in 2019. In contrast, the number of donors after cardiac death (DCDs) (white solid bars) has decreased since the revision of the law, falling to approximately 30 in recent years. In 2020, after detection of the first COVID-19-positive patients in Japan, the number of BDDs and DCDs decreased to 68 and 9, respectively

has decreased, with no organ donations in December, 2020. It is noteworthy that the number of DCDs, which require a long waiting period for transplant doctors, has dropped significantly since early 2020, to only nine cases in 2020. This represents the first single-digit figure in the records, and highlights the significant impact of the COVID-19 pandemic on organ donation in Japan (Fig. 2).

As a result, the annual number of SOTs from deceased donors decreased significantly in 2020 compared with the number in 2019, with the exception of small-intestine transplants (Fig. 3). There were 84 cases of heart transplantation in 2019 vs. 54 in 2020 (64% of the year-on-year average) and 79 cases of lung transplantation in 2019 vs. 58 in 2020 (73% of the year-on-year average). Regarding abdominal organ transplantation, there were 88 cases of liver transplantation in 2019 vs. 63 in 2020 (72% of the year-on-year average) and 176 cases of kidney transplantation, including 46 cases of simultaneous pancreas transplantation (SPK) and 6 cases of simultaneous liver transplantation (SLK), in 2019 vs. 124 in 2020 (SPK, $n=24$; SLK, $n=5$; 71% of the

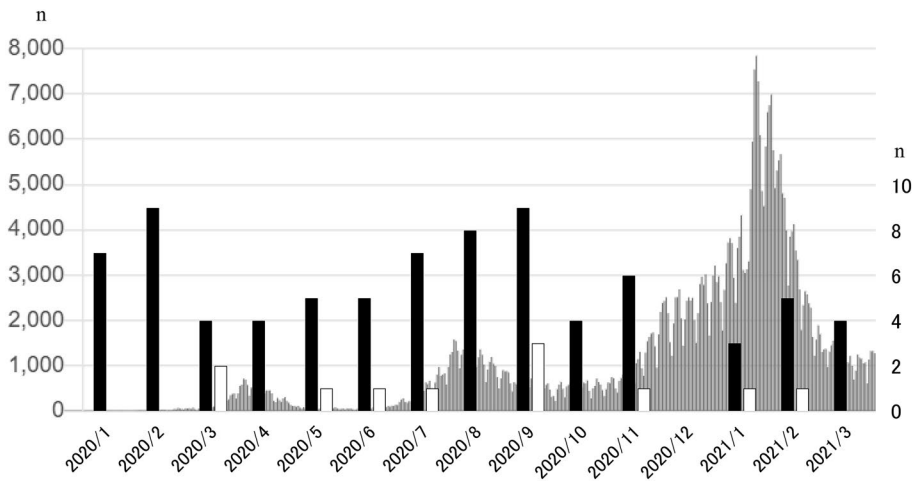

Fig. 2 Numbers of COVID-19-positive patients and deceased donors in 2020. The change in the number of COVID-19-positive patients is displayed as solid gray bars, and the monthly numbers of organ donations from BDDs and DCDs since January 2020 are shown as solid black bars and solid white bars, respectively. Since the autumn of 2020, when the third wave of the COVID-19 pandemic started, the number of organ donations has decreased. In December 2020, there were no organ donations. It is noteworthy that the number of DCDs, which require a long waiting period for transplant doctors, has dropped significantly since early 2020

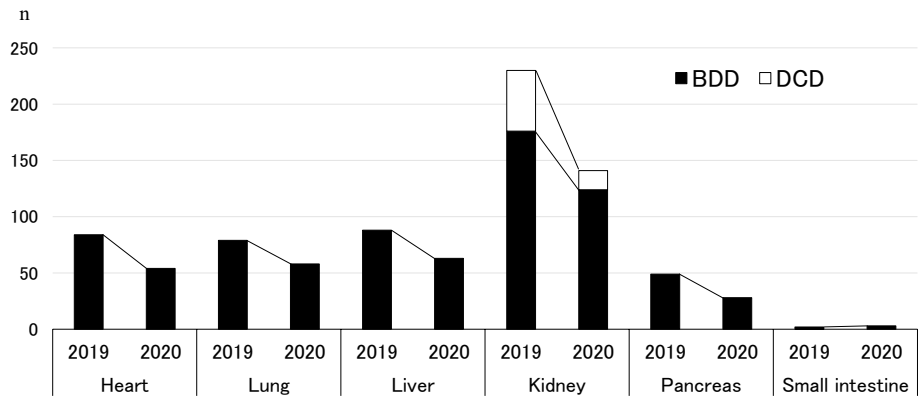

Fig. 3 Annual numbers of transplantations from deceased donors in 2019 and 2020 in Japan. There were 84 cases of heart transplantation in 2019 vs. 54 in 2020 (64% of the year-on-year average) and 79 cases of lung transplantation in 2019 vs. 58 in 2020 (73% of the year-on-year average). For abdominal organ transplantation, there were 88 cases of liver transplantation in 2019 vs. 63 in 2020 (72% of the year-on-year average) and 176 cases of kidney transplantation, including 46 of simultaneous pancreas transplantation (SPK) and 6 of simultaneous liver transplantation (SLK), in 2019 vs. 124 (SPK, $n=24$; SLK, $n=5$; 71% of the year-on-year average) in 2020. Pancreas transplants also decreased from 49 cases in 2019 to 28 in 2020 (57% of the year-on-year average). Small-intestine transplants increased slightly from two cases in 2019 to three in 2020

year-on-year average). Pancreas transplants also decreased from 49 cases in 2019 to 28 in 2020 (57% of the year-on-year average), whereas small-intestine transplants increased slightly from 2 cases in 2019 to 3 in 2020.

Current status of transplant medical care at transplant centers in Japan

We received questionnaire responses from 177 of the 206 centers, representing a response rate of 86% (heart centers, 100%; lung centers, 90%; liver centers, 100%; kidney centers, 79%; pancreas centers, 100%; small-intestine centers, 92%).

Table 1 summarizes the medical care for COVID-19 (other than transplants) that was provided in transplant centers. Among the responding centers, 98 (55%) were designated hospitals for infection (Q1), and 155 (88%), including those other than designated hospitals for infection, had wards dedicated to the treatment of COVID-19-positive patients (Q3). ICUs were set up in-hospital at 172 centers (97%) (Q4), and patients with severe COVID-19 sequelae were treated in the ICU at 144 centers (81%) (Q5). Regarding in-hospital tests for COVID-19, PCR testing was performed at 169 centers (95%) (Q6), antigen tests were performed at 151 centers (85%) (Q7), and antibody tests were performed at 90 centers (51%) (Q8). A total of 161 centers (90%) had established rules on surgical treatment (including surgery other than transplantation) during the COVID-19 pandemic (Q9).

Table 2 summarizes the results of the questionnaire on the status of transplant programs at transplant centers in Japan during the COVID-19 pandemic. Regarding the continuation of providing transplant medical care, following discussions held at 151 centers (85%) (Q10), 85 centers (48%) suspended transplant medical care because of the COVID-19 pandemic (Q12). While no center discontinued its transplant surgery for heart and lung transplants, one center (4%) suspended liver transplants, 80 (78%) suspended kidney transplants, and 4 (22%) suspended pancreas transplants (Fig. 4a). In 41 centers (23%), this discussion involved a single department, in 57 (32%) it involved multiple departments concerned with SOT, and in 44 (25%) it involved the whole hospital (Q11). The reasons for suspending transplant surgeries (Q13) were as follows: there were COVID-19-positive patients in the hospital ($n=12$; 7%), there were COVID-19-positive patients in the prefecture ($n=26$; 15%), the in-hospital medical care system or examination system was inadequate for assessing COVID-19 ($n=34$; 19%), all surgical treatment (including transplantation) was restricted ($n=33$; 19%), and transplant surgery was suspended in accordance with the guidelines of the Japan Society for Transplantation ($n=57$; 32%) (Fig. 4b). Fifty-six centers (31%) suspended all transplants, including both deceased and living donor transplantation, 25 (14%) suspended only living donor transplantation, and 1 (1%) suspended only deceased donor transplantation (Fig. 4c) (Q14).

During the period of the questionnaire (December, 2020–January, 2021), transplant surgery was still suspended at seven centers (4%), all of which were kidney transplant programs. The reasons for resuming transplant surgeries (Q15) were as follows: reduction in the number of COVID-19 infections at the hospital ($n=9$; 5%), lack of spread of COVID-19 infection confirmed in the hospital ($n=11$; 6%), reduction in the number of COVID-19 infections in the local area ($n=29$; 16%), establishment of an in-hospital medical

Table 1 Medical care for COVID-19 in transplant centers

		Answer	Overall (%) $n=177$	Heart $n=11$	Lung $n=9$	Liver $n=25$	Kidney $n=103$	Pancreas $n=18$	Small intestine $n=11$
Q1	Is your center an infectious disease designated hospital?	Yes	98 (55)	2 (18)	6 (67)	18 (72)	52 (50)	12 (67)	8 (73)
		No	79 (45)	9 (82)	3 (33)	7 (28)	51 (50)	6 (33)	3 (27)
Q2	Do you have a special outpatient clinic that provides care for patients with fever in your hospital?	Yes	127 (72)	5 (45)	6 (67)	18 (72)	79 (77)	12 (67)	7 (64)
		No	49 (28)	6 (55)	3 (33)	7 (28)	23 (22)	6 (33)	4 (36)
Q3	Do you have a ward dedicated to treating COVID-19 infected patients in your hospital?	Yes	155 (88)	11 (100)	9 (100)	20 (80)	90 (87)	17 (94)	8 (73)
		No	22 (12)	0 (0)	0 (0)	5 (20)	13 (13)	1 (6)	3 (27)
Q4	Do you have an ICU in your hospital?	Yes	172 (97)	11 (100)	9 (100)	25 (100)	98 (95)	18 (100)	11 (100)
		No	5 (3)	0 (0)	0 (0)	0 (0)	5 (5)	0 (0)	0 (0)
Q5	Does the ICU accept treatment for patients infected with COVID-19?	Yes	144 (81)	11 (100)	9 (100)	23 (92)	76 (74)	15 (83)	10 (91)
		No	32 (19)	0 (0)	0 (0)	2 (8)	26 (25)	3 (17)	1 (9)
Q6	Is it possible to perform PCR tests in-hospital for COVID-19 in your center?	Yes	169 (95)	11 (100)	9 (100)	25 (100)	95 (92)	18 (100)	11 (100)
		No	7 (4)	0 (0)	0 (0)	0 (0)	7 (7)	0 (0)	0 (0)
Q7	Is it possible to perform antigen tests in-hospital for COVID-19 in your center?	Yes	151 (85)	9 (82)	8 (89)	20 (80)	90 (87)	16 (89)	8 (73)
		No	21 (12)	0 (0)	1 (11)	3 (12)	13 (13)	2 (11)	2 (18)
Q8	Is it possible to perform antibody tests in-hospital for COVID-19 in your center?	Yes	90 (51)	8 (73)	6 (67)	14 (56)	46 (45)	10 (56)	6 (55)
		No	78 (44)	2 (18)	3 (33)	9 (36)	54 (52)	7 (39)	3 (27)
Q9	Do you have any rules related to COVID-19 concerning the performance of surgical treatment (including surgery other than transplantation) in your center?	Yes	161 (90)	9 (82)	9 (100)	23 (92)	94 (91)	17 (94)	9 (82)
		No	12 (7)	0 (0)	0 (0)	1 (4)	8 (8)	1 (6)	2 (18)

care system and testing for COVID-19 ($n=51$; 29%), restrictions on surgeries other than transplantation ($n=28$; 16%), and surgeries re-established in accordance with the guidelines of the Japan Society for Transplantation ($n=34$; 19%).

Of the centers with ongoing transplant surgery at the time of the questionnaire, 112 (63%) were providing transplant medical care without special restrictions, while 34 (19%) were limiting transplant surgery to cases considered difficult to postpone (Fig. 4d) (Q16). Depending on the future spread of the COVID-19 pandemic, only 30 centers (17%) answered that they would continue to provide transplant medical care without any restrictions, while 92 (52%) answered that they would consider suspending their transplant surgeries depending on the presence of COVID-19 in the ICU or hospital. Thirty-four centers answered that they would discontinue transplant surgeries in the event of nosocomial COVID-19 infection (Q17).

During the COVID-19 pandemic, 21 centers (12%) answered that they had been restricted from dispatching to organ recovery (Q18), and 14 centers (8%) answered that they had abandoned organ recovery efforts because of the COVID-19 pandemic (Q19). Even when organ recovery was possible, 12 centers (7%) reported that they had abandoned transplant surgery because of the COVID-19 pandemic (Q20).

Before any transplant surgery, 161 institutions (90%) performed a preoperative COVID-19 screening test of SOT recipients (Q21). A total of 112 centers (63%) answered that the post-transplant follow-up systems had changed in accordance with the COVID-19 pandemic (Q22), and most (123 centers, 69%) answered that follow-up outpatient visits after transplantation were set at longer intervals (Q23).

Discussion

The findings of this study confirmed that the COVID-19 pandemic reduced the number of organ donations, especially from DCDs. In Japan, organ donation from DCDs was performed without the withdrawal of life-support including respiration, which sometimes forces the organ recovery team to wait a long time in the donor's hospital. This was considered why DCDs were so markedly reduced by the COVID-19 pandemic. Our questionnaire survey revealed the organ donation situation in Japan. In addition to a reduction in the number of organ donations, half of the transplant centers suspended transplant surgery, particularly abdominal organ transplant surgeries, because of the COVID-19 pandemic. While transplant surgeries were resuming in most institutions when the questionnaire was distributed, approximately 20% of the transplant centers limited SOT surgery to those patients whose prognosis would have been severely affected by postponing surgery, and about 10% of centers indicated that it was necessary to abandon organ recovery or SOT in

Table 2 Results of the questionnaire on the status of transplant programs

		Answer	Overall (%) $n=177$	Heart $n=11$	Lung $n=9$	Liver $n=25$	Kidney $n=103$	Pancreas $n=18$	Small intestine $n=11$
Q10	Have you ever discussed the continuation of the transplant surgeries in the hospital during the COVID-19 pandemic?	Yes	151 (85)	8 (73)	6 (67)	20 (80)	94 (91)	15 (83)	8 (73)
		No	26 (15)	3 (27)	3 (33)	5 (20)	9 (9)	3 (17)	3 (27)
Q11	To what extent did that discussion take place?	Single department	41 (23)	0 (0)	1 (17)	5 (25)	30 (32)	3 (20)	2 (25)
		Multiple department	57 (32)	5 (63)	0 (0)	9 (45)	31 (33)	8 (53)	4 (50)
		All over hospital	44 (25)	3 (38)	5 (83)	5 (25)	25 (27)	4 (27)	2 (25)
		Others	7 (4)	0 (0)	0 (0)	1 (5)	6 (6)	0 (0)	0 (0)
Q12	Have the organ transplant surgeries in your hospital been stopped due to the COVID-19 pandemic?	Yes	85 (48)	0 (0)	0 (0)	1 (4)	80 (78)	4 (22)	0 (0)
		No	92 (52)	11 (100)	9 (100)	24 (96)	23 (22)	14 (78)	11 (100)
Q13	What was the reason for the decision to suspend the organ transplant surgeries? (Multiple answers allowed)	Presence of COVID-19-positive patients after transplantation in the hospital	0 (0)	N/A	N/A	0 (0)	0 (0)	0 (0)	N/A
		Presence of COVID-19-positive patients in the hospital	12 (7)	N/A	N/A	1 (100)	11 (14)	0 (0)	N/A
		Presence of COVID-19-positive patients in the area (prefecture)	26 (15)	N/A	N/A	0 (0)	26 (33)	0 (0)	N/A
		In-hospital medical care system or examination system inadequate for assessing COVID-19	34 (19)	N/A	N/A	1 (100)	33 (41)	0 (0)	N/A
		All surgical treatments restricted, including transplantation	33 (19)	N/A	N/A	1 (100)	30 (38)	2 (50)	N/A
		Following the guidelines of the Japan Society for Transplantation	57 (32)	N/A	N/A	0 (0)	54 (68)	3 (75)	N/A
		Others	16 (9)	N/A	N/A	0 (0)	15 (19)	1 (25)	N/A
Q14	What kind of organ transplants were suspended?	Both deceased donor transplants and living donor transplantation	56 (31)	N/A	N/A	1 (100)	51 (64)	4 (100)	N/A
		Only living donor transplantation	25 (14)	N/A	N/A	0 (0)	25 (31)	0 (0)	N/A
		Only high-risk transplantation including ABO incompatible cases	0 (0)	N/A	N/A	0 (0)	0 (0)	0 (0)	N/A
		Deceased donor transplantation	1 (1)	N/A	N/A	0 (0)	1 (1)	0 (0)	N/A
		Others	3 (2)	N/A	N/A	0 (0)	3 (4)	0 (0)	N/A

Table 2 (continued)

		Answer	Overall (%) $n=177$	Heart $n=11$	Lung $n=9$	Liver $n=25$	Kidney $n=103$	Pancreas $n=18$	Small intestine $n=11$
Q15	What was the reason for resuming the organ transplant surgeries? (Multiple answers allowed)	Reduction in numbers of COVID-19 infections in the hospital	9 (5)	N/A	N/A	0 (0)	8 (11)	1 (25)	N/A
		A lack of spread of COVID-19 infection confirmed in the hospital	11 (6)	N/A	N/A	1 (100)	8 (11)	2 (50)	N/A
		Reduction in numbers of COVID-19 infections in the local area	29 (16)	N/A	N/A	0 (0)	27 (36)	2 (50)	N/A
		Establishment of an in-hospital medical care system and examination system for COVID-19	51 (29)	N/A	N/A	1 (100)	48 (64)	2 (50)	N/A
		Restrictions on surgeries other than transplantation lifted	28 (16)	N/A	N/A	1 (100)	25 (33)	2 (50)	N/A
		Following the guidelines of the Japan Society for Transplantation	34 (19)	N/A	N/A	0 (0)	32 (43)	2 (50)	N/A
		Others	8 (4)	N/A	N/A	0 (0)	8 (11)	0 (0)	N/A
Q16	What kind of organ transplants are being performed if the program is ongoing?	Without any particular restrictions	112 (63)	11 (100)	6 (67)	14 (56)	66 (69)	9 (50)	6 (55)
		Limited to cases considering being difficult to postpone	34 (19)	0 (0)	1 (11)	9 (36)	15 (16)	5 (28)	4 (36)
		Others	18 (10)	0 (0)	1 (11)	2 (8)	10 (10)	4 (22)	1 (9)
Q17	If the COVID-19 epidemic expands more in the near future, how do you think that organ transplants be carried out in your hospital?	Without any particular restrictions	30 (17)	5 (45)	1 (11)	4 (16)	13 (14)	4 (22)	3 (27)
		Considering discontinuing their transplant surgeries depending on the presence of COVID-19 patients in the ICU	60 (34)	5 (45)	7 (78)	15 (60)	20 (21)	6 (33)	7 (64)
		Considering discontinuing their transplant surgeries depending on the presence of COVID-19 patients in the hospital	32 (18)	1 (9)	0 (0)	6 (24)	19 (20)	3 (17)	3 (27)
		Discontinue the transplant surgeries should nosocomial COVID-19 infection be observed	34 (19)	1 (9)	0 (0)	2 (8)	30 (31)	0 (0)	1 (9)
		Not decided, yet	24 (13)	2 (18)	1 (11)	2 (8)	15 (16)	4 (22)	0 (0)
		Others	23 (13)	0 (0)	0 (0)	3 (12)	16 (17)	4 (22)	0 (0)
Q18	Have you placed any restrictions on the dispatch of organ recovery from your center during the COVID-19 pandemic?	Yes	21 (12)	0 (0)	0 (0)	1 (4)	18 (17)	1 (6)	1 (9)
		No	148	11 (100)	9 (100)	22 (88)	79 (77)	17 (94)	10 (91)
Q19	Have you experienced any cases in which organ recovery was abandoned due to a COVID-19 infection?	Yes	14 (8)	3 (27)	0 (0)	0 (0)	8 (8)	3 (17)	0 (0)
		No	156 (88)	8 (73)	9 (100)	23 (92)	90 (87)	15 (83)	11 (100)

Table 2 (continued)

		Answer	Overall (%) $n=177$	Heart $n=11$	Lung $n=9$	Liver $n=25$	Kidney $n=103$	Pancreas $n=18$	Small intestine $n=11$
Q20	Have you experienced any cases in which organ transplantation was abandoned due to a COVID-19 infection even though organ recovery was possible?	Yes	12 (7)	1 (9)	1 (11)	0 (0)	9 (9)	1 (6)	0 (0)
		No	158 (89)	10 (91)	8 (89)	23 (92)	89 (86)	17 (94)	11 (100)
Q21	How do you handle patients who are candidates for organ transplantation during the COVID-19 pandemic? (Multiple answers allowed)	Be sure to perform chest CT	125 (70)	8 (73)	6 (67)	11 (44)	85 (83)	13 (72)	2 (18)
		Perform chest CT if the patient has some symptoms	16 (9)	1 (9)	0 (0)	5 (20)	3 (3)	3 (17)	4 (36)
		Be sure to screen for COVID-19 (PCR test, antigen test, etc.)	161 (90)	9 (82)	9 (100)	22 (88)	93 (90)	18 (100)	10 (91)
		Screen for COVID-19 (PCR test, antigen test, etc.), if there are chest CT findings or the patient has some symptoms	6 (3)	1 (9)	0 (0)	2 (8)	2 (2)	0 (0)	1 (9)
		Others	6 (3)	1 (9)	0 (0)	0 (0)	5 (5)	0 (0)	0 (0)
Q22	Have there been any changes in the post-transplant follow-up systems during the COVID-19 pandemic in your hospital?	No change	65 (37)	6 (55)	3 (33)	9 (36)	37 (36)	6 (33)	4 (36)
		The system has changed a little	80 (45)	5 (45)	6 (67)	11 (44)	45 (44)	9 (50)	4 (36)
		The system has changed considerably	29 (16)	0 (0)	0 (0)	5 (20)	18 (17)	3 (17)	3 (27)
		The system has all changed	3 (2)	0 (0)	0 (0)	0 (0)	3 (3)	0 (0)	0 (0)
Q23	If you answered "yes" to Q22, please explain how the post-transplant follow-up systems have changed. (Multiple answers allowed)	Outpatient visits for patients after transplantation were set to be performed at longer intervals	123 (69)	6 (100)	4 (80)	16 (76)	77 (94)	12 (92)	8 (89)
		Try to give more medicine than usual	66 (37)	4 (67)	3 (60)	9 (43)	44 (54)	4 (31)	2 (22)
		Examination are limited as much as possible	14 (8)	0 (0)	1 (20)	2 (10)	9 (11)	2 (15)	0 (0)
		Try to patients stay in the out-patients clinic as short as possible	51 (29)	2 (33)	3 (60)	5 (24)	35 (43)	4 (31)	2 (22)
		Try to make each other patients avoid contact	36 (20)	3 (50)	2 (40)	5 (24)	21 (26)	2 (15)	3 (33)
		Others	21 (12)	2 (33)	3 (60)	5 (24)	8 (10)	1 (8)	2 (22)

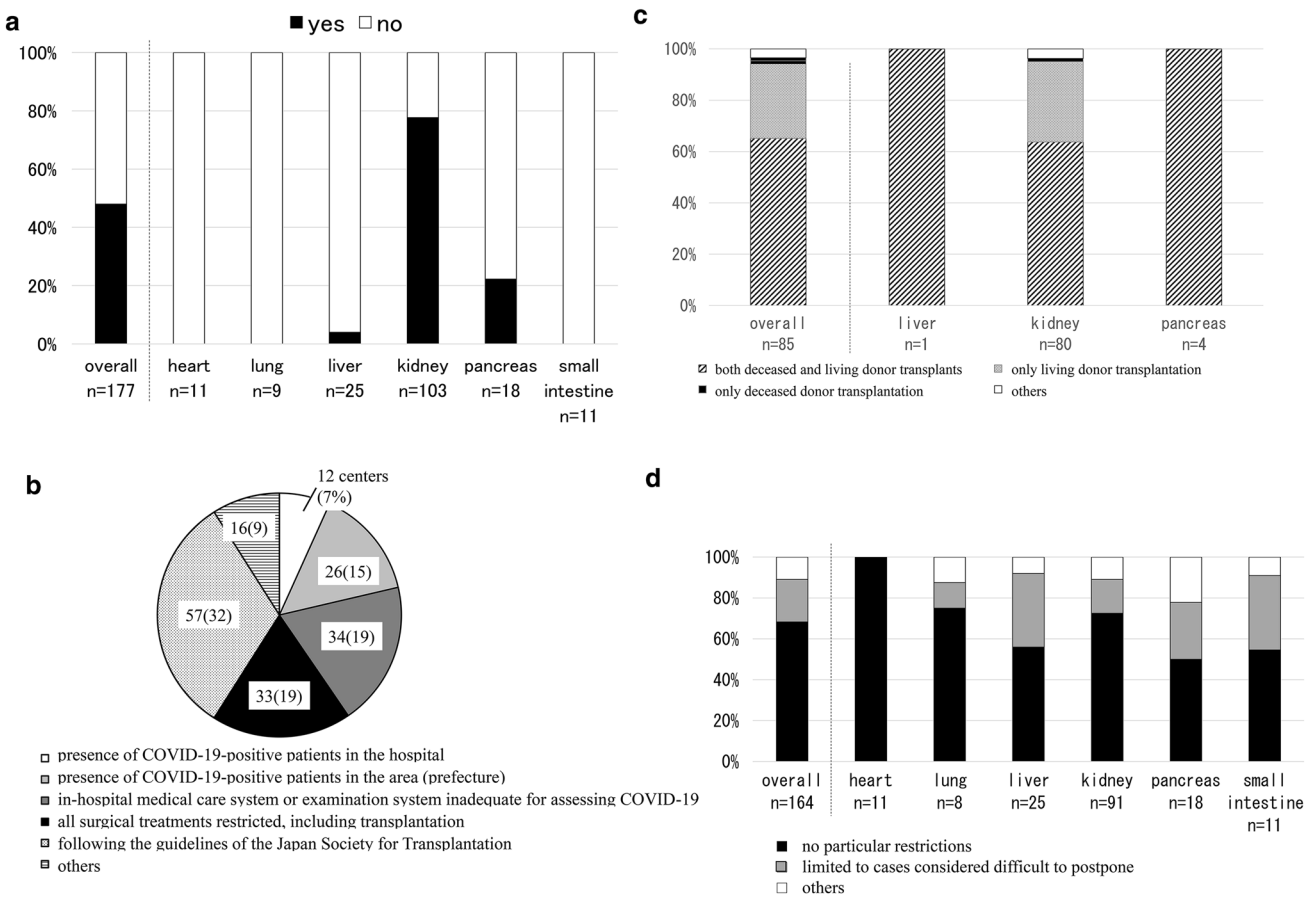

Fig. 4 Answers to questions about porting program continuation. Q12: Have organ transplant surgeries in your hospital been stopped due to the COVID-19 pandemic? (**a**), Q13: What was the reason for the decision to suspend organ transplant surgeries? (Multiple answers allowed) (**b**), Q14: What kind of organ transplants were suspended? (**c**), Q16: What kind of organ transplants are being performed if transplant surgery is ongoing? (**d**). Response summaries: Q12: While no center discontinued its transplant surgeries for heart and lung transplants, one center (4%) suspended its transplant surgeries for liver transplants, 80 (78%) suspended their transplant surgeries for kidney transplants, and 4 (22%) suspended their transplant surgeries for pancreas transplants (**a**). Q13: The reasons for discontinuing transplantation were as follows: COVID-19-positive patients in the hospital ($n=12$; 7%), COVID-19-positive patients in the prefecture ($n=26$; 15%), in-hospital medical care system or examination system inadequate for assessing COVID-19 ($n=34$; 19%), all surgical treatment (including transplantation) restricted ($n=33$; 19%), and suspended in accordance with guidelines of the Japan Society for Transplantation ($n=57$; 32%) (**b**). Q14: Fifty-six centers (31%) discontinued all transplants, including both deceased and living donor transplantation, 25 (14%) discontinued only living donor transplantation, and 1 (1%) discontinued only deceased donor transplantation (**c**). Q16: Of the centers with an ongoing transplant surgeries at the time of the questionnaire, 112 (63%) were providing transplant medical care without any specific restrictions, while 34 (19%) were limiting transplant surgery to cases when it was considered difficult to postpone (**d**)

some cases because of the COVID-19 pandemic. The present study confirmed that the COVID-19 pandemic has had a significantly negative impact on both organ donation and the performance of SOT.

In the United States, the number of patients registered as waiting for SOT and transplant surgery in April, 2020, was reported to have decreased in all United Network for Organ Sharing regions, and the mortality rate of these waiting patients had increased in more than half of the regions [34]. It was also reported that in March and April, 2020, when the COVID-19 pandemic began, the number of new wait-list patient enrollments, deceased-donor kidney transplants, and living-donor kidney transplants, fell below expectations by 18%, 24%, and 87%, respectively [35]. In Europe, the COVID-19 pandemic was reported to have had a similarly severe impact on transplant medical care, with the number of referrals of potential donors decreasing by 39% in the United Kingdom [36] and the number of potential deceased organ donors decreasing by 16% in comparison with previous years in France [37]. Conversely, in South Korea, (as in Japan), where the COVID-19 pandemic manifested relatively early with a less impact than in the United States and Europe, there was no significant change reported in the number of liver transplantations or kidney transplantations as of March and April, 2020 [38, 39], respectively, from the previous year, for both living donor transplants and BDD

transplants. These findings showed that the ability to perform organ transplantation is dependent on the severity of the spread of COVID-19 in a given country; however, as these reports relate to the situation in spring 2020, subsequent reports on the overall situation of organ transplantation in 2020 are awaited.

Unfortunately, during the severe COVID-19 pandemic at the present time, in many countries, including Japan, available medical resources are likely to be assigned to countermeasures against the COVID-19 pandemic, necessitating a reduction in transplantation activity. In several countries, newly developed vaccines are improving the impact of the COVID-19 pandemic [40–45], and facilitating the rebuilding of a normal lifestyle. It is thought that the acquisition of herd immunity through vaccination will improve the survival of patients with organ failure who are awaiting transplantation and promote transplant medical care.

The present study had several limitations. The overall response rate to the questionnaire was 86%, which may be considered relatively high; however, the response rate of the kidney transplant centers was approximately 80%, which is slightly low. The questionnaire survey in this study was conducted from December, 2020 to January, 2021, when the background of the COVID-19 pandemic in Japan was in a state of flux. In particular, the number of COVID-19-positive patients in the third wave increased rapidly, and from January 2021, a state of emergency was declared in some cities, including Tokyo. The movement of people was greatly restricted and the situation was changing, which may have affected organ recovery; thus, the answers to our questionnaire survey might have varied greatly depending on the time of the response. Furthermore, the number of living donor organ transplantations was not mentioned in this paper, as the effects of the COVID-19 pandemic on the state of living transplantation in Japan is being investigated in another study.

Conclusion

At the end of March, 2021, the number of patients infected with COVID-19 in the third wave of the pandemic began to decline. Although the COVID-19 pandemic in Japan is less severe than in other countries, it has had a large impact on the overall transplantation activity, suspending transplantation surgeries in 48% of the transplantation centers, including 78% of the kidney transplantation centers, and reducing the number of organ donations to 61% of the year-on-year average. This situation should be monitored closely.

Acknowledgements We like to thank the 177 transplant centers that responded to the questionnaire during the national COVID-19 pandemic crisis.

Funding This research was funded by Health, Labour and Welfare Policy Research Grants.

Declarations

Conflict of interest We have no conflicts of interest to declare in association with this study.

References

1. Soyama A, Eguchi S. The current status and future perspectives of organ donation in Japan: learning from the systems in other countries. Surg Today. 2016;46(4):387–92.
2. Soyama A, Eguchi S, Egawa H. Liver transplantation in Japan. Liver Transpl. 2016;22(10):1401–7.
3. Fukushima N, Ono M, Saito S, Saiki Y, Kubota S, Tanoue Y, et al. Heart donation in Japan before and after the revision of the Japanese Transplantation Act. Transpl Proc. 2014;46(6):2050–3.
4. Egawa H, Tanabe K, Fukushima N, Date H, Sugitani A, Haga H. Current status of organ transplantation in Japan. Am J Transpl. 2012;12(3):523–30.
5. Fukushima N, Ono M, Saiki Y, Sawa Y, Nunoda S, Isobe M. Registry report on heart transplantation in Japan (June 2016). Circ J. 2017;81(3):298–303.
6. Ito T, Kenmochi T, Aida N, Kurihara K, Tomimaru Y, Ito T. Impact of the revision of the law on pancreatic transplants in Japan—an analysis of the Japanese Pancreas Transplants Registry. J Hepatobiliary Pancreat Sci. 2021;28(4):353-64.
7. Liu X, Huang J, Li C, Zhao Y, Wang D, Huang Z, et al. The role of seasonality in the spread of COVID-19 pandemic. Environ Res. 2021;195:110874.
8. Gholizadeh P, Sanogo M, Oumarou A, Mohamed MN, Cissoko Y, Saliou Sow M, et al. Fighting COVID-19 in the West Africa after experiencing the Ebola epidemic. Health Promot Perspect. 2021;11(1):5–11.
9. Kliem F. ASEAN and the EU amidst COVID-19: overcoming the self-fulfilling prophecy of realism. Asia Eur J. 2021;13:1–19.
10. Chowell G, Mizumoto K. The COVID-19 pandemic in the USA: what might we expect? Lancet. 2020;395(10230):1093–4.
11. Novelli G, Biancolella M, Mehrian-Shai R, Erickson C, Godri Pollitt KJ, Vasiliou V, et al. COVID-19 update: the first 6 months of the pandemic. Hum Genom. 2020;14(1):48.
12. Furuse Y, Ko YK, Saito M, Shobugawa Y, Jindai K, Saito T, et al. Epidemiology of COVID-19 outbreak in Japan, from January-March 2020. Jpn J Infect Dis. 2020;73(5):391–3.
13. Amengual O, Atsumi T. COVID-19 pandemic in Japan. Rheumatol Int. 2021;41(1):1–5.
14. Hayakawa S, Komine-Aizawa S, Mor GG. COVID-19 pandemic and pregnancy. J Obstet Gynaecol Res. 2020;46(10):1958–66.

15. Mori M, Ikeda N, Taketomi A, Asahi Y, Takesue Y, Orimo T, et al. COVID-19: clinical issues from the Japan Surgical Society. Surg Today. 2020;50(8):794–808.
16. Suka M, Yamauchi T, Yanagisawa H. Changes in health status, workload, and lifestyle after starting the COVID-19 pandemic: a web-based survey of Japanese men and women. Environ Health Prev Med. 2021;26(1):37.
17. Fava A, Cucchiari D, Montero N, Toapanta N, Centellas FJ, Vila-Santandreu A, et al. Clinical characteristics and risk factors for severe COVID-19 in hospitalized kidney transplant recipients: a multicentric cohort study. Am J Transpl. 2020;20(11):3030–41.
18. Sanchez-Alvarez JE, Perez Fontan M, Jimenez Martin C, Blasco Pelicano M, Cabezas Reina CJ, Sevillano Prieto AM, et al. SARS-CoV-2 infection in patients on renal replacement therapy Report of the COVID-19. Registry of the Spanish Society of Nephrology (SEN). Nefrologia. 2020;40(3):272–8.
19. Cravedi P, Suraj SM, Azzi Y, Haverly M, Farouk S, Perez-Saez MJ, et al. COVID-19 and kidney transplantation: results from the TANGO International Transplant Consortium. Am J Transpl. 2020;20(11):3140-8.
20. Alberici F, Delbarba E, Manenti C, Econimo L, Valerio F, Pola A, et al. A report from the Brescia Renal COVID Task Force on the clinical characteristics and short-term outcome of hemodialysis patients with SARS-CoV-2 infection. Kidney Int. 2020;98(1):20–6.
21. Tortonese S, Scriabine I, Anjou L, Loens C, Michon A, Benabdelhak M, et al. COVID-19 in patients on maintenance dialysis in the Paris region. Kidney Int Rep. 2020;5(9):1535–44.
22. Keller N, Chantrel F, Krummel T, Bazin-Kara D, Faller AL, Muller C, et al. Impact of first-wave COronaVIrus disease 2019 infection in patients on haemoDIALysis in Alsace: the observational COVIDIAL study. Nephrol Dial Transpl. 2020;35(8):1338–411.
23. Corbett RW, Blakey S, Nitsch D, Loucaidou M, McLean A, Duncan N, et al. Epidemiology of COVID-19 in an Urban Dialysis Center. J Am Soc Nephrol. 2020;31(8):1815–23.
24. Valeri AM, Robbins-Juarez SY, Stevens JS, Ahn W, Rao MK, Radhakrishnan J, et al. Presentation and outcomes of patients with ESKD and COVID-19. J Am Soc Nephrol. 2020;31(7):1409–15.
25. Ng JH, Hirsch JS, Wanchoo R, Sachdeva M, Sakhiya V, Hong S, et al. Outcomes of patients with end-stage kidney disease hospitalized with COVID-19. Kidney Int. 2020;98(6):1530–9.
26. Caillard S, Anglicheau D, Matignon M, Durrbach A, Greze C, Frimat L, et al. An initial report from the French SOT COVID Registry suggests high mortality due to COVID-19 in recipients of kidney transplants. Kidney Int. 2020;98(6):1549–58.
27. Webb GJ, Marjot T, Cook JA, Aloman C, Armstrong MJ, Brenner EJ, et al. Outcomes following SARS-CoV-2 infection in liver transplant recipients: an international registry study. Lancet Gastroenterol Hepatol. 2020;5(11):1008–16.
28. Colmenero J, Rodriguez-Peralvarez M, Salcedo M, Arias-Milla A, Munoz-Serrano A, Graus J, et al. Epidemiological pattern, incidence, and outcomes of COVID-19 in liver transplant patients. J Hepatol. 2021;74(1):148–55.
29. Ketcham SW, Adie SK, Malliett A, Abdul-Aziz AA, Bitar A, Grafton G, et al. Coronavirus disease-2019 in heart transplant recipients in Southeastern Michigan: a case series. J Card Fail. 2020;26(6):457–61.
30. Rivinius R, Kaya Z, Schramm R, Boeken U, Provaznik Z, Heim C, et al. COVID-19 among heart transplant recipients in Germany: a multicenter survey. Clin Res Cardiol. 2020;109(12):1531–9.
31. Iacovoni A, Boffini M, Pidello S, Simonato E, Barbero C, Sebastiani R, et al. A case series of novel coronavirus infection in heart transplantation from 2 centers in the pandemic area in the North of Italy. J Heart Lung Transpl. 2020;39(10):1081–8.
32. Aversa M, Benvenuto L, Anderson M, Shah L, Robbins H, Pereira M, et al. COVID-19 in lung transplant recipients: a single center case series from New York City. Am J Transpl. 2020;20(11):3072–80.
33. Ortiz-Brizuela E, Leal-Vega F, Cuellar-Rodriguez J, Bobadilla-Del-Valle M, Ponce-de-Leon A. Vaccine-derived varicella zoster infection in a kidney transplant recipient after zoster vaccine live administration. Vaccine. 2019;37(27):3576–9.
34. Cholankeril G, Podboy A, Alshuwaykh OS, Kim D, Kanwal F, Esquivel CO, et al. Early impact of COVID-19 on solid organ transplantation in the United States. Transplantation. 2020;104(11):2221–4.
35. Boyarsky BJ, Werbel WA, Durand CM, Avery RK, Jackson KR, Kernodle AB, et al. Early national and center-level changes to kidney transplantation in the United States during the COVID-19 epidemic. Am J Transpl. 2020;20(11):3131–9.
36. Manara AR, Mumford L, Callaghan CJ, Ravanan R, Gardiner D. Donation and transplantation activity in the UK during the COVID-19 lockdown. Lancet. 2020;396(10249):465–6.
37. Legeai C, Malaquin G, Lamotte C, Antoine C, Averland B, Jasseron C, et al. Impact of coronavirus disease 2019 on organ donation and transplantation in France. Transpl Int. 2021;34(1):204–6.
38. Lee JM. Effect of COVID-19 on liver transplantation in Korea. Transpl Infect Dis. 2020;22(5):e13384.
39. Lee J, Huh KH. Kidney transplantation trends in South Korea during the COVID-19 pandemic. Kidney Int. 2020;98(2):512–3.
40. Hall VJ, Foulkes S, Saei A, Andrews N, Oguti B, Charlett A, et al. COVID-19 vaccine coverage in health-care workers in England and effectiveness of BNT162b2 mRNA vaccine against infection (SIREN): a prospective, multicentre, cohort study. Lancet. 2021;397(10286):1725–35.
41. Abu-Raddad LJ, Chemaitelly H, Yassine HM, Benslimane FM, Al Khatib HA, Tang P, et al. Pfizer-BioNTech mRNA BNT162b2 COVID-19 vaccine protection against variants of concern after one versus two doses. J Travel Med. 2021. https://doi.org/10.1093/jtm/taab083.
42. Voysey M, Costa Clemens SA, Madhi SA, Weckx LY, Folegatti PM, Aleyet PK, et al. Single-dose administration and the influence of the timing of the booster dose on immunogenicity and efficacy of ChAdOx1 nCoV-19 (AZD1222) vaccine: a pooled analysis of four randomised trials. Lancet. 2021;397(10277):881–91.
43. Abu-Raddad LJ, Chemaitelly H, Butt AA. Effectiveness of the BNT162b2 COVID-19 vaccine against the B.1.1.7 and B.1.351 variants. N Engl J Med. 2021;385(2):187–9.
44. Baden LR, El Sahly HM, Essink B, Kotloff K, Frey S, Novak R, et al. Efficacy and safety of the mRNA-1273 SARS-CoV-2 vaccine. N Engl J Med. 2021;384(5):403–16.
45. Chemaitelly H, Yassine HM, Benslimane FM, Al Khatib HA, Tang P, Hasan MR, et al. mRNA-1273 COVID-19 vaccine effectiveness against the B.1.1.7 and B.1.351 variants and severe COVID-19 disease in Qatar. Nat Med. 2021. https://doi.org/10.1038/s41591-021-01446-y.

Journal of Rural Medicine

Original article

A multicentric study on the newly developed reconstruction locking plate for midshaft clavicular fracture

Takeshi Ogawa[1, 2], Masafumi Uesugi[3], Yuki Hara[2], Yuichi Yoshii[4], and Masashi Yamazaki[2]

[1]*Department of Orthopaedic Surgery, National Hospital Organization, Mito Medical Center, Japan*
[2]*Department of Orthopaedic Surgery, Faculty of Medicine, University of Tsukuba, Japan*
[3]*Department of Orthopaedic Surgery, Ibaraki Seinan Medical Centre Hospital, Japan*
[4]*Department of Orthopaedic Surgery, Tokyo Medical University Ibaraki Medical Center, Japan*

Abstract

Objectives: To examine the efficacy and clinical and radiological outcomes of the use of a streamlined clavicle plate® (MEIRA, Aichi, Japan) for midshaft clavicular fractures.
Methods: This was a retrospective cohort study of 155 patients with displaced midshaft clavicular fractures treated using a streamlined clavicle plate between 2015 and 2019 in 18 hospitals across Japan. A questionnaire regarding bone union and postoperative complications was used, and 136 cases were followed up for one year or until bone union. Plate fitting was evaluated retrospectively using surgical records, radiographic findings, and surgeon's opinion.
Results: During surgery, plate bending was needed in 19 cases (12.3%), poor fitting was observed in 8 cases (5.2%), and bone union was achieved in 133 cases (97.8%). Total implantation failure, including plate breakage and screw loosening, occurred in 10 cases (6.5%) from the intraoperative to postoperative period. Subjective complications were observed in 26 cases (16.8%): incongruity around the surgical scar or in the anterior chest in 23, and contracture of the shoulder in three. Plate removal was performed in 66 cases (48.5%) per patient's request.
Conclusion: The use of a streamlined clavicle plate is effective for midshaft fractures of the clavicle, and the success rates of bone union and implantation using this approach are comparable to those of other existing plates.

Key words: clavicle midshaft fracture, multicentric study, superior plate of the clavicle

(J Rural Med 2021; 16(3): 148–153)

Introduction

Clavicle fractures are common injuries in adults, accounting for 5% of all fractures. Eighty percent of clavicular fractures in adults occur in the middle one-third of the bone[1, 2]. There are various methods for treating midshaft clavicle fractures, such as the use of intramedullary Kirschner wires, Steinmann pin fixation, and plate fixation[3–7]. Currently, open reduction and internal fixation of severely displaced fractures of the middle third of the clavicle are recommended for adult patients[8]. In particular, plate fixation can help in obtaining a stable anatomical reduction in severely displaced or comminuted fractures. Plates such as reconstruction and reconstruction locking compression plates (LCPs), which can be bent to accommodate the S-shaped curvature of the clavicle, are preferred[9–11]. Plate fixation can be technically difficult because of the complex anatomy of the clavicle, with its S-shaped curvature and cephalad-to-caudad bow[2]. To address this problem, pre-contoured anatomic plates have been developed. Some anatomical clavicle plates include the LCP Superior Anterior Clavicle plate® (Depuy Synthes, Massachusetts, USA), VariAx Clavicle Locking Plate System® (Stryker Corporation, Michigan, USA), and Locking Clavicle Plating System® (Acumed, Oregon, USA), each with features that are low-profile and designed to fit

Received: March 10, 2021
Accepted: March 15, 2021
Correspondence: Takeshi Ogawa, Department of Orthopaedic Surgery, National Hospital Organization, Mito Medical Center, 280 Sakuranosato, Ibarakimachi, Ibaraki 311-3193, Japan
E-mail: ogawat@md.tsukuba.ac.jp

the superior surface of the clavicle with minimal soft-tissue irritation. A streamlined clavicle plate® (MEIRA, Aichi, Japan; SC plate) was developed based on the computed tomography (CT) data of Japanese patients; its thickness was 2.9 mm—the thinnest among the locking plates—with a strength of no less than the existing plates. There are several reports and single-center studies on patients treated through plate fixation; however, there are few studies that involve multiple centers and a large sample size[1]. In this multicenter study, we aimed to assess the safety, adaptability, efficacy, and clinical and radiological outcomes of using the SC plate®, a reconstruction locking plate, for midshaft clavicular fractures.

Materials and Methods

This was a retrospective cohort study of patients with displaced midshaft clavicular fractures treated using an SC plate between 2015 and 2019 in 18 hospitals across Japan. The ethics committee of the University of Tsukuba Hospital approved the study (reference number: R01-044), and informed consent was obtained from all participants. The inclusion criteria included surgical cases with midshaft fractures that were evaluated to require surgery by orthopedic surgeons in each hospital. The exclusion criterion was the distal or proximal end of the clavicle fracture. We collected relevant information on 155 cases using a questionnaire at each facility. In addition to the patient's basic information (age, sex, mechanism of injury, radiographic findings, waiting period from the injury, and so on), the questionnaire asked about the size of the plate used for fixation (eight, nine, ten holes), whether plate bending was needed, the quality of fit between the plate and the clavicle, the time of surgery, and occurrence of any complications during the surgery. The SC plate length ranged between 85 mm (eight holes) and 105 mm (ten holes), and the width between 24.8 mm (eight holes) and 31.1 mm (nine and ten holes), all of which passed the mechanical load tests under the approval number 22800BZX00003000. The injury patterns were classified according to the guidelines of the Orthopaedic Trauma Association/Arbeitsgemeinschaft fur Osteosynthesefragen (OTA/AO) and Robinson's classification[12]. The quality of the plate fitting was retrospectively evaluated from the surgical records, radiographs, and surgeon's opinion. We also investigated the achievement of bone union, the occurrence of implantation failure, and the need for reoperation due to implantation failure. In 136 cases, follow-up was performed for more than one year or until bone union to observe any postoperative complications. Unfortunately, we could not follow-up 19 cases because the patients dropped out or were transferred to another hospital. The indication and the technique of the surgery, as well as the rehabilitation plans, were decided by each hospital.

One orthopedic surgeon in each facility retrospectively evaluated bone healing using radiographs. The level of bone healing was judged by three or more cortical bone continuity in two directions of the radiographic images. In case of any difficulty in assessing the bone union using the radiographic images, a consensus was reached between the surgeon and the first author.

Furthermore, we investigated the quality of the fitting in 22 patients who had undergone CT postoperatively at the first author's facility. The quality of the fitting was defined as good (no overhang), fair (mild anterior or posterior overhang of the plate over the clavicle), or poor (both anterior and posterior plate overhang or screw-hole overhang). The decision regarding the quality was made via a three-dimensional CT (3DCT) using the modified Huang's evaluation[2].

Results

A total of 155 patients (123 men and 32 women; mean age, 41.7 ± 19.7 years) underwent SC plate fixation for midshaft clavicular fractures between April 2015 and December 2019 at the institutes included in this study. Eighty-seven patients had fractures on the right side, whereas 68 had fractures on the left side. Thirty-two patients were smokers, and 94 patients were non-smokers. Smoking status remained unknown in 28 patients. Regarding the mechanism of injury, high-energy incidents, including traffic accidents, falls from great heights or during sports, occurred in 79 patients; low-energy incidents, such as falling down, occurred in 72 patients, and the mechanism was unknown in four patients. According to the OTA/AO classification, 27, 76, and 52 patients were categorized as 15.2A, B, and C, respectively. According to Robinson's classification, four, five, 98, and 48 patients were categorized as Types 2A1, A2, B1, and B2, respectively (Table 1). Eight-hole, nine-hole, and ten-hole plates were used for 67, 62, and 26 patients, re-

Table 1 Patient characteristics and the number of each patient

Patient characteristics	Number of patients
Gender	Male 123, Female 32
Age, average (range)	41.2 (13–87) years
Smoking, current	Yes 32, No 94, Unknown 28
Mechanism of injury	High 79, Low 72, Unknown 4
Fracture type (AO classification)	
A	27
B	76
C	52
Fracture type (Robinson classification)	
A1	4
A2	5
B1	98
B2	48

spectively. During the surgery, plate bending was needed in 19 patients (12.3%), and poor fitting was confirmed in eight patients (5.2%). The average time of surgery was 91 minutes (range: 51–156 minutes). Intrasurgical complications occurred in three cases (breakage of the plate during plate bending occurred in one case and difficulty in insertion of the most proximal screw occurred in two cases). Bone union was achieved in 133 (97.8%) of the 136 patients who could be followed up for over one year or until bone union had been achieved. The average time to bone union was 153.1 days (range: 44–482 days). Postoperative complications, including screw loosening, were observed in seven patients (5.1%), and plate breakage did not occur. Total implantation failure occurred in ten patients (6.5%) from the intraoperative to postoperative period. Subjective complications were seen in 26 patients (16.8%): a sense of incongruity around the surgical scar or anterior chest in 23 patients and contracture of the shoulder in three patients. Plate removal was implemented per patient's request in 66 (48.5%) of the 136 patients who will be followed up for over one year or until bone union (Table 2).

Upon evaluation of the quality of the plate fitting in 22 cases using 3DCT, the fitting was found to be good in ten patients, fair in four patients, and poor in eight patients. The summary of the representative cases is as follows:

In case 1, a 35-year-old man sustained a Robinson 2B1 clavicular fracture. The fracture was fixed with a ten-hole SC plate, and bone union was achieved after three months. The fitting of the plate was good in the 3DCT scan using the modified Huang's evaluation[2] (Figure 1). He exhibited excellent function but retained a sense of incongruity around the surgical scar; thus, the plate was removed one year after the surgery.

In case 2, a 17-year-old boy sustained a Robinson 2A2

Table 2 Outcomes. The total number of patients is 155; however, bone union was evaluated in only 136 patients

Outcomes	The number of patients
Plate size	Total 155
8 hole	67
9 hole	62
10 hole	26
Plate bending	
Yes	19
No	136
Plate fitting	
Good	147
Not good	8
Implant failure	10
Bone union	Total 136
Yes	133
No	3

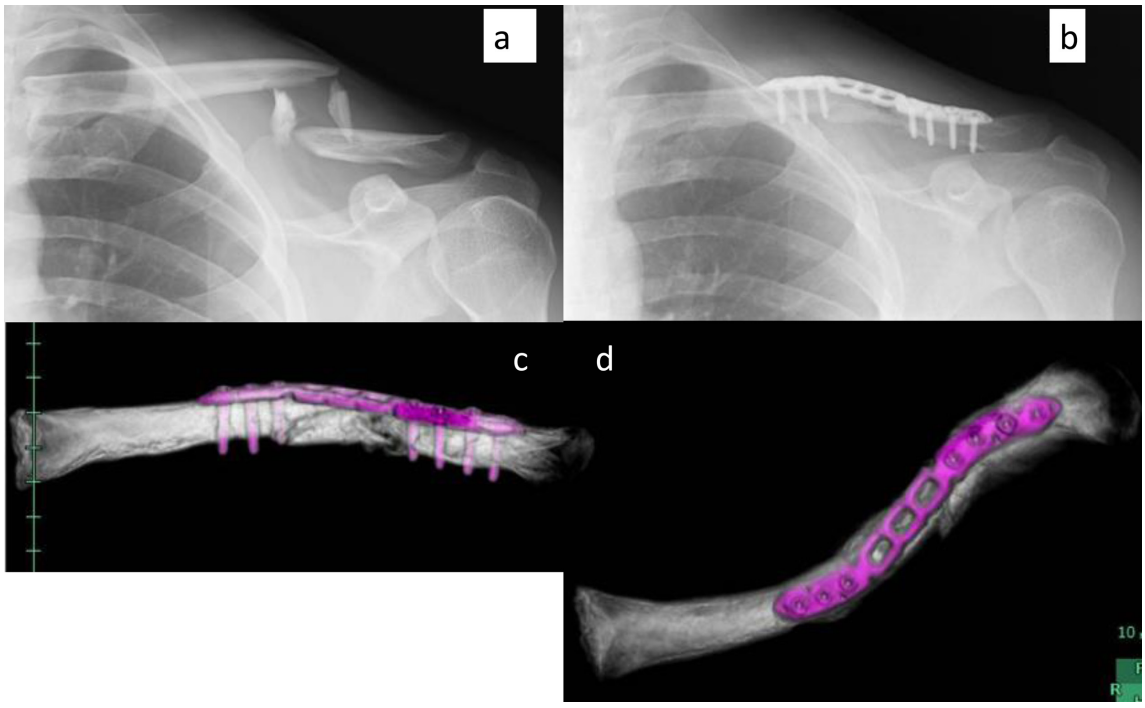

Figure 1 a: Robinson 2B1 clavicular fracture (39-year-old man). b: Fracture fixated using a ten-hole SC plate. c: Bone union achieved after three months. d: 3DCT shows a good quality plate fitting.

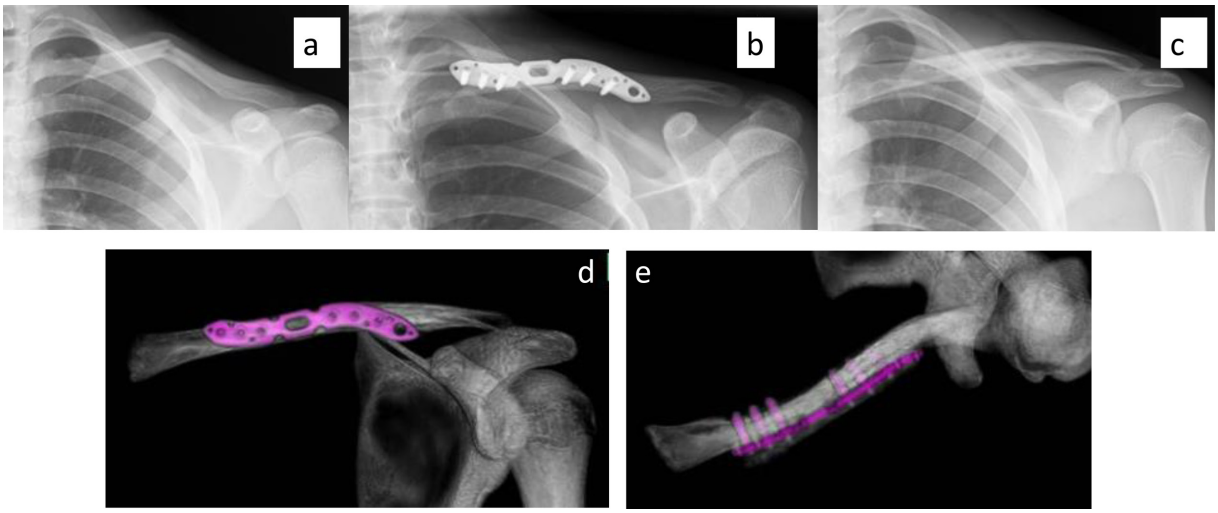

Figure 2 a: Robinson 2A2 clavicular fracture (17-year-old boy). b: Fracture fixated using an eight-hole SC plate. c: The plate removed one year after surgery. d: 3DCT performed three months after surgery indicates poor fitting; the plate was anteriorly set. e: Bone union achieved three months after surgery.

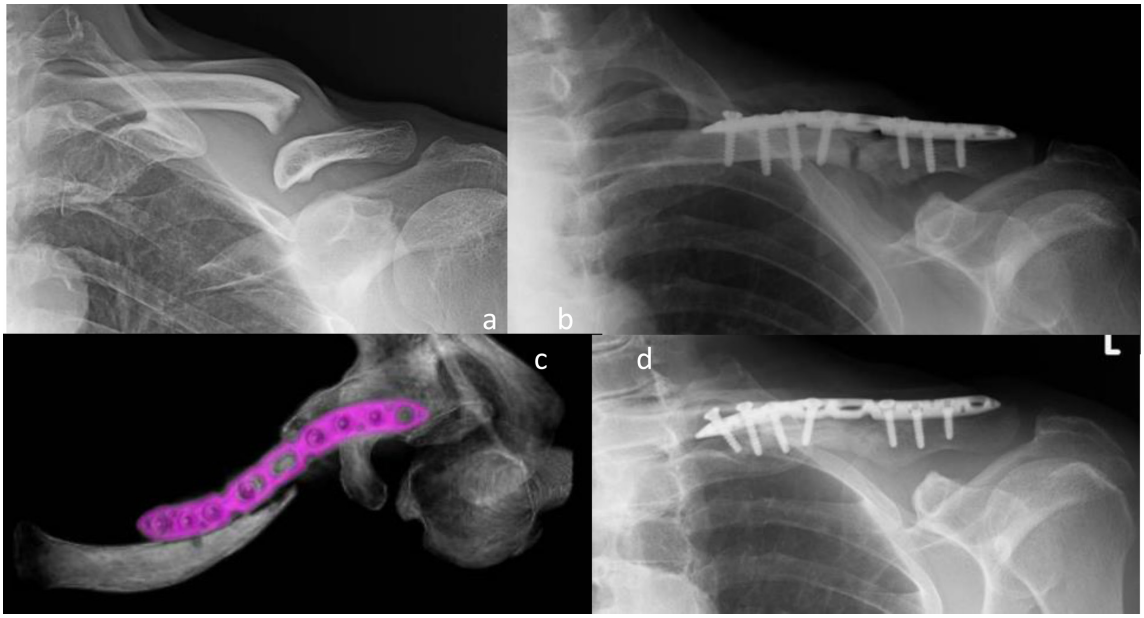

Figure 3 a: Robinson 2B1 clavicular fracture (69-year-old man). b: Fracture fixated using a nine-hole SC plate. c: 3DCT performed one month after surgery indicates poor fitting. d: Loosening of the two proximal screws; however, bone union was achieved three months after surgery.

clavicular fracture, which was fixed with an eight-hole SC plate. From the 3DCT results performed three months after surgery, we realized that the distal part of the plate was placed anterior to the bone. The plate fitting quality was evaluated as poor; however, bone union was achieved three months after surgery. Plate removal was performed one year after the surgery (Figure 2).

In case 3, a 69-year-old man sustained a Robinson 2B1 clavicular fracture, which was fixed with a nine-hole SC plate. One month after surgery, 3DCT showed that the quality of the plate fitting was poor. At three months after surgery, loosening of the two proximal screws was observed; nevertheless, bone union was achieved by limiting the shoulder's range of motion for two months after surgery (Figure 3).

Discussion

This was a multicenter study that included a larger number of cases of midshaft fracture treated with plate fixation for the clavicle than in previous studies[1, 9, 13]. The bone union rate was 97.8%, while the implantation failure rate was 6.5% (10/155 cases). Woltz *et al.* described the rate of implantation failure to be 12.6% in their retrospective cohort study[1]. Gilde *et al.* reported significantly more implant-related complications when using a reconstruction plate than when using a dynamic compression plate (8.5% vs. 1.2%, p=0.03). Although their plate was an anteroinferior type plate, unlike our superior reconstruction locking plate, it is expected to be a more durable and effective implant[9]. Robinson *et al.* described a reoperation rate of 2.3% in 86 cases due to implantation failure of the locking clavicle plating system® (Acumed, Oregon, USA)[13]. Their plate system had two direction types (anterior and superior), and all surgeries were performed by shoulder specialists (Table 3).

In our study, orthopedic specialists or residents performed several surgeries. Plate breakage or deviations may thus have been caused by both the lack of strength of the plate, as well as by technical problems by the surgeons. However, in superior types of clavicle plates, insertion of proximal screws is difficult because it is obstructed by the patient's head. Hence, in several cases, a cortical screw was selected for the proximal hole to lean in the direction of the insertion. A locking screw was not used because of the poor angle of insertion in some cases. These problems may lead to loosening of the screw; however, the strength and durability of our plates are not inferior to those of other existing plates. The SC plates in our study feature slight elasticity, allowing them to pull up the bone in the proper reduction position. The three locking holes on both sides create slightly smaller hole distances, unlike in other existing plates, helping to reduce the mechanical load on both sides. There are also some notches on the plate to be used for wiring in the case of comminuted fractures; therefore, the bending of the plate is easier in the SC plate compared to that in the other existing plates.

This SC plate was designed to set the upper part of the clavicle, and the quality of the fitting was good in 132 cases (94.8%). Although plate bending was needed in 19 cases (12.3%), all these cases had good quality plate fitting according to the surgeon's opinion. In contrast, another study reported poor fitting in eight of 22 cases, suggested by 3DCT findings with the modified Huang's method[2]. Although bone union was achieved in all these cases, technical errors, including poor reduction or poor setting position of the plate, were revealed. Ordinarily, CT is not used to investigate the achievement of bone union, except when patients exhibit any complications; however, it is true that plate setting is difficult if the fracture site is too distal or too proximal. In such cases, fair fitting may not be inevitable using this SC plate, as it only has three size options and a superior type of setting. Further development of this plate is needed to address several types of midshaft clavicle fractures. Kim et al. described a real-size 3D-printed model as a preoperative and intraoperative tool for minimally invasive plating of comminuted midshaft clavicle fractures[14]. Such trials are useful for providing more precise treatment, as well as for developing new types of plates.

There are some limitations to this multicenter study. First, we conducted a retrospective study using questionnaires; thus, the evaluations were sourced from several investigators. In order to assess the quality of plate fitting, we depended on the surgical records and the surgeon's opinion. We evaluated only 22 cases using 3DCT; however, due to the harmful effects of radiation, it is inappropriate to use CT for patients who follow a favorable recovery process. Second, it could not be directly compared with other plates or treatment methods, such as conservative or intramedullary nails. Further research is warranted to address these limitations.

Conclusion

In conclusion, this multicenter study demonstrated the effectiveness of our SC plate for treating midshaft clavicle fractures. The rates of bone union and implant failure were 97.8% and 6.5%, respectively, indicating that this plate may have sufficient strength for bone union and would not lead to serious complications. Therefore, this SC plate is not considered inferior to the existing plates.

Table 3 Summary of literature: nonunion, implant failure, and plate removal rates

Study	Number of patients	Plate type		Nonunion (%)	Implant failure (%)	Plate removal (%)
Shin *et al.*, 2012 [11]	125	Recon.	Superior		12	
Robinson *et al.*, 2013 [12]	86	Precontoured locking	Superior/Anterior	1.7	2.3	11.6
Waltz *et al.*, 2016 [1]	111	3.5 mm Recon.	all directions	2.7	8.1	37.8
Gilde *et al.*, 2014 [9]	85	2.7 mm DCP	Anteroinferior	1.2	1.2	11.8
	71	2.7 mm Recon.	Anteroinferior	7	8.5	7
Ours	155	2.8 mm Recon. Locking	Superior	2.2	6.5	48.5

Funding: No benefits in any form have been received or will be received by the authors related directly or indirectly to the subject of this article.

Conflicts of interest: None.

Acknowledgments

The authors would like to thank all the investigating members, who are specialists in orthopedics at the University of Tsukuba and related facilities, for their contributions to this study. We present their names and the hospitals to which they are affiliated in the list below.

Dr. Akira Ikumi, M.D., Ph.D.
– Takahagi Kyodo Hospital and Mito Kyodo General Hospital
Dr. Arata Watanabe, M.D., Ph.D.
– Ichihara Hospital
Dr. Hisanori Gamada, M.D.
– Ibaraki Western Medical Center
Dr. Katsuya Aoto, M.D., Ph.D.
– National Hospital Organization Kasumigaura Medical Center
Dr. Kazuhiro Ikeda, M.D.
– Kikkoman General Hospital
Dr. Kensei Katsura, M.D.
– Total Moriya Daiichi Clinics
Dr. Masato Murakami, M.D.
– Ryugasaki Saiseikai Hospital
Dr. Ryuhei Michinobu, M.D.
– University of Tsukuba Hospital
Dr. Satoshi Nakamura, M.D.
– Tsukuba Central Hospital
Drs. Satoki Ii, M.D., Kazuo Ohyama, M.D., Jun Nishine, M.D., and Takamasa Kudo, M.D.
– Tokyo Medical University Ibaraki Medical Center
Dr. Shigeo Izawa, M.D.
– Tsukuba Gakuen Hospital
Dr. Shota Nakagawa, M.D.
– Matsudo City General Hospital
Dr. Takumi Hirabayasi, M.D.
– General Hospital in Hitachinaka
Dr. Tomohiro Yoshizawa, M.D., Ph.D.
– Tsukuba Medical Center Hospital
Dr. Yohei Tomaru, M.D., Ph.D.
– Namegata District General Hospital
Dr. Yosuke Ogata, M.D.
– Japanese Red Cross Mito Hospital

The authors also thank Mr. Yoshitaka Okayama and Mr. Ryo Namiki, who are sales representatives of MEIRA Corporation Inc., for serving as liaisons between the authors and the above investigators.

References

1. Woltz S, Duijff JW, Hoogendoorn JM, *et al*. Reconstruction plates for midshaft clavicular fractures: a retrospective cohort study. Orthop Traumatol Surg Res 2016; 102: 25–29. [Medline] [CrossRef]
2. Huang JI, Toogood P, Chen MR, *et al*. Clavicular anatomy and the applicability of precontoured plates. J Bone Joint Surg Am 2007; 89: 2260–2265. [Medline] [CrossRef]
3. Hulsmans MH, van Heijl M, Houwert RM, *et al*. Surgical fixation of midshaft clavicle fractures: a systematic review of biomechanical studies. Injury 2018; 49: 753–765. [Medline] [CrossRef]
4. Huttunen TT, Launonen AP, Berg HE, *et al*. Trends in the incidence of clavicle fractures and surgical repair in Sweden: 2001–2012. J Bone Joint Surg Am 2016; 98: 1837–1842. [Medline] [CrossRef]
5. Honeycutt MW, Fisher M, Riehl JT. Orthopaedic Tips: A comprehensive review of midshaft clavicle fractures. J Orthop Physician Assistants 2019; 7: e0053. [CrossRef]
6. van der Meijden OA, Gaskill TR, Millett PJ. Treatment of clavicle fractures: current concepts review. J Shoulder Elbow Surg 2012; 21: 423–429. [Medline] [CrossRef]
7. Zlowodzki M, Zelle BA, Cole PA, *et al*. Evidence-Based Orthopaedic Trauma Working Group Treatment of acute midshaft clavicle fractures: systematic review of 2144 fractures: on behalf of the Evidence-Based Orthopaedic Trauma Working Group. J Orthop Trauma 2005; 19: 504–507. [Medline] [CrossRef]
8. Hill JM, McGuire MH, Crosby LA. Closed treatment of displaced middle-third fractures of the clavicle gives poor results. J Bone Joint Surg Br 1997; 79: 537–539. [Medline] [CrossRef]
9. Gilde AK, Jones CB, Sietsema DL, *et al*. Does plate type influence the clinical outcomes and implant removal in midclavicular fractures fixed with 2.7-mm anteroinferior plates? A retrospective cohort study. J Orthop Surg Res 2014; 9: 55. [Medline] [CrossRef]
10. Hsiao YC, Lin TY, Wang YC, *et al*. Prognostic factors and outcomes of secondary surgery after plate fixation for midshaft clavicle fracture: Comparison of traditional DCP and pre-contoured locking plate. Injury 2020; 51: 2241–2244. [Medline] [CrossRef]
11. Shin SJ, Do NH, Jang KY. Risk factors for postoperative complications of displaced clavicular midshaft fractures. J Trauma Acute Care Surg 2012; 72: 1046–1050. [Medline] [CrossRef]
12. Robinson CM. Fractures of the clavicle in the adult. Epidemiology and classification. J Bone Joint Surg Br 1998; 80: 476–484. [Medline] [CrossRef]
13. Robinson CM, Goudie EB, Murray IR, *et al*. Open reduction and plate fixation versus nonoperative treatment for displaced midshaft clavicular fractures: a multicenter, randomized, controlled trial. J Bone Joint Surg Am 2013; 95: 1576–1584. [Medline] [CrossRef]
14. Kim HN, Liu XN, Noh KC. Use of a real-size 3D-printed model as a preoperative and intraoperative tool for minimally invasive plating of comminuted midshaft clavicle fractures. J Orthop Surg Res 2015; 10: 91. [Medline] [CrossRef]

Journal of Orthopaedic Science xxx (xxxx) xxx

Contents lists available at ScienceDirect

Journal of Orthopaedic Science

journal homepage: http://www.elsevier.com/locate/jos

Original Article

High-definition magnetic resonance images on medial elbow injuries in preadolescent Little Leaguers

Tomomi Kajiwara [a], Takeshi Ogawa [b, *], Naotaka Mamizuka [c], Ryuhei Michinobu [d], Toshiyuki Irie [e], Atsushi Hirano [d]

[a] Department of Internal Medicine, Mito Clinical Education and Training Center, University of Tsukuba Hospital, Mito Kyodo General Hospital, 3-2-7 Miya-Machi, Mito, Ibaraki, 310-0015, Japan
[b] Department of Orthopedic Surgery, National Hospital Organization Mito Medical Center, 280 Sakuranosato, Ibarakimachi, Ibaraki, 311-3193, Japan
[c] Baseball and Sports Clinic, 2-228-1 Kosugi, Park city Musashikosugi the Garden Towers West 1st Floor W4, Nakahara-ward, Kawasaki-city, Kanagawa, 211-0063, Japan
[d] Department of Orthopaedic Surgery and Sports Medicine, Mito Clinical Education and Training Center, University of Tsukuba Hospital, Mito Kyodo General Hospital, 3-2-7 Miya-Machi, Mito, Ibaraki, 310-0015, Japan
[e] Department of Radiology, Mito Clinical Education and Training Center, University of Tsukuba Hospital, Mito Kyodo General Hospital. 3-2-7 Miya-Machi, Mito, Ibaraki, 310-0015, Japan

ARTICLE INFO

Article history:
Received 15 July 2021
Received in revised form
9 December 2021
Accepted 14 December 2021
Available online xxx

ABSTRACT

Background: The incidence of throwing-related elbow injuries is still rising. The study aimed to enhance the pathology of acute medial elbow injuries among young Little Leaguers by examining the medial elbows of symptomatic 9–10 years old Little Leaguers using High-Definition Magnetic Resonance Images (HDMRI), which uses a small-diameter surface coil on the target area, leading to greater image resolution.

Method: We identified Little Leaguers aged 9–10 years old. To minimize the detection of the chronic adaptative changes, players who experienced the medial elbow pain previously and whose HDMRI had not been taken within 4 weeks from the onset of medial elbow pain were excluded. This study considered 21 players, and the mean age was 9.4 ± 0.5 years.

Result: The fragmentation of the medial epicondyle apophysis via HDMRI was found in 15 elbows (71.4%), while the avulsion was seen in three cases. The signal hyperintensity at the medial epicondyle apophysis was observed in 2 cases. Our data showed abnormal changes to the medial epicondyle apophysis and surrounding structures, such as the ulnar collateral ligament (UCL), flexor-pronator tendons or the coronoid process of the ulna. We detected 11 abnormalities on X-ray imaging, while 20 subjects showed some abnormal findings via HDMRI.

Discussion: The current study showed that initial medial elbow injury in Little Leaguers without a history of previous elbow injury could be attributed to multi-structure injury. Over 90% of subjects were injured in the perichondrium, while 71.4% demonstrated a fragmentation of the secondary ossification center, and 14.3% experienced an avulsion of the medial epicondyle apophysis. Because the injuries were not limited to bony structures, HDMRI may be beneficial for the appropriate evaluation of medial elbow pain. The pathology of initial medial elbow injuries in young baseball players may be due to acute trauma instead of repetitive microtrauma.

1. Introduction

In 1960, Brogdon and Crow first defined “Little Leaguer's elbow” as the symptomatic separation and fragmentation of the medial epicondyle apophysis among Little League pitchers. Subsequent researchers have shown various possible risk factors of elbow injuries such as amount of pitching, poor pitching biomechanics,

* Corresponding author. Fax: +81 29 240 7788
E-mail address: ogawat@tsukuba-seikei.jp (T. Ogawa).

https://doi.org/10.1016/j.jos.2021.12.011
0949-2658/

fatigue, pitch velocity, pitch count, year-round participation, greater pressure, or earlier single sports specialization [1–7]. Major League Baseball and USA Baseball released guidelines to reduce throwing-related injuries based on these scientific data. However, 20%–30% of 8–12-year-old Little Leaguers have experienced elbow pain [8]. Some studies have shown that the number of emergency visits resulting from baseball-related elbow injuries has increased from 2006 to 2016, compared with injuries to other body parts such as shoulders, knees, ankles, or wrists. Ulnar collateral ligament (UCL) reconstruction in youth pitchers increased between 1994 and 2010 [1] and increased by 343% between 2003 and 2014 [9].

While the little leaguer's elbow is known as the result of chronic repetitive trauma to the most vulnerable component of the elbow among young players, it is true that there are some patients present after an acute injury [10]. However, little is known about the acute pathology of the medial elbow injury among young overhead-throwing athletes. The increase in the number of elbow injuries must be explained by a bad adherence or a mal-understanding of the guideline at least partially, but there may be other factors behind it since the guideline mainly focuses on preventing overuse.

The purpose of this study was to enhance the pathology of acute medial elbow injuries among young Little Leaguers by examining the medial elbows of symptomatic 9–10 years old Little Leaguers by using High-definition MRI (HDMRI), which uses a small-diameter surface coil on the target area, leads to greater image resolution by having a better signal-to-noise ratio and a smaller voxel size.

2. Methods

In this descriptive case series, we identified Little Leaguers aged 9–10 years old who visited our hospital with medial elbow pain from 2014 to 2018 and included those boys that had HDMRI results for the evaluation. To minimize the detection of the chronic adaptative changes, players who experienced the medial elbow pain previously and whose HDMRI had not been taken within 4 weeks from the onset of medial elbow pain were excluded. We recognized HDMRIs of 50 Little Leaguers and excluded seven players who had histories of previous elbow injuries and 20 whose HDMRI had been taken later than 4 weeks of the onset. Two players injured by direct trauma to the medial elbow were also excluded. Thus, 21 players were considered in this study (Fig. 1). A 1.5 or 3-T magnetic resonance apparatus (Magnetom Symphony, Siemens, Munich, Germany) with a small-diameter surface coil (Loop Flex Coil, Siemens) was used to evaluate all subjects. Images were evaluated in the coronal plane with a series of fat-suppressed T2 weight fast spine-echo images (T2FS), proton density-weight images (PDW), and GRE T2*-weighted images (T2*). The morphological abnormality of UCL (rupture or sagging of the UCL) and the perichondrium (rupture or translocation of the perichondrium) were evaluated with PDW and T2*, respectively. The signal abnormality of UCL and its surrounding structures, and the secondary ossification center and the coronoid process of the ulna were evaluated in T2FS. We also examined the radiographs of the elbow of the anteroposterior view with full extension and at 45° of flexion to compare the findings against HDMRI. The X-ray was taken on the day of the first visit. Two orthopedic surgeons and one radiologist evaluated the images independently and retrospectively. A consensus was reached when different MRI readings were observed among the three.

3. Results

One person out of 21 players was left-handed. The mean age was 9.4 ± 0.5 years (range, 9–10-years). Twenty patients played rubber-ball baseball, and only one patient played hard-ball baseball. Their actual years of baseball-playing experience are unknown. The average days from the onset of pain to the imaging date was 18.1 ± 6.2 days. The fragmentation of the secondary ossification center via HDMRI (Fig. 2) was found in 15 elbows (71.4%), while the avulsion of the medial epicondyle apophysis (Fig. 3) was seen in three (14.3%). The signal hyperintensity at the secondary ossification center of the medial epicondyle apophysis without fragmentation was observed in two cases (9.5%). Translocation or rupture of

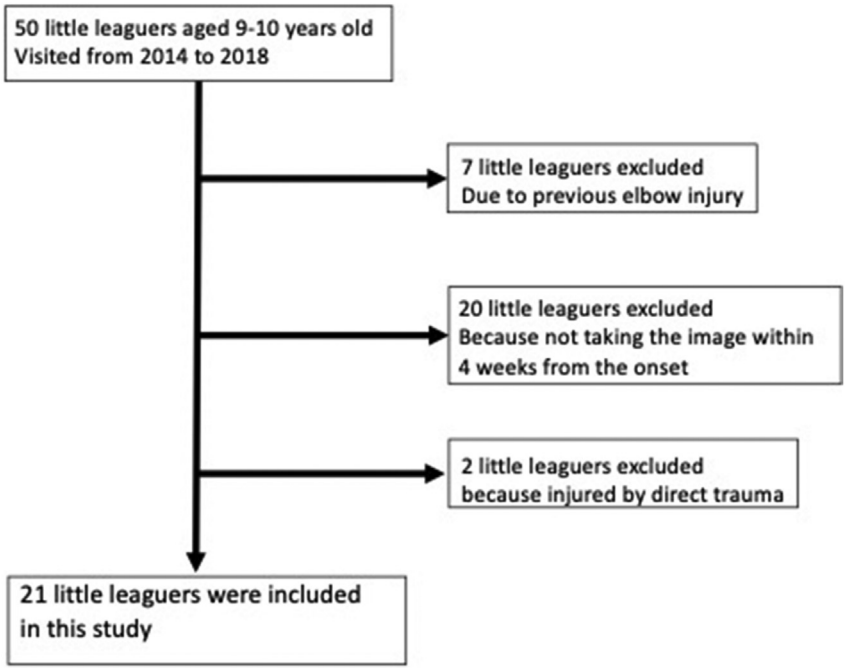

Fig. 1. Inclusion and exclusion criteria.

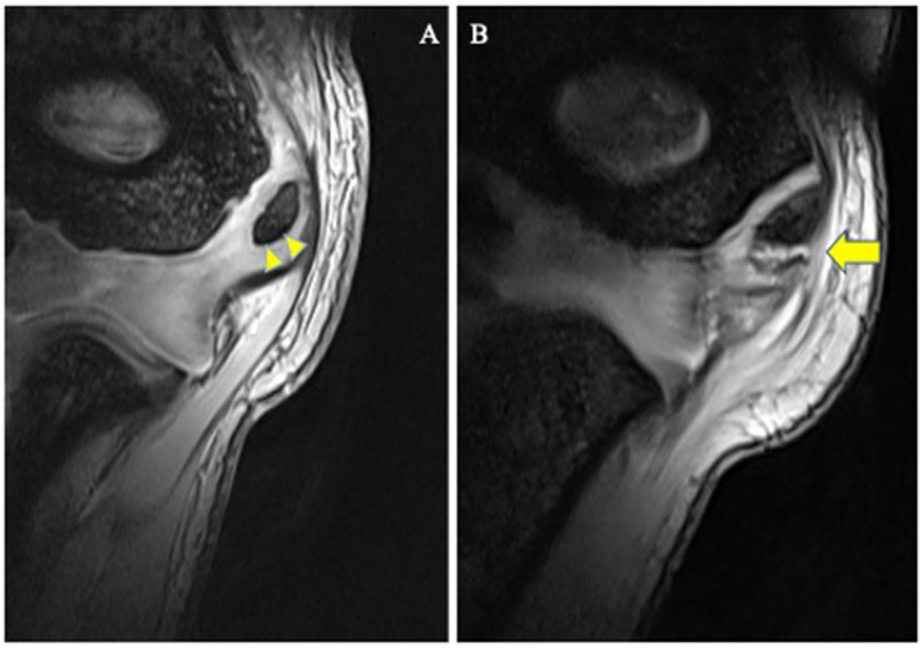

Fig. 2. A: Normal secondary ossification center at medial elbow (T2*) (arrow head). B: Fragmented secondary ossification center (T2*) (arrow).

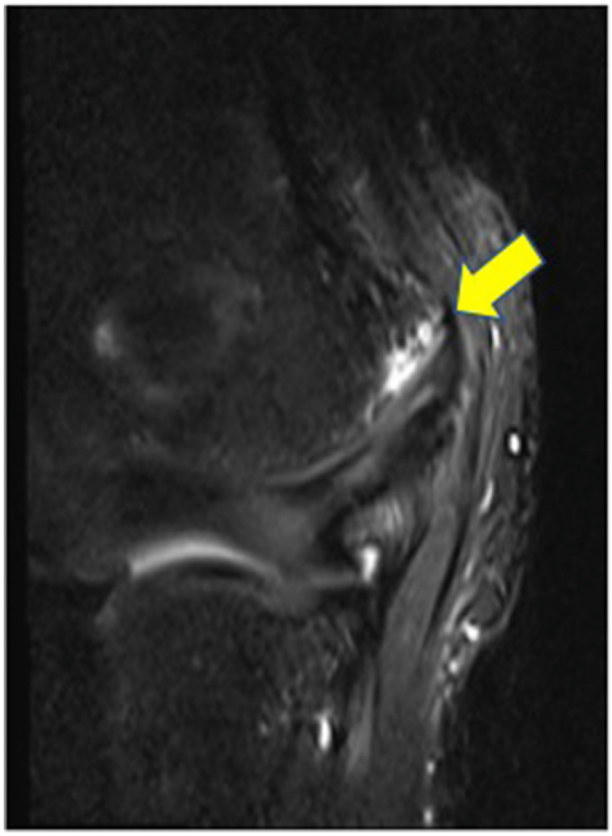

Fig. 3. High-signal intensity at the proximal part of the medial epicondyle apophysis (arrow) indicating avulsed apophysis (T2FS).

the perichondrium (Fig. 4) was observed in 19 players (90.5%). Morphological abnormalities, such as the sagging of the anterior oblique bundle of UCL (Fig. 5), were found in 16 players (76.2%). Of these 16 cases, 4 (19%) demonstrated signal hyperintensity of the UCL. The signal hyperintensity around the UCL, including flexor-pronator tendons, was observed in 13 players (61.9%). Signal hyperintensity at the subchondral bone just below the coronoid process of the ulna was found in 9 players (42.9%). All players demonstrated signal changes via HDMRI in more than two structures. The separations of the secondary ossification center of medial epicondyle were seen in 11 players via X-ray imaging, while 9 players had no signs of injury on X-ray imaging. One player missed an X-ray of the elbow that was taken at the first visit. The results are summarized in Table 1. Fourteen players (66.7%) reported that they could remember a specific single throwing motion that caused their medial elbow pain.

3.1. Representative case

A 9-year-old boy who played first base and short stop felt a sudden pain at the medial elbow when he threw a rubber baseball. The pain worsened when he released a ball. He visited our hospital on day X+12. The X-ray of the A-P view with full extension showed no abnormality of the medial epicondyle (Fig. 6A). On the other hand, the X-ray of the A-P view with 45° of flexion might seem like the fragmentation at the tip of the ossification center of the medial epicondyle, although it is unclear (Fig. 6B, arrow). However, the HDMRI, which was taken on day X+23, clearly showed a rupture of the perichondrium and an avulsion of the medial epicondyle apophysis (Fig. 7A and B).

4. Discussion

We limited our subjects to 9–10 years old baseball players since it has been reported that the UCL could be thickened or there would be the sclerotic bony changes among asymptomatic baseball pitchers aged 15–19 years old with ten years' experience in pitching, possibly due to the positive adaptation or the initiation of degenerative change [11]. The younger the pitchers are, the fewer the chances of having pre-existing irregular MRI changes because the duration of playing baseball is shorter, and the cumulative number of throwing is considered to be smaller. Players can

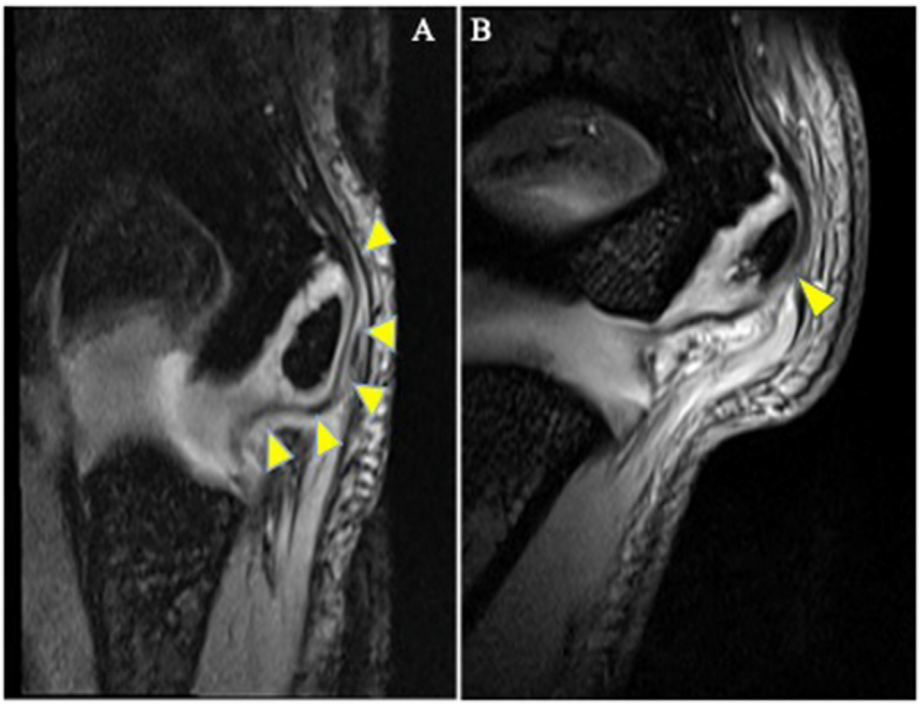

Fig. 4. A: Normal perichondrium shown as a low signal intensity line, just medial to the apophysis (T2*). B: The ruptured perichondrium shown as the low signal intensity line was discontinued (T2*).

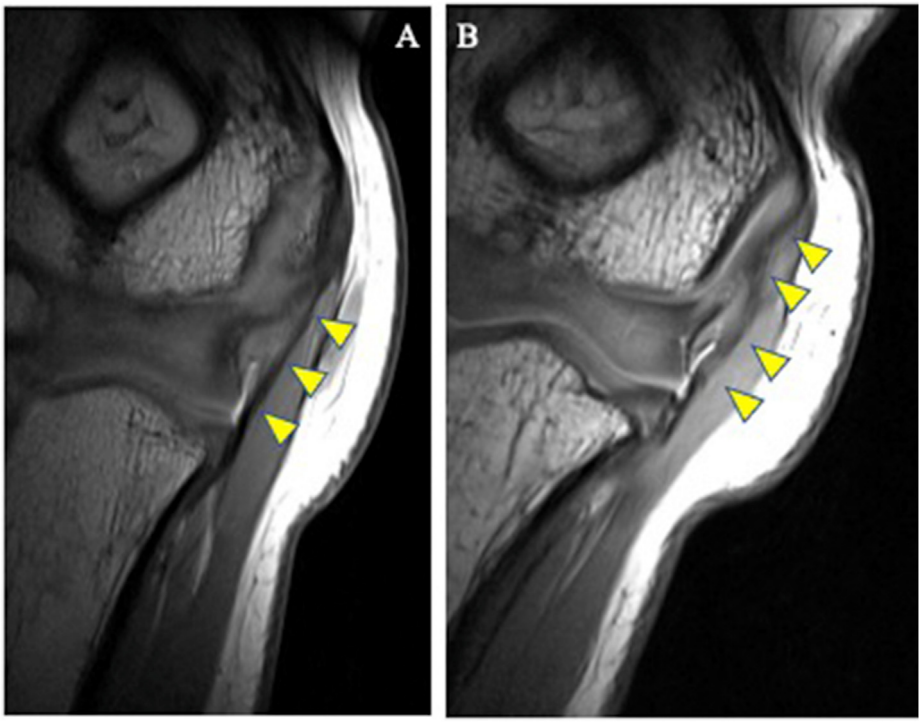

Fig. 5. A: Normal UCL shown as straight low signal intensity line (PDW). B: UCL was sagged, and the signal hyperintensity was seen (PDW).

participate in Little Leaguer's "major division" as young as 9 years old; it is important to evaluate 9–10 years old players to minimize the possibility of adaptive changes as shown in the images. We included players whose HDMRI were taken 4 weeks from the onset of pain. As Frank et al. stated, the healing of ligaments is variable and unpredictable [12]; thus, it is difficult to decide when chronic changes after a traumatic event are shown in HDMRI images. Animal models have not shown remaining gross external changes at week 4 for a mild sprain and slight local thickening of the ligament at week 7 in the case of a severe sprain [13]. Hence, we decided that 4 weeks was a reasonable timeframe in which to capture acute changes and eliminate chronic changes.

Our data showed abnormal changes not only to the medial epicondyle apophysis but also to the surrounding structures, such

Table 1
The list of abnormal findings by structures on imaging.

MRI	Percentage	Number
1. Medial epicondyle apophysis		
TOTAL	**95.2**	**20**
i) Fragmentation	71.4	15
ii) Avulsion	14.3	3
iii) Signal hyperintensity at secondary ossification center only	9.5	2
2. Perichondrium		
TOTAL	**90.4**	**19**
i) Rupture	42.9	9
ii) Translocation	47.6	10
3. UCL		
TOTAL	**76.2**	**16**
i) Morphological change	76.2	16
ii) Signal hyperintensity (overlapped)	19.0	4
4. Signal hyperintensity around UCL (includes flexor-pronator tendons)	61.9	13
5. Signal hyperintensity at coronoid process of ulna	42.9	9
X-ray		
Abnormal findings of the medial elbow	55.0	11
no X-ray imaging at the first visit	–	1

as the UCL, flexor-pronator tendons, or the coronoid process of ulna. Furthermore, we found a thin, linear area of low signal intensity wrapping around the medial epicondyle of the humerus to the medial side of the trochlea of the ulna; this is known as the perichondrium (Fig. 4A). Laor et al. described the perichondrium as the thin layer that envelops the physis and continues longitudinally around the most adjacent newly formed trabecula of the metaphysis [14]. It shows low signal intensity on all sequences of MRI. It was stated that a tear of the perichondrium might be helpful to detect minimally displaced fractures of the knee in children [14]. There are no known studies evaluating the perichondrium of adolescent baseball players with medial elbow pain. The current study showed that the translocation or the rupture of the perichondrium existed in 90.5% of the initial medial elbow pain among young baseball players. This may enlighten the possibility that the perichondrium involves the acute pathology of the medial elbow pain.

The morphological change of the UCL was observed in 76.2% players, while the signal change within the UCL was seen in only 19.0% of the subjects. Zell et al. stated that the origin of UCL always remained medial to the cartilaginous interface of the apophysis and was centered approximately 3 mm medial to the lateral edge of the apophysis [15], which may indicate that the UCL originates from the perichondrium. We hypothesized that the UCL was not always damaged but sagged because it originated from the ruptured or translocated perichondrium. Thus, the possibility exists that the instability against the valgus stress could happen without avulsion or fragmentation of the medial epicondyle apophysis or the secondary ossification center. In addition, our data showed that 66.7% of players complained of pain after one specific throwing motion. This may indicate that the acute pathology of the initial medial elbow pain among preadolescent Little Leaguers is more often than we have recognized, and the principal pathology may be on the perichondrium.

We detected 11 abnormalities on X-ray imaging, while all subjects demonstrated some abnormal findings via HDMRI. One subject missed X-ray imaging; however, we decided to include it to the study because the findings of the HDMRI were valuable. Given that HDMRI had 100% sensitivity, nine out of 20 (45%) structural abnormalities on the medial elbow might have been missed via x-ray imaging. The example case is shown in Figs. 6 and 7. Wei et al. stated that the underlying etiology of Little Leaguer's elbow might be related not only to skeletal changes but also to the flexor-pronator muscles or the common tendon; thus, the X-ray imaging may understate the injury [16]. Yoshioka et al. showed that HDMRI with a small-diameter surface coil helped characterize the normal anatomy and depict injuries of the elbow [17]. MRI is an efficient tool to evaluate soft tissues, but Wei also stated that the MRI did not change the clinical management of Little Leaguer's elbow; thus, he did not recommend routine evaluation using MRI. Since little is known about the treatment of the ruptured or translocated perichondrium, the meaning of evaluating the medial elbow via MRI or HDMRI needs to be discussed further.

This study had several limitations. First, we only examined the symptomatic side of the elbow without considering an analysis of the unaffected part of the elbow. Second, we selected subjects with no previous history of elbow injury as far as they or their parents

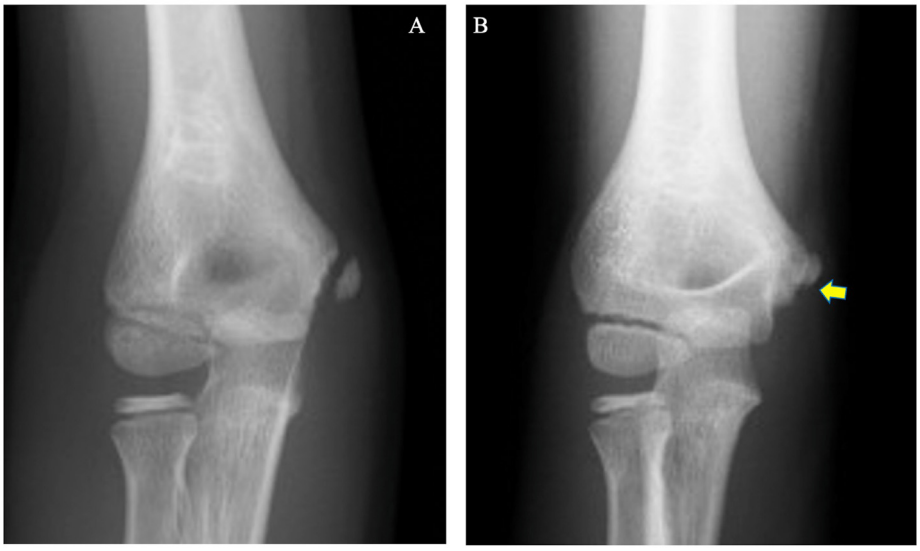

Fig. 6. Right elbow of a 9-year-old boy on the X-ray. A: anteroposterior (A–P) view with full extension. B: AP view with 45° of flexion. The avulsion at the tip of the ossification center of the medial epicondyle might be shown on B (arrow), but it was unclear on A.

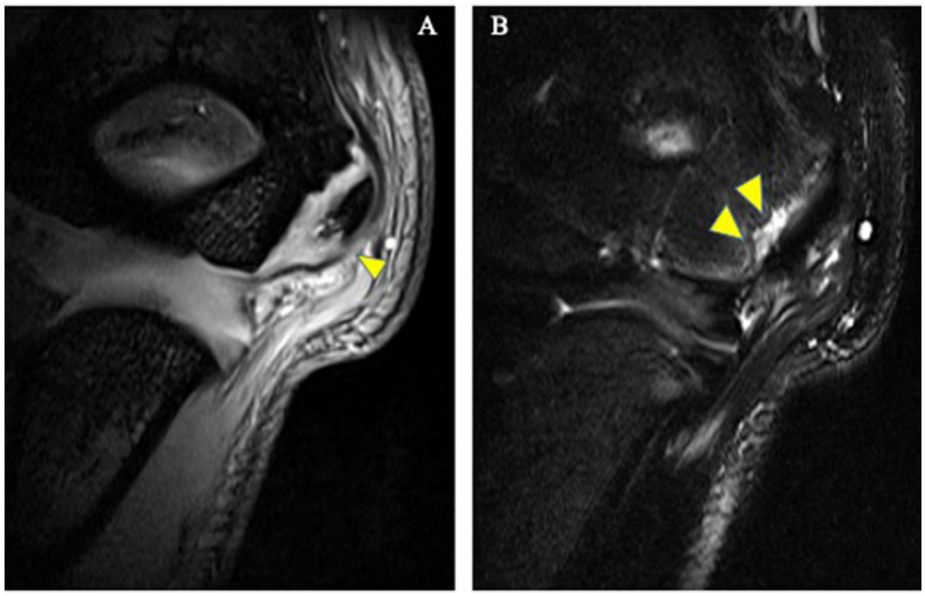

Fig. 7. 9-year-old boy (same patient as Fig. 4). A: HDMRI revealed the rupture of the perichondrium (T2*). B: HDMRI (T2FS) revealed the high signal intensity (arrow head). It shows an avulsion of the medial epicondyle apophysis.

could remember; there might be a bias. Actually, fragmentation at the secondary ossification center was observed in 15 cases; however, of these, three did not demonstrate signal hyperintensity at the region, which may indicate the presence of chronic changes. Third, we considered only 4-week-old HDMRI imaging and were unsure if the players had been symptomatic or not at the time of imaging; some players were symptomatic only when they performed overhead throwing. We did not encourage throwing as we were not aware of their symptoms. This means that they may have been asymptomatic on the day of HDMRI; therefore, our findings might have captured some normal variation. Fourth, the sample size was small and selected from outpatients of a single facility. Lastly, the perichondrium needs to be verified histologically.

5. Conclusion

The current study showed that the initial medial elbow injury in Little Leaguers without a history of previous elbow injury could be attributed to multi-structure injury, including perichondrium or UCL. Because the injuries were not limited to bony structures, HDMRI may be beneficial for the appropriate evaluation of medial elbow pain. Furthermore, medial elbow injuries in preadolescent baseball players could occur via acute trauma, which requires further study.

Declaration of competing interest

This work was supported by JSPS KAKENHI Grant Number JP19K11435.

Acknowledgments

The authors thank Katsutoshi Kobayashi and Takuya Hirochi, radiological technicians at the Mito Kyodo General Hospital, for their contributions to MRI analysis. In addition, we also thank Atsuko Taya, medical clerks at the Mito Kyodo General Hospital, for her contributions to data collection. Moreover, we would like to thank Editage for English language editing services.

References

[1] Fleisig GS, Andrews JR. Prevention of elbow injuries in youth baseball pitchers. Sports Health 2012 Sep;4(5):419–24.
[2] Chalmers PN, Erickson BJ, Ball B, Romeo AA, Verma NN. Fastball pitch velocity helps predict ulnar collateral ligament reconstruction in major league baseball pitchers. Am J Sports Med 2016 Aug;44(8):2130–5.
[3] Yukutake T, Kuwata M, Yamada M, Aoyama T. A preseason checklist for predicting elbow injury in little league baseball players. Orthop J Sport Med 2015 Jan 13;3(1):1–7.
[4] Hibberd E, Hoffer J, Brown R. Optimal management of ulnar collateral ligament injury in baseball pitchers. Open Access J Sport Med 2015 Nov 11:343–52.
[5] Pennock AT, Pytiak A, Stearns P, Roocroft JH, Dwek J, Kruk P, et al. Preseason assessment of radiographic abnormalities in elbows of little league baseball players. J Bone Jt Surg - Am 2016 May 4;98(9):761–7.
[6] Pytiak AV, Stearns P, Bastrom TP, Dwek J, Kruk P, Roocroft JH, et al. Are the current little league pitching guidelines adequate ? A single-season prospective MRI study. Orthop J Sports Med 2017 May 19;5(5).
[7] Norton R, Honstad C, Joshi R, Silvis M, Chinchilli V, Dhawan A. Risk factors for elbow and shoulder injuries in adolescent baseball players: a systematic review. Am J Sports Med 2019 Mar;47(4):982–90.
[8] Gregory B, Nyland J. Medial elbow injury in young throwing athletes. Muscles, Ligaments Tendons J 2013 Jul 9;3(2):91–100. Vol. 3.
[9] Mahure SA, Mollon B, Shamah SD, Kwon YW, Rokito AS. Disproportionate trends in ulnar collateral ligament reconstruction: projections through 2025 and a literature review. J Shoulder Elbow Surg 2016 Jun;25(6):1005–12.
[10] Barco R, Antuña SA. Medial elbow pain. EFORT Open Rev 2017 Aug 30;2(8):362–71.
[11] Hurd WJ, Eby S, Kaufman KR, Murthy NS. Magnetic resonance imaging of the throwing elbow in the uninjured, high school-aged baseball pitcher. Am J Sports Med 2011 Apr;39(4):722–8.
[12] Frank C, Shrive N, Phil D, Bray R. Ligament healing: a review of some current clinical and experimental concepts. Iowa Orthop J 1992;12(Mcl):21.
[13] Clayton M, Miles J, Abdulla M. Experimental investigations of ligamentous healing. Clin Orthop Relat Res 1968 Nov-Dec;61:146–53.
[14] Laor T, Jaramillo D. It's time to recognize the perichondrium. Pediatr Radiol 2020 Feb;50(2):153–60.
[15] Zell M, Dwek JR, Edmonds EW. Origin of the medial ulnar collateral ligament on the pediatric elbow. J Child Orthop 2013 Oct;7(4):323–8.
[16] Wei AS, Khana S, Limpisvasti O, Crues J, Podesta L, Yocum LA. Clinical and magnetic resonance imaging findings associated with little league elbow. J Pediatr Orthop 2010 Oct-Nov;30(7):715–9.
[17] Yoshioka H, Ueno T, Tanaka T, Kujiraoka Y, Shindo M, Takahashi N, et al. High-resolution MR imaging of the elbow using a microscopy surface coil and a clinical 1.5 T MR machine: preliminary results. Skeletal Radiol 2004 May;33(5):265–71.

Journal of Tissue Viability 30 (2021) 621–625

Contents lists available at ScienceDirect

Journal of Tissue Viability

journal homepage: www.elsevier.com/locate/jtv

Case report

Squamous cell carcinoma arising from an ischial pressure ulcer initially suspected to be necrotizing soft tissue infection: A case report

Takehiro Kasai [a,*], Tetsuya Isayama [a], Mitsuru Sekido [b]

[a] Department of Plastic and Reconstructive Surgery, National Hospital Organization Mito Medical Center, Ibaraki, 311-3193, Japan
[b] Department of Plastic and Reconstructive Surgery, Faculty of Medicine, University of Tsukuba, Ibaraki, 305-8576, Japan

ARTICLE INFO

Keywords:
Squamous cell carcinoma
Marjolin's ulcer
Pressure ulcer
Chronic wound
Tissue biopsy
Necrotizing soft tissue infection

ABSTRACT

Background: Pressure ulcers are the most common complications in bedridden patients or those with spinal cord injuries. Marjolin's ulcer refers to a malignant transformation arising from burn scars or chronic nonhealing wounds—such as pressure ulcers—over many years. Squamous cell carcinoma is the major histopathologic type of Marjolin's ulcer, and the gold standard for diagnosis is tissue biopsy. Medical professionals may have difficulty distinguishing pressure ulcers from Marjolin's ulcer, especially when the latter presents with invasive infections. Thus, malignant transformations arising from pressure ulcers are frequently overlooked. Herein, we describe a case of squamous cell carcinoma arising from pressure ulcers on the left ischium, which was initially identified as a necrotizing soft tissue infection.

Case report: A 59-year-old paraplegic patient presented with stage 3 left ischial pressure ulcer, which involves full-thickness skin loss and extends into deep subcutaneous tissue, and arrived at our hospital with suspected sepsis. Upon physical examination, the patient presented with fever and shivering. Initial examination and imaging findings revealed the presence of necrotizing soft tissue infections. Three weeks later, rapid increase in granulation in the deep part of the ulcer was observed. Samples from multiples ulcer sites were collected for tissue biopsy. Finally, histological examination revealed well-differentiated squamous cell carcinoma. The patient received radiation therapy and chemotherapy and died 11 months after the diagnosis.

Conclusion: Malignant transformations arising from pressure ulcers may closely resemble pressure ulcer infections. In these cases, tissue biopsies should be performed during primary care for the infection to exclude malignant transformations.

1. Introduction

Pressure ulcers are the most common complication in bedridden patients or those with spinal cord injuries because of lower body paralysis. Marjolin's ulcer refers to malignant transformations arising from burn scars and chronic nonhealing wounds, such as pressure ulcers, over many years [1,2]. Squamous cell carcinoma (SCC) is the major histopathologic type of Marjolin's ulcer [3]; the gold standard for its diagnosis is tissue biopsy of the chronic nonhealing wound [4].

However, malignant transformations arising from pressure ulcers are frequently overlooked. Physicians and medical professionals may have difficulty distinguishing pressure ulcers from Marjolin's ulcers upon physical examination, especially when the pressure ulcers present with invasive infections. This delay in diagnosis may result in a worse prognosis.

Herein, we describe a case of SCC arising from longstanding pressure ulcers on the left ischium initially identified as a necrotizing soft tissue infection (NSTI).

2. Case report

A 59-year-old paraplegic male patient was admitted with infective complications in a left ischial pressure ulcer. His paraplegia was caused by a traffic accident at the age of 20. Prior to being admitted to our hospital, he had undergone two operations for ischial pressure ulcers, at another hospital. The first operation was performed over 20 years ago and involved a right ischial pressure ulcer, while the second one was performed 19 years ago and involved a left ischial pressure ulcer. Once

* Corresponding author.Department of Plastic and Reconstructive Surgery, National Hospital Organization Mito Medical Center, Sakuranosato 280, ibaraki-machiHigashiibaraki-gun, Ibaraki-ken, 311-3193, Japan.
E-mail address: takehiro.kasai0725@gmail.com (T. Kasai).

https://doi.org/10.1016/j.jtv.2021.01.002
Received 26 November 2020; Accepted 3 January 2021
Available online 8 January 2021

these pressure ulcers were completely cured, approximately one year after the second surgery the recent left ischial pressure ulcer appeared close to the last left ischial pressure ulcer. This time, he was transferred to our hospital with suspected sepsis. The patient presented with a 6-cm slit-shaped left ischial pressure ulcer involving full-thickness skin loss and a 4-cm subcutaneous pocket extending into the deeper subcutaneous tissue (Fig. 1); the ulcer was classified as stage 3 according to the National Pressure Ulcer Advisory Panel [5].

Upon physical examination, the patient had a fever of 39.0 °C, tachycardia, and shivers. Laboratory examination revealed a white blood cell count of 12,800/μL, and C-reactive protein, hemoglobin, sodium, creatinine, and glucose levels of 20.05 mg/dL, 9.7 g/dL, 134 mmol/L, 0.46 mg/dL, and 101 mg/dL, respectively. The Laboratory Risk Indicator for Necrotizing Fasciitis score was 8 at admission, indicating a high risk of necrotizing fasciitis. Microbiological culture in the wound detected the presence of *Staphylococcus aureus*. His left gluteal region was slightly reddish and painful (Fig. 1). Initial examination and imaging findings showed the presence of NSTIs, from which the suspicion of sepsis originated. Upon computed tomography, abscess formation and the presence of gas were observed in the left gluteus maximus muscle (Fig. 2); subsequently, emergency debridement was performed and empiric antibiotic therapy was administered to treat the NSTI. The symptoms of infection rapidly improved thereafter (Fig. 3). After the infection completely subsided, negative pressure wound therapy was administered to his ischial tissue wound.

Four weeks after the first debridement, with the patient still hospitalized, a rapid increase in granulation tissue originating from the deep part of the wound was observed (Fig. 4). Samples from multiple wound and ulcer sites were collected for tissue and left lymph node biopsies. Finally, histological examination confirmed the diagnosis of well-differentiated SCC (Fig. 5).

Computed tomography revealed enlarged lymph nodes in the left groin and left common iliac areas. The tumor had likely spread to the patient's pelvic bones, left lung, or distant lymph nodes. The result of the left groin lymph node biopsy confirmed the diagnosis of metastatic SCC.

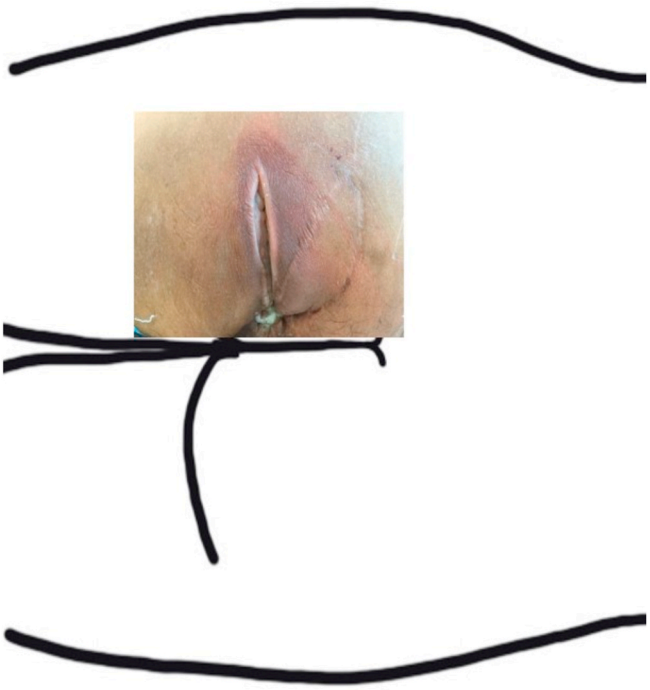

Fig. 1. Photo and schema of ulcer presentation. Patient presented with a slit-shaped pressure ulcer of approximately 6 cm. His left gluteal region was slightly reddish and warm to the touch.

After discussing with the patient and his family, the decision was made to attempt radiation therapy (50 Gy in 20 fractions) and chemotherapy. He received radiation therapy and chemotherapy (cisplatin 75 mg/m^2 and doxorubicin 50 mg/m^2). Eleven months after the SCC diagnosis, the patient died due to cancer-related complications.

3. Discussion

Marjolin's ulcer tends to be more aggressive and quicker to metastasize than other skin cancers. Moreover, Marjolin's ulcer has a higher fatality rate when malignant transformation occurs in pressure ulcers than in other chronic nonhealing wounds and burn scars [6]. Pressure ulcers undergo malignant transformation in 0.5% of cases [7], with a latency period of 20–22 years [6,10]. In contrast, burn scars undergo this transformation in 30–45 years [8–10]. Marjolin's ulcers arising from pressure ulcers resemble common pressure ulcers, resulting in difficulty in recognizing such transformation. This may cause delay in diagnosis and worse prognosis. Particularly, patients with spinal cord injuries have 2-year mortality rates of 67%–80% in cases of pressure ulcer-related malignancies [6,7,11].

The case presented herein allowed us to identify two important clinical issues. First, when the malignant transformation occurs under the skin and is accompanied by infections, the possibility of misdiagnosing it as pressure ulcer infections or NSTIs increases. In our case, the findings indicating infection, such as swelling and redness, were more prominent than those indicating malignant transformation, such as irregular granulation and malodor.

The characteristics of malignant transformation include everted wound edges, exophytic growth, irregular base or margin, excess granulation tissue extending beyond the wound margins, and translucent or shiny granulation tissue affecting the ulcer margins. Moreover, the patient may experience an increase in pain, bleeding, exudate, malodor, and ulcer size despite appropriate treatment [4,12]. A case report described the development of a tumor under normal skin after pressure ulcer operation [13]. Therefore, when characteristic features are not present and the malignant transformation occurs under the skin, physicians encounter increased difficulty in recognizing the malignancy at an early stage.

Despite the existence of few reports regarding pressure ulcer carcinoma accompanied by infection, a case report described a case of SCC arising from hidradenitis suppurativa that was initially misdiagnosed as NSTI [14]. In our case, the pressure ulcer lacked malignant characteristics and imaging examination showed abscess formation and the presence of gas in the left gluteus maximus muscle. Thus, in accordance with NSTI treatment guidelines, wound debridement was promptly performed. Pressure ulcer-related NSTIs have been reported to occur in regions such as the sacral region [15,16], with a recent Japanese study reporting a mortality rate of 38% for these cases [17]. Moreover, pressure ulcers significantly increase the risk of developing Fournier's gangrene, an NSTI of the perineum, in patients with spinal cord injuries [18]. Patients with grade 3 and 4 pressure ulcers also have a significantly increased risk of developing necrotizing fasciitis [15]. Thus, when the ulcer appears infected, the appropriate treatments—such as wide-open incision and drainage, lavage drainage, and debridement—should be quickly administered because of the infection rapid progress. When the pressure ulcer infection is severe, treatment of the infection requires priority.

The second important clinical issue involves excluding the possibility of a malignant tumor while treating infections. When the malignant transformation is accompanied by infections, the clinical picture may become obfuscated [14]. Therefore, physicians should actively investigate the presence of a malignant tumor in tandem with treating infections. Particularly, conducting multiple tissue biopsies of pressure ulcers in patients with spinal cord injuries undergoing long-term pressure ulcer treatment should be incorporated as a routine examination and part of the infection treatment protocol.

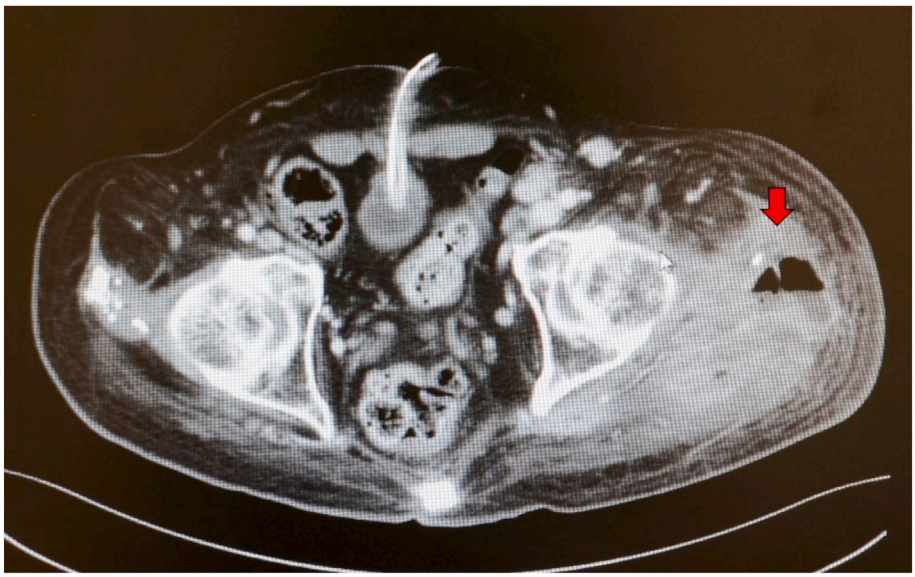

Fig. 2. Computed tomography scan of the patient's left gluteal muscle showing fluid retention and the presence of gas (red arrow). (For interpretation of the references to colour in this figure legend, the reader is referred to the Web version of this article.)

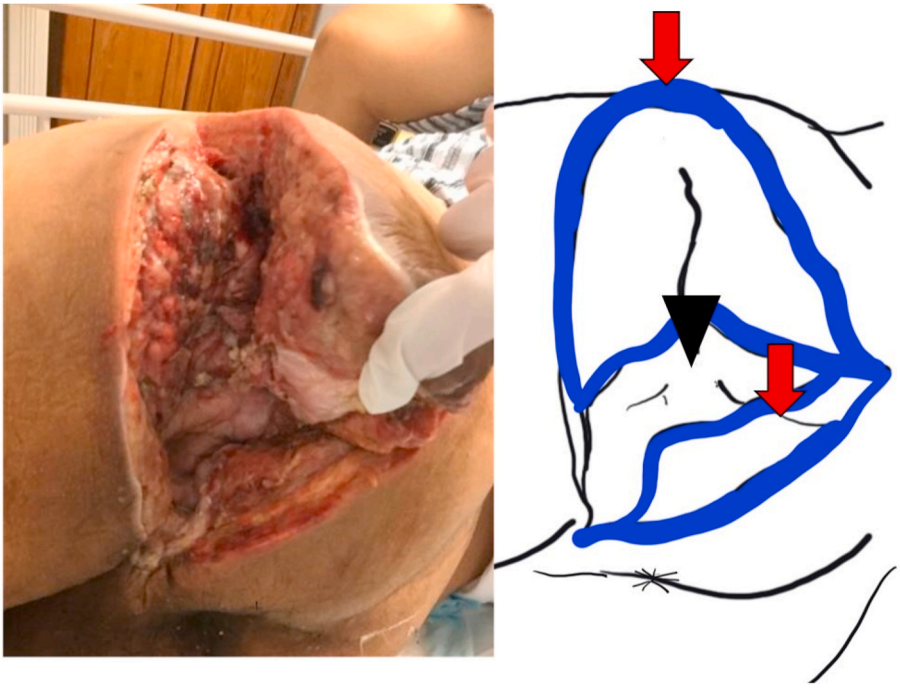

Fig. 3. Left: Patient's left ischial pressure ulcer after debridement. Right: Schema illustrating the debridement process; blue lines represent incisions; red arrows show debridement areas; Arrow head indicates primal pressure ulcer location. (For interpretation of the references to colour in this figure legend, the reader is referred to the Web version of this article.)

Generally, the prognosis of non-metastatic SCC is positive, with a 5-year survival rate of 90% [9] In contrast, the prognosis of Marjolin's ulcer or pressure ulcer-derived malignancy is poor [19,20]. The ratio of metastasis in pressure ulcer carcinomas has been reported as high as 61% [7]. Additionally, 80% of patients with this type of carcinoma died of recurrence within 18 months after operation [6]. This malignant transformation easily invades deep structures such as bones, causing hematogenous or lymphogenous metastases [21]. The sacral and gluteal areas have a rich lymphatic drainage system to the pelvic region, which explains the high lymphogenous metastatic rate [13]. This metastatic tendency results in advanced-stage malignancies at the time of diagnosis [4,21].

In patients with long-term pressure ulcers and spinal cord injuries, biopsies should be performed routinely to detect a possible malignancy at an early stage. Additionally, a single tissue biopsy may not reveal the presence of SCC [22]. Therefore, active tissue biopsies at multiple sites are important for early diagnosis and treatment and to ensure that a possible SCC will not be overlooked.

This disease will exist as long as patients do not receive adequate treatment for chronic nonhealing wounds. In addition, chronic wounds such as pressure ulcers will not decrease in the future as the number of bedridden patients increases as a result of an aging society. As illustrated

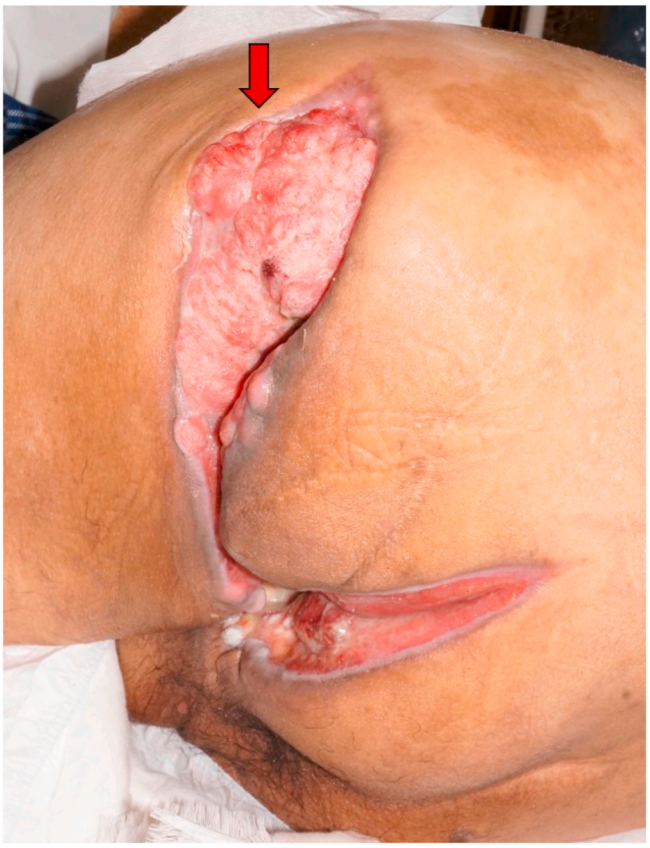

Fig. 4. Clinical Photo after 4 weeks. Everted wound edges, exophytic growth, and excess granulation tissue (red arrow) were observed in the debridement incisions. Tissue biopsies were performed using samples from multiple wound and ulcer sites. (For interpretation of the references to colour in this figure legend, the reader is referred to the Web version of this article.)

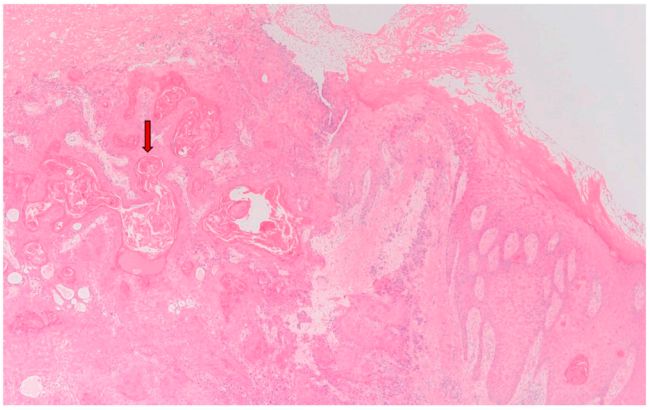

Fig. 5. Histopathology of the patient's left ischial pressure ulcer revealing a well-differentiated squamous cell carcinoma with infiltrative pattern areas and the presence of keratin pearls (red arrow) (magnification ×40; hematoxylin and eosin stain). (For interpretation of the references to colour in this figure legend, the reader is referred to the Web version of this article.)

by this case, overlooking malignant tumors originating from pressure ulcers may be fatal. On the other hand, this case seems to contribute to the improvement of pressure ulcer management in the future.

In conclusion, when pressure ulcer-derived malignant transformation occurs under the skin with concurrent infection, this malignancy may be overlooked and misdiagnosed as a pressure ulcer infection or NSTIs. To avoid a misdiagnosis, physicians must actively investigate the presence of a malignant tumor while treating the infection. Particularly, patients with spinal cord injuries undergoing long-term pressure ulcer treatment must undergo routine tissue biopsies at multiple ulcer sites.

Declaration of competing interest

None.

Acknowledgements

The authors would like to thank Y. Fujisawa M.D. Ph.D. and the staff of the Department of Dermatology, Faculty of Medicine, University of Tsukuba, for technical assistance with the treatments.

Appendix A. Supplementary data

Supplementary data to this article can be found online at https://doi.org/10.1016/j.jtv.2021.01.002.

Funding

This research did not receive any specific grant from funding agencies in the public, commercial, or not-for-profit sectors.

Ethical considerations

This study has been approved by the research ethics committee of National Hospital Organization Mito Medical Center (process number: 2020–80). Written informed consent was obtained from the patient for publication of this case report and accompanying images.

References

[1] Barr LH, Menard JW. Marjolin's ulcer. The LSU experience. Cancer 1983;52:173–5. https://doi.org/10.1002/1097-0142(19830701)52:1<173:AID-CNCR2820520131>3.0.CO.2-6.
[2] Esther RJ, Lamps L, Schwartz HS. Marjolin ulcers: secondary carcinomas in chronic wounds. J South Orthop Assoc 1999;8:181–7.
[3] Copcu E, Aktas A, Şişman N, Oztan Y. Thirty-one cases of Marjolin's ulcer. Clin Exp Dermatol 2003;28:138–41. https://doi.org/10.1046/j.1365-2230.2003.01210.x.
[4] Enoch S, Miller DR, Price PE, Harding KG. Early diagnosis is vital in the management of squamous cell carcinomas associated with chronic non healing ulcers: a case series and review of the literature. Int Wound J 2004;1:165–75. https://doi.org/10.1111/j.1742-4801.2004.00056.x.
[5] Edsberg LE, Black JM, Goldberg M, McNichol L, Moore L, Sieggreen M. Revised national pressure ulcer advisory Panel pressure injury staging system: revised pressure injury staging system. J Wound, Ostomy Cont Nurs 2016;43:585–97. https://doi.org/10.1097/WON.0000000000000281.
[6] Grotting JC, Bunkis J, Vasconez LO. Pressure sore carcinoma. Ann Plast Surg 1987;18:527–32. https://doi.org/10.1097/00000637-198706000-00012.
[7] Mustoe T, Upton J, Marcellino V, Tun CJ, Rossier AB, Hachend HJ. Carcinoma in chronic pressure sores: a fulminant disease process. Plast Reconstr Surg 1986;77:116–21. https://doi.org/10.1097/00006534-198601000-00017.
[8] Türegün M, Nişanci M, Güler M. Burn scar carcinoma with longer lag period arising in previously grafted area. Burns 1997;23:496–7. https://doi.org/10.1016/S0305-4179(97)00041-7.
[9] Tutela RR, Granick M, Benevenia J. Marjolin's ulcer arising in a pressure ulcer. Adv Skin Wound Care 2004;17:462–7. https://doi.org/10.1097/00129334-200411000-00010.
[10] Huang CY, Feng CH, Hsiao YC, Chuang SS, Yang JY. Burn scar carcinoma. J Dermatol Treat 2010;21:350–6. https://doi.org/10.3109/09546630903386580.
[11] Eltorai IM, Montroy RE, Kobayashi M, Jakowatz J, Guttierez P. Marjolin's ulcer in patients with spinal cord injury. J Spinal Cord Med 2002;25:191–6. https://doi.org/10.1080/10790268.2002.11753621.
[12] Khan K, Giannone AL, Mehrabi E, Khan A, Giannone RE. Marjolin's ulcer complicating a pressure sore: the clock is ticking. Am J Case Rep 2016;17:111–4. https://doi.org/10.12659/AJCR.896352.
[13] Knudsen MA, Biering-Sørensen F. Development of Marjolin's ulcer following successful surgical treatment of chronic sacral pressure sore. Spinal Cord 2008;46:239–40. https://doi.org/10.1038/sj.sc.3102090.
[14] Harview CL, Truong AK, Worswick SD, Sarantopoulos GP, Hsiao JL. Squamous cell carcinoma of the perineum masquerading as necrotizing hidradenitis suppurativa. Dermatol Online J 2018;24.
[15] Citak M, Backhaus M, Tilkorn DJ, O'Loughlin PF, Meindl R, Muhr G, et al. Necrotizing fasciitis in patients with spinal cord injury: an analysis of 25 patients.

Spine (Phila Pa 1976;36:E1225–9. https://doi.org/10.1097/BRS.0b013e3182059950. 2011.
[16] Mizokami F, Furuta K, Isogai Z. Necrotizing soft tissue infections developing from pressure ulcers. J Tissue Viability 2014;23:1–6. https://doi.org/10.1016/j.jtv.2013.11.001.
[17] Oonishi S, Koide T, Shiogama K, Tsutsumi Y. A case of decubitus-related gas-producing necrotizing fasciitis caused by group G β-hemolytic streptococcus. Japanese J Press Ulcers 2005;7:848–52.
[18] Backhaus M, Citak M, Tilkorn DJ, Meindl R, Schildhauer TA, Fehmer T. Pressure sores significantly increase the risk of developing a Fournier's gangrene in patients with spinal cord injury. Spinal Cord 2011;49:1143–6. https://doi.org/10.1038/sc.2011.75.
[19] Bostwick 3rd J, Pendergrast Jr WJ, Vasconez LO. Marjolin's ulcer: An immunologically privileged tumor? Plast Reconstr Surg 1976;57:66–9.
[20] Copcu E. Marjolin's ulcer: a preventable complication of burns? Plast Reconstr Surg 2009;124. https://doi.org/10.1097/PRS.0b013e3181a8082e. 156e–64e.
[21] Homma K, Sugihara T, Yoshida T, Ishikawa T, Minakawa H, Matsumoto T, et al. Pressure Sore Carcinoma -Report of five cases and review of the Japanese literature-. J Jpn. Soc Plast Reconstr Surg 1990;10:636–48.
[22] Pavlovic S, Wiley E, Guzman G, Morris D, Braniecki M. Marjolin ulcer: an overlooked entity. Int Wound J 2011;8:419–24. https://doi.org/10.1111/j.1742-481X.2011.00811.x.

IDCases 27 (2022) e01410

Contents lists available at ScienceDirect

IDCases

journal homepage: www.elsevier.com/locate/idcases

Case report

Emphysematous cystitis due to *Streptococcus salivarius* infection in a patient with a neurogenic bladder

Shuhei Okada, Yasushi Ichimura, Masahiro Iinuma*

Department of Urology, Mito Medical Center, 280 Sakuranosato, Ibaraki-machi, Higashi-Ibaraki-gun, Ibaraki-ken 311-3193, Japan

ARTICLE INFO

Article history:
Received 18 October 2021
Received in revised form 17 January 2022
Accepted 17 January 2022

Keywords:
Emphysematous cystitis
Streptococcus salivarius
Neurogenic bladder
Urinary tract infections
Putamen hemorrhage

ABSTRACT

Streptococcus salivarius (*S. salivarius*) is an oral commensal bacterium that rarely causes disease. Here, we report a case of emphysematous cystitis due to *S. salivarius* infection in a patient with a neurogenic bladder. A 56-year-old woman was hospitalized and managed for left putamen hemorrhage. Afterward, she developed poor oral intake. Although the patient was afebrile, laboratory test results suggested an inflammatory response. Urinalysis revealed pyuria and hematuria. Abdominal computed tomography revealed a thickened urinary bladder wall and intraluminal gas. Additionally, she was diagnosed with a neurogenic bladder as she had approximately 200 mL of residual urine. The patient was diagnosed with emphysematous cystitis, and *S. salivarius* was isolated from urine culture specimens. The patient's condition improved immediately after treatment, which included bladder drainage and administration of appropriate antibiotics. We could not find any report on *S. salivarius* causing urinary tract infections, such as emphysematous cystitis. Accordingly, we report this case along with a review of the literature.

Introduction

Streptococcus salivarius (*S. salivarius*) is a viridans streptococcus, that is relatively commonly isolated from the tongue, palate, and saliva. It has low pathogenicity and is occasionally isolated from the intestine or vagina. We could not find any report on *S. salivarius* causing urinary tract infections. Herein, we report a case of emphysematous cystitis due to *S. salivarius* infection, along with a review of the literature.

Case presentation

A 56-year-old female patient, who had been generally healthy, was admitted to the Department of Neurosurgery at our hospital and managed for a left putamen hemorrhage on February 5, 2020. There was no relevant family, medical, or medication history. She gradually recovered through conservative treatment and was scheduled to be transferred to another hospital for further rehabilitation. However, she developed poor oral intake around February 19, 2020, but was afebrile. The patient was referred to our department on February 22, 2020, following routine blood sampling and an abdominal computed tomography (CT) scan. The blood sample revealed an elevated inflammatory response, and the scan showed a thickened bladder wall and intraluminal gas.

Physical examination revealed a blood pressure of 135/82 mmHg, pulse rate of 106/min, SpO_2 of 96% (room air), and body temperature of 97.3 °F. Suprapubic tenderness was observed on abdominal palpation; however, bilateral costovertebral angle tenderness was not detected.

Laboratory findings

Elevated inflammatory response and renal dysfunction were observed. A complete blood count revealed a white blood cell count of 28,600/μL; the C-reactive protein (CRP) level was 47.2 mg/dL, while blood urea nitrogen and serum creatinine levels were 97.0 mg/dL and 2.49 mg/dL, respectively. Urinalysis revealed hematuria and pyuria. These findings are shown in Table 1.

Culture

Only *S. salivarius* was detected in the urine culture (10^6 CFU/mL). Four days were required for confirmation, and no drug resistance was observed. *Peptostreptococcus anaerobius* was detected in the blood cultures; however, it was thought to have resulted from contamination. This is because only one of the two sets of blood cultures was positive, and confirmation of findings took seven days. Notably, images of the culture media are unavailable.

* Corresponding author.
E-mail address: iinuma.masahiro.nv@mail.hosp.go.jp (M. Iinuma).

https://doi.org/10.1016/j.idcr.2022.e01410
2214-2509/

Table 1
Laboratory findings on February 22, 2021.

TP	7.3	g/dL	WBC	28,600	/μL
ALB	3.7	g/dL	RBC	4.88×10^6	/μL
AST	16	U/L	Hb	17.1	g/dL
ALT	37	U/L	Ht	50.6	%
ALP	485	U/L	MCV	103.7	fL
LDH	388	U/L	MCH	35.0	pg
T-BIL	1.3	mg/dL	MCHC	33.8	g/dL
BUN	97.0	mg/dL	PLT	306×10^3	/μL
CRE	2.49	mg/dL	PT	18.2	sec
CK	38	U/L	PT(INR)	1.43	
Na	143	mmol/L	APTT	49.8	sec
K	5.5	mmol/L	D-dimer	4.7	μ./mL
Cl	104	mmol/L			
CRP	47.2	mg/dL			

TP: total protein; ALB: albumin; AST: aspartate aminotransferase; ALT: alanine aminotransferase; ALP: alkaline phosphatase; LDH: lactate dehydrogenase; T-BIL: total bilirubin; BUN: blood urea nitrogen; CRE: creatinine; CK: creatine kinase; Na: sodium; K: potassium; Cl: chloride; CRP: C-reactive protein; WBC: white blood cell; RBC: red blood cell; Hb: hemoglobin; Ht: hematocrit; MCV: mean corpuscular volume; MCH: mean corpuscular hemoglobin; MCHC: mean corpuscular hemoglobin concentration; PLT: platelet; PT: prothrombin time; INR: international normalized ratio; APTT: activated partial thromboplastin time.

Imaging

A plain CT was performed after inserting an indwelling bladder catheter; therefore, the bladder was collapsed. The bladder wall was thickened compared to the previous CT scan performed on admission. In addition, perivesical fat stranding was observed (Fig. 1); however, perirenal fat stranding and hydronephrosis were not observed bilaterally. No other abnormal findings were observed. The bladder was considered the focus of inflammation, and air bubbles were observed around the bladder wall. Although iatrogenic gas contamination could not be ruled out, emphysematous cystitis was most suspected because of a severe inflammation localized to the bladder. Since other diseases could also cause gas contamination into the bladder, colovesical fistula and vesicovaginal fistula were ruled out based on CT findings. Since an abscess continuous from the umbilicus to the dome of the bladder was not observed, a urachal abscess was similarly ruled out.

Urination

Communication with the patient was difficult; however, according to her family, she experienced no disturbance on urination before admission. In addition, the CT scan on admission showed no thickening or deformation of the bladder wall. In our hospital, acute care physicians occasionally perform a whole-body CT scan regardless of chief complaints; however, it is not routine in many centers.

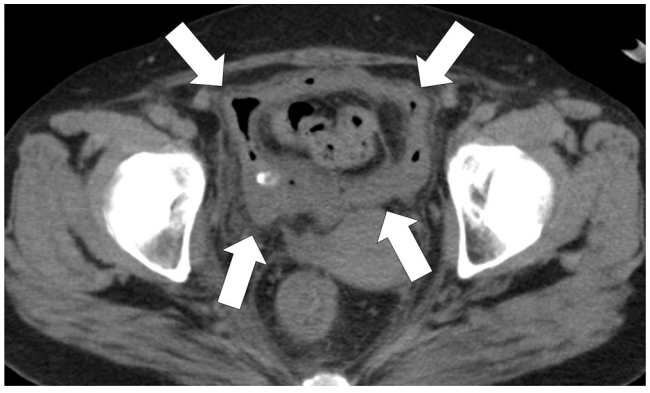

Fig. 1. Computed tomography after urethral catheterization. Arrows indicate the thickened bladder wall and air bubbles around the bladder wall (the axial slice).

An indwelling bladder catheter was inserted on February 5, 2020, and removed on February 10, 2020. On the day of catheter removal, the residual urine volume was 291 mL, which was measured only once. Afterward, her medical record did not report lower abdominal distension. However, nurses only checked whether or not the diaper was wet with urine, and the residual urine volume was not measured. The residual urine volume was approximately 250 mL when an indwelling bladder catheter was re-inserted on February 22, 2020. Therefore, we speculated that the residual urine volume was more than 200 mL after removing the indwelling bladder catheter. There was no history of diabetes mellitus or pelvic surgery. Therefore, increased residual urine volume was supposedly caused by a neurogenic bladder associated with the left putamen hemorrhage.

Diagnosis

Based on the above findings, we diagnosed the patient with emphysematous cystitis due to *S. salivarius* infection. Neurogenic bladder associated with left putamen hemorrhage is supposedly one of the causes of this disease.

Clinical course

Pyuria drainage was achieved by re-inserting an indwelling bladder catheter. Meropenem (2 g/day) and clindamycin (1200 mg/day) were administered intravenously from February 22, 2020. The dose of meropenem was reduced from 3 g/day to 2 g/day due to renal dysfunction. The inflammatory response and renal function gradually improved and were almost normalized on March 1, 2020 (white blood cell count: 6800/μL, C-reactive protein: 0.94 mg/dL, blood urea nitrogen: 9.1 mg/dL, and serum creatinine: 0.50 mg/dL). On March 2, 2020, we changed the antibiotic to levofloxacin (500 mg/day), based on antibiotic susceptibility testing. On March 15, 2020, levofloxacin was discontinued, and no relapse of the inflammatory reaction was observed (Fig. 2). The patient was transferred to another hospital for further rehabilitation on March 24, 2020. Since she could not perform intermittent self-catheterization, we inserted an indwelling bladder catheter. After hospital discharge, the patient was scheduled to be examined for neurogenic bladder at our department.

Discussion

Emphysematous cystitis is caused by gas-forming bacteria. The mean age of emphysematous cystitis occurrence is approximately 66 years, and it occurs twice as often in women than in men [1]. Diabetes mellitus and urinary stasis are well-recognized risk factors [2].

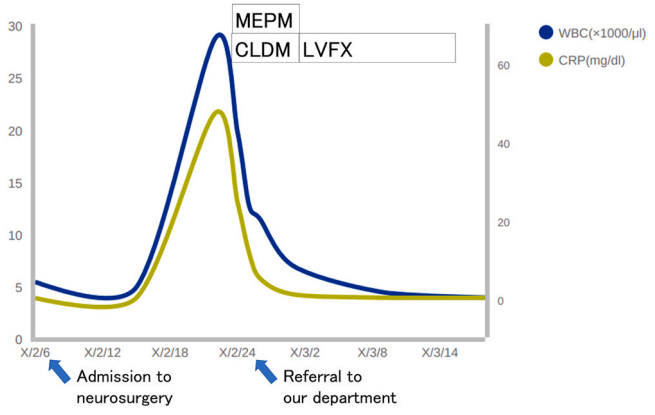

Fig. 2. Clinical course post-admission. MEPM, meropenem hydrate; CLDM, clindamycin phosphate; LVFX, levofloxacin hydrate.

In emphysematous cystitis, *Escherichia coli* and *Klebsiella pneumoniae* are often isolated from urine cultures [1]. As for the genus Streptococcus, group D streptococcus has been reported to cause emphysematous cystitis [1]. To the best of our knowledge, there are no reports of *S. salivarius* as the causative pathogen of urinary tract infections, such as emphysematous cystitis [3]. *S. salivarius* is a viridans streptococcus, which has low pathogenicity. It is relatively commonly isolated from the tongue, palate, and saliva, and is occasionally isolated from the intestine or vagina [4–6]. Its presence in the vagina is considered to inhibit the growth of Group B Streptococcus [4]. According to previous reports, it causes bacteremia, meningitis, endocarditis, sinusitis, and liver abscesses [5–10]. There are two possible mechanisms by which *S. salivarius* causes bacteremia: (1) iatrogenic contamination associated with an invasive procedure, such as spinal anesthesia, and (2) invasion associated with disruption of the gastrointestinal mucosa [5,11,12]. In this case, these mechanisms were unlikely because the patient did not have bacteremia. The route of infection was supposedly retrograde, with *S. salivarius* arising from feces or vaginal discharge. However, this was not verified since culture tests of feces and vaginal discharge were not performed. In addition, iatrogenic contamination of *S. salivarius* was possible through the saliva of medical staff during the insertion of an indwelling bladder catheter on admission. However, this is considered unlikely because all emergency room staff at our hospital wear personal protective equipment. As mentioned above, since plain CT was performed after inserting an indwelling bladder catheter, we could not deny the possibility of gas contamination. The collection of gas in the bladder wall, which is characteristic of emphysematous cystitis, was difficult to recognize because the bladder was collapsed. In addition, according to the medical record, the indwelling bladder catheter was inserted at 11:00 am, and the plain CT scan was performed at 2:00 pm. Thus, approximately 3 h had passed, during which the intramural and intraluminal gas may have decreased. However, emphysematous cystitis was suspected because of strong inflammation localized to the bladder. Although emphysematous cystitis is characterized by cobblestone and beaded-necklace appearance on abdominal X-ray [13], such findings may not be observed when an indwelling bladder catheter is inserted. Hence, CT is useful for establishing diagnoses, as in this case. Besides emphysematous cystitis, pyocystis (bladder abscess) also presents with strong inflammation localized to the bladder. However, pyocystis is unlikely in this case because it has been reported in oliguric patients, such as patients with supravesical urinary diversion or hemodialysis-dependent patients [14]. Although there is no report of emphysematous cystitis due to *S. salivarius* infection [1,2,15,16], *S. salivarius* can lead to gas formation. The urease system in *S. salivarius* breaks down urea to ammonia and CO_2 [17]. Since substances other than glucose are supposedly substrates for gas formation, it is feasible that urea was a substrate for gas formation in this case. The initial management of emphysematous cystitis consists of drainage of the bladder by catheter placement, appropriate antibiotics administration, and treatment of predisposing conditions, such as glycemic control [15]. If these treatments are ineffective, surgical treatment, including cystectomy, may be required [15]. The overall death rate from emphysematous cystitis has been reported to be approximately 7%; however, if emphysematous pyelonephritis occurs, the mortality rate increases to 14–20% [1,15]. Therefore, early detection of emphysematous cystitis is desirable. Additionally, we considered what could have been done to diagnose this case earlier. Emphysematous cystitis can vary from asymptomatic cases to sepsis. The frequent chief complaints of patients with emphysematous cystitis are suprapubic pain, gross hematuria, fever, and pneumaturia [15]. In this case, gross hematuria was not observed, and the patient had been afebrile. Due to the acute left putamen hemorrhage, it was difficult for the patient to complain of suprapubic pain. If pneumaturia existed, it was difficult to recognize because she was incontinent. In addition, even if she had residual urine retention, it was difficult to complain because of the acute left putamen hemorrhage. Therefore, in the acute phase of cerebrovascular disease, residual urine measurement and urinalysis after removing an indwelling bladder catheter should be performed periodically to prevent emphysematous cystitis.

Conclusion

We reported a case of emphysematous cystitis due to *S. salivarius* infection in a patient with a neurogenic bladder. We could not find any reports of *S. salivarius* causing urinary tract infections, including emphysematous cystitis. Infectious diseases can be detected by clinical signs and blood work in afebrile patients as well. In the acute stage of cerebrovascular disease, it may be difficult for a patient to complain of bladder irritability or suprapubic pain. Therefore, emphysematous cystitis should be understood not only by urologists but also by neurologists.

Ethical approval

This study has been approved by the institutional review board of Mito medical center.

Funding

This research did not receive any specific grant from funding agencies in the public, commercial, or not-for-profit sectors.

CRediT authorship contribution statement

Shuhei Okada: Conceptualization, Investigation, Writing – original draft. **Yasushi Ichimura:** Conceptualization, Investigation. **Masahiro Iinuma:** Writing – review & editing, Supervision, Project administration.

Declaration of interest

None.

Acknowledgments

None.

Approval of research protocol

Not applicable.

Consent

Written informed consent was obtained from the patient for publication of this case report and accompanying images. A copy of the written consent is available for review by the Editor-in-Chief of this journal on request.

Registry and registration number

Not applicable.

References

[1] Schicho A, Stroszczynski C, Wiggermann P. Emphysematous cystitis: mortality, risk factors, and pathogens of a rare disease. Clin Pract 2017;7:54–5. https://doi.org/10.4081/cp.2017.930

[2] Adeyemi OA, Flaherty JP. Emphysematous cystitis. Cureus 2020;12:e11723https://doi.org/10.7759/cureus.11723

[3] Facklam R. What happened to the streptococci: overview of taxonomic and nomenclature changes. Clin Microbiol Rev 2002;15:613–30. https://doi.org/10.1128/CMR.15.4.613-630.2002
[4] Patras KA, Wescombe PA, Rösler B, Hale JD, Tagg JR, Doran KS. Streptococcus salivarius K12 limits Group B Streptococcus vaginal colonization. Infect Immun 2015;83:3438–44. https://doi.org/10.1128/IAI.00409-15
[5] Legier JF. Streptococcus salivarius meningitis and colonic carcinoma. South Med J 1991;84:1058–9. https://doi.org/10.1097/00007611-199108000-00031
[6] Elsawy AM, Faidah HS, Redwan EM. Streptococcus salivarius meningitis in immunocompetent: a case report. Int Arch Med Microbiol 2018;1. https://doi.org/10.23937/iamm-2017/1710004
[7] Nilson B, Olaison L, Rasmussen M. Clinical presentation of infective endocarditis caused by different groups of non-beta haemolytic streptococci. Eur J Clin Microbiol Infect Dis 2016;352:215–8. https://doi.org/10.1007/s10096-015-2532-5
[8] Radosz-Komoniewska H, Kapp-Burzyńska Z, Kłaptocz B, Wilk I, Ekiel A. Tlenowa i beztlenowa flora bakteryjna w przewlekłym zapaleniu zatok przynosowych u dorosłych [Aerobic and anaerobic bacterial flora in chronic sinusitis in adults]. Med Dosw Mikrobiol 1997;49:89–94.
[9] Ruiz-Tovar J, Gamallo C. Streptococcus salivarius causing multiple liver abscesses in a patient with situs inversus. Surg Infect 2012;132:130–1. https://doi.org/10.1089/sur.2011.082
[10] Kamachi S, Otsuka T, Tsuji C, Nakashita S, Ide Y, Mizuta T. A case of multiple liver abscesses associated with Streptococcus salivarius in a patient with chronic periodontitis. Nihon Shokakibyo Gakkai Zasshi Jpn J Gastro-Enterol 2014;111:1602–8.
[11] Veringa E, van Belkum A, Schellekens H. Iatrogenic meningitis by Streptococcus salivarius following lumbar puncture. J Hosp Infect 1995;29:316–8. https://doi.org/10.1016/0195-6701(95)90283-x
[12] Idigoras P, Valiente A, Iglesias L, Trieu-Cout P, Poyart C. Meningitis due to Streptococcus salivarius. J Clin Microbiol 2001;39:3017. https://doi.org/10.1128/JCM.39.8.3017.2001
[13] Middela S, Green E, Montague R. Emphysematous cystitis: radiological diagnosis of complicated urinary tract infection. BMJ Case Rep 2009;bcr05.2009:1832. https://doi.org/10.1136/bcr.05.2009.1832
[14] Elsayed M, Finn A, Dapaah-Afriyie K. Unusual organism causing pyocystis in an immunosuppressed haemodialysis patient. BMJ Case Rep 2016;bcr2015214264. https://doi.org/10.1136/bcr-2015-214264
[15] Amano M, Shimizu T. Emphysematous cystitis: a review of the literature. Intern Med 2014;53:79–82. https://doi.org/10.2169/internalmedicine.53.1121
[16] Thomas AA, Lane BR, Thomas AZ, Remer EM, Campbell SC, Shoskes DA. Emphysematous cystitis: a review of 135 cases. BJU Int 2007;100:17–20. https://doi.org/10.1111/j.1464-410X.2007.06930.x
[17] Zlatkovic N, Aleksić G, Gašić K. Biology of oral streptococci. Microbiol Spectr 2018;6. https://doi.org/10.1128/microbiolspec.GPP3-0042-2018

Case Report

Extramedullary plasmacytoma of the ureter

Shuhei Okada, Yasushi Ichimura and Masahiro Iinuma

Department of Urology, Mito Medical Center, Higashiibaraki-gun, Ibaraki-ken, Japan

Abbreviations & Acronyms
AMY = amylase
CT = computed tomography
EAU = European Association of Urology
EMP = extramedullary plasmacytoma
Ig = immunoglobulin
SBP = solitary bone plasmacytoma
T-BIL = total bilirubin
UC = urothelial carcinoma
UTUC = upper tract urothelial carcinoma

Correspondence: Masahiro Iinuma, M.D., Department of Urology, Mito Medical Center, 280 Sakuranosato, Ibaraki-machi, Higashiibaraki-gun, Ibaraki-ken 311-3193, Japan.
Email: iinuma.masahiro.nv@mail.hosp.go.jp

How to cite this article: Okada S, Ichimura Y, Iinuma M. Extramedullary plasmacytoma of the ureter. *IJU Case Rep*. 2021; https://doi.org/10.1002/iju5.12373.

Received 26 July 2021; accepted 30 August 2021.

Introduction: We report a rare case of an extramedullary plasmacytoma of the ureter.
Case presentation: A 77-year-old man was referred to our hospital because of left hydronephrosis. Computed tomography showed a tumor in the left ureter, and tumor invasion into the periureteric fat was suspected. Urine cytology showed Eatypical cells whose nuclei were hyperchromatic (class IIIb). The left ureteral tumor was diagnosed as urothelial carcinoma (cT3N0M0) preoperatively. Subsequently, we performed laparoscopic radical nephroureterectomy with bladder cuff excision. The tumor was pathologically diagnosed as a plasmacytoma. Postoperative positron emission tomography did not reveal abnormal uptake, and bone marrow aspiration findings were normal. Consequently, the left ureter tumor was diagnosed as an extramedullary plasmacytoma of the ureter.
Conclusion: Extramedullary plasmacytoma commonly occurs in the upper respiratory tract or upper gastrointestinal tract. Extramedullary plasmacytoma of the ureter is rare. This is only the fourth reported case of extramedullary plasmacytoma of the ureter.

Key words: extramedullary plasmacytoma, hydronephrosis, tumor, ureter, urothelial carcinoma.

Keynote message

The ureter is a rare location for an EMP. Therefore, preoperative diagnosis is challenging. To the best of our knowledge, this is only the fourth reported case of EMP of the ureter.

Introduction

Solitary plasmacytoma is defined as a localized mass of neoplastic monoclonal plasma cells. EMP arises from soft tissue throughout the body. An EMP often occurs in the upper respiratory or gastrointestinal tract, accounting for approximately 80% of cases.[1] The ureter is a rare location for an EMP. Here, we report a case of a primary EMP of the ureter.

Case presentation

A 77-year-old man who presented with abdominal pain was referred to our hospital because an ultrasound sonogram revealed left hydronephrosis. The patient's height was 165.5 cm and his body weight was 55.45 kg. The patient's medical history included constipation, hyperuricemia, benign prostatic hyperplasia, auditory disturbance, and lower back pain. The patient's regular medications included elobixibat hydrate, febuxostat, silodosin, loxoprofen sodium hydrate, and senna. Regarding family history, the patient's father died of lung cancer and his mother died of unknown causes. The patient had smoked 20 cigarettes per day for 10 years. CT revealed a tumor in the left ureter with a diameter of approximately 2.5 cm (Fig. 1). Tumor invasion into the periureteric fat was suspected. Distant metastasis and regional node involvement were not found on CT. Urine cytology showed atypical cells whose nuclei were hyperchromatic (class IIIb). UC was suspected. The left ureteral tumor was diagnosed as UC (cT3N0M0) preoperatively.

An increased level of creatinine was observed (1.96 mg/dL). Laboratory findings are shown in Table 1. This renal impairment was partly due to atrophy of the right kidney. Segmental ureterectomy was considered to be challenging because the diameter of the left ureteral tumor was approximately 2.5 cm and tumor invasion into the periureteric fat was suspected. Subsequently, we performed laparoscopic radical nephroureterectomy with bladder cuff excision.

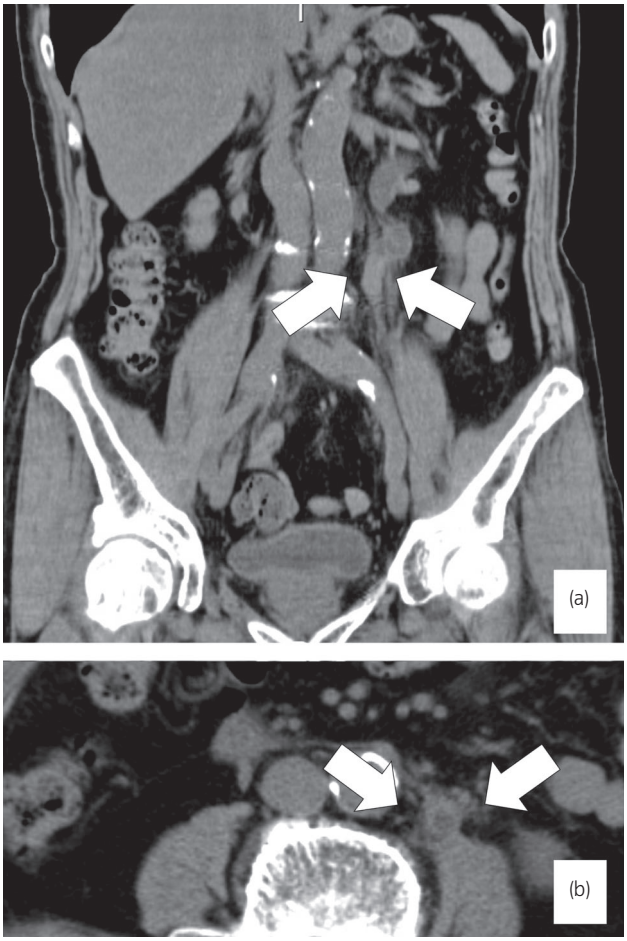

Fig. 1 Abdominal CT image showing a left ureteral mass (arrows) causing hydronephrosis. (a) Coronal view. (b) Axial view.

Table 1 Laboratory findings

TP	7.4	g/dL	WBC	5200	/μL
ALB	4.1	g/dL	RBC	4.12×10^6	/μL
AST	14	U/L	Hb	12.1	g/dL
ALT	8	U/L	Ht	36.5	%
ALP	281	U/L	MCV	88.6	fl
LDH	179	U/L	MCH	29.4	pg
T-BIL	0.5	mg/dL	MCHC	33.2	g/dL
BUN	26.1	mg/dL	PLT	256×10^3	/μL
CRE	1.96	mg/dL	PT	13.8	sec
UA	6.4	mg/dL	PT(INR)	1.05	
AMY	48	IU/L	APTT	38.5	sec
Na	140	mmol/L			
K	4.8	mmol/L			
Cl	108	mmol/L			
Ca	9.0	mg/dL			
CRP	0.49	mg/dL			

Although the serum creatinine level increased to 3.75 mg/dL after surgery, hemodialysis was not required. He was discharged on postoperative day 13. Macroscopically, a solid tumor (20 × 15 mm) was observed in the middle of the left ureter. Histopathological findings revealed inflammatory cell infiltration and atypical cells, which included numerous eosinophil granules (Fig. 2). No UC component was observed in the tumor. Immunohistochemical staining revealed that atypical cells were positive for CD138 and CD79a, characteristic markers of B cells or plasma cells. In addition, we detected light chain restriction (Igκ > Igγ). Therefore, the left ureter tumor was pathologically diagnosed as a plasmacytoma.

After the diagnosis of EMP, the patient was referred to a hematologist. A postoperative positron emission tomography scan did not show abnormal uptake, and bone marrow aspiration findings were normal. No monoclonal protein was detected in the patient's blood and urine. Therefore, we diagnosed the left ureter tumor as a primary EMP of the ureter. The patient survived without renal replacement therapy and showed no evidence of multiple myeloma, local recurrence, or distant metastasis until 22 months after surgery.

Discussion

Solitary plasmacytoma is defined as a localized mass of neoplastic monoclonal plasma cells. SBP is characterized by a sole lesion of bone. EMP arises from soft tissue throughout the body.[1] The International Myeloma Working Group defines EMP using the following criteria: (i) a tumor comprising of monoclonal plasma cells in a single extramedullary site, (ii) no lesion in the whole-body bone, (iii) no lesion in the bone marrow, (iv) no involvement of organs, and (v) no monoclonal Ig in serum or urine.[2] Since our patient met the above criteria, the left ureter tumor was diagnosed as a primary EMP of the ureter. An EMP usually occurs in the upper respiratory or gastrointestinal tract, accounting for approximately 80% of cases.[3] The ureter is a rare location for an EMP. To the best of our knowledge, this is only the fourth reported case of EMP of the ureter (Table 2). Compared with EMP, SBP has a significantly higher risk for progression to multiple myeloma than EMP. Therefore, SBP has poor prognosis in comparison with EMP. Symptoms of EMP vary depending on the tumor occurrence site. Alexiou *et al.*[4] reported approximately 65% of EMP had no recurrence and did not progress to multiple myeloma after treatment. Younger age was reported as a good independent prognostic factor.[5] In contrast, anaplastic type plasmacytoma, a higher histologic grade, and a high level of angiogenesis were reported as poor prognostic factors.[6,7] Solitary plasmacytoma is highly radiosensitive. It has been reported that a local control rate of 94% was achieved by doses over 40 Gy.[8] Radiotherapy should encompass the primary tumor with a margin of at least 2 cm.[9] Adjuvant chemotherapy might be considered for the tumor larger than 5 cm and/or of a high histological grade.

Complete resection of EMP is considered equivalent to radiotherapy. Since EMP is a highly radiosensitive tumor, postoperative radiotherapy is recommended for patients with inadequate surgical margins or local recurrence. Our case was diagnosed as a UC before surgery. As the diameter of the left ureteral tumor was approximately 2.5 cm and tumor invasion into the periureteric fat was suspected, segmental ureteral resection was considered challenging; therefore, we performed laparoscopic radical nephroureterectomy with bladder cuff excision. Although Landsmann *et al.*[10] reported segmental ureter resection and ureterocystostomy for an EMP of the

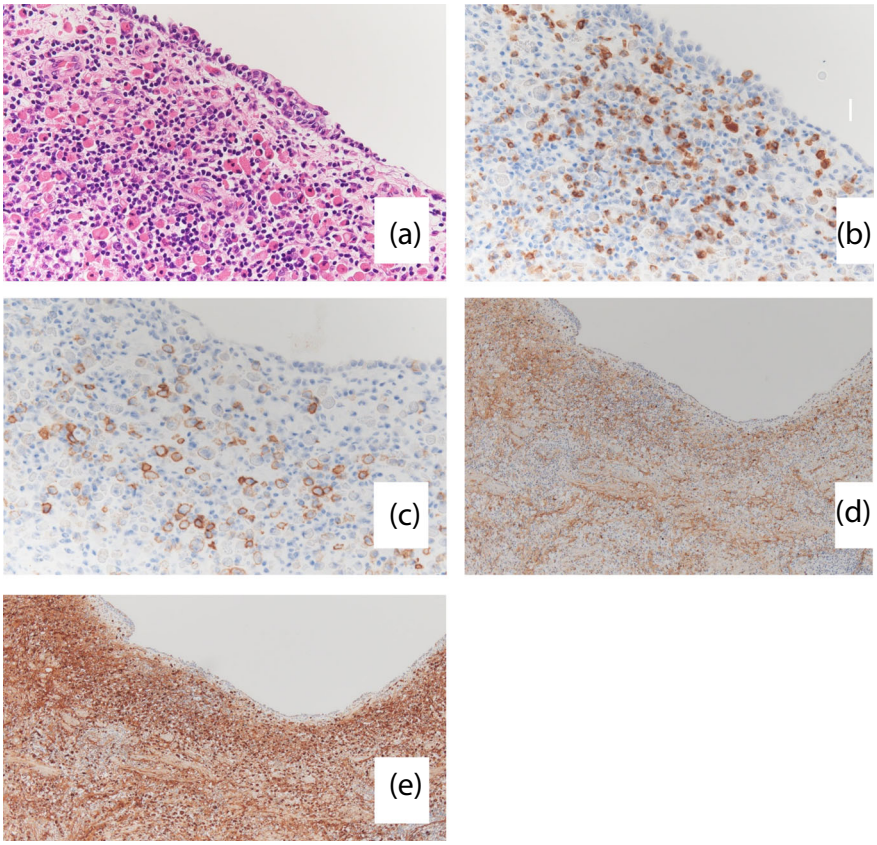

Fig. 2 Hematoxylin and eosin staining showing (a) inflammatory cell infiltration and atypical cells, which include numerous eosinophil granules, and tumor cells positive for (b) CD79a, (c) CD138, (d) Igλ, and (e) Igκ. Staining is more pronounced for Igκ than for Igλ (light chain restriction). Magnification, ×100.

Table 2 Clinical features of reported cases of EMP of the ureter

Case number	1	2	3	4
Authors	Landsmann S	Klein T	Nagai T	Okada S
Year	2009	2010	2016	2021
Age	80	82	45	77
Sex	Female	Female	Male	Male
Chief complaint	Renal colic	Hematuria	Hematuria	Abdominal pain
Preoperative ureteroscopy	Not mentioned	Not performed	Not performed	Not performed
Preoperative diagnosis	Not mentioned	Not mentioned	UC (cT2N0M0)	UC (cT3N0M0)
Treatment	Segmental ureterectomy	Nephro-ureterectomy (open)	Nephro-ureterectomy (laparoscopic)	Nephro-ureterectomy (laparoscopic)
Follow-up (months)	Not mentioned	Not mentioned	5	22
Postoperative dialysis	Not required	Not required	Not required	Not required
Outcome	No evidence of disease	No evidence of disease	No evidence of disease	No evidence of disease

ureter, Klein *et al.*[11] and Nagai *et al.*[3] reported that radical nephroureterectomy with bladder cuff excision was performed because UC was suspected before surgery.

The EAU guidelines on upper UTUC define high-risk UTUC by the following criteria: (i) multifocal disease, (ii) tumor size ≥2 cm, (iii) high-grade cytology, (iv) high-grade ureterorenoscopy biopsy, (v) local invasion on CT, (vi) hydronephrosis, (vii) previous radical cystectomy for high-grade bladder cancer, and (viii) variant histology. Our case met three of these high-risk UTUC criteria: tumor size ≥2 cm, local invasion on CT, and hydronephrosis. Per the EAU guidelines on UTUC, radical nephroureterectomy is the standard treatment for high-risk UTUC in the middle or proximal ureter. Therefore, we performed laparoscopic radical nephroureterectomy. Indeed, without a biopsy of the ureteral tumor, preoperative diagnosis of an EMP of the ureter is almost impossible. The differential diagnoses for ureteral tumors include UC, EMP, neuroendocrine tumor, metastatic tumor, paraganglioma, fibroepithelial polyp, and inflammatory myofibroblastic tumor. Among these tumors, EMP is a highly

radiosensitive tumor.[12–16] If we had preoperatively diagnosed the ureteral tumor as EMP, we would have been able to choose radiotherapy instead of nephroureterectomy. We did not perform diagnostic ureteroscopy because we considered the left ureteral tumor as a high-risk UTUC before surgery. In addition, the use of diagnostic ureteroscopy has been associated with a higher risk of developing bladder recurrence after radical nephroureterectomy.[17,18] The possibility of cancer dissemination has also been reported.[18–20] Segmental ureteral resection is considered as another treatment option.[21] In segmental ureteral resection for the tumor in the middle or proximal ureter, when end-to-end anastomosis of the ureter is challenging, an ileal-ureteral substitution is required, which is technically challenging and more invasive.

In our case, the tumor size was ≥2 cm and tumor invasion into the periureteric fat was suspected on preoperative CT. Segmental ureteral resection was considered challenging. Therefore, we performed laparoscopic radical nephroureterectomy. However, if we had preoperatively diagnosed the ureteral tumor as EMP, we would have been able to choose radiotherapy instead of nephroureterectomy.

Conclusion

We report a rare case of a primary EMP of the ureter. The patient survived without recurrence after laparoscopic radical nephroureterectomy.

Conflict of interest

The authors declare no conflict of interest.

Approval of the research protocol by an Institutional Reviewer Board

Not applicable.

Informed consent

Informed consent for publication was obtained from the patient.

Registry and the Registration No. of the study/trial

Not applicable.

References

1 Kilciksiz S, Karakoyun-Celik O, Agaoglu FY, Haydaroglu A. A review for solitary plasmacytoma of bone and extramedullary plasmacytoma. *Sci. World J.* 2012; **2012**: 895765.
2 International Myeloma Working Group. Criteria for the classification of monoclonal gammopathies, multiple myeloma and related disorders: a report of the International Myeloma Working Group. *Br. J. Haematol.* 2003; **121**: 749–57.
3 Nagai T, Okamura T, Taki Y *et al*. Extramedullary plasmacytoma of the ureter in an HIV-positive patient. *Int. Cancer Conf. J.* 2017; **6**: 171–4.
4 Alexiou C, Kau RJ, Dietzfelbinger H *et al*. Extramedullary plasmacytoma: tumor occurrence and therapeutic concepts. *Cancer* 1999; **85**: 2305–14.
5 Kilciksiz S, Celik OK, Pak Y *et al*. Clinical and prognostic features of plasmacytomas: a multicenter study of Turkish Oncology Group-Sarcoma Working Party. *Am. J. Hematol.* 2008; **83**: 702–7.
6 Kumar S, Fonseca R, Dispenzieri A *et al*. Prognostic value of angiogenesis in solitary bone plasmacytoma. *Blood* 2003; **101**: 1715–7.
7 Susnerwala SS, Shanks JH, Banerjee SS, Scarffe JH, Farrington WT, Slevin NJ. Extramedullary plasmacytoma of the head and neck region: clinicopathological correlation in 25 cases. *Br. J. Cancer* 1997; **75**: 921–7.
8 Mendenhall CM, Thar TL, Million RR. Solitary plasmacytoma of bone and soft tissue. *Int. J. Radiat. Oncol. Biol. Phys.* 1980; **6**: 1497–501.
9 Soutar R, Lucraft H, Jackson G *et al*. Guidelines on the diagnosis and management of solitary plasmacytoma of bone and solitary extramedullary plasmacytoma. *Clin. Oncol.* 2004; **2004**: 405–13.
10 Landsmann S, Todorov J, Streitberg U, Seitz G, Weingärtner K. Plasmocytoma of the ureter – a rare cause of hydronephrosis: case report and review of the literature. *Aktuelle Urol.* 2009; **40**: 175–8.
11 Klein T, Holz A, Neid M, Hinkel A, Noldus J. The first description of an extramedullary plasmacytoma of the ureter. *Urol. Int.* 2010; **84**: 122–4.
12 Li F, Guo H, Qiu H *et al*. Ureteral inflammatory myofibroblastic tumor: a case report and literature review. *Medicine* 2018; **97**: e13177.
13 Wang Z, Yang J *et al*. Primary retroperitoneal paraganglioma mimicking a ureteral tumor: a case report and literature review. *Postgrad. Med.* 2020; **132**: 657–61.
14 Hu J, Deng J, Guo J, Fu B. Ureteral involvement by metastatic malignant disease. *Clin. Exp. Metastasis* 2019; **36**: 499–509.
15 Wang H, Ma C, Jie W *et al*. Clinicopathologic features of the ureteral neuroendocrine tumors. *Pathol. Res. Pract.* 2020; **216**: 152788.
16 Gupta M, Roy S, Wann C *et al*. Giant fibroepithelial polyp of the ureter. *BMJ Case Rep.* 2017; **2017**: bcr2016218999.
17 Marchioni M, Primiceri G, Cindolo L *et al*. Impact of diagnostic ureteroscopy on intravesical recurrence in patients undergoing radical nephroureterectomy for upper tract urothelial cancer: a systematic review and meta-analysis. *BJU Int.* 2017; **120**: 313–9.
18 Guo RQ, Hong P, Xiong GY *et al*. Impact of ureteroscopy before radical nephroureterectomy for upper tract urothelial carcinomas on oncological outcomes: a meta-analysis. *BJU Int.* 2018; **121**: 184–93.
19 Hendin BN, Streem SB, Levin HS, Klein EA, Novick AC. Impact of diagnostic ureteroscopy on long-term survival in patients with upper tract transitional cell carcinoma. *J. Urol.* 1999; **161**: 783–5.
20 Territo A, Gallioli A, Meneghetti I *et al*. Diagnostic ureteroscopy for upper tract urothelial carcinoma: friend or foe? *Arab. J. Urol.* 2021; **19**: 46–58.
21 Ou YC, Hu CY, Cheng HL, Yang WH. Long-term outcomes of total ureterectomy with ileal-ureteral substitution treatment for ureteral cancer: a single-center experience. *BMC Urol.* 2018; **18**: 73.

Cureus

Open Access Original Article

DOI: 10.7759/cureus.22421

Effects of Magnetic Resonance Imaging With Axial Traction of the Thumb Carpometacarpal Joint on Articular Cartilage Visibility: A Feasibility Study

Review began 01/28/2022
Review ended 02/13/2022
Published 02/21/2022

Akira Ikumi [1, 2], Sho Kohyama [3], Shun Okuwaki [2], Masaki Tatsumura [1], Yuki Hara [4], Takeo Mammoto [1], Takeshi Ogawa [5], Yuichi Yoshii [6], Haruo Kawamura [2], Masashi Yamazaki [4]

1. Department of Orthopedic Surgery and Sports Medicine, Tsukuba University Hospital Mito Clinical Education and Training Center, Ibaraki, JPN 2. Department of Orthopedic Surgery, Kenpoku Medical Center Takahagi Kyodo Hospital, Ibaraki, JPN 3. Department of Orthopedic Surgery, Kikkoman General Hospital, Chiba, JPN 4. Department of Orthopedic Surgery, Faculty of Medicine, University of Tsukuba, Ibaraki, JPN 5. Department of Orthopedic Surgery, National Hospital Organization, Mito Medical Center, Ibaraki, JPN 6. Department of Orthopedic Surgery, Tokyo Medical University Ibaraki Medical Center, Ibaraki, JPN

Corresponding author: Akira Ikumi, ikumi@tsukuba-seikei.jp

Abstract

Objectives

The objective of this study was to verify the usefulness of magnetic resonance imaging (MRI) with axial traction of the thumb for observing articular cartilage.

Materials and methods

Eleven healthy adult volunteers (39.7 ± 7.4 years) without thumb carpometacarpal joint arthritis or trauma were included in this study. A 3-tesla (3T) MRI (Magnetom Skyra, Siemens Healthineers AG, Munich, Germany) of the right thumb with axial traction applied by a finger trap with three traction weights (0, 2, and 5 kg) was performed. A 3D T2* multiecho data imaging combination (MEDIC) was selected to visualize the articular cartilage. After multiplanar reconstruction, sagittal and coronal images of the thumb carpometacarpal joint were used to evaluate the articular cartilage visibility and joint space widths at five locations. Articular cartilage visibility was evaluated using our original classification method that used the percentage of the cartilage detectable area. The Friedman test was used to compare the differences between each traction weight and location.

Results

Articular cartilage visibility significantly improved with axial traction. The average joint space widths with the 5-kg application were 1.9 ± 0.8, 3.9 ± 0.6, 2.0 ± 0.9, 3.9 ± 1.1, and 2.5 ± 1.4 mm at the center, volar edge, dorsal edge, radial edge, and ulnar edge, respectively. The joint space widths significantly increased proportionally with the traction weight at all locations. The joint space widths at the volar and radial edges were significantly greater than those at other locations.

Conclusion

Applying axial traction to the thumb increased the joint space widths and improved the visibility of the articular cartilage in the carpometacarpal joint on MRI.

Categories: Radiology, Orthopedics
Keywords: joint space width, articular cartilage visibility, thumb carpometacarpal joint, magnetic resonance imaging, axial traction

Introduction

The thumb carpometacarpal (CMC) joint is a saddle joint that connects the first metacarpal bone and the trapezium and can be moved in multiple different directions during daily activities such as pinching or grasping due to its anatomical characteristics [1,2]. The incidence of thumb CMC joint arthritis is high, occurring in >15% of adults aged >30 years and one-third of postmenopausal women, despite it being a non-weight-bearing joint [3-6]. Thumb CMC joint arthritis is usually diagnosed on the basis of the patient's history, physical examination, and radiographs. The Eaton and Littler classification system is widely used to determine the staging and severity of such types of arthritis [7,8]. However, the degree of damage in the thumb CMC joint cartilage is not accurately assessed because the Eaton and Littler classification is based only on radiographs. A study reported that the intra- and inter-examiner reliabilities of this classification are low [9]; other studies have reported a poor correlation with clinical symptoms and intraoperative

articular cartilage findings [10,11].

Magnetic resonance imaging (MRI) is widely used to evaluate the damage to articular cartilage. However, accurate evaluation of the thumb CMC joint cartilage is difficult due to its anatomical complexity and relatively small size compared with large joints such as the hip and knee. Although some reports have evaluated the articular cartilage of the thumb CMC joint using MRI [12-14], an accurate method of evaluation has not yet been established because of the overlap of the articular cartilage between the first metacarpal bone and the trapezium as well as the underestimation of the degree of cartilage damage compared with other pathological findings [15]. Therefore, to enhance the visibility of the articular cartilage, we have attempted to perform MRI while applying axial traction to the joint. This method of applying axial traction to improve visualization of articular cartilage has been previously used to observe other joints, including for osteochondritis dissecans in the capitellum [16].

This study aimed to examine the effects of MRI with axial traction of the thumb CMC joint on the visibility of articular cartilage among healthy volunteers.

Materials And Methods

Study population

This study was approved by the institutional review board (IRB) of the first author's hospital (no. R2-06) and was performed following the ethical standards laid down in the 1964 Declaration of Helsinki and its later amendments or comparable ethical standards. We enrolled 11 healthy volunteers without a history of a thumb injury and symptoms. All volunteers were hospital staff members. The first author provided detailed information about the study (after IRB approval) within the hospital premises and recruited the volunteers. Informed consent was obtained from each volunteer after thoroughly explaining the objective, method, and any expected complications of the study.

Image acquisition

MRI was performed at the Kenpoku Medical Center Takahagi Kyodo Hospital between January 2021 and March 2021. We used a 3-tesla (3T) whole-body MRI system (Magnetom Skyra, Siemens Healthineers AG, Munich, Germany) using a four-channel 3T special purpose coil (Siemens Healthineers AG, Munich, Germany). For the MRI sequence, a three-dimensional T2* multiecho data imaging combination (MEDIC) scan was used with the following parameters: slice thickness, 0.2 mm; slice gap, 0.15 mm; field of vision, 130 mm × 130 mm × 78 mm; matrix, 384 × 292; time to repeat, 20 ms; echo time, 11.0 ms; and flip angle, 25°. The required time according to the protocol was 5 min and 43 s for each imaging. The volunteers were asked to lay supine on the table with their arms outstretched and forearms in pronation at the side of the body. The hand under observation was centered parallel to the long axis of the gantry.

Application of axial traction during MRI

MRI was initially performed without traction, followed by MRI with traction. After performing the initial MRI without traction, the volunteer’s thumb was enclosed within a Chinese finger trap (Allen® Sterile Mesh Finger Traps, AliMed, Inc., Massachusetts, USA) using a rope. The other end of the rope was hung over the edge of the MR table via a pulley system and attached to nonmagnetic traction weights (Figure *1*).

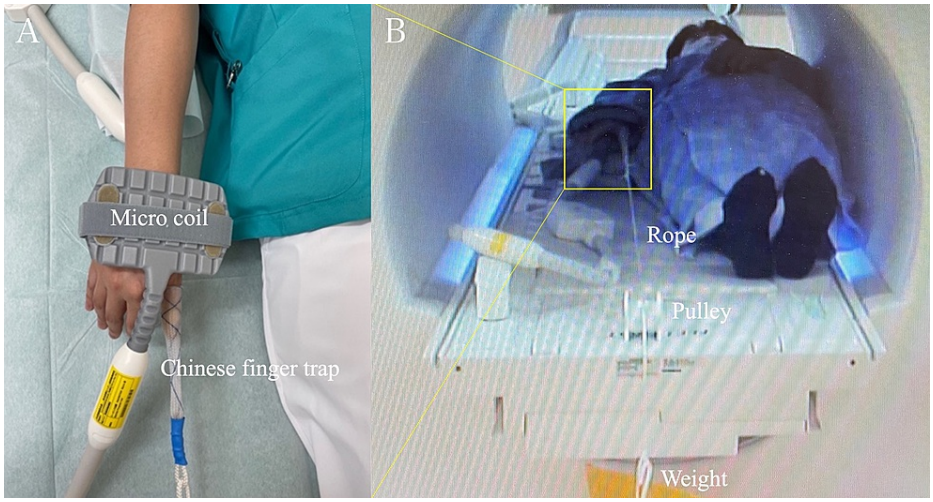

FIGURE 1: Application of axial traction during thumb carpometacarpal joint MRI

(A) The volunteer's thumb was enclosed within a Chinese finger trap and pulled distally. (B) The Chinese finger trap was connected to the traction weight using a nonelastic rope routed through the pulley system.

The ideal traction weight for the thumb has not been determined to date; therefore, traction weights of 2 and 5 kgs were used based on previous literature [17].

Image analysis

We evaluated the following items: the effects of traction on the joint space width, articular cartilage outline visibility, and pain and discomfort during imaging with traction. In this study, joint space width was defined as the space between opposing articular cartilages within the target joint. All MR images were independently evaluated by two orthopedic surgeons (with 13 and six years of clinical experience, respectively). All study images were interpreted on a workstation (Materialise Mimics, version 20.0; Materialise, Belgium); this workstation was also used to obtain multiplanar reconstructed (MPR) images. Specifically, coronal and sagittal images were reconstructed such that they were parallel to the longitudinal axis of the first metacarpal bone. This procedure was performed by the first author for all images. The images were initially enlarged, and the gray-scale contrast was adjusted to optimize the visualization of the structure being assessed. The images were then randomly numbered to minimize bias among examiners.

Measurement of the joint space width

The joint space width was measured on the sagittal and coronal images at the center of the proximal articular surface of the first metacarpal bone. On the sagittal image, the AB line, the line through both the volar (point A) and dorsal (point B) borders at the proximal articular surface of the first metacarpal, and the CD line, the line through both volar (point C) and dorsal (point D) borders of the distal articular surface of trapezium, were drawn at first. Then, a perpendicular line was then drawn at the center of the AB line, and the intersection points of the articular surface of the first metacarpal were labeled as point E and the intersection points of the articular surface of the trapezium were labeled as point F. Furthermore, the intersection points of the perpendicular line drawn from point A and B to the CD line were labeled as points G and H. On the sagittal image, the IJ line, the line through the radial (point I) and ulnar (point J) borders of the proximal articular surface of the first metacarpal, and the KL line, the line through the radial (point K) and ulnar (point L) borders at the distal articular surface of the trapezium, were drawn first. Subsequently, the intersection points of the perpendicular line drawn from points K and L to the IJ line were defined as points M and N. The distance between points E and F was defined as the center of the joint space width, that of points A-G and B-H was defined as volar and dorsal of the joint space width, and that of points I-M and J-N was defined as radial and ulnar of the joint space width (Figure *2*).

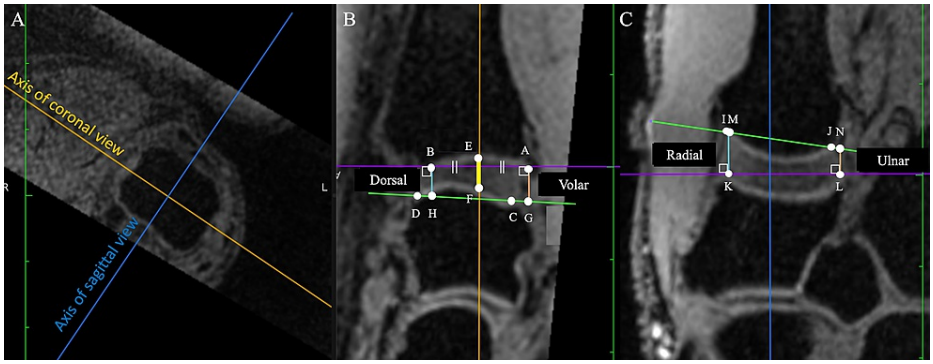

FIGURE 2: Definition of measurement points

(A) The coronal and sagittal axes were defined using the axial plane at the first metacarpal bone head. (B) Sagittal image of first carpometacarpal joint. Distances E-F, A-G, and B-H were defined as the center, volar, and dorsal distances, respectively. (C) Coronal image at the first carpometacarpal joint. Distances K-M and L-N were defined as radial and ulnar, respectively.

Assessment of the articular cartilage outline visibility

Articular cartilage outline visibility was graded using the following three-point scale on each sagittal and coronal image in which the joint space width was measured: 2 (complete), when 100% of the articular cartilage outline was clearly visible in the entire range when facing the opposing articular cartilage; 1 (intermediate), when ⩾50% but <100% of the articular cartilage outline was clearly visible in the range when facing the opposing articular cartilage; and 0 (poor), when the articular cartilage outline was visible in <50% of the entire range when facing the opposing articular cartilage (Figure *3*).

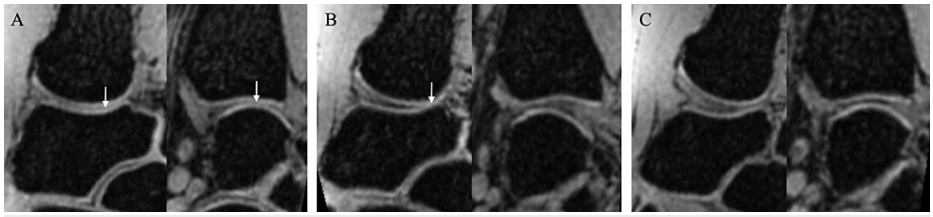

FIGURE 3: Articular cartilage outline visibility grade

(A) Grade 0 (poor): The articular cartilage outline was visible in <50% of the entire range when facing the opposing articular cartilage. (B) Grade 1 (intermediate): ≥50% but <100% of the articular cartilage outline was clearly visible in the range when facing the opposing articular cartilage. (C) Grade 2 (complete): 100% of the articular cartilage outline was clearly visible in the entire range when facing the opposing articular cartilage. The contact area of each articular cartilage is indicated by the white arrows.

Assessment of pain and discomfort during MRI with axial traction

The visual analog scale (VAS) was in a questionnaire format to assess the pain and discomfort during MRI with axial traction and was completed by each volunteer immediately after undergoing MRI with axial traction (0, minimum; 100, maximum).

Statistical analyses

We used GraphPad Prism 8 (GraphPad Software, LLC., CA, USA) for all statistical analyses. All data were tested for normal distribution using the Shapiro-Wilk test. Only the VAS score followed the normal distribution. We used a one-way analysis of variance (ANOVA) to assess the differences in the VAS scores for each traction weight. None of the data on articular cartilage outline visibility and joint space width followed normal distribution due to the small sample size. Therefore, the Friedman test was used to assess the differences in the joint space widths and articular cartilage outline visibility between each traction weight. A P-value < 0.05 was considered significant.

Results

In this study, six of the 11 volunteers were men and five were women, with a mean age of 39.4 ± 7.4 (range, 27-49) years. Demographic data of the volunteers are presented in Table *1*.

No.	Sex	Age (Years)	History of thumb CMC joint injury	Symptoms of thumb CMC joint arthritis
1	Male	37	None	None
2	Male	49	None	None
3	Female	45	None	None
4	Female	43	None	None
5	Male	29	None	None
6	Male	30	None	None
7	Male	40	None	None
8	Female	41	None	None
9	Male	27	None	None
10	Female	49	None	None
11	Female	43	None	None

TABLE 1: Demographic data of the volunteers

CMC: Carpometacarpal.

The joint space width significantly increased at all points with the 5-kg traction than with no traction. No significant differences in the joint space widths were observed between the 2-kg traction and non-traction at all points (Figure *4*).

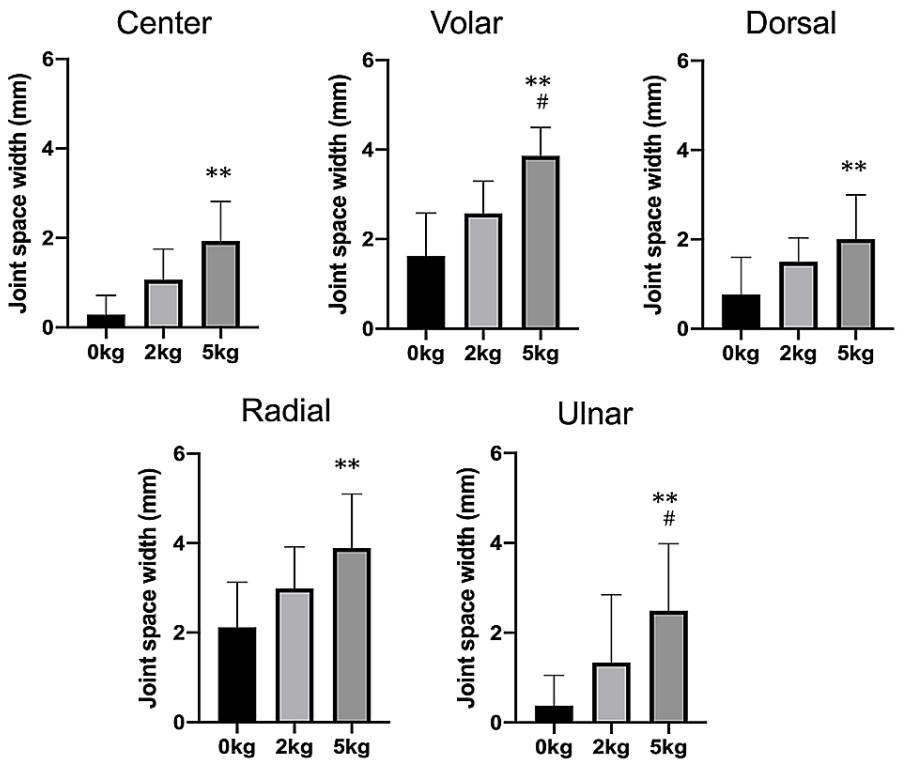

FIGURE 4: Joint space widths at each point (median ± standard deviation)

Joint space widths gradually widened after axial traction. At all points, significant differences were observed between the 0-kg and 5-kg tractions.

**P < 0.01 compared with 0-kg traction.

#P < 0.05 compared with 2-kg traction.

On comparing each point, the volar and radial points were found to have significantly wider joint space width for all traction weights than the center, dorsal, and ulnar. The visibility of the articular cartilage outlines significantly improved with the 5-kg traction (P < 0.01), with approximately 82% of volunteers showing complete visibility of the articular cartilage with the 5-kg traction (Figure *5*).

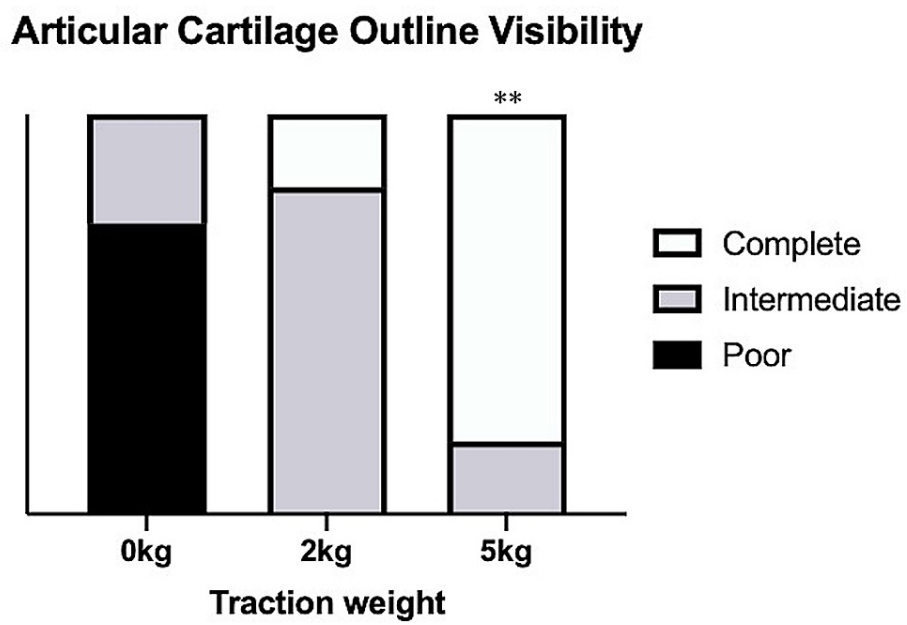

FIGURE 5: Visibility of the articular cartilage outlines

**P < 0.01 compared with the 0-kg traction.

The mean VAS score for pain and discomfort during MRI with axial traction was 0 (0-0) in non-traction, 25 (10-47) in 2-kg traction, and 52 (33-89) in 5-kg traction (Figure *6*).

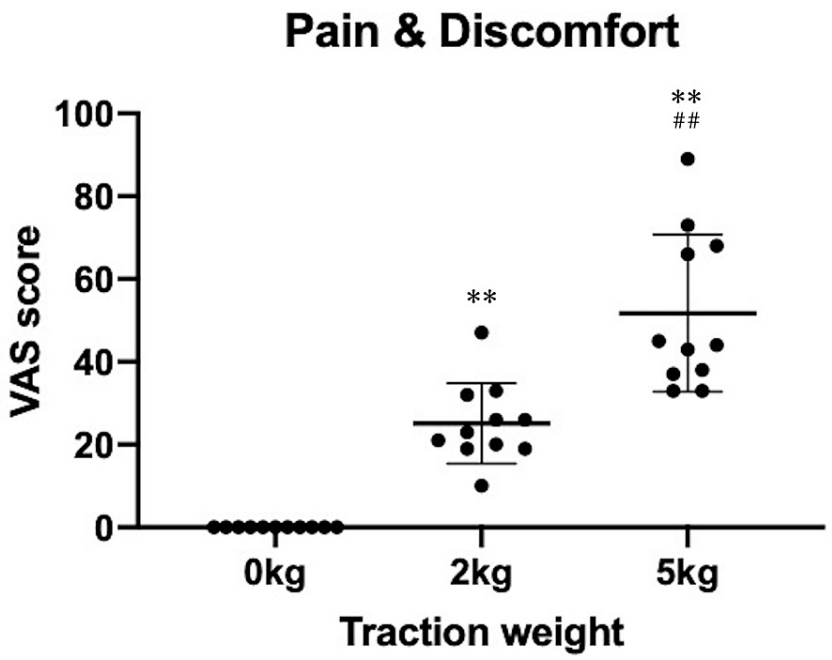

FIGURE 6: Visual analog scale scores of the pain and discomfort during traction

VAS: Visual analog scale.

**P < 0.01 compared with the 0-kg traction.

##P < 0.01 compared with the 2-kg traction.

The scores significantly increased with traction ($P < 0.01$); however, the pain and discomfort were resolved within 15 min after completing the traction and removing the finger trap in all volunteers.

Discussion

Our results showed that the cartilage outline visibility of the thumb CMC joint on MRI was significantly better when axial traction was applied to the thumb.

Traction of the thumb

Joint traction during diagnostic testing and treatment has already been applied in multiple situations [18,19]. Guntern et al. recently demonstrated that a 3-kg distraction load on the wrist significantly expands the radiocarpal and midcarpal joints, particularly the radioscaphoid and lunocapitate spaces [18]. Lee et al. reported that traction significantly improves the cartilage surface visibility for standard MRI of the wrist, although the effect was not as obvious as that seen with MR arthrography or MR arthrography with traction [17]. Orthopedic surgeons have also used axial traction of the wrist for treatment and diagnosis. The distraction of the wrist by axial traction helps realign the fragments after displacement fractures of the distal radius. Axial traction has been used as a carpal stress test in the diagnosis of scapholunate ligament injuries in radiology [20]. Furthermore, four previous studies have reported the advantages of applying axial traction during MR arthrography: one at the shoulder [21], two at the hip [22,23], and one at the knee [24]. Although the articular cartilage visibility significantly improved by increasing the traction weight, the pain and discomfort caused by traction were also significantly increased in this study. An increase in the traction weight results in increased tightness of the finger being tested. We suspected that the pain during traction was caused by vascular insufficiency due to the use of the Chinese finger trap. The maximal traction weight in this study (5 kg) is acceptable in a clinical setting because 4.5 kg (10 pounds) of traction is usually applied for fingers when performing wrist or thumb arthroscopy [17,19,25]. However, the traction of the thumb in patients with thumb CMC joint arthritis may exacerbate pain and other symptoms, although these symptoms disappear within a short period in healthy volunteers. Further research is warranted to determine the optimal traction weight for the thumb.

MRI sequences to observe the articular cartilage

MEDIC was used to evaluate the articular cartilage in this study. Its T2*-weighted gradient-echo sequence is specifically designed for musculoskeletal and neuroradiological purposes and combines up to six echoes in a single image, leading to a higher signal-to-noise ratio (SNR) and reduced susceptibility [26-28]. A 3D-MEDIC is useful in the diagnosis of fibrocartilaginous and ligamentous pathologies due to its high intrinsic SNR and high resolution of the 3D data stack [26,27]. Compared to other 3D sequences of the wrist, 3D-MEDIC exhibits a high contrast and SNR as well as the best visibility of fibrocartilaginous and ligamentous tissues [26]. In this study, articular cartilage is defined as a white line contacting the subchondral bone. Therefore, our results suggest that the MEDIC sequence can describe articular cartilage in the same way that it can be used to describe fibrocartilaginous and ligamentous tissues. Therefore, the optimal sequence to describe the articular cartilage in MRI should be examined in a study that compares several MRI sequences in the future.

Importance of articular cartilage evaluation for the thumb CMC joint

Various surgical techniques have been previously reported for thumb CMC joint arthritis [29]. For patients with mild osteoarthritic changes (Eaton classification stage 1 or 2), ligamentoplasty, arthroscopic synovectomy, and first metacarpal osteotomy are selected for thumb CMC joint preservation surgery, whereas, for patients with advanced osteoarthritic changes (Eaton classification stage 3 or 4), arthroplasty such as ligament reconstruction and tendon interposition, arthrodesis, and artificial joint replacement is generally selected as the thumb CMC joint non-preservation surgery. Although the clinical outcome is generally good with each type of treatment [30], Ogawa et al. have reported symptomatic improvement with joint preservation surgery even in patients with advanced osteoarthritic changes [25]. We believe that joint preservation surgery is preferable for younger patients or those who are involved in heavy labor, although a risk of osteoarthritic change progression exists even after a long-term joint preservation surgery.

Badia et al. reported a treatment algorithm based on intraoperative thumb CMC joint arthroscopic findings in 2006 [11]. Depending on the degree of articular cartilage damage or loss, joint preservation or non-preservation surgery is selected in this algorithm. This algorithm is more innovative than the Eaton classification as it assesses the articular cartilage damage and loss with higher accuracy before deciding the surgical technique. However, several limitations, such as the inability to preoperatively evaluate the articular cartilage, invasiveness, and the need to decide the surgical technique intraoperatively, were encountered. Our results demonstrated that the axial traction MRI of the thumb CMC joint could be used to preoperatively evaluate the articular cartilage condition, which will allow the selection of the optimal surgical technique that reflects the articular cartilage condition rather than depending on the Eaton classification.

This study has several limitations. First, the number of study participants was small. Second, we did not examine the use of MRI with axial traction for patients with thumb CMC joint arthritis. Third, the axial traction system in this study could not control the rotation force for the thumb CMC joint. A slight twist caused by axial traction may affect the measurement of joint space widths at each point. Therefore, adding

a system to control the rotation force during axial traction is necessary in future studies. Finally, we did not validate the concordance rate between MRI findings and intraoperative or pathological findings. To address these problems, the usefulness of this method should be verified in patients with thumb CMC joint arthritis, and the concordance rate must be verified with intraoperative and pathological findings in the future.

Conclusions

Axial traction of the thumb increased the joint space widths and improved the visibility of articular cartilage in the thumb CMC joint on MRI. Our results suggest that axial traction MRI can be used to evaluate the articular cartilage in a noninvasive manner in patients with thumb CMC joint arthritis, and it can be used to obtain useful information that will help to select the optimal surgical procedure.

Additional Information

Disclosures

Human subjects: Consent was obtained or waived by all participants in this study. Kenpoku Medical Center Takahagi Kyodo Hospital issued approval R2-06. **Animal subjects:** All authors have confirmed that this study did not involve animal subjects or tissue. **Conflicts of interest:** In compliance with the ICMJE uniform disclosure form, all authors declare the following: **Payment/services info:** All authors have declared that no financial support was received from any organization for the submitted work. **Financial relationships:** All authors have declared that they have no financial relationships at present or within the previous three years with any organizations that might have an interest in the submitted work. **Other relationships:** All authors have declared that there are no other relationships or activities that could appear to have influenced the submitted work.

Acknowledgements

The authors would like to thank Kazuki Hiruma and staff of the radiology department for performing MRI as the radiology technician and Enago (www.enago.jp) for the English language review.

References

1. Cooney WP 3rd, Chao EY: Biomechanical analysis of static forces in the thumb during hand function . J Bone Joint Surg Am. 1977, 59:27-36.
2. Strauch RJ, Behrman MJ, Rosenwasser MP: Acute dislocation of the carpometacarpal joint of the thumb: an anatomic and cadaver study. J Hand Surg Am. 1994, 19:93-98. 10.1016/0363-5023(94)90229-1
3. Armstrong AL, Hunter JB, Davis TR: The prevalence of degenerative arthritis of the base of the thumb in post-menopausal women. J Hand Surg Br. 1994, 19:340-341. 10.1016/0266-7681(94)90085-x
4. Dillon CF, Hirsch R, Rasch EK, Gu Q: Symptomatic hand osteoarthritis in the United States: prevalence and functional impairment estimates from the third U.S. National Health and Nutrition Examination Survey, 1991-1994. Am J Phys Med Rehabil. 2007, 86:12-21. 10.1097/phm.0b013e31802ba28e
5. Haara MM, Heliövaara M, Kröger H, et al.: Osteoarthritis in the carpometacarpal joint of the thumb. Prevalence and associations with disability and mortality. J Bone Joint Surg Am. 2004, 86:1452-7. 10.2106/00004623-200407000-00013
6. Sodha S, Ring D, Zurakowski D, Jupiter JB: Prevalence of osteoarthrosis of the trapeziometacarpal joint . J Bone Joint Surg Am. 2005, 87:2614-8. 10.2106/JBJS.E.00104
7. Eaton RG, Littler JW: Ligament reconstruction for the painful thumb carpometacarpal joint . J Bone Joint Surg Am. 1973, 55:1655-1666.
8. Eaton RG, Glickel SZ: Trapeziometacarpal osteoarthritis. Staging as a rationale for treatment . Hand Clin. 1987, 3:455-471.
9. Berger AJ, Momeni A, Ladd AL: Intra- and interobserver reliability of the Eaton classification for trapeziometacarpal arthritis: a systematic review. Clin Orthop Relat Res. 2014, 472:1155-9. 10.1007/s11999-013-3208-z
10. Hoffler CE 2nd, Matzon JL, Lutsky KF, Kim N, Beredjiklian PK: Radiographic stage does not correlate with symptom severity in thumb basilar joint osteoarthritis. J Am Acad Orthop Surg. 2015, 23:778-82. 10.5435/JAAOS-D-15-00329
11. Badia A: Trapeziometacarpal arthroscopy: a classification and treatment algorithm . Hand Clin. 2006, 22:153-63. 10.1016/j.hcl.2006.02.006
12. Kroon FP, Conaghan PG, Foltz V, et al.: Development and reliability of the OMERACT thumb base osteoarthritis magnetic resonance imaging scoring system. J Rheumatol. 2017, 44:1694-8. 10.3899/jrheum.161099
13. Connell DA, Pike J, Koulouris G, van Wettering N, Hoy G: MR imaging of thumb carpometacarpal joint ligament injuries. J Hand Surg Br. 2004, 29:46-54. 10.1016/s0266-7681(03)00170-0
14. Cardoso FN, Kim HJ, Albertotti F, Botte MJ, Resnick D, Chung CB: Imaging the ligaments of the trapeziometacarpal joint: MRI compared with MR arthrography in cadaveric specimens. AJR Am J Roentgenol. 2009, 192:W13-9. 10.2214/AJR.07.4010
15. Saltzherr MS, Coert JH, Selles RW, et al.: Accuracy of magnetic resonance imaging to detect cartilage loss in severe osteoarthritis of the first carpometacarpal joint: comparison with histological evaluation. Arthritis Res Ther. 2017, 19:55. 10.1186/s13075-017-1262-8
16. Kohyama S, Tanaka T, Shimasaki K, Kobayashi S, Ikumi A, Yanai T, Ochiai N: Effect of elbow MRI with axial traction on articular cartilage visibility-a feasibility study. Skeletal Radiol. 2020, 49:1555-66. 10.1007/s00256-020-03455-3

17. Lee RK, Griffith JF, Tang WK, Ng AW, Yeung DK: Effect of traction on wrist joint space and cartilage visibility with and without MR arthrography. Br J Radiol. 2017, 90:20160932. 10.1259/bjr.20160932
18. Guntern D, Becce F, Richarme D, Palhais NS, Meuli R, Theumann N: Direct magnetic resonance arthrography of the wrist with axial traction: a feasibility study to assess joint cartilage. J Magn Reson Imaging. 2011, 34:239-44. 10.1002/jmri.22615
19. Lee RK, Griffith JF, Ng AW, Nung RC, Yeung DK: Wrist traction during MR arthrography improves detection of triangular fibrocartilage complex and intrinsic ligament tears and visibility of articular cartilage. AJR Am J Roentgenol. 2016, 206:155-61. 10.2214/AJR.15.14948
20. Fortems Y, Mawhinney I, Lawrence T, Stanley JK: Traction radiographs in the diagnosis of chronic wrist pain. J Hand Surg Br. 1994, 19:334-7. 10.1016/0266-7681(94)90083-3
21. Chan KK, Muldoon KA, Yeh L, et al.: Superior labral anteroposterior lesions: MR arthrography with arm traction. AJR Am J Roentgenol. 1999, 173:1117-22. 10.2214/ajr.173.4.10511190
22. Llopis E, Cerezal L, Kassarjian A, Higueras V, Fernandez E: Direct MR arthrography of the hip with leg traction: feasibility for assessing articular cartilage. AJR Am J Roentgenol. 2008, 190:1124-8. 10.2214/AJR.07.2559
23. Nishii T, Nakanishi K, Sugano N, Masuhara K, Ohzono K, Ochi T: Articular cartilage evaluation in osteoarthritis of the hip with MR imaging under continuous leg traction. Magn Reson Imaging. 1998, 16:871-5. 10.1016/s0730-725x(98)00009-5
24. Palhais NS, Guntern D, Kagel A, Wettstein M, Mouhsine E, Theumann N: Direct magnetic resonance arthrography of the knee: utility of axial traction. Eur Radiol. 2009, 19:2225-31. 10.1007/s00330-009-1389-3
25. Ogawa T, Tanaka T, Asakawa S, Tatsumura M, Mammoto T, Hirano A: Arthroscopic synovectomy for the treatment of stage II to IV trapeziometacarpal joint arthritis. J Rural Med. 2018, 13:76-81. 10.2185/jrm.2962
26. Rehnitz C, Klaan B, von Stillfried F, Amarteifio E, Burkholder I, Kauczor HU, Weber MA: Comparison of modern 3D and 2D MR imaging sequences of the wrist at 3 Tesla. Rofo. 2016, 188:753-62. 10.1055/s-0042-104512
27. Dorenbeck U, Schreyer AG, Schlaier J, Held P, Feuerbach S, Seitz J: Degenerative diseases of the cervical spine: comparison of a multiecho data image combination sequence with a magnetisation transfer saturation pulse and cervical myelography and CT. Neuroradiology. 2004, 46:306-9. 10.1007/s00234-004-1175-5
28. Schmid MR, Pfirrmann CW, Koch P, Zanetti M, Kuehn B, Hodler J: Imaging of patellar cartilage with a 2D multiple-echo data image combination sequence. AJR Am J Roentgenol. 2005, 184:1744-8. 10.2214/ajr.184.6.01841744
29. Wilkens SC, Meghpara MM, Ring D, Coert JH, Jupiter JB, Chen NC: Trapeziometacarpal arthrosis. JBJS Rev. 2019, 7:e8. 10.2106/JBJS.RVW.18.00020
30. Gottschalk MB, Patel NN, Boden AL, Kakar S: Treatment of basilar thumb arthritis: a critical analysis review . JBJS Rev. 2018, 6:e4. 10.2106/JBJS.RVW.17.00156

Cureus

Open Access Original Article

DOI: 10.7759/cureus.22421

Effects of Magnetic Resonance Imaging With Axial Traction of the Thumb Carpometacarpal Joint on Articular Cartilage Visibility: A Feasibility Study

Review began 01/28/2022
Review ended 02/13/2022
Published 02/21/2022

Akira Ikumi [1, 2], Sho Kohyama [3], Shun Okuwaki [2], Masaki Tatsumura [1], Yuki Hara [4], Takeo Mammoto [1], Takeshi Ogawa [5], Yuichi Yoshii [6], Haruo Kawamura [2], Masashi Yamazaki [4]

1. Department of Orthopedic Surgery and Sports Medicine, Tsukuba University Hospital Mito Clinical Education and Training Center, Ibaraki, JPN 2. Department of Orthopedic Surgery, Kenpoku Medical Center Takahagi Kyodo Hospital, Ibaraki, JPN 3. Department of Orthopedic Surgery, Kikkoman General Hospital, Chiba, JPN 4. Department of Orthopedic Surgery, Faculty of Medicine, University of Tsukuba, Ibaraki, JPN 5. Department of Orthopedic Surgery, National Hospital Organization, Mito Medical Center, Ibaraki, JPN 6. Department of Orthopedic Surgery, Tokyo Medical University Ibaraki Medical Center, Ibaraki, JPN

Corresponding author: Akira Ikumi, ikumi@tsukuba-seikei.jp

Abstract

Objectives

The objective of this study was to verify the usefulness of magnetic resonance imaging (MRI) with axial traction of the thumb for observing articular cartilage.

Materials and methods

Eleven healthy adult volunteers (39.7 ± 7.4 years) without thumb carpometacarpal joint arthritis or trauma were included in this study. A 3-tesla (3T) MRI (Magnetom Skyra, Siemens Healthineers AG, Munich, Germany) of the right thumb with axial traction applied by a finger trap with three traction weights (0, 2, and 5 kg) was performed. A 3D T2* multiecho data imaging combination (MEDIC) was selected to visualize the articular cartilage. After multiplanar reconstruction, sagittal and coronal images of the thumb carpometacarpal joint were used to evaluate the articular cartilage visibility and joint space widths at five locations. Articular cartilage visibility was evaluated using our original classification method that used the percentage of the cartilage detectable area. The Friedman test was used to compare the differences between each traction weight and location.

Results

Articular cartilage visibility significantly improved with axial traction. The average joint space widths with the 5-kg application were 1.9 ± 0.8, 3.9 ± 0.6, 2.0 ± 0.9, 3.9 ± 1.1, and 2.5 ± 1.4 mm at the center, volar edge, dorsal edge, radial edge, and ulnar edge, respectively. The joint space widths significantly increased proportionally with the traction weight at all locations. The joint space widths at the volar and radial edges were significantly greater than those at other locations.

Conclusion

Applying axial traction to the thumb increased the joint space widths and improved the visibility of the articular cartilage in the carpometacarpal joint on MRI.

Categories: Radiology, Orthopedics
Keywords: joint space width, articular cartilage visibility, thumb carpometacarpal joint, magnetic resonance imaging, axial traction

Introduction

The thumb carpometacarpal (CMC) joint is a saddle joint that connects the first metacarpal bone and the trapezium and can be moved in multiple different directions during daily activities such as pinching or grasping due to its anatomical characteristics [1,2]. The incidence of thumb CMC joint arthritis is high, occurring in >15% of adults aged >30 years and one-third of postmenopausal women, despite it being a non-weight-bearing joint [3-6]. Thumb CMC joint arthritis is usually diagnosed on the basis of the patient's history, physical examination, and radiographs. The Eaton and Littler classification system is widely used to determine the staging and severity of such types of arthritis [7,8]. However, the degree of damage in the thumb CMC joint cartilage is not accurately assessed because the Eaton and Littler classification is based only on radiographs. A study reported that the intra- and inter-examiner reliabilities of this classification are low [9]; other studies have reported a poor correlation with clinical symptoms and intraoperative

articular cartilage findings [10,11].

Magnetic resonance imaging (MRI) is widely used to evaluate the damage to articular cartilage. However, accurate evaluation of the thumb CMC joint cartilage is difficult due to its anatomical complexity and relatively small size compared with large joints such as the hip and knee. Although some reports have evaluated the articular cartilage of the thumb CMC joint using MRI [12-14], an accurate method of evaluation has not yet been established because of the overlap of the articular cartilage between the first metacarpal bone and the trapezium as well as the underestimation of the degree of cartilage damage compared with other pathological findings [15]. Therefore, to enhance the visibility of the articular cartilage, we have attempted to perform MRI while applying axial traction to the joint. This method of applying axial traction to improve visualization of articular cartilage has been previously used to observe other joints, including for osteochondritis dissecans in the capitellum [16].

This study aimed to examine the effects of MRI with axial traction of the thumb CMC joint on the visibility of articular cartilage among healthy volunteers.

Materials And Methods

Study population

This study was approved by the institutional review board (IRB) of the first author's hospital (no. R2-06) and was performed following the ethical standards laid down in the 1964 Declaration of Helsinki and its later amendments or comparable ethical standards. We enrolled 11 healthy volunteers without a history of a thumb injury and symptoms. All volunteers were hospital staff members. The first author provided detailed information about the study (after IRB approval) within the hospital premises and recruited the volunteers. Informed consent was obtained from each volunteer after thoroughly explaining the objective, method, and any expected complications of the study.

Image acquisition

MRI was performed at the Kenpoku Medical Center Takahagi Kyodo Hospital between January 2021 and March 2021. We used a 3-tesla (3T) whole-body MRI system (Magnetom Skyra, Siemens Healthineers AG, Munich, Germany) using a four-channel 3T special purpose coil (Siemens Healthineers AG, Munich, Germany). For the MRI sequence, a three-dimensional T2* multiecho data imaging combination (MEDIC) scan was used with the following parameters: slice thickness, 0.2 mm; slice gap, 0.15 mm; field of vision, 130 mm × 130 mm × 78 mm; matrix, 384 × 292; time to repeat, 20 ms; echo time, 11.0 ms; and flip angle, 25°. The required time according to the protocol was 5 min and 43 s for each imaging. The volunteers were asked to lay supine on the table with their arms outstretched and forearms in pronation at the side of the body. The hand under observation was centered parallel to the long axis of the gantry.

Application of axial traction during MRI

MRI was initially performed without traction, followed by MRI with traction. After performing the initial MRI without traction, the volunteer’s thumb was enclosed within a Chinese finger trap (Allen® Sterile Mesh Finger Traps, AliMed, Inc., Massachusetts, USA) using a rope. The other end of the rope was hung over the edge of the MR table via a pulley system and attached to nonmagnetic traction weights (Figure *1*).

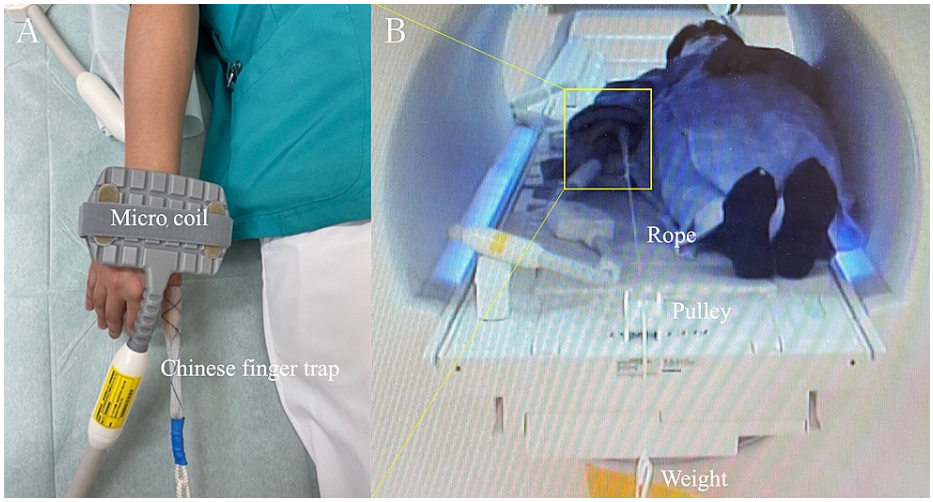

FIGURE 1: Application of axial traction during thumb carpometacarpal joint MRI

(A) The volunteer's thumb was enclosed within a Chinese finger trap and pulled distally. (B) The Chinese finger trap was connected to the traction weight using a nonelastic rope routed through the pulley system.

The ideal traction weight for the thumb has not been determined to date; therefore, traction weights of 2 and 5 kgs were used based on previous literature [17].

Image analysis

We evaluated the following items: the effects of traction on the joint space width, articular cartilage outline visibility, and pain and discomfort during imaging with traction. In this study, joint space width was defined as the space between opposing articular cartilages within the target joint. All MR images were independently evaluated by two orthopedic surgeons (with 13 and six years of clinical experience, respectively). All study images were interpreted on a workstation (Materialise Mimics, version 20.0; Materialise, Belgium); this workstation was also used to obtain multiplanar reconstructed (MPR) images. Specifically, coronal and sagittal images were reconstructed such that they were parallel to the longitudinal axis of the first metacarpal bone. This procedure was performed by the first author for all images. The images were initially enlarged, and the gray-scale contrast was adjusted to optimize the visualization of the structure being assessed. The images were then randomly numbered to minimize bias among examiners.

Measurement of the joint space width

The joint space width was measured on the sagittal and coronal images at the center of the proximal articular surface of the first metacarpal bone. On the sagittal image, the AB line, the line through both the volar (point A) and dorsal (point B) borders at the proximal articular surface of the first metacarpal, and the CD line, the line through both volar (point C) and dorsal (point D) borders of the distal articular surface of trapezium, were drawn at first. Then, a perpendicular line was then drawn at the center of the AB line, and the intersection points of the articular surface of the first metacarpal were labeled as point E and the intersection points of the articular surface of the trapezium were labeled as point F. Furthermore, the intersection points of the perpendicular line drawn from point A and B to the CD line were labeled as points G and H. On the sagittal image, the IJ line, the line through the radial (point I) and ulnar (point J) borders of the proximal articular surface of the first metacarpal, and the KL line, the line through the radial (point K) and ulnar (point L) borders at the distal articular surface of the trapezium, were drawn first. Subsequently, the intersection points of the perpendicular line drawn from points K and L to the IJ line were defined as points M and N. The distance between points E and F was defined as the center of the joint space width, that of points A-G and B-H was defined as volar and dorsal of the joint space width, and that of points I-M and J-N was defined as radial and ulnar of the joint space width (Figure *2*).

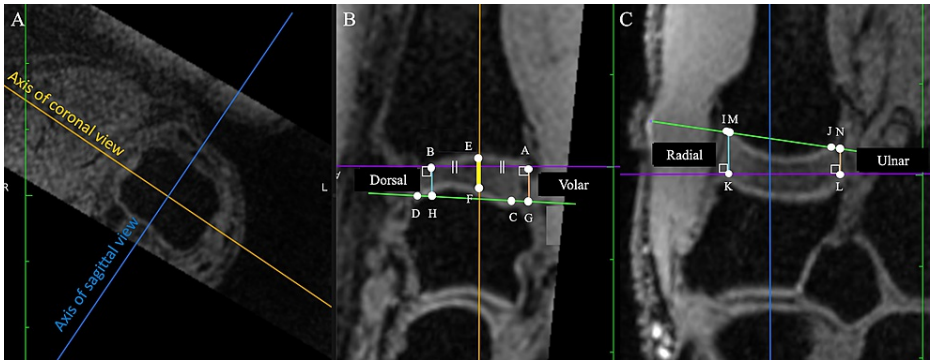

FIGURE 2: Definition of measurement points

(A) The coronal and sagittal axes were defined using the axial plane at the first metacarpal bone head. (B) Sagittal image of first carpometacarpal joint. Distances E-F, A-G, and B-H were defined as the center, volar, and dorsal distances, respectively. (C) Coronal image at the first carpometacarpal joint. Distances K-M and L-N were defined as radial and ulnar, respectively.

Assessment of the articular cartilage outline visibility

Articular cartilage outline visibility was graded using the following three-point scale on each sagittal and coronal image in which the joint space width was measured: 2 (complete), when 100% of the articular cartilage outline was clearly visible in the entire range when facing the opposing articular cartilage; 1 (intermediate), when ⩾50% but <100% of the articular cartilage outline was clearly visible in the range when facing the opposing articular cartilage; and 0 (poor), when the articular cartilage outline was visible in <50% of the entire range when facing the opposing articular cartilage (Figure *3*).

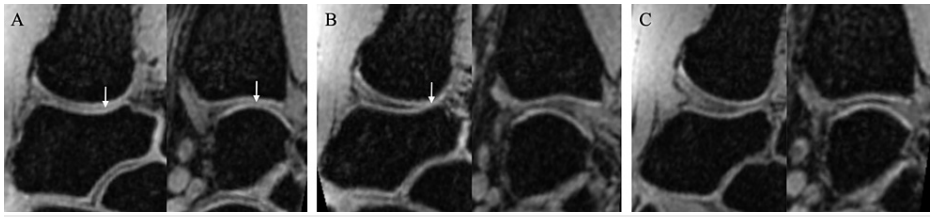

FIGURE 3: Articular cartilage outline visibility grade

(A) Grade 0 (poor): The articular cartilage outline was visible in <50% of the entire range when facing the opposing articular cartilage. (B) Grade 1 (intermediate): ≥50% but <100% of the articular cartilage outline was clearly visible in the range when facing the opposing articular cartilage. (C) Grade 2 (complete): 100% of the articular cartilage outline was clearly visible in the entire range when facing the opposing articular cartilage. The contact area of each articular cartilage is indicated by the white arrows.

Assessment of pain and discomfort during MRI with axial traction

The visual analog scale (VAS) was in a questionnaire format to assess the pain and discomfort during MRI with axial traction and was completed by each volunteer immediately after undergoing MRI with axial traction (0, minimum; 100, maximum).

Statistical analyses

We used GraphPad Prism 8 (GraphPad Software, LLC., CA, USA) for all statistical analyses. All data were tested for normal distribution using the Shapiro-Wilk test. Only the VAS score followed the normal distribution. We used a one-way analysis of variance (ANOVA) to assess the differences in the VAS scores for each traction weight. None of the data on articular cartilage outline visibility and joint space width followed normal distribution due to the small sample size. Therefore, the Friedman test was used to assess the differences in the joint space widths and articular cartilage outline visibility between each traction weight. A P-value < 0.05 was considered significant.

Results

In this study, six of the 11 volunteers were men and five were women, with a mean age of 39.4 ± 7.4 (range, 27-49) years. Demographic data of the volunteers are presented in Table *1*.

No.	Sex	Age (Years)	History of thumb CMC joint injury	Symptoms of thumb CMC joint arthritis
1	Male	37	None	None
2	Male	49	None	None
3	Female	45	None	None
4	Female	43	None	None
5	Male	29	None	None
6	Male	30	None	None
7	Male	40	None	None
8	Female	41	None	None
9	Male	27	None	None
10	Female	49	None	None
11	Female	43	None	None

TABLE 1: Demographic data of the volunteers

CMC: Carpometacarpal.

The joint space width significantly increased at all points with the 5-kg traction than with no traction. No significant differences in the joint space widths were observed between the 2-kg traction and non-traction at all points (Figure *4*).

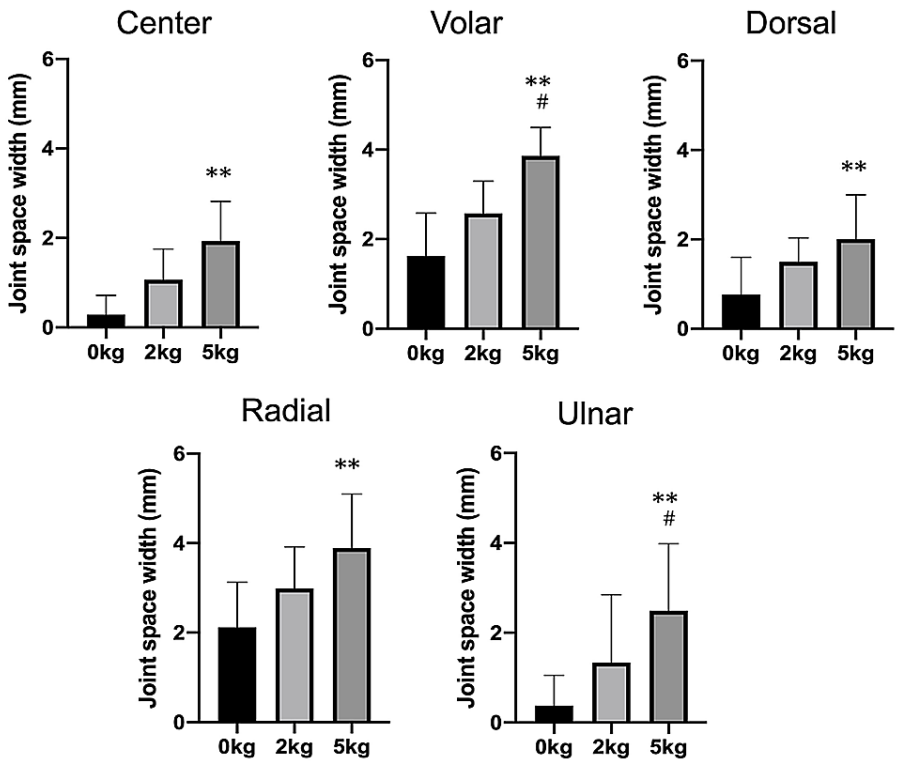

FIGURE 4: Joint space widths at each point (median ± standard deviation)

Joint space widths gradually widened after axial traction. At all points, significant differences were observed between the 0-kg and 5-kg tractions.

**P < 0.01 compared with 0-kg traction.

#P < 0.05 compared with 2-kg traction.

On comparing each point, the volar and radial points were found to have significantly wider joint space width for all traction weights than the center, dorsal, and ulnar. The visibility of the articular cartilage outlines significantly improved with the 5-kg traction (P < 0.01), with approximately 82% of volunteers showing complete visibility of the articular cartilage with the 5-kg traction (Figure *5*).

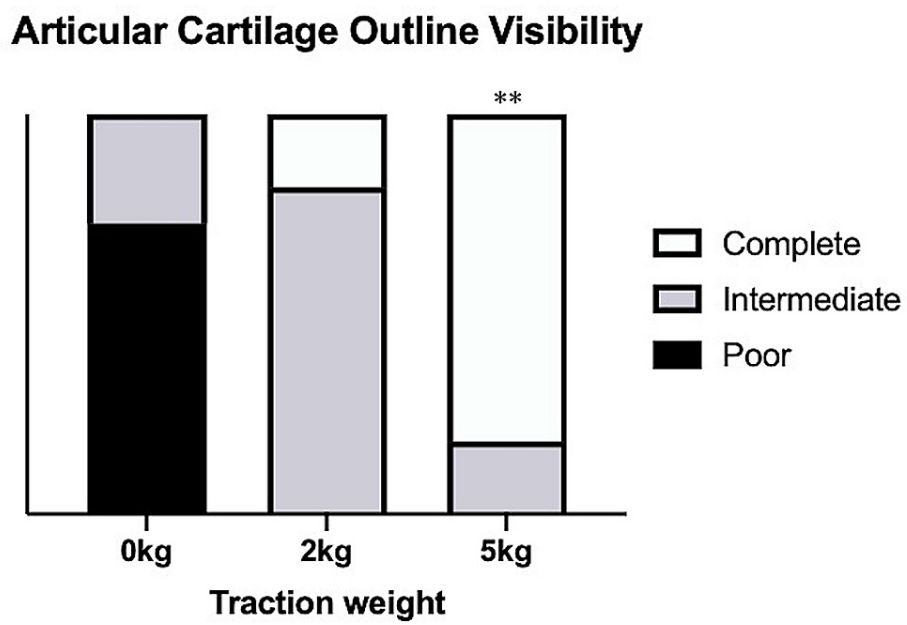

FIGURE 5: Visibility of the articular cartilage outlines

**P < 0.01 compared with the 0-kg traction.

The mean VAS score for pain and discomfort during MRI with axial traction was 0 (0-0) in non-traction, 25 (10-47) in 2-kg traction, and 52 (33-89) in 5-kg traction (Figure *6*).

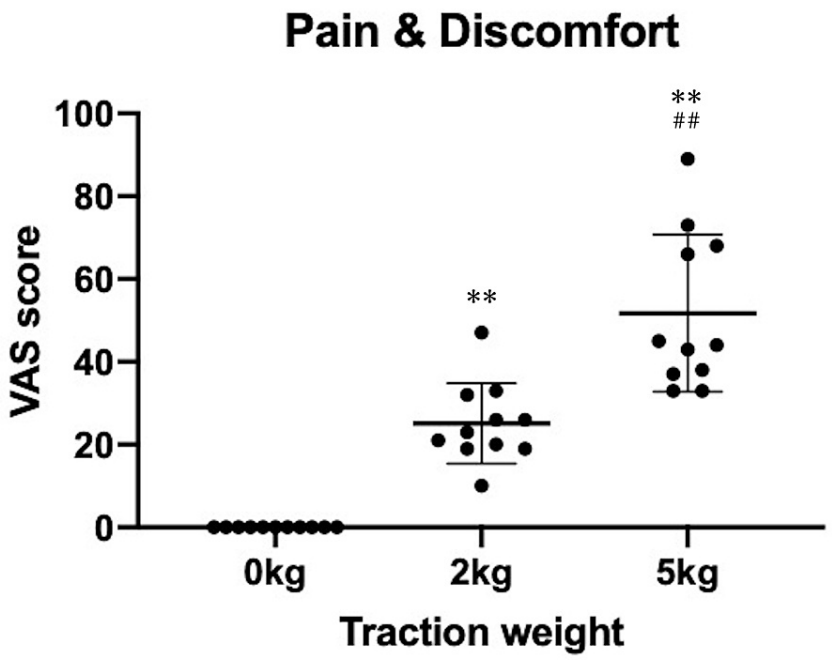

FIGURE 6: Visual analog scale scores of the pain and discomfort during traction

VAS: Visual analog scale.

**P < 0.01 compared with the 0-kg traction.

##P < 0.01 compared with the 2-kg traction.

The scores significantly increased with traction ($P < 0.01$); however, the pain and discomfort were resolved within 15 min after completing the traction and removing the finger trap in all volunteers.

Discussion

Our results showed that the cartilage outline visibility of the thumb CMC joint on MRI was significantly better when axial traction was applied to the thumb.

Traction of the thumb

Joint traction during diagnostic testing and treatment has already been applied in multiple situations [18,19]. Guntern et al. recently demonstrated that a 3-kg distraction load on the wrist significantly expands the radiocarpal and midcarpal joints, particularly the radioscaphoid and lunocapitate spaces [18]. Lee et al. reported that traction significantly improves the cartilage surface visibility for standard MRI of the wrist, although the effect was not as obvious as that seen with MR arthrography or MR arthrography with traction [17]. Orthopedic surgeons have also used axial traction of the wrist for treatment and diagnosis. The distraction of the wrist by axial traction helps realign the fragments after displacement fractures of the distal radius. Axial traction has been used as a carpal stress test in the diagnosis of scapholunate ligament injuries in radiology [20]. Furthermore, four previous studies have reported the advantages of applying axial traction during MR arthrography: one at the shoulder [21], two at the hip [22,23], and one at the knee [24]. Although the articular cartilage visibility significantly improved by increasing the traction weight, the pain and discomfort caused by traction were also significantly increased in this study. An increase in the traction weight results in increased tightness of the finger being tested. We suspected that the pain during traction was caused by vascular insufficiency due to the use of the Chinese finger trap. The maximal traction weight in this study (5 kg) is acceptable in a clinical setting because 4.5 kg (10 pounds) of traction is usually applied for fingers when performing wrist or thumb arthroscopy [17,19,25]. However, the traction of the thumb in patients with thumb CMC joint arthritis may exacerbate pain and other symptoms, although these symptoms disappear within a short period in healthy volunteers. Further research is warranted to determine the optimal traction weight for the thumb.

MRI sequences to observe the articular cartilage

MEDIC was used to evaluate the articular cartilage in this study. Its T2*-weighted gradient-echo sequence is specifically designed for musculoskeletal and neuroradiological purposes and combines up to six echoes in a single image, leading to a higher signal-to-noise ratio (SNR) and reduced susceptibility [26-28]. A 3D-MEDIC is useful in the diagnosis of fibrocartilaginous and ligamentous pathologies due to its high intrinsic SNR and high resolution of the 3D data stack [26,27]. Compared to other 3D sequences of the wrist, 3D-MEDIC exhibits a high contrast and SNR as well as the best visibility of fibrocartilaginous and ligamentous tissues [26]. In this study, articular cartilage is defined as a white line contacting the subchondral bone. Therefore, our results suggest that the MEDIC sequence can describe articular cartilage in the same way that it can be used to describe fibrocartilaginous and ligamentous tissues. Therefore, the optimal sequence to describe the articular cartilage in MRI should be examined in a study that compares several MRI sequences in the future.

Importance of articular cartilage evaluation for the thumb CMC joint

Various surgical techniques have been previously reported for thumb CMC joint arthritis [29]. For patients with mild osteoarthritic changes (Eaton classification stage 1 or 2), ligamentoplasty, arthroscopic synovectomy, and first metacarpal osteotomy are selected for thumb CMC joint preservation surgery, whereas, for patients with advanced osteoarthritic changes (Eaton classification stage 3 or 4), arthroplasty such as ligament reconstruction and tendon interposition, arthrodesis, and artificial joint replacement is generally selected as the thumb CMC joint non-preservation surgery. Although the clinical outcome is generally good with each type of treatment [30], Ogawa et al. have reported symptomatic improvement with joint preservation surgery even in patients with advanced osteoarthritic changes [25]. We believe that joint preservation surgery is preferable for younger patients or those who are involved in heavy labor, although a risk of osteoarthritic change progression exists even after a long-term joint preservation surgery.

Badia et al. reported a treatment algorithm based on intraoperative thumb CMC joint arthroscopic findings in 2006 [11]. Depending on the degree of articular cartilage damage or loss, joint preservation or non-preservation surgery is selected in this algorithm. This algorithm is more innovative than the Eaton classification as it assesses the articular cartilage damage and loss with higher accuracy before deciding the surgical technique. However, several limitations, such as the inability to preoperatively evaluate the articular cartilage, invasiveness, and the need to decide the surgical technique intraoperatively, were encountered. Our results demonstrated that the axial traction MRI of the thumb CMC joint could be used to preoperatively evaluate the articular cartilage condition, which will allow the selection of the optimal surgical technique that reflects the articular cartilage condition rather than depending on the Eaton classification.

This study has several limitations. First, the number of study participants was small. Second, we did not examine the use of MRI with axial traction for patients with thumb CMC joint arthritis. Third, the axial traction system in this study could not control the rotation force for the thumb CMC joint. A slight twist caused by axial traction may affect the measurement of joint space widths at each point. Therefore, adding

a system to control the rotation force during axial traction is necessary in future studies. Finally, we did not validate the concordance rate between MRI findings and intraoperative or pathological findings. To address these problems, the usefulness of this method should be verified in patients with thumb CMC joint arthritis, and the concordance rate must be verified with intraoperative and pathological findings in the future.

Conclusions

Axial traction of the thumb increased the joint space widths and improved the visibility of articular cartilage in the thumb CMC joint on MRI. Our results suggest that axial traction MRI can be used to evaluate the articular cartilage in a noninvasive manner in patients with thumb CMC joint arthritis, and it can be used to obtain useful information that will help to select the optimal surgical procedure.

Additional Information

Disclosures

Human subjects: Consent was obtained or waived by all participants in this study. Kenpoku Medical Center Takahagi Kyodo Hospital issued approval R2-06. **Animal subjects:** All authors have confirmed that this study did not involve animal subjects or tissue. **Conflicts of interest:** In compliance with the ICMJE uniform disclosure form, all authors declare the following: **Payment/services info:** All authors have declared that no financial support was received from any organization for the submitted work. **Financial relationships:** All authors have declared that they have no financial relationships at present or within the previous three years with any organizations that might have an interest in the submitted work. **Other relationships:** All authors have declared that there are no other relationships or activities that could appear to have influenced the submitted work.

Acknowledgements

The authors would like to thank Kazuki Hiruma and staff of the radiology department for performing MRI as the radiology technician and Enago (www.enago.jp) for the English language review.

References

1. Cooney WP 3rd, Chao EY: Biomechanical analysis of static forces in the thumb during hand function . J Bone Joint Surg Am. 1977, 59:27-36.
2. Strauch RJ, Behrman MJ, Rosenwasser MP: Acute dislocation of the carpometacarpal joint of the thumb: an anatomic and cadaver study. J Hand Surg Am. 1994, 19:93-98. 10.1016/0363-5023(94)90229-1
3. Armstrong AL, Hunter JB, Davis TR: The prevalence of degenerative arthritis of the base of the thumb in post-menopausal women. J Hand Surg Br. 1994, 19:340-341. 10.1016/0266-7681(94)90085-x
4. Dillon CF, Hirsch R, Rasch EK, Gu Q: Symptomatic hand osteoarthritis in the United States: prevalence and functional impairment estimates from the third U.S. National Health and Nutrition Examination Survey, 1991-1994. Am J Phys Med Rehabil. 2007, 86:12-21. 10.1097/phm.0b013e31802ba28e
5. Haara MM, Heliövaara M, Kröger H, et al.: Osteoarthritis in the carpometacarpal joint of the thumb. Prevalence and associations with disability and mortality. J Bone Joint Surg Am. 2004, 86:1452-7. 10.2106/00004623-200407000-00013
6. Sodha S, Ring D, Zurakowski D, Jupiter JB: Prevalence of osteoarthrosis of the trapeziometacarpal joint . J Bone Joint Surg Am. 2005, 87:2614-8. 10.2106/JBJS.E.00104
7. Eaton RG, Littler JW: Ligament reconstruction for the painful thumb carpometacarpal joint . J Bone Joint Surg Am. 1973, 55:1655-1666.
8. Eaton RG, Glickel SZ: Trapeziometacarpal osteoarthritis. Staging as a rationale for treatment . Hand Clin. 1987, 3:455-471.
9. Berger AJ, Momeni A, Ladd AL: Intra- and interobserver reliability of the Eaton classification for trapeziometacarpal arthritis: a systematic review. Clin Orthop Relat Res. 2014, 472:1155-9. 10.1007/s11999-013-3208-z
10. Hoffler CE 2nd, Matzon JL, Lutsky KF, Kim N, Beredjiklian PK: Radiographic stage does not correlate with symptom severity in thumb basilar joint osteoarthritis. J Am Acad Orthop Surg. 2015, 23:778-82. 10.5435/JAAOS-D-15-00329
11. Badia A: Trapeziometacarpal arthroscopy: a classification and treatment algorithm . Hand Clin. 2006, 22:153-63. 10.1016/j.hcl.2006.02.006
12. Kroon FP, Conaghan PG, Foltz V, et al.: Development and reliability of the OMERACT thumb base osteoarthritis magnetic resonance imaging scoring system. J Rheumatol. 2017, 44:1694-8. 10.3899/jrheum.161099
13. Connell DA, Pike J, Koulouris G, van Wettering N, Hoy G: MR imaging of thumb carpometacarpal joint ligament injuries. J Hand Surg Br. 2004, 29:46-54. 10.1016/s0266-7681(03)00170-0
14. Cardoso FN, Kim HJ, Albertotti F, Botte MJ, Resnick D, Chung CB: Imaging the ligaments of the trapeziometacarpal joint: MRI compared with MR arthrography in cadaveric specimens. AJR Am J Roentgenol. 2009, 192:W13-9. 10.2214/AJR.07.4010
15. Saltzherr MS, Coert JH, Selles RW, et al.: Accuracy of magnetic resonance imaging to detect cartilage loss in severe osteoarthritis of the first carpometacarpal joint: comparison with histological evaluation. Arthritis Res Ther. 2017, 19:55. 10.1186/s13075-017-1262-8
16. Kohyama S, Tanaka T, Shimasaki K, Kobayashi S, Ikumi A, Yanai T, Ochiai N: Effect of elbow MRI with axial traction on articular cartilage visibility-a feasibility study. Skeletal Radiol. 2020, 49:1555-66. 10.1007/s00256-020-03455-3

17. Lee RK, Griffith JF, Tang WK, Ng AW, Yeung DK: Effect of traction on wrist joint space and cartilage visibility with and without MR arthrography. Br J Radiol. 2017, 90:20160932. 10.1259/bjr.20160932
18. Guntern D, Becce F, Richarme D, Palhais NS, Meuli R, Theumann N: Direct magnetic resonance arthrography of the wrist with axial traction: a feasibility study to assess joint cartilage. J Magn Reson Imaging. 2011, 34:239-44. 10.1002/jmri.22615
19. Lee RK, Griffith JF, Ng AW, Nung RC, Yeung DK: Wrist traction during MR arthrography improves detection of triangular fibrocartilage complex and intrinsic ligament tears and visibility of articular cartilage. AJR Am J Roentgenol. 2016, 206:155-61. 10.2214/AJR.15.14948
20. Fortems Y, Mawhinney I, Lawrence T, Stanley JK: Traction radiographs in the diagnosis of chronic wrist pain. J Hand Surg Br. 1994, 19:334-7. 10.1016/0266-7681(94)90083-3
21. Chan KK, Muldoon KA, Yeh L, et al.: Superior labral anteroposterior lesions: MR arthrography with arm traction. AJR Am J Roentgenol. 1999, 173:1117-22. 10.2214/ajr.173.4.10511190
22. Llopis E, Cerezal L, Kassarjian A, Higueras V, Fernandez E: Direct MR arthrography of the hip with leg traction: feasibility for assessing articular cartilage. AJR Am J Roentgenol. 2008, 190:1124-8. 10.2214/AJR.07.2559
23. Nishii T, Nakanishi K, Sugano N, Masuhara K, Ohzono K, Ochi T: Articular cartilage evaluation in osteoarthritis of the hip with MR imaging under continuous leg traction. Magn Reson Imaging. 1998, 16:871-5. 10.1016/s0730-725x(98)00009-5
24. Palhais NS, Guntern D, Kagel A, Wettstein M, Mouhsine E, Theumann N: Direct magnetic resonance arthrography of the knee: utility of axial traction. Eur Radiol. 2009, 19:2225-31. 10.1007/s00330-009-1389-3
25. Ogawa T, Tanaka T, Asakawa S, Tatsumura M, Mammoto T, Hirano A: Arthroscopic synovectomy for the treatment of stage II to IV trapeziometacarpal joint arthritis. J Rural Med. 2018, 13:76-81. 10.2185/jrm.2962
26. Rehnitz C, Klaan B, von Stillfried F, Amarteifio E, Burkholder I, Kauczor HU, Weber MA: Comparison of modern 3D and 2D MR imaging sequences of the wrist at 3 Tesla. Rofo. 2016, 188:753-62. 10.1055/s-0042-104512
27. Dorenbeck U, Schreyer AG, Schlaier J, Held P, Feuerbach S, Seitz J: Degenerative diseases of the cervical spine: comparison of a multiecho data image combination sequence with a magnetisation transfer saturation pulse and cervical myelography and CT. Neuroradiology. 2004, 46:306-9. 10.1007/s00234-004-1175-5
28. Schmid MR, Pfirrmann CW, Koch P, Zanetti M, Kuehn B, Hodler J: Imaging of patellar cartilage with a 2D multiple-echo data image combination sequence. AJR Am J Roentgenol. 2005, 184:1744-8. 10.2214/ajr.184.6.01841744
29. Wilkens SC, Meghpara MM, Ring D, Coert JH, Jupiter JB, Chen NC: Trapeziometacarpal arthrosis. JBJS Rev. 2019, 7:e8. 10.2106/JBJS.RVW.18.00020
30. Gottschalk MB, Patel NN, Boden AL, Kakar S: Treatment of basilar thumb arthritis: a critical analysis review . JBJS Rev. 2018, 6:e4. 10.2106/JBJS.RVW.17.00156

RESEARCH ARTICLE

Difference in Rupture Risk Between Familial and Sporadic Intracranial Aneurysms

An Individual Patient Data Meta-analysis

Charlotte C.M. Zuurbier, MD, Liselore A. Mensing, MD, Marieke J.H. Wermer, MD, PhD, Seppo Juvela, MD, PhD, Antti E. Lindgren, MD, PhD, Timo Koivisto, MD, PhD, Juha E. Jääskeläinen, MD, PhD, Tomosato Yamazaki, MD, PhD, Rob Molenberg, BsC, J. Marc C. van Dijk, MD, PhD, Maarten Uyttenboogaart, MD, PhD, Marlien Aalbers, MD, Akio Morita, MD, PhD, Shinjiro Tominari, MD, PhD, Hajime Arai, MD, PhD, Kazuhiko Nozaki, MD, PhD, Yuichi Murayama, MD, Toshihiro Ishibashi, MD, Hiroyuki Takao, MD, PhD, Gabriel J.E. Rinkel, prof MD, PhD, Jacoba P. Greving, PhD, and Ynte M. Ruigrok, MD, PhD

Correspondence
Dr. Ruigrok
ij.m.ruigrok@umcutrecht.nl

Neurology® 2021;97:e2195-e2203. doi:10.1212/WNL.0000000000012885

Abstract

Background and Objectives

We combined individual patient data (IPD) from prospective cohorts of patients with unruptured intracranial aneurysms (UIAs) to assess to what extent patients with familial UIA have a higher rupture risk than those with sporadic UIA.

Methods

For this IPD meta-analysis, we performed an Embase and PubMed search for studies published up to December 1, 2020. We included studies that (1) had a prospective study design; (2) included 50 or more patients with UIA; (3) studied the natural course of UIA and risk factors for aneurysm rupture including family history for aneurysmal subarachnoid haemorrhage and UIA; and (4) had aneurysm rupture as an outcome. Cohorts with available IPD were included. All studies included patients with newly diagnosed UIA visiting one of the study centers. The primary outcome was aneurysmal rupture. Patients with polycystic kidney disease and moyamoya disease were excluded. We compared rupture rates of familial vs sporadic UIA using a Cox proportional hazard regression model adjusted for PHASES score and smoking. We performed 2 analyses: (1) only studies defining first-degree relatives as parents, children, and siblings and (2) all studies, including those in which first-degree relatives are defined as only parents and children, but not siblings.

Results

We pooled IPD from 8 cohorts with a low and moderate risk of bias. First-degree relatives were defined as parents, siblings, and children in 6 cohorts (29% Dutch, 55% Finnish, 15% Japanese), totaling 2,297 patients (17% familial, 399 patients) with 3,089 UIAs and 7,301 person-years follow-up. Rupture occurred in 10 familial cases (rupture rate: 0.89%/person-year; 95% confidence interval [CI] 0.45–1.59) and 41 sporadic cases (0.66%/person-year; 95% CI 0.48–0.89); adjusted hazard ratio (HR) for familial cases 2.56 (95% CI 1.18–5.56). After adding the 2 cohorts excluding siblings as first-degree relatives, resulting in 9,511 patients, the adjusted HR was 1.44 (95% CI 0.86–2.40).

Discussion

The risk of rupture of UIA is 2.5 times higher, with a range from a 1.2 to 5 times higher risk, in familial than in sporadic UIA. When assessing the risk of rupture in UIA, family history should be taken into account.

From the Department of Neurology and Neurosurgery, UMC Utrecht Brain Center (C.C.M.Z., L.A.M., G.J.E.R., Y.M.R.), and Julius Centre for Health Sciences and Primary Care (J.P.G.), University Medical Center Utrecht; Department of Neurology (M.J.H.W.), Leiden University Medical Center, the Netherlands; Department of Clinical Neurosciences (S.J.), University of Helsinki; Neurosurgery of NeuroCenter (A.E.L., T.K., J.E.J.), University of Eastern Finland, Kuopio, Finland; Department of Neurosurgery (T.Y.), National Hospital Organization, Mito Medical Center, Japan; Departments of Neurosurgery (R.M., J.M.C.v.D., M.U., M.A.), University Medical Center Groningen, the Netherlands; University of Tokyo–Nippon Medical School (A.M.); Department of Health Informatics, School of Public Health (S.T.), Kyoto University; Department of Neurosurgery (H.A.), Juntendo University Medical School, Tokyo; Department of Neurosurgery (K.N.), Shiga University of Medical Science; and Department of Endovascular Neurosurgery (Y.M., T.I., H.T.), Tokyo Jikei University School of Medicine, Japan.

Go to Neurology.org/N for full disclosures. Funding information and disclosures deemed relevant by the authors, if any, are provided at the end of the article.

Glossary

aSAH = aneurysmal subarachnoid hemorrhage; **CI** = confidence interval; **HR** = hazard ratio; **QUIPS** = Quality in Prognosis Studies; **UIA** = unruptured intracranial aneurysm.

Persons with a positive family history of aneurysmal subarachnoid hemorrhage (aSAH) or unruptured intracranial aneurysms (UIAs) have a 10% risk of having a UIA.[1] A higher rupture risk of UIA has been suggested in these patients compared to patients without such a history. The Familial Intracranial Aneurysm study reported a 17 times higher rupture rate for individuals with a family history of aSAH plus hypertension or smoking, or both, compared to individuals with sporadic UIA. However, these data lack precision as they are based on 2 cases of aSAH in 113 patients with UIAs.[2] Another prospective, single-center cohort with familial patients not selected for smoking or hypertension, and taking risk factors for rupture into account, found a not statistically significant 3 times higher risk.[3]

The definition of a positive family history may also play a role in the level of risk of rupture of familial UIA.[4] In most countries, first-degree relatives are defined as parents, siblings, or children, while in some other countries, first-degree relatives are defined as only parents and children, but not siblings. We recently showed that within families, siblings have a higher risk of UIA and aSAH than parents and children.[4] Thus, to assess the risk of rupture of familial aneurysms, it is important to include siblings in the category of first-degree relatives.

We aimed to assess to what extent patients with familial UIA have a higher risk of rupture than those with sporadic UIA, when defining first-degree relatives as parents, siblings, or children. Secondly, we assessed this association in cohorts both including and excluding siblings in the definition of first-degree relatives.

Methods

Search Strategy and Selection Criteria

We performed a systematic search in Embase and PubMed to retrieve all studies on rupture risk of UIA published up to December 1, 2020. Our search strategy included the keywords "(intracranial aneurysm[s] or cerebral aneurysm[s]) and (risk of rupture or aneurysm rupture or risk factors or rupture or unruptured or subarachnoid hemorrhage) and (follow-up or natural history or natural course)" (eFigure 1, available from Dryad: doi.org/10.5061/dryad.3bk3j9kjz). We searched the reference list of all relevant publications for additional studies. We included studies that (1) had a prospective study design; (2) included 50 or more patients with UIA; (3) studied the natural course of UIA and risk factors for aneurysm rupture including family history for aSAH and UIA; and (4) had aneurysm rupture as an outcome. There was no language restriction other than the requirement of an abstract in English. One author (C.C.M.Z.) performed the literature search, checked the titles and abstracts of search records, and assessed eligible articles to decide which met the predefined inclusion criteria.

Study Design

For the eligible studies meeting the inclusion criteria, we approached the research groups that performed these studies asking if they could provide us with their individual patient data. Only cohorts with available individual patient-level data were included in our meta-analysis.

Data Collection

Data requested for each patient at baseline of the different included studies were the following: age, sex, history of aSAH, smoking status, positive family history for aSAH or UIA, hypertension status, number of aneurysms, maximum diameter of aneurysms, and aneurysm location. For each patient, we summarized the data on the different risk factors for rupture by calculating the PHASES score.[5] Data requested for each patient during follow-up were the following: occurrence of rupture, date of rupture, data of a surgical or endovascular intervention, date of death, date of last follow-up assessment, and whether a patient was lost to follow-up. Individuals with a positive family history were defined as individuals with at least 2 affected first-degree relatives with aSAH whether or not in combination of first-degree relatives with UIA. A smoker was defined as a former or current smoker and a person with hypertension as a history of a systolic blood pressure >140 mm Hg or diastolic blood pressure >90 mm Hg or use of antihypertensive drugs. The location of the aneurysm was classified into the categories internal carotid artery, posterior communicating artery, anterior cerebral arteries (including the anterior cerebral artery, anterior communicating artery, and pericallosal artery), middle cerebral artery, or posterior circulation (including the vertebral artery, basilar artery, cerebellar arteries, and posterior cerebral artery). Patients with polycystic kidney disease and moyamoya disease were excluded as we are not sure whether the rupture risk of patients with familial UIA and these diseases is similar to the rupture risk of patients with sporadic UIA with these diseases or patients with familial UIA without these diseases. The primary outcome was the rupture of an UIA. We followed Preferred Reporting Items for Systematic Reviews and Meta-Analyses (PRISMA) guidelines throughout our review. We assessed the quality of the observational studies using the Quality in Prognosis Studies (QUIPS) tool.[6]

Statistical Approach

Information on the outcome measure and aneurysm characteristics was complete for all patients. In 4 studies, no data on family history were available for a small subset of patients, and

Figure 1 Preferred Reporting Items for Systematic Reviews and Meta-Analyses (PRISMA) Flow Diagram

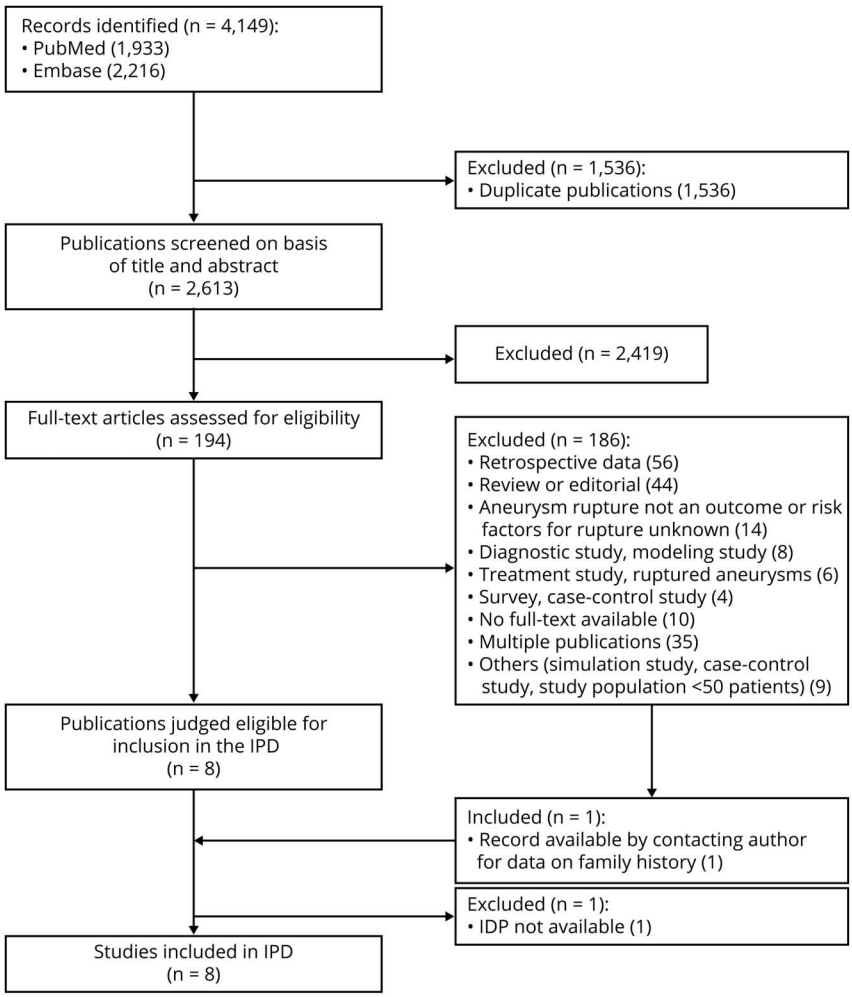

IPD = individual patient data.

these patients were excluded from the pooled analysis (146 patients excluded).[7-10] Information on patient characteristics was also complete except for smoking, which was available in 9,276/9,511 (97.5%) patients, and for hypertension, which was available in 9,424/9,511 (99.1%) patients. These missing data were imputed using multiple imputation. In one study, smokers were defined as current smokers and no data on former smoking were availaible.[9] Forty-two patients were included in 2 Japanese cohorts[10,11] and 11 patients were included in 2 Dutch cohorts[3,8] and these patients were excluded in one of these cohorts in the pooled analysis. For data analysis, we categorized according to the presence of a family history of aSAH or UIA (familial UIAs) or not (sporadic UIAs). Categorical variables of baseline characteristics were compared using the χ^2 test. Continuous variables of baseline characteristics were compared among groups using the Mann-Whitney *U* test or the Student *t* test. A *p* value ≤0.05 was considered statistically significant. We analyzed rupture rates per patient in all cohorts. In case of multiple aneurysms, the largest aneurysm was used for analysis. In addition, we performed an aneurysm-based analysis, where all UIAs were analyzed. Rupture rate was analyzed with a Cox proportional hazard regression model and adjusted for the PHASES score[5] and smoking. A 2-stage approach was used with random effect for cohort, because beforehand we expected heterogeneity as studies were performed in different countries that used different treatment regimens, and a fixed effect for the PHASES score and smoking. In the 2-stage IPD meta-analysis, individual patient data from each study were analyzed separately in order to obtain hazard ratios in each study, Next, these were combined by a random effect meta-analysis model. Proportional hazard assumptions were checked using diagnostics based on the scaled Schoenfeld residuals.[12] Follow-up data for patients started at time of UIA diagnosis and were censored at the time of an aneurysm rupture, death, last follow-up assessment, or at the time of surgical or endovascular aneurysm occlusion. Regarding the definition of first-degree relatives, we performed our primary analysis on studies including parents, siblings, or children as affected first-degree relatives and our secondary analysis on all studies including those in which first-degree relatives are defined as only parents and children, but not siblings. A sensitivity analysis was performed with cohorts from European and Japanese populations.

Role of the Funding Source

The funders of the study had no role in study design, data collection, data analysis, data interpretation, writing of the report, or the decision to submit for publication. All authors had full access to all the data in the study; the corresponding author had final responsibility for the decision to submit for publication.

Data Availability

All study data are available on request.

Results

We found 8 studies that fulfilled the inclusion criteria,[3,7-11,13,14] and 7 research groups provided us with their individual patient data.[3,7-11,13] All studies included patients with newly diagnosed UIA visiting one of the study centers. We also found one additional cohort study on UIA, which did not report on family in the PubMed search,[15] but authors of this study provided unpublished data on family history for aSAH, and therefore we could include this cohort as well. This prospective cohort study consisted of data on patients with UIA collected between 1980 and 2017 from the IA database of Neurosurgery of Kuopio University Hospital. This database included 1,181 patients with 1,653 UIA, of whom 248 had a positive family history. In total, 8 studies met our inclusion criteria (Figure 1). In these studies, 68 patients with polycystic kidney disease and 2 patients with moyamoya disease were excluded. In 6 studies, first-degree relatives were defined as parents, siblings, or children,[3,7-10,15] while in 2 studies, only parents and children were referred to as first-degree relatives.[11,13] The 8 cohorts are listed in Table 1 and the baseline characteristics of patients in all separate cohorts in eTable 1 (available from Dryad: doi.org/10.5061/dryad.3bk3j9kjz). Quality assessment of included cohort studies by QUIPS tool is shown in eTable 2 (available from Dryad: doi.org/10.5061/dryad.3bk3j9kjz). The 6 cohorts that defined first-degree relatives as parents, siblings, and children totaled 2,297 patients with 3,089 UIA and 7,301 person-years of follow-up. Baseline characteristics are shown in Table 2. The mean age was 56 ± 12 years, 399 patients (17%) had a positive family history for aSAH and UIA, and patients came from Dutch (29%), Finnish (55%), and Japanese (15%) populations. Patients with familial UIA were younger, less often had hypertension, and more often were smokers than patients with sporadic aneurysms. Familial cases more often had small UIA and aneurysms were more often located at the middle cerebral artery compared to sporadic cases. These described characteristics are all included in the PHASES score except smoking.[6] Patients with familial UIA had a similar median PHASES score of 7.0 (range 0–19) as patients with sporadic UIA (7.0; range 0–21), but the mean PHASES score was lower in patients with familial UIA (7.1; SD 3.5) compared to sporadic UIA (7.7; SD 3.6). The mean follow-up time for patients with familial UIA was 2.8 ± 4.5 years (median 1.0 [0–35] year) and for patients with sporadic UIA 3.3 ± 6.2 years (median 1.1 [0–52] year). Preventive neurosurgical or endovascular treatment during follow-up occurred in 47% of familial UIA (median 107 days) and in 37% of sporadic UIA (median 121 days). When assessing the baseline aneurysm characteristics on aneurysm level instead of patient level, results were similar (data not shown). Baseline characteristics of 9,511 patients with 11,647 UIA included in all cohorts including those in which first-degree relatives are defined as only parents and children, but not siblings, are provided in eTable 3 (available from Dryad: doi.org/10.5061/dryad.3bk3j9kjz).

In 53 patients, UIA rupture occurred. Of these 53 patients, 11 patients had multiple UIA, and in 51 of 53 patients (96%), the

Table 1 Characteristics of Included Studies

	Country	Recruitment period	Patients, n	UIAs, n	First-degree relatives including siblings	Patients with positive family history	Age, y, mean (range)	Follow-up, y, median (range)	aSAHs during follow-up, n
Juvela et al.[7]	Finland	1956–1978	93	116	Yes	9	42 (15–61)	27.2 (1–52)	22
Lindgren et al.[a]	Finland	1977–2016	1,181	1,658	Yes	248	56 (16–85)	0.5 (0–23)	14
Mensing et al.[3]	The Netherlands	1994–2016	474	633	Yes	62	56 (22–81)	0.8 (0–21)	10
Morita et al.[11]	Japan	2001–2004	5,702	6,675	No	327	63 (23–98)	1.0 (0–9)	111
Murayama et al.[13]	Japan	2003–2012	1,561	1942	No	184	66 (25–100)	3.2 (0–11)	56
Wermer et al.[8]	The Netherlands	2002–2004	89	119	Yes	26	50 (20–69)	2.2 (1–15)	1
Molenberg et al.[9]	The Netherlands	1998–2017	122	159	Yes	33	55 (33–77)	1 (0–2)	0
Sonobe et al.[10]	Japan	2000–2004	349	419	Yes	31	62 (23–89)	3.2 (0–7)	6

Abbreviations: aSAH = aneurysmal subarachnoid hemorrhage; UIA = unruptured intracranial aneurysm.
[a] Unpublished data.

Table 2 Baseline Characteristics of Patients in Cohorts Defining First-Degree Relatives as Parents, Children, and Siblings

Pooled data	Familial	Sporadic	Total	*p* Value
Patients	399	1,898	2,297	
Women	265 (66)	1,169 (62)	1,434 (62)	0.07
Age,[a] y, mean (range)	51 (20–80)	57 (15–89)	56 (15–89)	<0.01
Hypertension[a]	139 (35)	818 (43)	957 (42)	<0.01
Ever smoker	212 (53)	931 (49)	1,143 (50)	0.138
Previous aSAH[a]	34 (9)	242 (13)	276 (12)	0.018
Population[a]				
Finnish	257 (64)	1,018 (54)	1,274 (55)	<0.01
Dutch	111 (28)	563 (30)	674 (29)	
Japanese	31 (8)	318 (17)	349 (15)	
Multiple aneurysms	122 (31)	511 (27)	633 (28)	0.227
Aneurysm size, mm[a]				
<7.0	322 (81)	1,321 (70)	1,643 (72)	<0.01
7.0–9.9	43 (11)	301 (16)	344 (15)	
10.0–19.9	30 (8)	220 (12)	250 (11)	
>20.0	4 (1)	56 (3)	60 (3)	
Aneurysm location				
Internal carotid artery	83 (21)	413 (22)	496 (22)	0.065
Middle cerebral artery	189 (47)	783 (41)	972 (42)	
Anterior and posterior circulation	127 (32)	702 (37)	829 (36)	
Aneurysm treatment during follow-up[a]	186 (47)	702 (37)	888 (38)	<0.01
PHASES score,[a] median (range); mean ± SD	7.0 (0–19); 7.1 ± 3.5	7.0 (0–21); 7.7 ± 3.6	7.0 (0–21); 7.6 ± 3.6	<0.01

Abbreviation: aSAH = aneurysmal subarachnoid hemorrhage.
Values are n (%) unless otherwise specified.
[a] Statistically significant difference.

largest aneurysm ruptured. Rupture of the largest aneurysm occurred in 10 patients with familial UIA (rupture rate 0.89%/person-year; 95% confidence interval [CI] 0.45–1.59) and in 41 patients with sporadic UIA (0.66%/person-year; 95% CI 0.48–0.89). Characteristics of ruptured aneurysms are shown in Table 3. Characteristics of ruptured aneurysms in all cohorts including those in which first-degree relatives are defined as only parents and children but not siblings are provided in eTable 4 (available from Dryad: doi.org/10.5061/dryad.3bk3j9kjz).

The unadjusted hazard rate (HR) of patients with familial compared to those with sporadic aneurysms was 1.49 (95% CI 0.73–3.07) in cohorts defining first-degree relatives as parents, children, and siblings. After adjustment for the PHASES score and smoking, the adjusted HR was 2.56 (95% CI 1.18–5.56, I^2 = 0%; Figure 2). In the aneurysm-based analysis, the results were essentially the same (Figure 3). A sensitivity analysis with European and Japanese populations provided similar results (eFigure 2, available from Dryad: doi.org/10.5061/dryad.3bk3j9kjz). The unadjusted HR of patients with familial aneurysms compared to those with sporadic aneurysms in all cohorts including those in which first-degree relatives are defined as only parents and children, but not siblings, was 1.02 (95% CI 0.62–1.67) and 1.44 (95% CI 0.86–2.40, I^2 = 0%; eFigures 3–5, available from Dryad: doi.org/10.5061/dryad.3bk3j9kjz) after adjustment for the PHASES score and smoking.

Discussion

In this individual patient data meta-analysis, we found a higher risk of rupture for familial compared to sporadic UIA, with a point estimate of a 2.5 times higher risk, and a range from a 1.2 to 5 times higher risk, when restricting our analysis to cohorts referring to affected first-degree relatives as parents, siblings,

Table 3 Characteristics of Ruptured Intracranial Aneurysms in Cohorts Defining First-Degree Relatives as Parents, Children, and Siblings per Aneurysm

	Familial	Sporadic	Total
Ruptured IA, n	10	43	53
Largest IA ruptured[a]	10	41	41
Not largest IA ruptured	0	2	2
Women	6 (60)	28 (65)	34 (64)
Age, y, mean (range)	58 (33–74)	52 (23–80)	53 (23–80)
Hypertension	1 (10)	23 (54)	24 (45)
Ever smoker	3 (30)	24 (56)	27 (51)
Previous aSAH	3 (30)	20 (47)	23 (43)
Population			
Finnish	7 (70)	29 (70)	36 (70)
Netherlands	3 (30)	8 (18)	11 (20)
Japanese	0	6 (13)	6 (10)
Multiple aneurysms	0	11 (28)	11 (21)
Aneurysm size at time of detection, mm			
<7.0	6 (60)	23 (54)	29 (55)
7.0–9.9	1 (10)	10 (23)	11 (21)
10.0–19.9	3 (30)	9 (21)	12 (23)
>20.0	0	1 (2)	1 (2)
Aneurysm location			
Internal carotid artery	1 (10)	11 (26)	12 (23)
Middle cerebral artery	5 (50)	15 (35)	20 (38)
Anterior circulation and posterior circulation	4 (40)	17 (40)	21 (42)
PHASES score, median (range); mean ± SD	8.0 (2–16); 8.8 ± 4.7	9.0 (2–20); 9.5 ± 4.1	8.0 (2–20); 9.4 ± 4.2

Abbreviations: aSAH = aneurysmal subarachnoid hemorrhage; IA = intracranial aneurysm.
Values are n (%) unless otherwise specified.
[a] In case of multiple aneurysms, the largest aneurysm was used for analysis.

and children in defining a positive family history. We found a slightly but not statistically significantly increased risk of aneurysm rupture for familial compared to sporadic UIA when we analyzed all cohorts including those in which first-degree relatives are defined as only parents and children, but not siblings. When assessing the risk of rupture in UIA, the family history that includes affected siblings as first-degree relatives should be taken into account.

Our study showed a less strongly increased risk of rupture rate in persons with a positive family history for aSAH/UIA than reported in the previous Familial Intracranial Aneurysm study.[2] In this study, individuals diagnosed with an UIA were compared with historic controls[14] and all patients had a positive family history together with a positive history of smoking or hypertension. The higher risk in this highly selective population can be explained because this population already had a higher risk of UIA rupture due to the presence of the additional risk factors smoking and hypertension.[2] Our findings are consistent with a previous cohort study on the natural course of UIA in patients with and without a positive family history.[3] In our study we found a statistically significant higher risk of UIA rupture for familial compared to sporadic patients, while in the previous cohort study, a statistically nonsignificant effect was found, which can be explained by the smaller number of patients included. However, both our and the previous cohort study[3] found an increased risk for rupture in familial patients, which is much lower than the 17 times higher risk found in the Familial Intracranial Aneurysm study.[2]

Relatives of patients with familial aSAH have a higher incidence of aSAH than relatives without such a family history.[16] The higher incidence of aSAH in relatives of patients with familial aSAH is in part explained by a higher prevalence of UIA in these relatives.[17] Our study shows that a higher rupture risk of familial UIA also contributes to the higher incidence of aSAH in relatives with a family history of aSAH. This higher incidence of familial aSAH is likely due to shared genes and/or common environmental risk factors such as smoking and hypertension.[1] A prospective cohort study showed that smoking and hypertension were independent additional risk factors for the presence of IAs in persons with a positive family history of aSAH.[18] A population-based heritability study assessed the contribution of genetic factors to aSAH cohorts and reported a 41% heritability,[19] which is comparable with heritability estimates of other complex diseases.[20] In a genome-wide association study meta-analysis of intracranial aneurysms, half of this heritability could already be explained.[21]

The patients with familial UIA analyzed in this study had a lower PHASES score, thus indicating a lower risk of rupture than patients with sporadic UIA. A lower PHASES score in familial than in sporadic UIA was also found in a previous study analyzing patients with familial and sporadic UIA.[3] Numerous studies comparing the characteristics of familial UIA with those of sporadic UIA have found that familial UIA are more often located at the middle cerebral artery and rupture at a younger age.[22] These findings may explain the lower PHASES score in these patients. Alternatively, selection bias may have occurred, since the proportion of patients undergoing preventive treatment was higher in patients with familial than in patients with sporadic UIA. As a result, in the group of familial patients, the UIA with high PHASES scores may have been preventively treated more often. Despite the lower PHASES score and the shorter period of follow-up, both factors implying a lower risk of rupture, and the higher proportion of familial aneurysms undergoing preventive treatment, familial aneurysms still had a higher risk of rupture. If proportions of patients undergoing preventive treatment would have been similar for familial and sporadic UIA, the

Figure 2 Hazard Ratio (HR) of the Rupture Rate in Patients With Familial Aneurysms Compared to Sporadic Aneurysms Adjusted for the PHASES Score and Smoking in Cohorts Defining First-Degree Relatives as Parents, Children, and Siblings, Analyzing the Data per Patient

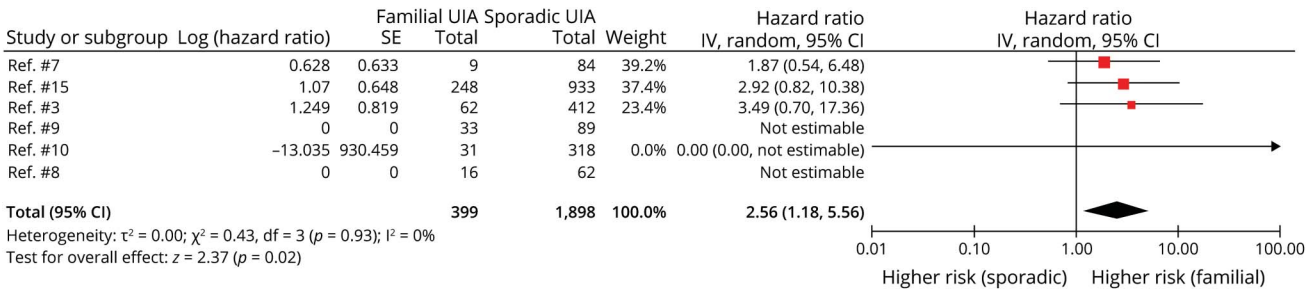

In the study by Wermer et al.,[8] 1 aneurysm ruptured in a patient with multiple aneurysms. The ruptured aneurysm was the smallest aneurysm and consequently this rupture was not included in the analysis per patient. CI = confidence interval; UIA = unruptured intracranial aneurysm.

rupture risk of familial UIA might have even been higher than we found.

A strength of our study is that we evaluated the association between a positive family history and the rupture risk of UIA using individual patient data from 8 prospective cohort studies, of which 6 cohorts defined first-degree relatives as parents, children, and siblings, and by that were able to include a large sample size with a large number of outcomes and person-years of follow-up. This allowed us to estimate the risk with high precision. In cohorts defining first-degree relatives as parents, children, and siblings the subgroup of familial patients was 17% of the total group of patients with UIA and included 399 patients with familial UIA. All studies had a prospective design and the quality was assessed with the QUIPS tool. A limitation of this study is that selection bias may have occurred due to informative censoring (loss to follow-up) within each cohort study. For example, in cohorts some patients were treated more aggressively and many patients received treatment during follow-up. In treated patients, growth of the UIA may have occurred, which is associated with a higher risk of rupture,[23] and consequently may have led to selection bias. Secondly, we performed patient-level analysis and in patients with multiple aneurysms we made the assumption that the largest aneurysms ruptured. In previous studies, a greater likelihood of multiple UIAs in patients with a positive family history is described.[24] In our study, familial cases did not have multiple IAs more often than sporadic cases when rupture occurred. Performing an additional analysis per aneurysm resulted in similar results, so this assumption did not influence our analysis. Thirdly, data on aspect ratio and irregular aneurysm shape were not available for either of the cohort studies included. Aspect ratio and irregular aneurysm shape are also known factors for UIA rupture,[25,26] and a higher prevalence of irregular aneurysms in familial cases may contribute to the difference in rupture. However, according to a previous study, the prevalence of these risk factors for aneurysm rupture was not higher in patients with aSAH compared to patients with sporadic aSAH.[27] Fourth, in our primary analysis, patients from Finnish populations were overrepresented (55%) compared to Dutch (29%) and Japanese (15%) populations. Across all populations a higher risk of rupture for familial compared to sporadic UIA was found, with the highest HR in the non-Finnish and non-Japanese cohort, so our results are generalizable to all populations. Fifth, the

Figure 3 Hazard Ratio of the Rupture Rate Adjusted for the PHASES Score and Smoking for Familial Aneurysms Compared to Sporadic Aneurysms in Cohorts Defining First-Degree Relatives as Parents, Children, and Siblings, Analyzing the Data per Aneurysm

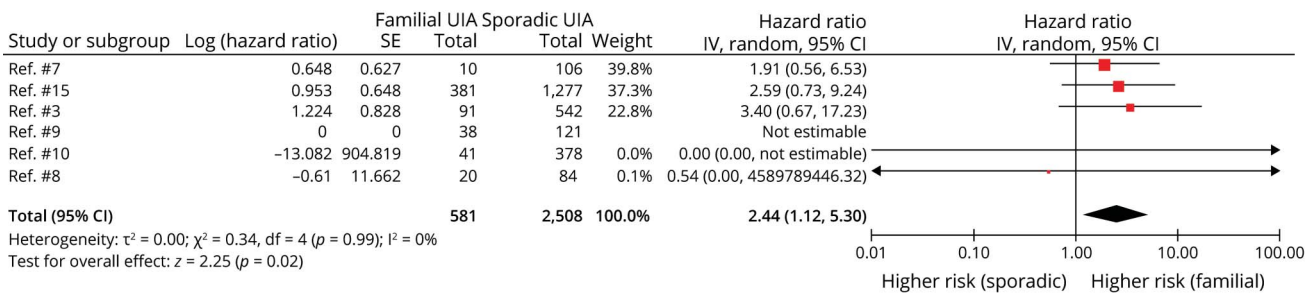

CI = confidence interval; UIA = unruptured intracranial aneurysm.

subgroup of familial patients was 17% of the total group of patients with UIA, ranging from 9% up to 29%. In previous studies, the proportion of familial cases is around 10%.[1] A possible explanation for this higher proportion in studies included in our meta-analysis could be that many included patients were treated in tertiary referral centers and that patients with a positive family history were referred to such centers more often. Regardless of the proportion of familial patients for all the different cohorts, a higher rupture risk of familial aneurysms was found, suggesting that despite differences in proportion of familial cases, our results are generalizable. Sixth, we had no data on confirmed consanguinity for the different cohorts. Finally, the difference in definition for a positive family history in all available studies resulted in systematic differences in the rupture risk. In 6 studies, siblings were included in the definition of first-degree relatives,[3,7-10] compared to 2 studies in which first-degree were defined as parents or children.[11,13] Consequently, the increased rupture risk in familial cases may have been diluted in these 2 studies because fewer patients are categorized as patients with familial UIA and because siblings with a positive family history are included in the group of patients with sporadic UIA. This effect cannot be counteracted by including both first-degree relatives and second-degree relatives in this family group. In this way, siblings are included in the familial group but also grandchildren and grandparents and these family relatives are likely to dilute the rupture risk in the familial group as they are known to have a risk of aSAH comparable to the general population.[23] Alternatively, in our data we were also not able to re-analyze the 6 cohorts excluding siblings in their definition as first-degree relatives. Future studies should assess the extent to which siblings influence the higher risk of rupture in familial cases.

We found a higher risk of rupture for familial compared to sporadic UIA, with a point estimate of a 2.5 times higher risk, and a range from a 1.2 to 5 times higher risk when using a definition for a positive family history that includes affected parents, siblings, and children. On analyzing all cohorts including those in which first-degree relatives are defined as only parents and children, but not siblings, a slightly but not statistically significantly increased risk of aneurysm rupture for familial compared to sporadic UIA was found. When assessing the risk of rupture of UIAs in familial patients defined as individuals with at least 2 affected first-degree relatives including parents, children, and siblings, this higher risk should be taken into account and a more aggressive treatment approach in these patients as compared to sporadic cases is justified. To assess whether this increased rupture risk should influence the current screening strategy of families of patients with familial UIA, an updated cost-effectiveness analysis with this increased rupture risk is needed.[28-30] Further studies are also needed on frequency of follow-up imaging in familial UIA. Growth of UIA is associated with a higher risk of rupture.[31] Thus, a higher frequency of follow-up imaging may detect growth before rupture, and provide the opportunity for targeted aggressive preventive treatment in familial UIA.

Study Funding

Supported by the Netherlands Cardiovascular Research Initiative: an initiative with support of the Dutch Heart Foundation, CVON2015-08 ERASE. This project has received funding from the European Research Council under the European Union's Horizon 2020 research and innovation program (grant agreement 852173).

Disclosure

The authors report no disclosures relevant to the manuscript. Go to Neurology.org/N for full disclosures.

Publication History

Received by *Neurology* February 9, 2021. Accepted in final form September 20, 2021.

Appendix Authors

Name	Location	Contribution
Charlotte C.M. Zuurbier, MD	University Medical Center Utrecht, the Netherlands	Literature search, statistical analysis, writing of the manuscript
Liselore A. Mensing, MD	University Medical Center Utrecht, the Netherlands	Data collection, review of manuscript
Marieke J.H. Wermer, MD, PhD	Leiden University Medical Center, the Netherlands	Data collection, review of manuscript
Seppo Juvela, MD, PhD	University of Helsinki, Finland	Data collection, review of manuscript
Antti E. Lindgren, MD, PhD	University of Eastern Finland, Kuopio	Data collection, review of manuscript
Timo Koivisto, MD, PhD	University of Eastern Finland, Kuopio	Data collection, review of manuscript
Juha E. Jääskeläinen, MD, PhD	University of Eastern Finland, Kuopio	Data collection, review of manuscript
Tomosato Yamazaki, MD, PhD	Department of Neurosurgery, National Hospital Organization, Mito Medical Center, Japan	Data collection, review of manuscript
Rob Molenberg, BsC	Departments of Neurosurgery, University Medical Center Groningen, the Netherlands	Data collection, review of manuscript
J. Marc C. van Dijk, MD, PhD	Departments of Neurosurgery, University Medical Center Groningen, the Netherlands	Data collection, review of manuscript
Maarten Uyttenboogaart, MD, PhD	Departments of Neurology and Medical Imaging Center, University Medical Center Groningen, the Netherlands	Data collection, review of manuscript
Marlien W. Aalbers, MD	Departments of Neurosurgery, University Medical Center Groningen, the Netherlands	Data collection, review of manuscript

Appendix *(continued)*

Name	Location	Contribution
Akio Morita, MD, PhD	University of Tokyo–Nippon Medical School, Tokyo, Japan	Data collection, review of manuscript
Shinjiro Tominari, MD, PhD	Department of Health Informatics, School of Public Health, Kyoto University, Japan	Data collection, review of manuscript
Hajime Arai, MD, PhD	Juntendo University Medical School, Tokyo, Japan	Data collection, review of manuscript
Kazuhiko Nozaki, MD, PhD	Shiga University of Medical Science, Japan	Data collection, review of manuscript
Yuichi Murayama, MD	Tokyo Jikei University School of Medicine, Japan	Data collection, review of manuscript
Toshihiro Ishibashi, MD	Tokyo Jikei University School of Medicine, Japan	Data collection, review of manuscript
Hiroyuki Takao, MD, PhD	Tokyo Jikei University School of Medicine, Japan	Data collection, review of manuscript
Gabriel J.E. Rinkel, MD, PhD	University Medical Center Utrecht, the Netherlands	Statistical analysis, review of manuscript
Jacoba P. Greving, PhD	University Medical Center Utrecht, the Netherlands	Statistical analysis, review of manuscript
Ynte M. Ruigrok, MD, PhD	University Medical Center Utrecht, the Netherlands	Outline of study, statistical analysis review of manuscript

References

1. Ruigrok YM, Rinkel GJ, Wijmenga C. Genetics of intracranial aneurysms. *Lancet Neurol.* 2005;4(3):179-189.
2. Broderick JP, Brown RD Jr., Sauerbeck L, et al. Greater rupture risk for familial as compared to sporadic unruptured intracranial aneurysms. *Stroke.* 2009;40(6):1952-1957.
3. Mensing LA, Greving JP, Verhoeff TA, Rinkel GJE, Ruigrok YM. Comparison of rupture risk of intracranial aneurysms between familial and sporadic patients. *Stroke.* 2019;50(6):1380-1383.
4. Zuurbier C, Greving JP, Rinkel G, Ruigrok YM. Higher risk of intracranial aneurysms and subarachnoid haemorrhage in siblings of families with intracranial aneurysms. *Eur Stroke J.* 2020;5(1):73-77.
5. Greving JP, Wermer MJ, Brown RD Jr., et al. Development of the phases score for prediction of risk of rupture of intracranial aneurysms: a pooled analysis of six prospective cohort studies. *Lancet Neurol.* 2014;13(1):59-66.
6. Hayden JA, Cote P, Bombardier C. Evaluation of the quality of prognosis studies in systematic reviews. *Ann Intern Med.* 2006;144(6):427-437.
7. Juvela S, Poussa K, Lehto H, Porras M. Natural history of unruptured intracranial aneurysms: a long-term follow-up study. *Stroke.* 2013;44(9):2414-2421.
8. Wermer MJ, van der Schaaf IC, Velthuis BK, Majoie CB, Albrecht KW, Rinkel GJ. Yield of short-term follow-up CT/MR angiography for small aneurysms detected at screening. *Stroke.* 2006;37(2):414-418.
9. Molenberg R, Aalbers MW, Metzemaekers JDM, et al. Clinical relevance of short-term follow-up of unruptured intracranial aneurysms. *Neurosurg Focus.* 2019;47(1):E7.
10. Sonobe M, Yamazaki T, Yonekura M, Kikuchi H. Small unruptured intracranial aneurysm verification study: Suave Study, Japan. *Stroke.* 2010;41(9):1969-1977.
11. UCAS Japan Investigators; Morita A, Kirino T, Hashi K, et al. The natural course of unruptured cerebral aneurysms in a Japanese cohort. *N Engl J Med.* 2012;366(1):2474-2482.
12. Grambsch TMT PM. Proportional hazards tests and diagnostics based on weighted residuals. *Biometrika.* 1994;81(1):515-526.
13. Murayama Y, Takao H, Ishibashi T, et al. Risk analysis of unruptured intracranial aneurysms: prospective 10-year cohort study. *Stroke.* 2016;47(2):365-371.
14. Wiebers DO, Whisnant JP, Huston J III, et al. Unruptured intracranial aneurysms: natural history, clinical outcome, and risks of surgical and endovascular treatment. *Lancet.* 2003;362(9378):103-110.
15. Lindgren AE, Koivisto T, Bjorkman J, et al. Irregular shape of intracranial aneurysm indicates rupture risk irrespective of size in a population-based cohort. *Stroke.* 2016;47(5):1219-1226.
16. Bor AS, Rinkel GJ, van Norden J, Wermer MJ. Long-term, serial screening for intracranial aneurysms in individuals with a family history of aneurysmal subarachnoid haemorrhage: a cohort study. *Lancet Neurol.* 2014;13(4):385-392.
17. Vlak MH, Algra A, Brandenburg R, Rinkel GJ. Prevalence of unruptured intracranial aneurysms, with emphasis on sex, age, comorbidity, country, and time period: a systematic review and meta-analysis. *Lancet Neurol.* 2011;10(7):626-636.
18. Rasing I, Nieuwkamp DJ, Algra A, Rinkel GJ. Additional risk of hypertension and smoking for aneurysms in people with a family history of subarachnoid haemorrhage. *J Neurol Neurosurg Psychiatry.* 2012;83(5):541-542.
19. Korja M, Silventoinen K, McCarron P, et al. Genetic epidemiology of spontaneous subarachnoid hemorrhage: Nordic Twin Study. *Stroke.* 2010;41(11):2458-2462.
20. Polderman TJ, Benyamin B, de Leeuw CA, et al. Meta-analysis of the heritability of human traits based on fifty years of twin studies. *Nat Genet.* 2015;47(7):702-709.
21. Bakker MK, van der Spek RAA, van Rheenen W, et al. Genome-wide association study of intracranial aneurysms identifies 17 risk loci and genetic overlap with clinical risk factors. *Nat Genet.* 2020;52(7):1303-1313.
22. Slot EMH, Rinkel GJE, Algra A, Ruigrok YM. Patient and aneurysm characteristics in familial intracranial aneurysms: a systematic review and meta-analysis. *PLoS One.* 2019;14(4):e0213372.
23. Bromberg JE, Rinkel GJ, Algra A, et al. Subarachnoid haemorrhage in first and second degree relatives of patients with subarachnoid haemorrhage. *BMJ.* 1995;311(7000):288-289.
24. Ruigrok YM, Rinkel GJ, Algra A, Raaymakers TW, Van Gijn J. Characteristics of intracranial aneurysms in patients with familial subarachnoid hemorrhage. *Neurology.* 2004;62(6):891-894.
25. Kleinloog R, de Mul N, Verweij BH, Post JA, Rinkel GJE, Ruigrok YM. Risk factors for intracranial aneurysm rupture: a systematic review. *Neurosurgery.* 2018;82(4):431-440.
26. Tominari S, Morita A, Ishibashi T, et al. Prediction model for 3-year rupture risk of unruptured cerebral aneurysms in Japanese patients. *Ann Neurol.* 2015;77(6):1050-1059.
27. Mensing LA, Rinkel GJ, Vlak MH, van der Schaaf IC, Ruigrok YM. Difference in aneurysm characteristics between patients with familial and sporadic aneurysmal subarachnoid haemorrhage. *PLoS One.* 2016;11(6):e0154281.
28. Takao H, Nojo T, Ohtomo K. Screening for familial intracranial aneurysms: decision and cost-effectiveness analysis. *Acad Radiol.* 2008;15(4):462-471.
29. Bor AS, Koffijberg H, Wermer MJ, Rinkel GJ. Optimal screening strategy for familial intracranial aneurysms: a cost-effectiveness analysis. *Neurology.* 2010;74(21):1671-1679.
30. Hopmans EM, Ruigrok YM, Bor AS, Rinkel GJ, Koffijberg H. A cost-effectiveness analysis of screening for intracranial aneurysms in persons with one first-degree relative with subarachnoid haemorrhage. *Eur Stroke J.* 2016;1(4):320-329.
31. Brinjikji W, Zhu YQ, Lanzino G, et al. Risk factors for growth of intracranial aneurysms: a systematic review and meta-analysis. *AJNR Am J Neuroradiol.* 2016;37(4):615-620.

diagnostics

MDPI

Article

Preoperative Evaluation and Surgical Simulation for Osteochondritis Dissecans of the Elbow Using Three-Dimensional MRI-CT Image Fusion Images

Sho Kohyama [1,*], Yasumasa Nishiura [2], Yuki Hara [3], Takeshi Ogawa [4], Akira Ikumi [5], Eriko Okano [3], Yasukazu Totoki [3], Yuichi Yoshii [6] and Masashi Yamazaki [3]

1 Department of Orthopaedic Surgery, Kikkoman General Hospital, Noda 278-0005, Japan
2 Tsuchiura Clinical Education and Training Center, Department of Orthopaedic Surgery, Tsukuba University Hospital, Tsuchiura 300-8585, Japan; ynishi@md.tsukuba.ac.jp
3 Department of Orthopaedic Surgery, Faculty of Medicine, University of Tsukuba, Tsukuba 305-8575, Japan; yukihara@md.tsukuba.ac.jp (Y.H.); eokano@tsukuba-seikei.jp (E.O.); yasutotoki@tsukuba-seikei.jp (Y.T.); masashiy@md.tsukuba.ac.jp (M.Y.)
4 Mito Medical Center, Department of Orthopaedic Surgery, National Hospital Organization, Ibaraki 311-3193, Japan; ogawat@md.tsukuba.ac.jp
5 Mito Medical Education and Training Center, Department of Orthopaedic Surgery, Tsukuba University Hospital, Mito 310-0015, Japan; bravelupus193@gmail.com
6 Department of Orthopaedic Surgery, Tokyo Medical University Ibaraki Medical Center, Tokyo 300-0395, Japan; yyoshii@tokyo-med.ac.jp
* Correspondence: sho_kohyama_1025@yahoo.co.jp

Citation: Kohyama, S.; Nishiura, Y.; Hara, Y.; Ogawa, T.; Ikumi, A.; Okano, E.; Totoki, Y.; Yoshii, Y.; Yamazaki, M. Preoperative Evaluation and Surgical Simulation for Osteochondritis Dissecans of the Elbow Using Three-Dimensional MRI-CT Image Fusion Images. *Diagnostics* **2021**, *11*, 2337. https://doi.org/10.3390/diagnostics11122337

Academic Editor: Ayman El-Baz

Received: 1 November 2021
Accepted: 9 December 2021
Published: 11 December 2021

Abstract: We used our novel three-dimensional magnetic resonance imaging-computed tomography fusion images (3D MRI-CT fusion images; MCFIs) for detailed preoperative lesion evaluation and surgical simulation in osteochondritis dissecans (OCD) of the elbow. Herein, we introduce our procedure and report the findings of the assessment of its utility. We enrolled 16 men (mean age: 14.0 years) and performed preoperative MRI using 7 kg axial traction with a 3-Tesla imager and CT. Three-dimensional-MRI models of the humerus and articular cartilage and a 3D-CT model of the humerus were constructed. We created MCFIs using both models. We validated the findings obtained from the MCFIs and intraoperative findings using the following items: articular cartilage fissures and defects, articular surface deformities, vertical and horizontal lesion diameters, the International Cartilage Repair Society (ICRS) classification, and surgical procedures. The MCFIs accurately reproduced the lesions and correctly matched the ICRS classification in 93.5% of cases. Surgery was performed as simulated in all cases. Preoperatively measured lesion diameters exhibited no significant differences compared to the intraoperative measurements. MCFIs were useful in the evaluation of OCD lesions and detailed preoperative surgical simulation through accurate reproduction of 3D structural details of the lesions.

Keywords: osteochondritis dissecans; elbow; magnetic resonance imaging; tomography; X-ray computed; imaging; three-dimensional; image interpretation; computer-assisted; simulation

1. Introduction

Osteochondritis dissecans of the elbow (OCD) is a rare intra-articular osteochondral lesion that is associated with overhead throwing sports [1–5]. The subchondral bone and articular cartilage of the humeral capitellum are affected, and several possible causes, including repetitive microtrauma and genetic factors, are implicated [3,4,6,7]. Although the stability and size of the lesion are considered important factors impacting lesion severity [6,8–10], no single imaging modality can adequately predict lesion severity [11–17], thereby presenting a challenge to elbow surgeons. A recent study by Pu et al. concluded that a combination of radiography, computed tomography (CT), and magnetic resonance

imaging (MRI) can most accurately determine OCD lesion stability by compensating for the respective flaws of the individual modalities [18]. However, at present, surgery is the only means of conclusively confirming the severity of OCD lesions using the classification proposed by the International Cartilage Repair Society (ICRS) [19–23].

Magnetic resonance arthrography (MRA) is another alternative modality for the evaluation of OCD lesions. As MRA involves the injection of contrast medium into the joint, the joint capsule distends, and visualization and differentiation of intra-articular structures can be enhanced [24,25]. Therefore, MRA could better depict articular cartilage. However, MRA is an invasive imaging modality and may cause pain, anxiety, and complications such as allergic reactions and infections [26,27]. As the majority of patients with OCD are children, it is important to minimize the use of invasive procedures. In addition, MRA alone cannot accurately evaluate the conditions of subchondral bone lesions such as sclerosis.

To address this difficulty, we developed and recently reported a method to create 3D MRI-CT fusion images (MCFIs) of the OCD lesions [28]. This computer-aided technique combines the advantages of CT and MRI and provides a minimally invasive, accurate preoperative evaluation of OCD lesions. In addition, detailed surgical simulation is possible, which could aid surgeons in intraoperative decision making.

There are various surgical options to effectively manage OCD lesions. In severe cases with unstable lesions, articular surface reconstruction must be considered. As the articular cartilage and subchondral lesion both require reconstruction, osteochondral autograft transplantation is a viable option. Generally, osteochondral autografts are harvested either from the knee using the osteochondral autograft transplantation system (OATS) or from the rib [1,6,11,29]. When the lesion is small but unstable, or the lesion is stable but resistant to conservative therapy, drilling of the lesion is an effective option. Drilling accelerates the union of the lesion and surrounding bone tissue by promoting bleeding from the bone marrow by puncturing the subchondral bone. If articular free bodies are present, their removal must be considered. Alternative surgical options include abrasion chondroplasty, microfracture, and in situ fixation of the lesion [1]. In this article, we introduce the use of MCFIs as a method of OCD lesion evaluation and surgical simulation for OCD lesions and report the findings of the assessment of the clinical applicability of the computer-aided technique. We aimed to assess the accuracy of MCFIs in evaluating OCD lesion severity and in facilitating surgical simulation.

2. Materials and Methods

2.1. Patient Selection

The institutional review board of the University of Tsukuba Hospital approved this study (Study Number: H29-58). Twenty-eight patients visited our facility and were diagnosed with OCD between July 2017 and March 2021. Among them, 16 patients whose lesions were evaluated using MCFIs were enrolled in this study. These patients subsequently underwent surgery. We obtained written informed consent from each patient. It was clearly stated that we would only use MCFIs for lesion evaluation and to decide the treatment strategy. All patients were boys (mean age: 14.0 $\pm$ 1.0 years, range: 12–16 years), and the right side was affected in fifteen patients, while the left side was affected in one patient. The average body weight of the patients was 56.9 (48.0–65.0) kg.

2.2. Obtaining the MR and CT Images

A 3-Tesla imager (MAGNETOM© Verio, Siemens, Munich, Germany) was used for MRI. We followed the procedures we published in a previous article on imaging sequence and settings, position of patients, and application of axial traction (7 kg) [28]. Axial traction widens the joint space and helps better visualize an outline of the articular cartilage of the humeral capitellum [28,30] (Figure 1).

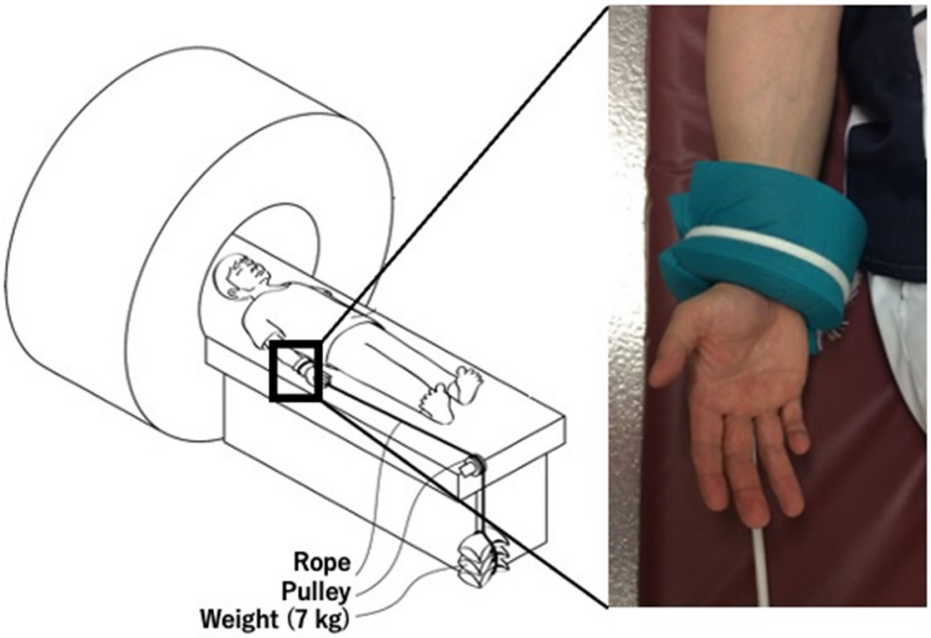

Figure 1. Acquisition of magnetic resonance images with axial traction. Axial traction (7 kg) was applied to the elbow to better visualize the articular cartilage of the humeral capitellum.

We used a 320-row scanner (Aquilion ONE^{TM}, Toshiba, Tokyo, Japan) for CT, and images were obtained with a 0.5 mm slice thickness. We did not apply axial traction during CT because CT data of the whole joint were not necessary for the procedure.

2.3. Creation of 3D Models

Using the obtained data, we created 3D MRI models of the humerus and articular cartilage and a 3D CT model of the humerus. The Materialise Mimics Innovation Suite version 20 (Materialise©, Leuven, Belgium) was used for this procedure. We referred to the MR signal intensity of the articular cartilage and humerus in each case for creation of 3D MRI models. As the participants in this study were skeletally immature, the growth cartilage was present in some cases. First, we set a threshold for the MR signal intensity for each target tissue. According to the set threshold, we selected the pixels that corresponded to the target tissue. The threshold was roughly set automatically and adjusted manually while simultaneously referring to the monitor to ensure correct selection of the target tissue. This procedure is called segmentation, which is crucial for creating better images. While segmenting the articular cartilage, we defined the articular cartilage fissures (ACFs) as the low-intensity lines within the articular cartilage, which penetrate or are perpendicular to the articular surface [12,15,31–33]. Articular surface deformity (ASD) was defined as irregularities in the outline of the articular cartilage [12,15] (Figure 2). The segmented structures, as well as the ACFs and ASDs were reconstructed and reproduced into 3D models. Similarly, we created 3D CT models of the humerus. During the procedure, the subchondral bone was considered segmented when the discontinuity of the subchondral bone to the floor was observed in all three planes: axial, sagittal, and coronal. We manually created a separate 3D model of segmented subchondral bone (SSB) and displayed it in red color for better visualization (Figure 3).

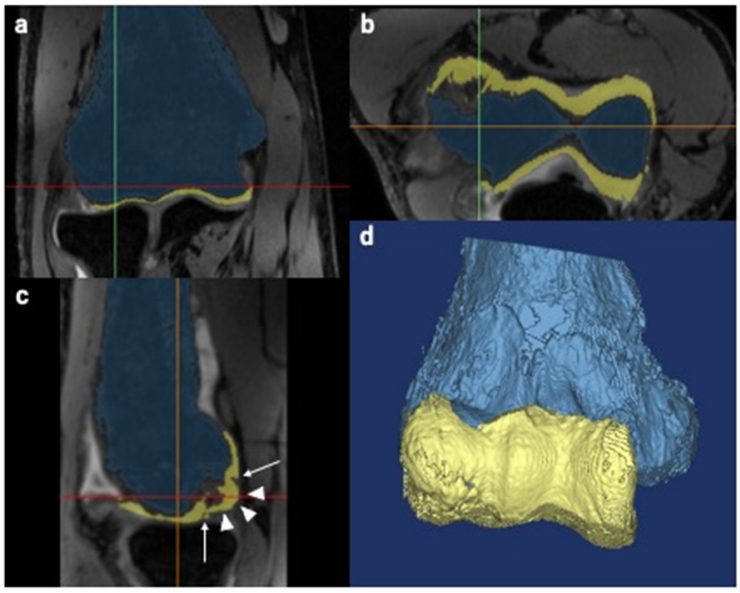

Figure 2. Creation of three-dimensional (3D) magnetic resonance imaging (MRI) models. The pixels correspond to the humerus and the articular cartilage which were independently selected based on the set threshold. The blue color represents the humerus, and the yellow color represents the articular cartilage. Green, red and orange lines are the reference lines correspond to sagittal, axial and coronal, respectively. (**a**) Coronal view. (**b**) Axial view. (**c**) Sagittal view. Arrow: articular cartilage fissures. Arrowheads: articular surface deformities. (**d**) Reconstructed 3D image of the humerus and articular cartilage.

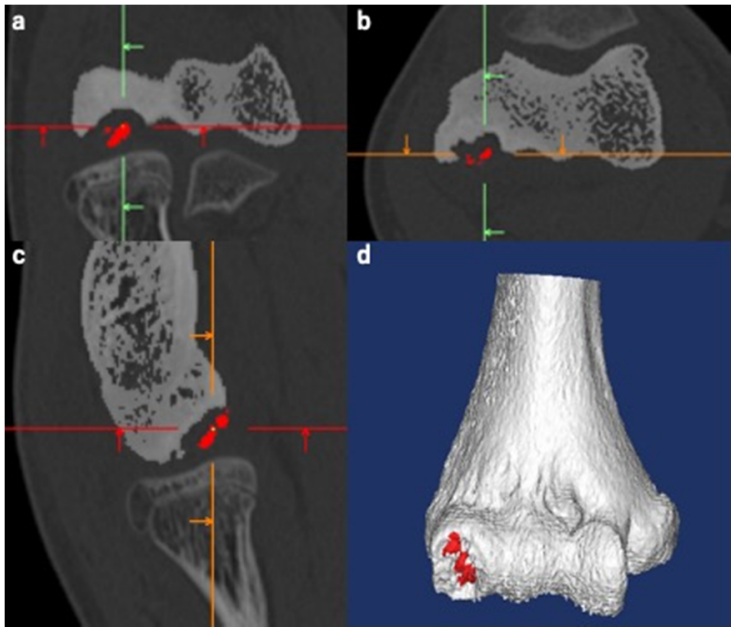

Figure 3. Creation of a three-dimensional (3D) computed tomography (CT) model of the humerus. The same procedure as used with magnetic resonance imaging was used. The segmented subchondral bone (SSB) was defined as the lesion whose continuity to the floor was lost in all three planes. The separate SSB model was created manually and is displayed in red for better visualization. Green, red and orange lines are the reference lines correspond to sagittal, axial and coronal, respectively. (**a**) Coronal view. (**b**) Axial view. (**c**) Sagittal view. (**d**) Reconstructed 3D image of the humerus.

2.4. Fusion of Created 3D Models

We used the 3-matic software version 12 (Materialise©, Belgium) to fuse the 3D models. First, we exported the created 3D models from the Materialise Mimics to the 3-matic. We then roughly fused both the 3D MRI and 3D CT models of the humerus using a function called N-point registration. This function enables two separate 3D models to be superimposed using an arbitrary number of corresponding points. In our procedure, we registered four corresponding points that are easy to recognize and belong to different planes, as reported in a previous study [28] (Figure 4a). Second, we used a function called global registration to fine-tune the position of the superimposed 3D models (Figure 4b). Using this function, the positions of the aligned 3D models can be automatically corrected depending on their shapes. Throughout the procedures, the 3D MRI model of the articular cartilage was set to move together with the 3D MRI model of the humerus in order to maintain the positional relationship between the structures. Finally, we completed the fusion of the 3D CT model of the humerus and the 3D MRI model of the articular cartilage by hiding the 3D MRI model of the humerus (Figure 4c). We termed this fusion model MCFI. The first author, an elbow surgeon with 14 years of clinical experience, created all MCFIs. The average interval between the MCFI creation and surgery was 26 (5–70) days.

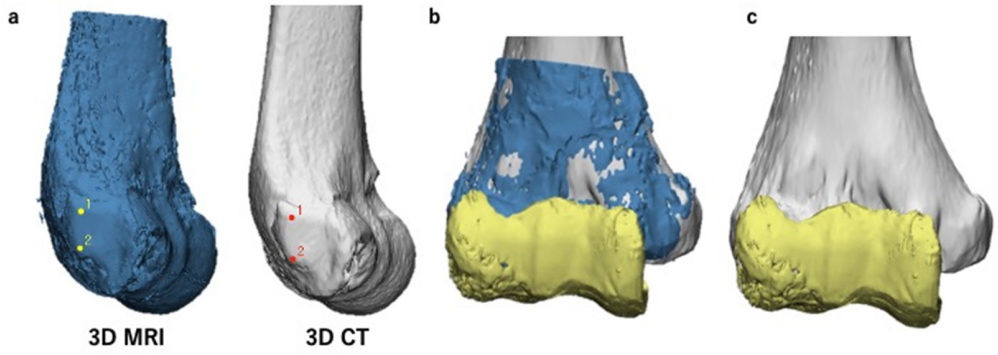

Figure 4. Procedures to create magnetic resonance imaging-computed tomography fusion images (MCFIs). The three-dimensional (3D) magnetic resonance imaging (MRI) model of the articular cartilage and 3D computed tomography (CT) model of the humerus were fused. (**a**) N-point registration of the 3D MRI and 3D CT models of the humerus for rough superimposition. The marked points in this figure are the two protuberances of the lateral epicondyle. (**b**) A superimposed 3D model after global registration (anteroposterior view). Here, the 3D CT and 3D MRI models of the humerus and the 3D MRI model of the articular cartilage are shown in gray, blue, and yellow, respectively. (**c**) A complete MCFI (anteroposterior view). The 3D MRI model of the humerus was hidden. This completed the creation of MCFIs.

Figure 4. Procedures to create magnetic resonance imaging-computed tomography fusion images (MCFIs). The three-dimensional (3D) magnetic resonance imaging (MRI) model of the articular cartilage and 3D computed tomography (CT) model of the humerus were fused. (**a**) N-point registration of the 3D MRI and 3D CT models of the humerus for rough superimposition. The marked points in this figure are the two protuberances of the lateral epicondyle. (**b**) A superimposed 3D model after global registration (anteroposterior view). Here, the 3D CT and 3D MRI models of the humerus and the 3D MRI model of the articular cartilage are shown in gray, blue, and yellow, respectively. (**c**) A complete MCFI (anteroposterior view). The 3D MRI model of the humerus was hidden. This completed the creation of MCFIs.

2.5. Lesion Evaluation Using MCFIs

The first author evaluated the OCD lesion immediately after image creation based on the MCFI. The evaluation was particularly focused on the findings of the articular cartilage and subchondral bone, such as the presence of ACFs, articular cartilage defect (ACD), or ASD (Figure 5a), and whether the subchondral bone was segmented or not. We recorded the findings of each case. In order to differentiate ASDs from ACDs, deformities were recorded as either protrusions or flattening of the articular surface. The positional relationship between the ACF and the SSB was evaluated by adjusting the transparency of the articular cartilage (Figure 5b). The articular surface of the humeral capitellum was considered elliptical in the anteroposterior view of the MCFI and divided into four areas, areas 1 to 4, clockwise from the anteromedial area (Figure 5c); we thereby recorded the location of each finding. Based on the findings reproduced in the MCFI, the vertical and horizontal diameters of the lesion were also measured (Figure 5d).

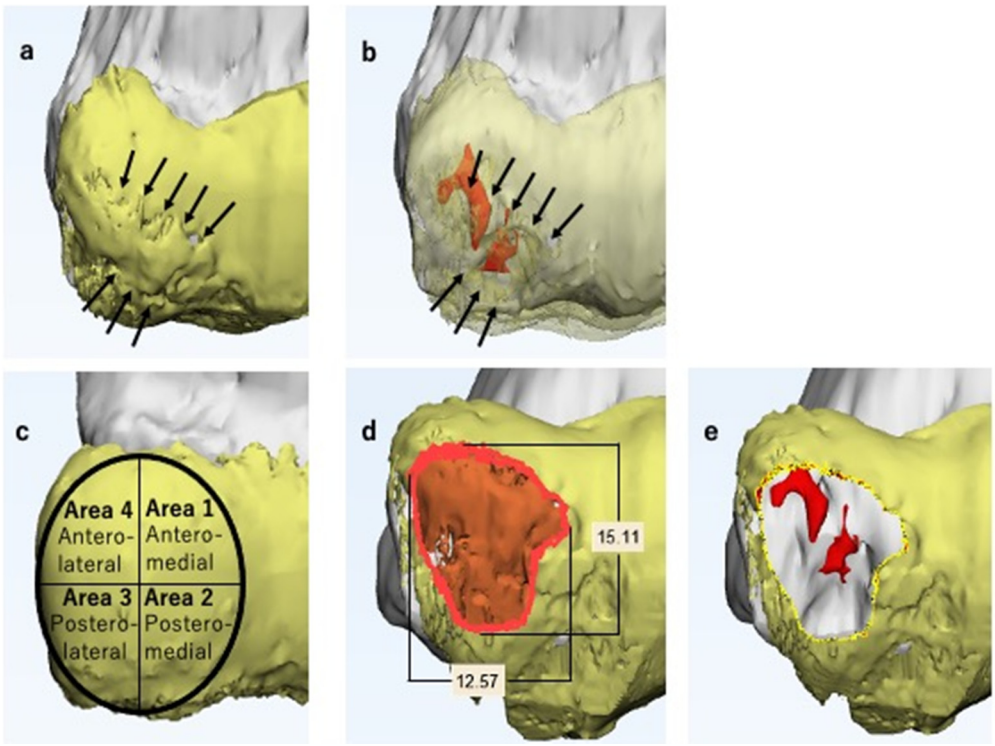

Figure 5. Magnetic resonance imaging-computed tomography fusion images (MCFIs). Here, the 3D CT model of the humerus and the 3D MRI model of the articular cartilage are shown in gray and yellow, respectively. (**a**) Anteroposterior view of the lesion (enlarged). The articular cartilage fissures (ACFs) can be observed (arrows). The articular surface is protruded and not smooth, particularly in the area surrounded by the fissure. (**b**) Anteroposterior view of the lesion with a transparent articular cartilage (enlarged). The segmented subchondral bone is shown in red and is located beneath the fissure (arrows). Considering all the findings, we predicted the lesion as unstable. (**c**) On the anteroposterior view of the MCFI, we divided the surface into four areas and recorded the location of each finding. (**d**) The lesion is marked in orange. The vertical and horizontal diameters of the lesion were measured. We determined the size of the lesion comprehensively based on the findings of the articular cartilage and subchondral lesion. (**e**) Simulated image of the lesion resection. We separated the area selected in Figure 5d from the original three-dimensional magnetic resonance imaging articular cartilage model and hid it to simulate lesion selection.

OCD lesions are defined as unstable when the lesion is displaced or dislocated, and thereby the articular surface is deformed [12,14–16,32–34]. We defined unstable OCD lesions in MCFIs as those with ACFs and/or ASDs, along with the SSB underneath. Based on the created MCFI, the ICRS classification [20] was predicted independently and comprehensively, respectively, by two surgeons (assessors 1 and 2) who had 13 and 12 years of clinical experience, respectively. The surgeons were requested to predict the ICRS classification at least 3 days preceding the patients' medical records. The two assessors participated as assistant surgeons in several surgeries performed in this study.

2.6. Surgical Simulation

We used the 3-matic software version 12 (Materialise©, Leuven, Belgium) for the surgical simulation. The first author performed all surgical simulations in this study.

Articular surface reconstruction by costal osteochondral autograft transplantation [19] is our first choice when the OCD lesion is unstable and its maximum diameter exceeds 10 mm; thus, we simulated the surgical procedure. First, we decided on the resection area according to the reproduced ACFs and ASDs (Figure 5d). After selecting the resection area, we separated the area from the original 3D model of the articular cartilage and created an

independent 3D model. This enabled us to freely hide the resection area, simulating the lesion resection (Figure 5e). Second, we simulated autograft transplantation. A 3D model of the average-sized costal osteochondral autograft was created in advance (Figure 6). We created this model based on the size of the actual autograft harvested from previously operated cases. This autograft model can be freely placed within the MCFI, and we simulated the position, direction, and depth of the transplantation (Figure 7).

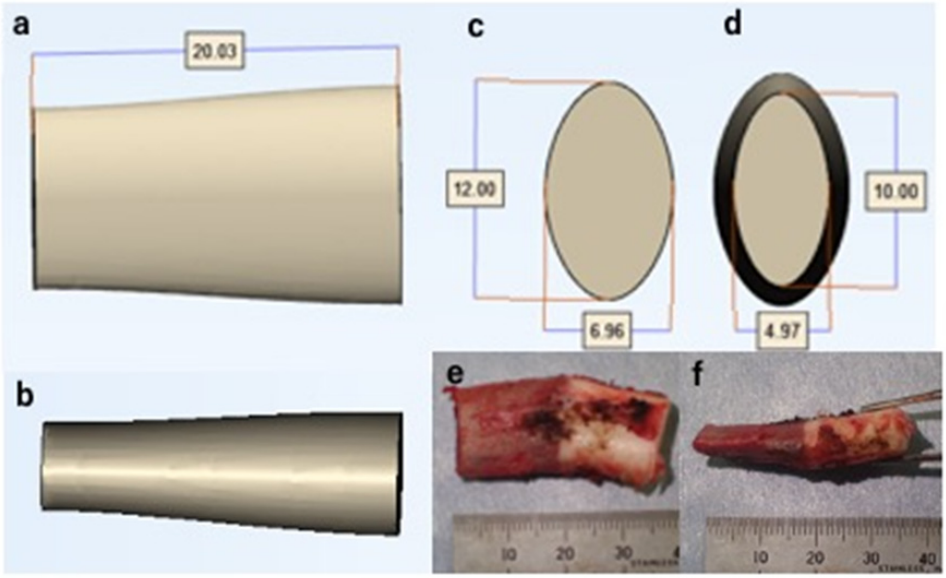

Figure 6. A three-dimensional model of an average-sized costal osteochondral autograft. (**a**) Anteroposterior view. (**b**) Lateral view. (**c**) Distal view. (**d**) Proximal view. (**e**) Anteroposterior view of a harvested costal osteochondral autograft. (**f**) Lateral view of a harvested costal osteochondral autograft.

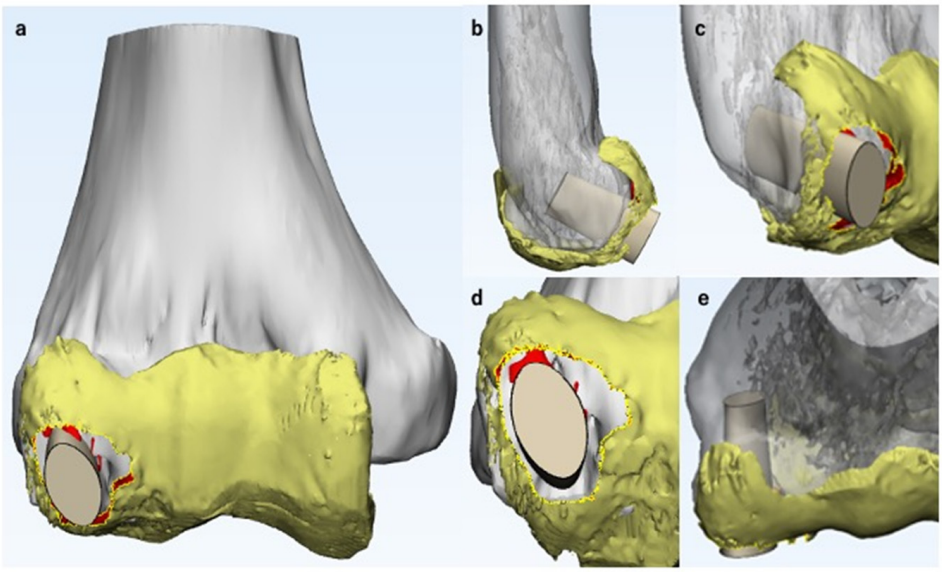

Figure 7. Simulation of costal osteochondral autograft transplantation. Here, the 3D CT model of the humerus and the 3D MRI model of the articular cartilage are shown in gray and yellow, respectively. The three-dimensional model of the costal osteochondral autograft was placed on the magnetic resonance imaging-computed tomography fusion image to simulate the position, direction, and depth of the transplant. (**a**) Anteroposterior view. (**b**) Lateral view. (**c**) Oblique view. (**d**) Distoproximal view. (**e**) Proximodistal view.

We simulated drilling when the OCD lesion was ICRS class IV and small, or when the lesion was stable, articular surface reconstruction was not necessary, and the lesion did not respond to conservative therapy. Generally, subchondral OCD lesions with a chronic history have a sclerotic component [1]. It is essential to penetrate the subchondral sclerosis to promote bone healing. Therefore, as the first step of the simulation of drilling, we manually selected the sclerotic region and highlighted it with a different color for better visualization. Second, we simulated the entry point, direction, and depth of drilling. When the lesion is stable and the articular surface is intact, it is important to avoid iatrogenic articular cartilage damage. Therefore, we simulated posteroanterior drilling for those cases (Figure 8).

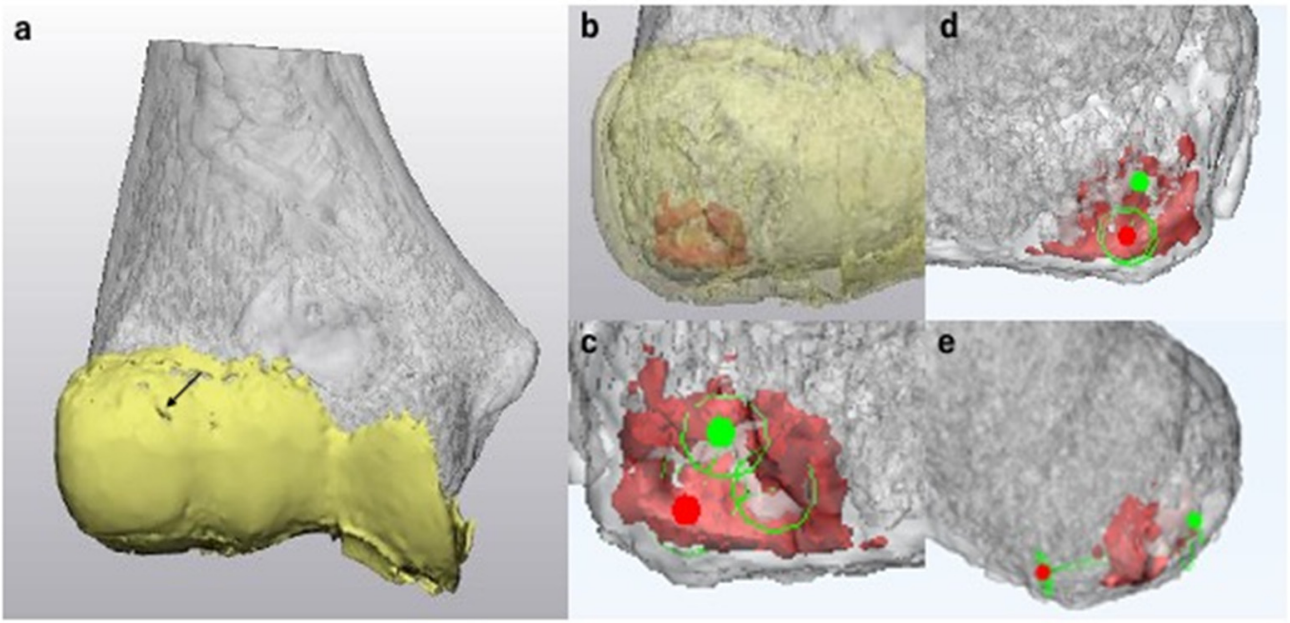

Figure 8. Surgical simulation of drilling. Here, the 3D CT model of the humerus and the 3D MRI model of the articular cartilage are shown in gray and yellow, respectively. (**a**) An anteroposterior view of the magnetic resonance imaging-computed tomography fusion image (MCFI) of case 1. The articular surface was smooth with only a small fissure in area 1 (arrow). (**b**) MCFI with a transparent articular cartilage. The subchondral lesion with sclerosis is shown in red. (**c**) Simulation of drilling (enlarged anteroposterior view without the articular cartilage). We simulated to penetrate the spots with sclerosis and cyst formation. The entry point is shown as a red spot, and the target point is shown in green. (**d**) Posteroanterior view. To avoid iatrogenic articular cartilage damage, we simulated posteroanterior drilling in these cases. The green circle with a red spot represents the entry point for drilling. (**e**) Lateral view. We simulated the direction and depth of drilling.

2.7. Intraoperative Evaluation of ICRS Classification

We evaluated all OCD lesions intraoperatively either under direct observation or using arthroscopic examination to determine the ICRS classification [20]. According to the definition, class I and II lesions are stable, while class III and IV lesions are unstable.

2.8. Evaluation of MCFIs

We compared the predicted values with the actual intraoperative findings for the ACFs, ACDs, ASDs, vertical and horizontal lesion diameters, and ICRS classification. The corresponding rate between each finding determined from the MCFI and those determined intraoperatively were evaluated. We calculated the corresponding rate as follows: (number of cases in which the findings determined by the MCFI corresponded to the actual intraoperative findings)/(total number of cases) [17].

Each finding and the corresponding ICRS classification were intraoperatively determined by both visual inspection and palpation. In class III lesions that underwent articular

reconstruction, the diameter of the resected lesion was recorded. In class IV lesions, the diameters of the articular cartilage defect were recorded. In 9 of 16 cases, where the first author conducted the surgery, another elbow surgeon with 23 years of clinical experience evaluated the intraoperative findings. This surgeon did not evaluate the lesion using the MCFI. The primary surgeon assessed the intraoperative findings in the remaining seven cases. Among the seven cases, six cases were assessed by an elbow surgeon with 23 years of clinical experience and one case by an elbow surgeon with 34 years of clinical experience. We compared the predicted and intraoperatively measured vertical and horizontal lesion diameters using the Mann–Whitney U test, which was selected because of the small sample size. Statistical significance was set at $p < 0.05$.

3. Results

3.1. Lesion Evaluation Using MCFIs

Tables 1–3 show the findings predicted by the MCFIs and intraoperatively determined findings for the ACFs, ACDs, and ASDs, respectively. The reproducibility of each finding was accurate in the MCFI, except for one case, in which the lesion was detached at the time of surgery, resulting in a corresponding rate of 93.8%. Table 4 depicts the measurements of the diameters of the lesions. The median values of the vertical diameter measured preoperatively and intraoperatively were 14.8 and 14.0 mm, respectively; there was no significant difference ($p = 0.78$). The median values of the horizontal diameter measured preoperatively and intraoperatively were 13.1 and 12.0 mm, respectively; there was no significant difference ($p = 0.14$). Figure 9 shows the intraoperative findings and corresponding MCFIs for representative cases.

3.2. ICRS Classifications

Table 5 presents the predicted and intraoperative ICRS classifications. The MCFI resulted in a corresponding rate of 93.8% for both examiners. This is because there was one case in which the lesion was detached at the time of surgery (case 15). We predicted this case as ICRS class III; however, the case was confirmed as class IV intraoperatively.

Table 1. Validation of the three-dimensional magnetic resonance imaging-computed tomography fusion images (3D MRI-CT fusion images; MCFIs) against intraoperative findings: articular cartilage fissures (ACFs). The reproducibility of the ACFs by the MCFIs was accurate in all cases.

Cases	Localization of Articular Cartilage Fissures (If Present)	
	Findings from 3D MRI-CT Fusion Images	Intraoperative Findings
1	Area 1	Area 1
2	Areas 1, 2, 3, and 4	Areas 1, 2, 3, and 4
3	None	None
4	Area 2	Area 2
5	Areas 1, 2, and 3	Areas 1, 2, and 3
6	None	None
7	Area 2	Area 2
8	Areas 2 and 3	Areas 2 and 3
9	Areas 1, 3, and 4	Areas 1, 3, and 4
10	Areas 1 and 4	Areas 1 and 4
11	Area 1	Area 1
12	Areas 1, 2, 3, and 4	Areas 1, 2, 3, and 4
13	Areas 2 and 3	Areas 2 and 3
14	Areas 2 and 3	Areas 2 and 3
15	Areas 1, 2, 3, and 4	Areas 1, 2, 3, and 4
16	Areas 2 and 3	Areas 2 and 3

Table 2. Validation of the magnetic resonance imaging-computed tomography fusion image (MCFI) against intraoperative findings: articular cartilage defects (ACDs). The reproducibility of the ACDs by MCFIs was accurate except for case 15, whose capitellar osteochondritis lesion was detached from the floor at the time of surgery.

Cases	Localization of Articular Cartilage Defects (If Present)	
	Findings from 3D MRI-CT Fusion Images	**Intraoperative Findings**
1	None	None
2	None	None
3	Areas 2 and 3	Areas 2 and 3
4	Areas 2 and 3	Areas 2 and 3
5	None	None
6	Area 2	Area 2
7	Areas 2 and 3	Areas 2 and 3
8	None	None
9	None	None
10	Area 1	Area 1
11	Area 1	Area 1
12	None	None
13	None	None
14	None	None
15	None	Areas 1, 2, 3, and 4 Lesion detached
16	None	None

Table 3. Validation of the magnetic resonance imaging-computed tomography fusion images (MCFIs) against intraoperative findings: articular surface deformities (ASDs). The MCFIs precisely reproduced the ASDs in all cases except for case 15. The lesion appeared to be protruded on the MCFI but was detached from the floor at the time of surgery.

Cases	Localization of Articular Surface Deformities (If Present)	
	Findings from 3D MRI-CT Fusion Images	**Intraoperative Findings**
1	None	None
2	Areas 2 and 3 (protrusion)	Areas 2 and 3 (protrusion)
3	None	None
4	None	None
5	Areas 2 and 3 (protrusion)	Areas 2 and 3 (protrusion)
6	None	None
7	None	None
8	Areas 2 and 3 (protrusion)	Areas 2 and 3 (protrusion)
9	Areas 2 and 3 (protrusion)	Areas 2 and 3 (protrusion)
10	Areas 1, 2, 3, and 4 (flattening)	Areas 1, 2, 3, and 4 (flattening)
11	Areas 1, 2, 3, and 4 (flattening)	Areas 1, 2, 3, and 4 (flattening)
12	Areas 2 and 3 (protrusion)	Areas 2 and 3 (protrusion)
13	Areas 2 and 3 (protrusion)	Areas 2 and 3 (protrusion)
14	Areas 2 and 3 (protrusion)	Areas 2 and 3 (protrusion)
15	Areas 1, 2, 3, and 4 (protrusion)	Areas 1, 2, 3, and 4 (lesion detached)
16	Areas 2 and 3 (protrusion)	Areas 2 and 3 (protrusion)

3.3. Surgical Simulation

We simulated drilling in four cases and osteochondral autograft transplantation in eleven cases. One case was indicated to perform free-body removal alone. All surgeries were conducted based on the simulations. We performed drilling for cases 1, 3, 11, and 15, free-body removal for cases 6 and 15, and costal osteochondral autograft transplantation for the remaining cases. Based on the MCFI, case 15 was indicated for articular surface reconstruction, but the patient did not consent to the surgical procedure and opted for the drilling procedure. We conducted all surgeries as simulated in all cases. Figure 10 shows the intraoperative findings and corresponding surgical simulation for representative cases.

Table 4. Validation of the magnetic resonance imaging-computed tomography fusion images (MCFIs) against intraoperative findings: vertical and horizontal lesion diameters. The reproducibility of the vertical and horizontal diameters of the lesions was accurate in the MCFI. In case 1, there were no articular cartilage defects or articular surface deformity. Therefore, it was impossible to measure the lesion size.

Cases	Vertical Diameters (mm)		Horizontal Diameters (mm)	
	MCFI	Intraoperative Findings	MDFIs	Intraoperative Findings
1				
2	19.7	18	12.3	12
3	7.9	8	11.5	11
4	13.6	12	14.5	14
5	16.1	14	15.6	15
6	11.6	10	8.8	8
7	12.1	15	14.3	13
8	18.7	17	12.5	12
9	19.4	19	14.1	14
10	16.9	16	14.7	12
11	19.5	20	16	15
12	16	18	12	12
13	11.6	11	7.8	8
14	14.8	14	11.8	10
15	13.5	13	14.2	11
16	12.5	12	13.1	10
Median value (interquartile range)	14.8 (12.1–16.9)	14.0 (11.5–17.5)	13.1 (11.8–14.3)	12.0 (10–14)
p-value		0.78		0.14

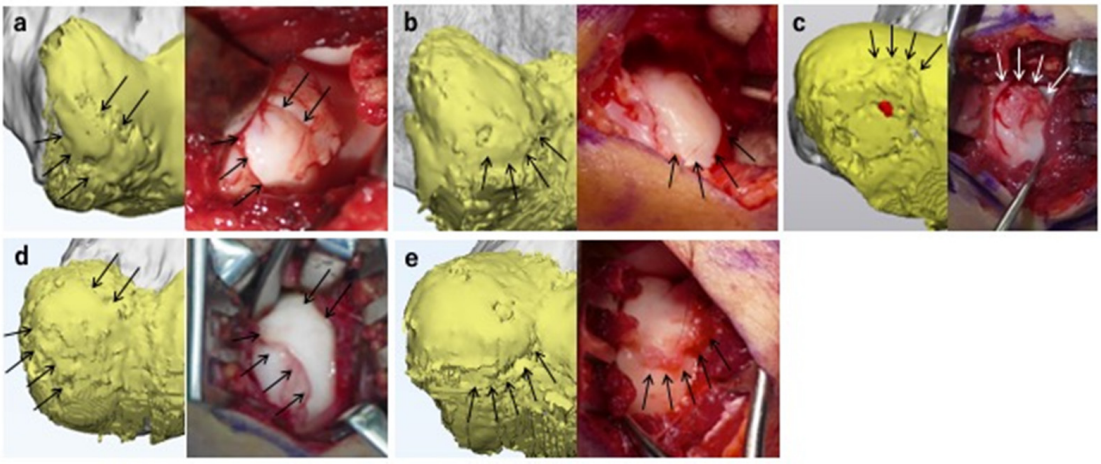

Figure 9. Magnetic resonance imaging-computed tomography fusion images (MCFIs) and corresponding intraoperative findings. The MCFIs are shown in the left panels, and the corresponding intraoperative findings are shown in the right panels. Here, the 3D CT model of the humerus and the 3D MRI model of the articular cartilage are shown in gray and yellow, respectively. (**a**) Case 12. The MCFI accurately reproduced the articular cartilage fissures (ACFs) in areas 1, 2, 3, and 4 (arrows). The lesion was predicted as unstable because the segmented subchondral bone (SSB) was present underneath the ACFs, and the articular surface was protruded. As predicted, the lesion was classified as unstable intraoperatively. (**b**) Case 8. The MCFI correctly reproduced the protrusion of the articular surface in areas 2 and 3 (arrows). The lesion was predicted as unstable owing to the presence of the articular surface deformity (ASD) and SSB underneath the ACF. The lesion was unstable on palpation, as predicted. (**c**) Case 16. The MCFI correctly reproduced the ACF and ASD in areas 2 and 3 (arrows). The lesion was predicted as unstable based on these findings and intraoperatively classified that the lesion was unstable. (**d**) Case 9. The MCFI correctly reproduced the ACFs in areas 1, 3, and 4 (arrows). The lesion was predicted as unstable based on the presence of the SSB underneath the ACF, as well as ASD. The lesion was unstable intraoperatively on palpation, as predicted. (**e**) Case 5. The MCFI correctly reproduced the ACF in areas 2 and 3 (arrows). The lesion was predicted as unstable because of the presence of ACF and the SSB underneath and ASD. The lesion was classified as unstable on palpation.

Table 5. Comparison of the International Cartilage Repair Society (ICRS) classification predicted by examiners and the actual intraoperative findings. The intraoperative ICRS classification accurately corresponded to the magnetic resonance imaging-computed tomography fusion image-based predictions in all cases except for case 15. The match rate was 93.8%.

Cases	MCFI		Intraoperative Findings
	Assessor 2	Assessor 3	
1	II	II	II
2	III	III	III
3	IV	IV	IV
4	IV	IV	IV
5	III	III	III
6	IV	IV	IV
7	IV	IV	IV
8	III	III	III
9	III	III	III
10	IV	IV	IV
11	IV	IV	IV
12	III	III	III
13	III	III	III
14	III	III	III
15	III	III	IV
16	III	III	III

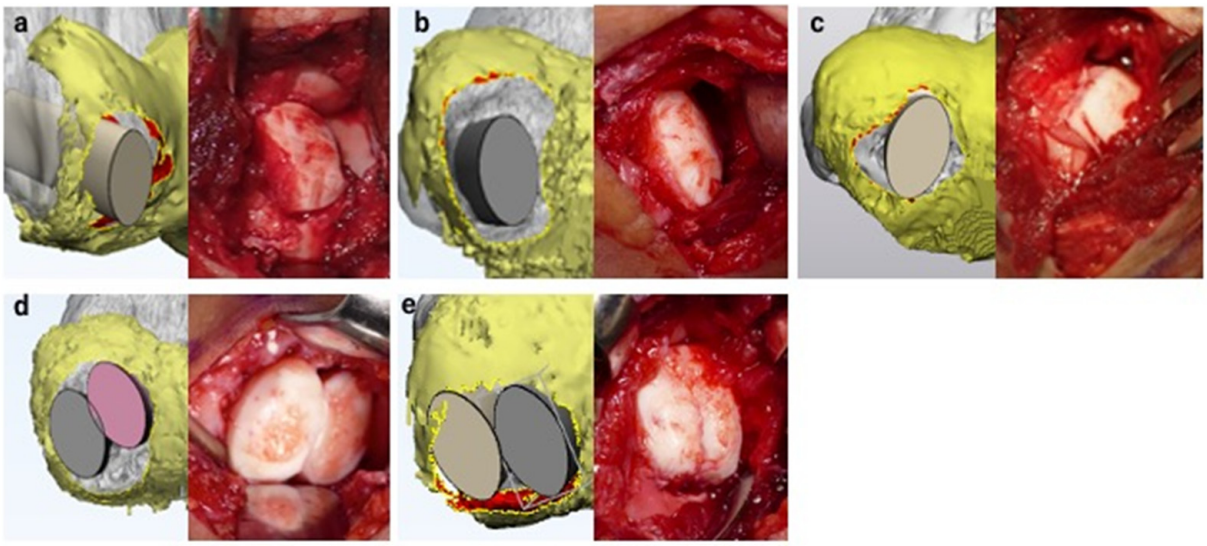

Figure 10. Surgical simulation using the magnetic resonance imaging-computed tomography fusion images and corresponding intraoperative findings. The surgical simulations are shown in the left panel, and corresponding intraoperative findings are shown in the right panel. Costal osteochondral autograft transplantation was simulated in all presented cases. All surgeries were conducted as simulated. Here, the 3D CT model of the humerus and the 3D MRI model of the articular cartilage are shown in gray and yellow, respectively. (**a**) Case 12. Reconstruction of the articular surface and lateral wall of the capitellum was necessary for this case. (**b**) Case 8. Reconstruction of the articular surface and lateral wall of the capitellum was necessary for this case. (**c**) Case 16. One costal osteochondral autograft transplantation procedure was sufficient to cover the articular surface defect. (**d**) Case 9. The predicted lesion was large; therefore, we simulated reconstruction of the articular surface by two costal osteochondral autografts to cover as much surface as possible. (**e**) Case 5. Two costal osteochondral autografts were necessary to reconstruct the large, predicted lesion.

4. Discussion

OCD lesion evaluation using MCFIs is a minimally invasive technique that enables prediction of lesion severity with high accuracy [28]. In developing this technique, we intended to maximize the advantages and compensate for the shortcomings of MRI and CT. The application of axial traction widens the joint space of the radio-capitellar joint and improves visualization of the articular cartilage outline of the humeral capitellum with minimum pain and discomfort [30,31], making the creation of accurate 3D models of the articular cartilage possible, and enabling images with a slice thickness of 0.4 mm to be obtained using a 3D sequence. We used a 7 kg traction weight according to previous studies [30,31]. There are no studies clarifying the ideal traction weight for elbow MRI in a skeletally immature population. Ideally, the traction weight must be decided on the basis of the body weight, size, and muscle development of the patient. Therefore, in the future, we will attempt to determine the ideal traction weight to lower discomfort during application of traction during MRI as much as possible.

The assessor can evaluate the 3D structure of the lesion from arbitrary angles using the MCFI. Additionally, it is possible to precisely obtain a positional relationship between the articular cartilage and the subchondral bone by adjusting the transparency of the articular cartilage, which is not visible to surgeons even during surgery. We accurately predicted the lesion severity in 15 out of 16 cases (93.8% accuracy). Although we predicted the case 15 lesion as ICRS class III, the lesion was diagnosed as class IV intraoperatively. This may be due to the high instability of the lesion, which could have caused the lesion to be displaced from the floor sometime between image acquisition and surgery. However, regarding the detection of unstable lesions, our technique achieved 100% accuracy. Diagnosing the stability of the lesion is extremely important in determining treatment strategies for patients with OCD [1,6,20]. Therefore, we believe that our technique is highly effective.

We simulated the surgical procedure in all cases and conducted surgery per the simulations in each case, which is another advantage of the MCFI. Among the surgical procedures we performed, articular surface reconstruction using a costal osteochondral autograft is the most complex surgery. Poor reconstruction of the articular surface leads to osteoarthritis in the future. However, owing to the anatomical feature of the elbow joint [35], articular surface reconstruction referring only to intraoperative findings can be challenging in some cases. Detailed surgical planning using MCFIs has the potential to minimize the process of intraoperative decision making by surgeons.

We selected costal osteochondral autograft transplantation for articular surface reconstruction because we are accustomed to the procedure; however, some surgeons prefer to harvest the osteochondral autograft from the knee using the OATS technique. Our surgical simulation technique is also applicable to surgeries that incorporate the OATS technique. When simulating the procedure, it is necessary to prepare a 3D model of a cylindrical autograft resembling the autograft harvested using the OATS technique instead of the 3D model of the costal osteochondral autograft. By preparing cylindrical autografts of various diameters, surgeons can precisely simulate the location and direction of the transplant, as well as the number of autografts necessary for the procedure (Figure 11).

A limitation of this technique is that the segmentation of the articular cartilage is time-consuming and technically demanding. Precise segmentation of the articular cartilage is the most crucial part of the procedure, but it must be partly executed manually. No available software can automatically and completely segment the articular cartilage, and it takes approximately 2 h per case to complete the procedure. Because we rely on the created MCFIs to determine the treatment strategies, it takes several weeks from the image acquisition to the surgery. This delay may lead to the deterioration of the OCD lesion in some cases, such as case 15, in which we misdiagnosed the ICRS classification. Therefore, we need to simplify the procedure and minimize the waiting period to avoid such consequences. In this study, evaluation of intraoperative findings was subjectively performed by each surgeon. We hope to achieve objective superposition of the MCFI and the surgical field in the future. Another limitation is that the number of cases was limited.

The accumulation of cases takes time as OCD is a rare condition. We will continue to work on the current study to further evaluate the consistency between intraoperative findings and MCFIs. Increasing the number of cases could lead to the development of software that can automatically create the MCFI for OCD patients. We also aim to conduct more quantitative evaluations of OCD lesions, including assessment of mild cases to predict the progression of lesion severity, in the future. In addition, we hope to apply this technique to other joints, with the aim of assisting surgeons in various fields treating intra-articular osteochondral lesions.

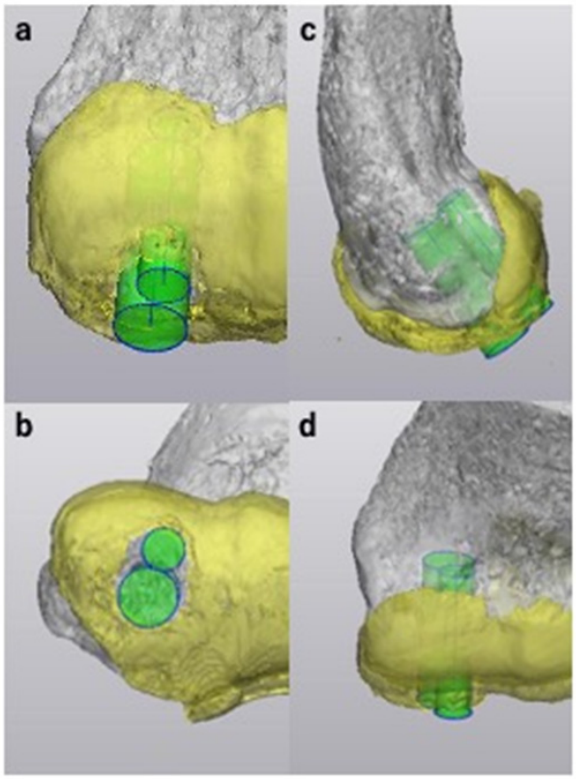

Figure 11. Sample simulation of articular surface reconstruction using the osteochondral autograft transplantation system technique with three-dimensional (3D) models of cylindrical autografts for case 16. We created two 3D models of cylindrical autografts with diameters of 4 mm and 7 mm. The 3D models were positioned to cover the lesion to simulate the location, direction, and depth of the transplant. Here, the 3D CT model of the humerus, the 3D MRI model of the articular cartilage and 3D models of cylindrical autografts are shown in gray, yellow and green, respectively. (**a**) Anteroposterior view. (**b**) Distoproximal view. (**c**) Lateral view. (**d**) Proximodistal view.

5. Conclusions

Herein, we introduced OCD lesion evaluation and surgical simulation using MCFIs of OCD, a novel tool developed by us. This computer-aided technique made the accurate evaluation of 3D structural details of the articular cartilage and subchondral bone possible, as well as lesion stability, without surgical intervention. A detailed surgical simulation is potentially useful for minimizing intraoperative decision making.

6. Patents

A patent for the 3D MRI-CT fusion image construction technique described in this article was applied for in Japan: 3D model generation method, 3D model generation device, and 3D model-generation program. Application No. 2018-066054, pending approval.

Author Contributions: Conceptualization, S.K.; Methodology, S.K., Y.N. and Y.H.; Validation, S.K.; Formal Analysis, S.K.; Investigation, S.K., Y.N., Y.H., T.O., A.I., E.O. and Y.T.; Data Curation, S.K., A.I., E.O. and Y.T.; Writing—Original Draft Preparation, S.K.; Writing—Review and Editing, Y.N., Y.H., T.O., A.I., E.O., Y.T., Y.Y. and M.Y.; Visualization, S.K.; Supervision, Y.N. and M.Y.; Project Administration, S.K., Y.N., Y.H. and M.Y. All authors have read and agreed to the published version of the manuscript.

Funding: This research received no external funding.

Institutional Review Board Statement: The study was conducted according to the guidelines of the Declaration of Helsinki and approved by the Institutional Review Board of the University of Tsukuba Hospital (Study Number: H29-58, approved 21 July 2017).

Informed Consent Statement: Informed consent was obtained from all subjects involved in the study.

Data Availability Statement: Not applicable.

Conflicts of Interest: The authors declare no conflict of interest.

References

1. Baker, C.L., III; Romeo, A.A.; Baker, C.L., Jr. Osteochondritis dissecans of the capitellum. *Am. J. Sports Med.* **2010**, *38*, 1917–1928. [CrossRef] [PubMed]
2. Brown, R.; Blazina, M.E.; Kerlan, R.K.; Carter, V.S.; Jobe, F.W.; Carlson, G.J. Osteochondritis of the capitellum. *J. Sports Med.* **1974**, *2*, 27–46. [CrossRef]
3. Edmonds, E.W.; Polousky, J. A review of knowledge in osteochondritis dissecans: 123 years of minimal evolution from König to the ROCK study group. *Clin. Orthop. Relat. Res.* **2013**, *471*, 1118–1126. [CrossRef]
4. Bruns, J.; Werner, M.; Habermann, C.R. Osteochondritis dissecans of smaller joints: The elbow. *Cartilage* **2021**, *12*, 407–417. [CrossRef] [PubMed]
5. Kessler, J.I.; Jacobs, J.C., Jr.; Cannamela, P.C.; Weiss, J.M.; Shea, K.G. Demographics and epidemiology of osteochondritis dissecans of the elbow among children and adolescents. *Orthop. J. Sports Med.* **2018**, *6*, 2325967118815846. [CrossRef] [PubMed]
6. Churchill, R.W.; Munoz, J.; Ahmad, C.S. Osteochondritis dissecans of the elbow. *Curr. Rev. Musculoskelet. Med.* **2016**, *9*, 232–239. [CrossRef]
7. Kessler, J.L.; Jacobs, J.C., Jr.; Cannamela, P.C.; Shea, K.G.; Weiss, J.M. Childhood obesity is associated with osteochondritis dissecans of the knee, ankle and elbow in children and adolescents. *J. Pediatr. Orthop.* **2018**, *38*, 296–299. [CrossRef]
8. Kirsch, J.M.; Thomas, J.; Bedi, A.; Lawton, J.N. Current concepts: Osteochondritis dissecans of the capitellum and the role of osteochondral autograft transplantation. *Hand* **2016**, *11*, 396–402. [CrossRef]
9. Shimada, K.; Tanaka, H.; Matsumoto, T.; Miyake, J.; Higuchi, H.; Gamo, K.; Fuji, T. Cylindrical costal osteochondral autograft for reconstruction of large defects of the capitellum due to osteochondritis dissecans. *J. Bone Jt. Surg. Am.* **2012**, *94*, 992–1002. [CrossRef] [PubMed]
10. Yamaguchi, N.; Yamamoto, S.; Aoki, A.; Ito, S.; Uchio, Y. Outcomes of surgical treatment for osteochondritis dissecans of the elbow: Evaluation by lesion location. *J. Shoulder Elb. Surg.* **2018**, *27*, 2262–2270.
11. Maruyama, M.; Takahara, M.; Satake, H. Diagnosis and treatment of osteochondritis dissecans of the humeral capitellum. *J. Orthop. Sci.* **2018**, *23*, 213–219. [CrossRef] [PubMed]
12. Itsubo, T.; Murakami, N.; Uemura, K.; Nakamura, K.; Hayashi, M.; Uchiyama, S.; Kato, H. Magnetic resonance imaging staging to evaluate the stability of capitellar osteochondritis dissecans lesions. *Am. J. Sports Med.* **2014**, *42*, 1972–1977. [CrossRef] [PubMed]
13. Satake, H.; Takahara, M.; Harada, M.; Maruyama, M. Preoperative imaging criteria for unstable osteochondritis dissecans of the capitellum. *Clin. Orthop. Relat. Res.* **2013**, *471*, 1137–1143. [CrossRef] [PubMed]
14. Iwasaki, N.; Kamishima, T.; Kato, H.; Funakoshi, T.; Minami, A. A retrospective evaluation of magnetic resonance imaging effectiveness on capitellar osteochondritis dissecans among overhead athletes. *Am. J. Sports Med.* **2012**, *40*, 624–630. [CrossRef]
15. Kohyama, S.; Ogawa, T.; Mamizuka, N.; Hara, Y.; Yamazaki, M. A magnetic resonance imaging-based staging system for osteochondritis dissecans of the elbow. A validation study against the international cartilage repair society classification. *Orthop. J. Sports Med.* **2018**, *6*, 2325967118794620. [CrossRef]
16. Nguyen, J.C.; Degnan, A.J.; Barrera, C.A.; Hee, T.P.; Ganley, T.J.; Kijowski, R. Osteochondritis dissecans of the elbow in children: MRI findings of instability. *AJR Am. J. Roentgenol.* **2019**, *213*, 1145–1151. [CrossRef]
17. Yoshizuka, M.; Sunagawa, T.; Nakashima, Y.; Shinomiya, R.; Masuda, T.; Makitsubo, M.; Adachi, N. Comparison of sonography and MRI in the evaluation of stability of capitellar osteochondritis dissecans. *J. Clin. Ultrasound* **2018**, *46*, 247–252. [CrossRef]
18. Pu, A.; Jauregui, J.J.; Salmons, H.I.; Weir, T.B.; Abzug, J.M.; Gilotra, M.N. Radiographic evaluation of osteochondritis dissecans of the humeral capitellum: A systematic review. *J. Orthop.* **2021**, *27*, 114–121. [CrossRef]
19. Takahara, M.; Mura, N.; Sasaki, J.; Harada, M.; Ogino, T. Classification, treatment, and outcome of osteochondritis dissecans of the humeral capitellum. *J. Bone Jt. Surg. Am.* **2007**, *89*, 1205–1214. [CrossRef]

20. ICRS Cartilage Injury Evaluation Package. Available online: https://cartilage.org/content/uploads/2014/10/ICRS_evaluation.pdf (accessed on 11 July 2017).
21. Zlotolow, D.A.; Bae, D.S. Osteochondral autograft transplantation in the elbow. *J. Hand Surg. Am.* **2014**, *39*, 368–372. [CrossRef]
22. Gouveia, K.; Zhang, K.; Kay, J.; Memon, M.; Simunovic, N.; Garrigues, G.E.; Pollock, J.W.; Ayeni, O.R. The use of elbow arthroscopy for management of the pediatric elbow: A systematic review of indications and outcomes. *Arthroscopy* **2021**, *37*, 1958–1970. [CrossRef] [PubMed]
23. Chow, H.Y.; Eygendaal, D.; The, B. Elbow arthroscopy—indications and technique. *J. Clin. Orthop. Trauma* **2021**, *19*, 147–153.
24. Sampath, S.C.; Sampath, S.C.; Bredella, M.A. Magnetic resonance imaging of the elbow: A structed approach. *Sports Health* **2013**, *5*, 34–39. [CrossRef] [PubMed]
25. Shahabpour, M.; Kichouh, M.; Laridon, E.; Gielen, J.L.; De Mey, J. The effectiveness of diagnostic imaging methods for the assessment of soft tissue and articular disorders of the shoulder and elbow. *Eur. J. Radiol.* **2008**, *65*, 194–200. [CrossRef]
26. Saupe, N.; Zanetti, M.; Pfirrmann, C.W.; Wels, T.; Schwenke, C.; Holder, J. Pain and other side effects after MR arthrography: Prospective evaluation in 1085 patients. *Radiology* **2009**, *250*, 830–838. [CrossRef] [PubMed]
27. Newberg, A.H.; Munn, C.S.; Robbins, A.H. Complications of arthrography. *Radiology* **1985**, *155*, 605–606. [CrossRef] [PubMed]
28. Kohyama, S.; Nishiura, Y.; Hara, Y.; Ogawa, T.; Ikumi, A.; Okano, E.; Totoki, Y.; Yamazaki, M. A novel three-dimensional MRI-CT image fusion technique for precise preoperative evaluation and treatment of capitellar osteochondritis dissecans. *Eur. Radiol.* **2021**, *31*, 5721–5733. [CrossRef]
29. Logli, A.L.; Leland, D.P.; Bernard, C.D.; Soleto, J.S.; Morrey, M.E.; O'Driscoll, S.W.; Krych, A.J.; Wang, Z.; Capm, C.L. Capitellar osteochondritis dissecans lesions of the elbow: A systematic review of osteochondral graft reconstruction options. *Arthroscopy* **2020**, *36*, 1747–1764. [CrossRef]
30. Kohyama, S.; Tanaka, T.; Shimasaki, K.; Kobayashi, S.; Ikumi, A.; Yanai, T.; Ochiai, N. Effect of elbow MRI with axial traction on articular cartilage visibility-a feasibility study. *Skelet. Radiol.* **2020**, *49*, 1555–1566. [CrossRef]
31. Lee, R.K.; Griffith, J.F.; Yuen, B.T.; Ng, A.W.; Yeung, D.K. Elbow MR arthrography with traction. *Br. J. Radiol.* **2016**, *89*, 20160378. [CrossRef]
32. Dipaola, J.D.; Nelson, D.W.; Colville, M.R. Characterizing osteochondral lesions by magnetic resonance imaging. *Arthroscopy* **1991**, *7*, 101–104. [CrossRef]
33. Jans, L.B.; Ditchfield, M.; Anna, G.; Jaremko, J.L.; Verstraete, K.L. MR imaging findings and MR criteria for instability in osteochondritis dissecans of the elbow in children. *Eur. J. Radiol.* **2012**, *81*, 1306–1310. [CrossRef] [PubMed]
34. Kijowski, R.; De Smet, A.A. MRI findings of osteochondritis dissecans of the capitellum with surgical correlation. *AJR Am. J. Roentgenol.* **2005**, *185*, 1453–1459. [CrossRef] [PubMed]
35. Kosaka, M.; Nakase, J.; Takahashi, R.; Toratani, T.; Ohashi, Y.; Kitaoka, K.; Tsuchiya, H. Outcomes and failure factors in surgical treatment for osteochondritis dissecans of the capitellum. *J. Pedriatr. Orthop.* **2013**, *33*, 719–724. [CrossRef]

Stroke

CLINICAL AND POPULATION SCIENCES

Sex Difference and Rupture Rate of Intracranial Aneurysms: An Individual Patient Data Meta-Analysis

Charlotte C.M. Zuurbier, MD, PhD; Rob Molenberg, BSc; Liselore A. Mensing, MD; Marieke J.H. Wermer, MD, PhD; Seppo Juvela, MD, PhD; Antti E. Lindgren, MD, PhD; Juha E. Jääskeläinen, MD, PhD; Timo Koivisto, MD, PhD; Tomosato Yamazaki, MD, PhD; Maarten Uyttenboogaart, MD, PhD; J. Marc C. van Dijk, MD, PhD; Marlien W. Aalbers, MD; Akio Morita, MD, PhD; Shinjiro Tominari, MD, PhD; Hajime Arai, MD, PhD; Kazuhiko Nozaki, MD, PhD; Yuichi Murayama, MD; Toshihiro Ishibashi, MD; Hiroyuki Takao, MD, PhD; Renato Gondar, MD; Philippe Bijlenga, MD, PhD; Gabriel J.E. Rinkel, MD, PhD; Jacoba P. Greving, PhD; Ynte M. Ruigrok, MD, PhD

BACKGROUND AND PURPOSE: In previous studies, women had a higher risk of rupture of intracranial aneurysms than men, but female sex was not an independent risk factor. This may be explained by a higher prevalence of patient- or aneurysm-related risk factors for rupture in women than in men or by insufficient power of previous studies. We assessed sex differences in rupture rate taking into account other patient- and aneurysm-related risk factors for aneurysmal rupture.

METHODS: We searched Embase and Pubmed for articles published until December 1, 2020. Cohorts with available individual patient data were included in our meta-analysis. We compared rupture rates of women versus men using a Cox proportional hazard regression model adjusted for the PHASES score (Population, Hypertension, Age, Size of Aneurysm, Earlier Subarachnoid Hemorrhage From Another Aneurysm, Site of Aneurysm), smoking, and a positive family history of aneurysmal subarachnoid hemorrhage.

RESULTS: We pooled individual patient data from 9 cohorts totaling 9940 patients (6555 women, 66%) with 12 193 unruptured intracranial aneurysms, and 24 357 person-years follow-up. Rupture occurred in 163 women (rupture rate 1.04%/person-years [95% CI, 0.89–1.21]) and 63 men (rupture rate 0.74%/person-years [95% CI, 0.58–0.94]). Women were older (61.9 versus 59.5 years), were less often smokers (20% versus 44%), more often had internal carotid artery aneurysms (24% versus 17%), and larger sized aneurysms (≥7 mm, 24% versus 23%) than men. The unadjusted women-to-men hazard ratio was 1.43 (95% CI, 1.07–1.93) and the adjusted women/men ratio was 1.39 (95% CI, 1.02–1.90).

CONCLUSIONS: Women have a higher risk of aneurysmal rupture than men and this sex difference is not explained by differences in patient- and aneurysm-related risk factors for aneurysmal rupture. Future studies should focus on the factors explaining the higher risk of aneurysmal rupture in women.

GRAPHIC ABSTRACT: A graphic abstract is available for this article.

Key Words: intracranial aneurysm ■ prevalence ■ risk factor ■ sex ■ subarachnoid hemorrhage

Correspondence to: Ynte M. Ruigrok, MD, PhD, UMC Utrecht Brain Center, Department of Neurology and Neurosurgery, room G03-228, University Medical Center Utrecht, Heidelberglaan 100, 3584 CX Utrecht, the Netherlands. Email ij.m.ruigrok@umcutrecht.nl

Supplemental Material is available at https://www.ahajournals.org/doi/suppl/10.1161/STROKEAHA.121.035187.

For Sources of Funding and Disclosures, see page 369.

Nonstandard Abbreviations and Acronyms

aSAH	aneurysmal subarachnoid hemorrhage
ISUIA	International Study of Unruptured Intracranial Aneurysms Investigators
PHASES	Population, Hypertension, Age, Size of Aneurysm, Earlier Subarachnoid Hemorrhage From Another Aneurysm, Site of Aneurysm
UIA	unruptured intracranial aneurysm

Approximately 3% of the general population has an unruptured intracranial aneurysm (UIA).[1] Rupture of an intracranial aneurysm results in aneurysmal subarachnoid hemorrhage (aSAH), a subtype of stroke which carries a high morbidity and case fatality.[2] UIA and aSAH occur more often in women than in men with overall 65% of the patients being women.[1,3]

In the decision whether to treat UIA with neurosurgical or endovascular treatment to prevent future aSAH, the risk of rupture and the risk of complications of preventive treatment have to be balanced.[4] The 5-year risk of rupture of UIA can be assessed using the PHASES score (Population, Hypertension, Age, Size of Aneurysm, Earlier Subarachnoid Hemorrhage From Another Aneurysm, Site of Aneurysm), which takes into account several patient- and aneurysm-related factors associated with rupture including geographic location, hypertension, age, history of aSAH, aneurysm size, and location.[5] The PHASES score is based on a pooled analysis of individual patient data from prospective cohort studies on rupture rates of UIAs and risk factors for rupture. In this pooled analysis, women had a higher risk of rupture, but in multivariable analysis, female sex was not an independent risk factor. Another meta-analysis including both retrospective and prospective studies reported a statistically significantly higher rupture risk in women compared to men, but whether female sex was an independent risk factor could not be investigated because multivariable analysis was not possible due to lack of individual patient data.[6] The higher risk of UIA rupture in women may therefore be explained by a higher prevalence of patient- or aneurysm-related risk factors for UIA rupture in women.

We performed a pooled analysis of individual patient data from prospective cohort studies to assess if sex is a risk factor for intracranial aneurysm rupture independent from other risk factors for rupture including the PHASES score, smoking, and a positive family history for aSAH.

METHODS

Search Strategy and Selection Criteria

We performed a systematic search of the Pubmed and Embase database to retrieve all studies on rupture risk published up to December 1, 2020. We used the keywords "(intracranial aneurysm(s) OR cerebral aneurysm(s) AND (risk of rupture OR aneurysm rupture OR risk factors OR rupture OR unruptured OR subarachnoid hemorrhage) AND (follow up OR natural history OR natural course)" (Figure S1). In addition, we checked the reference list of all relevant publications for further eligible studies. We performed our systematic review and meta-analysis according to the Preferred Reporting Items for Systematic Reviews and Meta-Analyses recommendations and Meta-Analysis of Observational Studies in Epidemiology guidelines.[7,8] We included studies that (1) used a prospective study design; (2) included at least 50 patients with UIA; and (3) studied the rupture rate of UIA and risk factors for aneurysm rupture. There was no language restriction other than the requirement of an abstract in English. When multiple publications reported on the same study population, the most recent publication was used. One author (C.C.M.Z.) performed the literature search, checked the titles and abstracts for studies meeting the inclusion criteria. Next, full-text copies of eligible studies were reviewed.

In total, 2613 articles were screened (Figure 1). For the eligible studies meeting the inclusion criteria, we approached the research groups that performed these studies asking if they could provide us with their individual patient data. Only cohorts with available individual patient-level data were included in our meta-analysis. We found twelve studies that fulfilled the inclusion criteria,[9–19] and 9 research groups provided us with their individual patient data.[12–19] One of these population-based cohort studies on UIA, did not report on family history,[20] but its authors could provide data including data on family history for aSAH for a selection of cases. These were data on patients with UIA collected between 1980 and 2017 from the IA database of Neurosurgery of Kuopio University Hospital and included 1181 patients with 1653 UIA, of whom 693 were women. The 9 cohorts are listed in Table 1, and the baseline characteristics of patients in all separate cohorts are listed in Table S1. Quality assessment of included cohort studies by QUIPS tool is shown in Table S2.

Data Extraction

Data requested for each patient of the different included studies were the following: age, sex, history of aSAH, smoking status, positive family history for aSAH, hypertension status, number of aneurysms, maximum diameter of aneurysms, aneurysm location. These data were collected at baseline only and not at later time points. These data were recorded individually and also summarized in the PHASES score which includes data on the risk factors geographic location, hypertension, age, history of aSAH, aneurysm size, and location.[5] Data requested for each patient during follow-up were the following: occurrence of rupture, date of rupture, data of a surgical or endovascular intervention, date of death, date of last follow-up assessment, and whether a patient was lost to follow-up. A smoker was defined as a former or current smoker, and person with hypertension as a systolic blood pressure >140 mm Hg or diastolic blood pressure >90 mm Hg or use of antihypertensive drugs. Individuals with a positive family history were defined as individuals with at least 2 affected first-degree relatives with aSAH whether or not in combination of first-degree relatives with UIA. The location of the aneurysm was classified as the

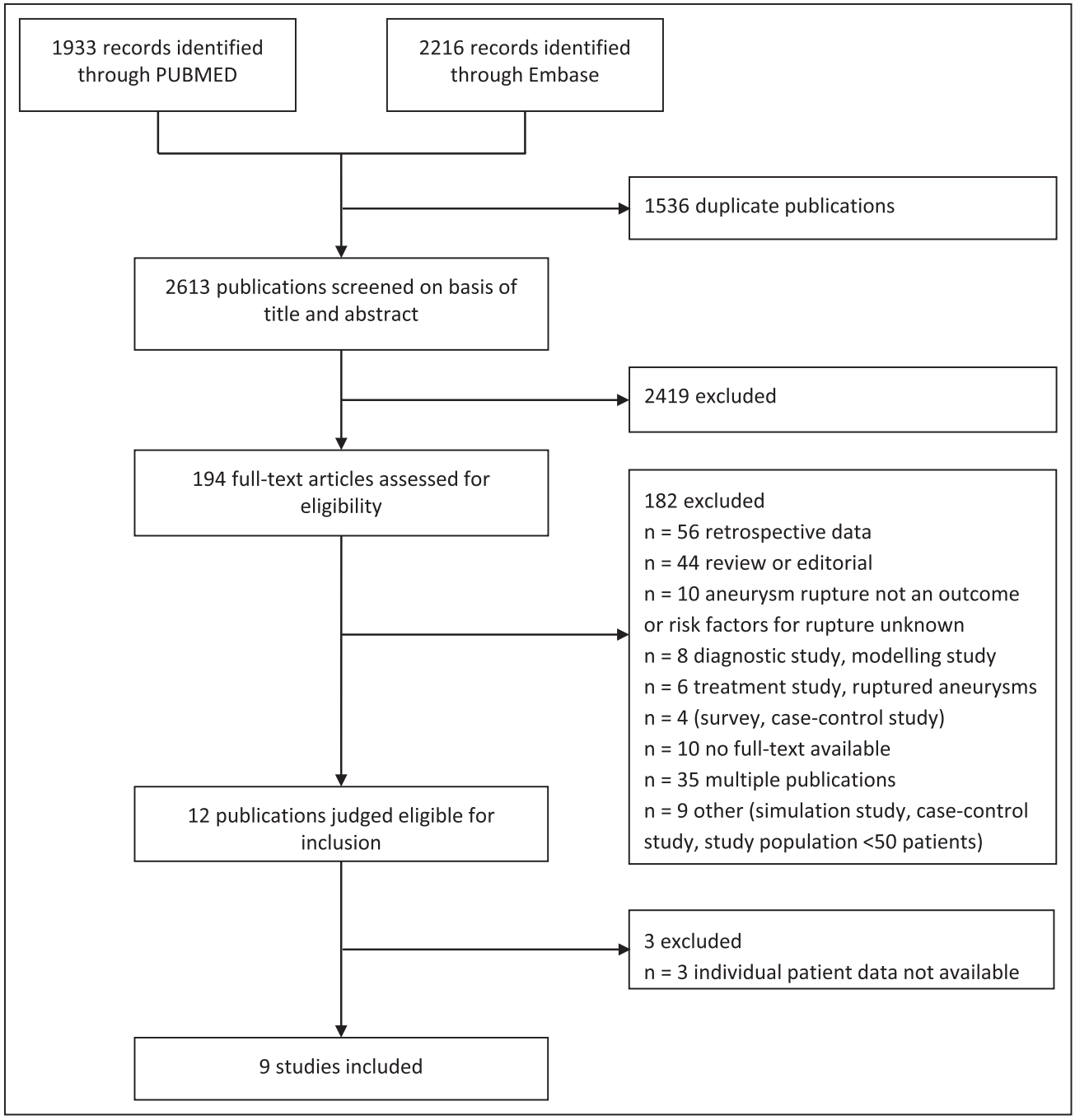

Figure 1. Preferred Reporting Items for Systematic Reviews and Meta-Analyses flow diagram.

internal carotid artery, posterior communicating artery, anterior cerebral arteries (including the anterior cerebral artery, anterior communicating artery, and pericallosal artery), middle cerebral artery, or posterior circulation (including the vertebral artery, basilar artery, cerebellar arteries, and posterior cerebral artery). Patients with polycystic kidney disease and moyamoya disease were excluded. We predefined the primary end point as the rupture of UIA.

Statistical Approach

Missing data were imputed for smoking, hypertension, and family history of aSAH within each cohort using the linear regression method (multivariable analyses). To assign values for these missing data, we performed multiple imputation creating 10 imputation datasets using all relevant prognostic factors and outcome. A sensitivity analysis was done by excluding participants for whom data were missing. In one study only data on current smoking was available but no data on former smoking, and therefore, in our analysis data on current smoking was considered as current or former smoking.[17] Fifty-seven Japanese patients were included both in the cohort of Morita et al[14] and of Murayama et al,[15] whereas 11 patients were included in both the cohort of Mensing et al[13] and of Wermer et al.[16] In the pooled analysis, these patients were removed from one of these cohorts. Categorical variables of baseline

 Stroke. 2022;53:362–369. DOI: 10.1161/STROKEAHA.121.035187

Table 1. Baseline Characteristics of Included Studies

Study	Country	Recruitment period	No. of patients	No. of UIA	Women (%)	Mean age in years (range)	Median follow-up in years (range)	No. of UIA rupture during follow-up
Juvela et al[12]	Finland	1956–1978	140	179	75 (54)	42 (15–61)	21.0 (0–52)	33
Lindgren et al[20]	Finland	1977–2016	1181	1658	693 (59)	56 (16–85)	0.5 (0–23)	14
Mensing at al[13]	the Netherlands	1994–2016	474	633	320 (68)	56 (22–81)	0.8 (0–21)	10
Morita et al[14]	Japan	2001–2004	5702	6675	3779 (66)	63 (23–98)	1.0 (0–9)	111
Murayama et al[15]	Japan	2003–2012	1561	1942	1039 (67)	66 (25–100)	3.2 (0–11)	56
Wermer et al[16]	the Netherlands	2002–2004	93	125	70 (75)	51 (20–69)	2.2 (1–15)	1
Molenberg et al[17]	the Netherlands	1998–2017	198	257	145 (73)	56 (28–79)	1 (0.3–2)	1
Sonobe et al[18]	Japan	2000–2004	368	441	236 (64)	62 (23–89)	3.2 (0–7)	6
Gondar et al[19]	Switzerland	2006–2014	291	367	225 (86)	55 (20–91)	2.5 (0–13)	3

UIA indicates unruptured intracranial aneurysm.

characteristics were compared using the χ^2 test. Continuous variables of baseline characteristics were compared among groups using the Mann-Whitney *U* test or the Student *t* test. A $p \leq 0.05$ was considered statistically significant. We pooled the individual patient data of the included studies and estimated sex-specific rupture rates for each cohort separately. In case of multiple UIAs, the largest UIA was used to categorize the patient regarding site and size of the aneurysm. In addition, we performed an aneurysm-based analysis where all UIAs were analyzed. Rupture rate was analyzed with a per-patient analysis and a per aneurysm analysis using a Cox proportional hazard regression model, adjusted for the PHASES score,[5] smoking, and positive family history for aSAH. A 2-stage approach was used with random effect for cohort because we expected heterogeneity since studies were performed in different countries which used different treatment regimes, and a fixed effect for the PHASES score, smoking, and positive family history for aSAH. As a sensitivity analysis, we also performed a one-stage model. Proportional hazard assumptions were checked in each individual cohort using diagnostics based on the scaled Schoenfeld residuals.[21] Follow-up data for patients started at time of UIA diagnosis and patients were followed up until aneurysmal rupture occurred. Patients were censored at the time of death, last follow-up assessment, or at the time of surgical or endovascular aneurysm treatment without preceding rupture. When patients underwent a surgical or endovascular aneurysm treatment, data from the period up to the time of the intervention were included in the analysis, whereas data from the period after the intervention were not included. The data that support the findings of this study are available from the corresponding author upon reasonable request.

RESULTS

We pooled individual patient data from 9940 patients with 12 193 UIAs and 24 357 person-years follow-up using data from nine prospective cohort studies.[12–20] Studies were at low and moderate risk of bias. Baseline characteristics of patients are shown in Table 2. Data on patient characteristics was almost complete except for smoking which was available in 9705/9940 (98%), for hypertension which was available in 9853/9940 (99%), and for family history of aSAH which was available in 9794/9940 (99%). Information on outcome measure was complete for all patients. The mean age was 61±12 years, 6555 patients (66%) were women, and patients came from Dutch (8%), Finnish (12%), Japanese (77%), and Swiss (4%) populations. Women were older (61.9 versus 59.5 years), less often smokers (20% versus 44%), and more often had internal carotid artery aneurysms (24% versus 17%) and larger aneurysms (≥7 mm, 24% versus 23%) than men. There were more women than men in cohorts from Japan (67% versus 33%), the Netherlands (70% versus 30%), Switzerland (77% versus 23%), whereas this difference was less pronounced in the cohort from Finland (58% versus 42%). The median PHASES score was the same in women (7.0 [range, 0–21]) and men (7.0 [range, 0–20]), and the mean PHASES score was 7.2±3.2 in women and 7.4±3.0 in men. In our pooled analysis, the mean follow-up time for women was 2.4±3.5 years (median: 1.5 (0-52) year) and 2.5±3.7 years (median: 1.5 (0-50) year) for men. Preventive neurosurgical or endovascular treatment during follow-up occurred in 36% of women (median: 60 days) and in 37% of men (median: 61 days). When assessing these characteristics per UIA, similar differences in characteristics were found (data not shown).

In 234 patients, rupture of the single, largest or another than the largest UIA occurred. Of these 234 patients, 67 patients had multiple UIA, and in 226 of 234 patients (97%), the single aneurysm (n=167) or the largest aneurysm in case of multiple aneurysms (n=59) ruptured. In 8 of the 67 patients with multiple aneurysm, another than the largest aneurysm ruptured. Of the 226 patients in whom the single or largest UIA ruptured, 163 were women (rupture rate 1.04%/person-years [95% CI, 0.89–1.21]), and 63 men (0.74%/person-years [95% CI, 0.58–0.94]). Characteristics of ruptured aneurysms are shown in Table 3.

The unadjusted women-to-men hazard ratio was 1.43 (95% CI, 1.07–1.93). After adjustment for the PHASES score, smoking, and positive family history for aSAH, the women-to-men hazard ratio was slightly lower

Table 2. Baseline Characteristics of Included Patients

Pooled data	Women, n (%)	Men, n (%)	Total, n (%)	Women-to-men difference* (95% CI)
No. of patients	6555	3385	9940	
Mean age (range)	61.9 (15 to 100)	59.5 (16 to 94)	61.1 (15 to 100)	0.004 (0.003 to 0.005)
Hypertension†	2913 (44)	1431 (42)	4344 (44)	0.019 (0.000 to 0.038)
Ever smoker†	1330 (20)	1500 (44)	2830 (29)	−0.264 (−0.284 to −0.244)
Previous aSAH	405 (6)	188 (6)	593 (6)	0.025 (−0.014 to 0.64)
Positive family history for aSAH†	676 (10)	316 (9)	992 (10)	0.028 (−0.003 to 0.059)
Population				0.061 (0.045 to 0.078)
Finnish	768 (12)	553 (16)	1321 (13)	
Japanese	5035 (77)	2539 (75)	7574 (76)	
Dutch	527 (8)	227 (7)	754 (8)	
Swiss	225 (4)	66 (2)	291 (3)	
Multiple aneurysms	1466 (22)	552 (16)	2018 (20)	0.083 (0.06 to 0.106)
Aneurysm size				0.010 (−0.003 to 0.023)
<7.0 mm	4951 (76)	2589 (77)	7540 (76)	
7.0–9.9 mm	887 (14)	475 (14)	1326 (14)	
10.0–919.9 mm	618 (9)	266 (8)	884 (9)	
>20.0 mm	99 (2)	55 (2)	154 (2)	
Aneurysm location				−0.043 (−0.055 to −0.031)
Internal carotid artery	1551 (24)	584 (17)	2135 (22)	
Middle cerebral artery	2305 (35)	1242 (37)	3547 (36)	
Anterior circulation or posterior circulation	2699 (41)	1559 (46)	4258 (43)	
PHASES score (median, range, mean, SD)	7.0 (0–921) 7.2±3.2	7.0 (0–920) 7.4±3.0	7.0 (0–921) 7.2±3.1	−0.005 (−0.008 to −0.002)

aSAH indicates aneurysmal subarachnoid hemorrhage; and PHASES, Population, Hypertension, Age, Size of Aneurysm, Earlier Subarachnoid Hemorrhage From Another Aneurysm, Site of Aneurysm.

*Unadjusted.

†Data are missing for hypertension in 87 persons (1%), for smoking in 235 persons (2%), and for family history of aSAH in 146 persons (1%).

(1.39 [95% CI, 1.02–1.90]; Figure 2). In the sensitivity analysis on the subset of patients with no missing data for smoking, hypertension, and family history of aSAH (n=9566), we found similar but nonstatistically significant results (Figure S2). We also performed a one-stage model which resulted in a hazard ratio of 1.36 (95% CI, 1.01–1.85). In the aneurysm-based analysis where all UIAs were analyzed, the results were essentially the same (Figure 3).

DISCUSSION

In our pooled analysis of individual patient data from prospective cohort studies, we found that women have a higher risk of aneurysmal rupture, and this increased rupture risk for women is not explained by differences in patient- and aneurysm-related risk factors for aneurysmal rupture, being risk factors of the PHASES score, smoking, and a positive family history for aSAH.

Some of the risk factors for rupture were more often present in women, but others in men. As the patient- and aneurysm-related risk factors for which we corrected in our analysis, do not explain the increased rupture risk in women, additional factors contributing to the increased risk remain to be detected. We had no data on the shape of the aneurysm in our data set. Because aspect ratio and irregular aneurysm shape are also known factors for UIA rupture,[22,23] a higher prevalence of irregular aneurysms in women than in men may contribute to the sex difference in rupture, but it is unlikely that such a difference would explain the sex difference in rupture completely. Because we could not find data in the literature on sex differences regarding shape of the aneurysms, it is currently unknown if or to what extent differences in shape of aneurysms between women and men play a role in the higher rupture risk in women.

Additional factors explaining the sex difference in risk of UIA rupture may be female-specific hormonal and reproductive factors. A previous systematic literature review on female risk factors for aSAH found an increased risk of aSAH for postmenopausal versus premenopausal women although the pathophysiology of this effect and its influence on the difference in incidence of SAH between the sexes remains unclear.[24] Alternatively, female-specific genetic factors, such as genetic factors of the X-chromosome, sex-specific effects of environmental risk factors, such as smoking[25] or other yet unknown clinical factors which occur more often or

 Stroke. 2022;53:362–369. DOI: 10.1161/STROKEAHA.121.035187

Table 3. Characteristics of Ruptured Intracranial Aneurysms, per Aneurysm

Pooled data	Women, n (%)	Men, n (%)	Total, n (%)	*P* value
No. of ruptured IA	169	65	234	
Largest IA ruptured*	163	63	226	
Not largest IA ruptured	6	2	8	
Mean age (range)	64.2 (23-93)	61.2 (28-87)	63.4 (23-93)	0.19
Hypertension	89 (53)	31 (48)	120 (52)	0.50
Ever smoker	28 (17)	33 (51)	61 (26)	<0.001
Previous aSAH	28 (17)	12 (19)	40 (17)	0.73
Positive family history for aSAH	18 (11)	8 (12)	26 (11)	0.72
Population				0.20
Finnish	30 (18)	17 (26)	47 (20)	
Japanese	129 (76)	43 (66)	172 (74)	
Dutch	9 (5)	3 (5)	12 (5)	
Swiss	1 (1)	2 (3)	3 (1)	
Multiple aneurysms	51 (30)	16 (25)	67 (29)	0.40
Aneurysm size				0.33
<7.0 mm	79 (47)	34 (52)	113 (48)	
7.0–9.9 mm	35 (21)	7 (11)	42 (18)	
10.0–19.9 mm	40 (24)	16 (25)	56 (24)	
>20.0 mm	15 (9)	8 (12)	23 (10)	
Aneurysm location				0.15
Internal carotid artery	26 (15)	4 (6)	30 (13)	
Middle cerebral artery	45 (27)	21 (32)	66 (28)	
Anterior circulation or posterior circulation	98 (58)	40 (62)	138 (59)	
PHASES score (median, range, mean, SD)	9.0 (2–919) 10.1±4.0	9.0 (4–920) 10.4±3.9	9.0 (2–920) 10.3±4.0	0.60

aSAH indicates aneurysmal subarachnoid hemorrhage; IA, intracranial aneurysm; and PHASE, Population, Hypertension, Age, Size of Aneurysm, Earlier Subarachnoid Hemorrhage From Another Aneurysm, Site of Aneurysm.
*In case of multiple aneurysms, the largest aneurysm was used for analysis.

have stronger effect in women than in men may explain the difference.

Our study has several strengths. It includes a large data set with individual patient data from several cohorts including risk factors for aneurysmal rupture. Also, almost all study cohorts included in this meta-analysis showed a higher rupture rate in women compared to men. This means that our data are consistent and generalizable for both Asian and European countries.

A first limitation of this study is that selection bias may have occurred due to informative censoring (loss to follow-up) within each cohort study. If men were treated more aggressively during follow-up than women for example upon growth of the UIA, which is associated

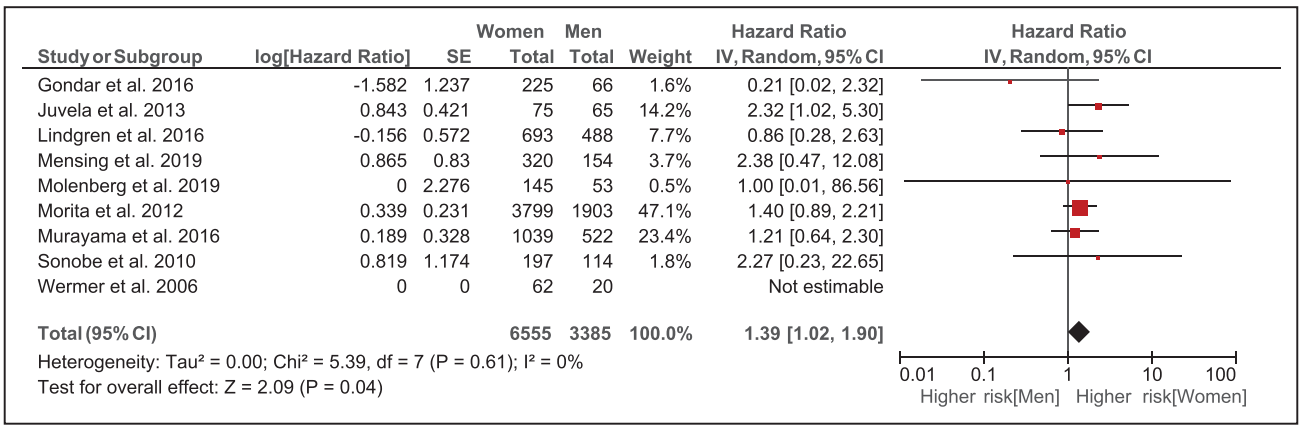

Figure 2. Hazard ratio of the rupture rate in women compared to men adjusted for the PHASES score (Population, Hypertension, Age, Size of Aneurysm, Earlier Subarachnoid Hemorrhage From Another Aneurysm, Site of Aneurysm), smoking and positive family history of aneurysmal subarachnoid hemorrhage, analyzing the data per patient.

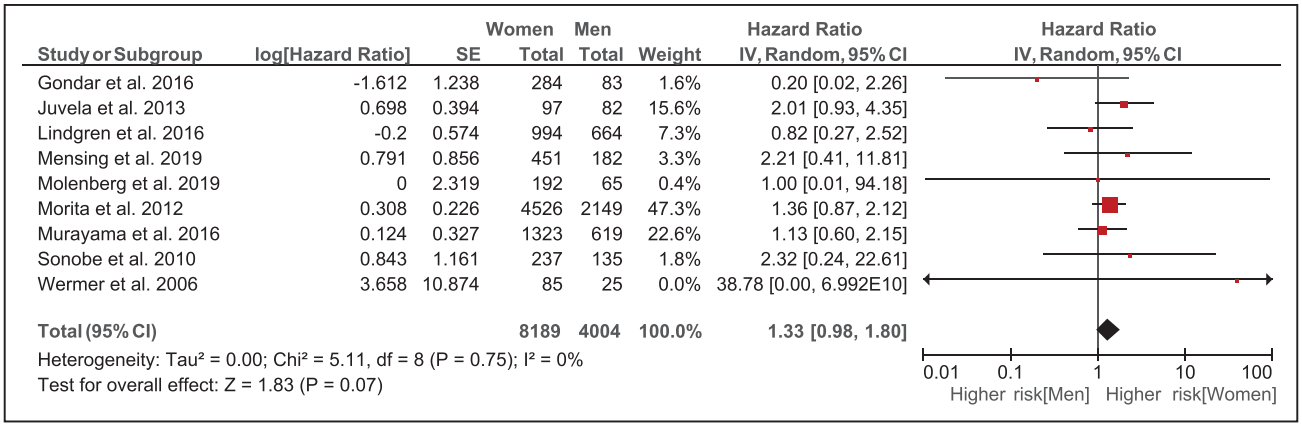

Figure 3. Hazard ratio of the rupture rate in women compared to men adjusted for the PHASES score (Population, Hypertension, Age, Size of Aneurysm, Earlier Subarachnoid Hemorrhage From Another Aneurysm, Site of Aneurysm), smoking and positive family history of aneurysmal subarachnoid hemorrhage, analyzing the data per aneurysm.

with a higher risk of rupture,[26] this may have led to selection bias. However, we found no difference in preventive neurosurgical or endovascular treatment during follow-up between men and women as it was done in 36% of women (median: 60 days) and in 37% of men (median: 61 days). Therefore, it is unlikely that differences in preventive treatment have influenced our results considerably. Second, in most studies, we only had data on smoking at the time of UIA detection but not for smoking status during follow-up. As a previous study showed that continuation of smoking is a significant risk factor for UIA rupture, no conclusions can be drawn about the effect of a change in smoking status after aneurysm detection during follow-up on our outcomes.[27] Cessation of smoking might have occurred more often in men during follow-up compared to women. Similarly, in most studies, we only had data on hypertension at time of UIA detection and not during follow-up. Better control of blood pressure might have been achieved in men during follow-up compared with women. Third, although 9 research groups[12–20] provided us with their individual patient data, 3 research groups[9–11] were not able to do so, which could possibly lead to a bias. However, the population characteristics between the three cohorts not included (Matsumoto et al[9]: 63% female, Güresir et al[10]: 78% female, and ISUIA [International Study of Unruptured Intracranial Aneurysms Investigators][11]: 75% female) and rupture risk (Matsumoto et al[9]: 6/111 patients, all female; Güresir et al[10]: 3/263 patients, all female; and ISUIA[11]: 51/1692, sex unknown) differed not much from those of the nine cohorts analyzed (66% [range, 54–86] female), and therefore, do not think that such a potential bias influences our conclusions. Fourth, in our analysis, patients from Japanese populations were overrepresented (77%) compared to Dutch (8%), Finnish (12%), and Swiss (4%) populations. Except for a small study in the Swiss population, in all populations, a higher risk of rupture for women compared to men was found, so we think our results are generalizable to all populations. Fifth, in our study, we performed patient-level analysis, and in patients with multiple UIAs, we analyzed data of the largest UIA, which is not always the UIA that actually ruptures.[28] However, in our analysis for rupture rate on aneurysm level, we found comparable results.

CONCLUSIONS

Our results show that UIAs in women have a higher rupture risk than UIAs in men, which is not explained by differences in patient- and aneurysm-related risk factors for aneurysmal rupture, being risk factors of the PHASES score, smoking, and a positive family history for aSAH. When assessing the risk of rupture of UIAs in women, this higher risk should be taken into account and a more aggressive treatment approach in women as compared to men is justified. Future studies should focus on the identification of the factors explaining the higher rupture risk of UIA in women, such as different approach during follow-up, female-specific hormonal and reproductive factors, or female-specific genetic and environmental risk factors.

ARTICLE INFORMATION

Received March 30, 2021; final revision received November 15, 2021; accepted December 3, 2021.

Affiliations

UMC Utrecht Brain Center, Department of Neurology and Neurosurgery (C.C.M.Z, L.A.M., G.J.E.R., Y.M.R.) and Julius Center for Health Sciences and Primary Care (J.P.G.), University Medical Center Utrecht, the Netherlands. Departments of Neurosurgery (R.M., J.M.C.v.D., M.W.A.) and Neurology and Medical Imaging Center (M.U.), University Medical Center Groningen, the Netherlands. Department of Neurology, Leiden University Medical Center, the Netherlands (M.J.H.W.). Department of Clinical Neurosciences, University of Helsinki, Finland (S.J.). Department of Clinical Radiology (A.E.L, J.E.J., T.K.) and Neurosurgery of NeuroCenter (A.E.L, J.E.J., T.K.), Kuopio University Hospital, Finland. Institute of Clinical Medicine, School of Medicine, Faculty of Health Sciences, University of Eastern Finland, Kuopio (A.E.L, J.E.J., T.K.). Department of Neurosurgery, National Hospital Organization, Mito Medical Center, Japan (T.Y.). Medical Center UCAS Japan Coordinating Office- University of Tokyo- Nippon Medical School, Neurological Surgery (A.M.). Department of Health Informatics, School of Public Health, Kyoto Uni-

versity, Japan (S.T.). Department of Neurosurgery, Juntendo University- Medical School, Tokyo, Japan (H.A.). Department of Neurosurgery, Shiga University of Medical Science, Japan (K.N.). Department of Endovascular Neurosurgery, Tokyo Jikei University School of Medicine, Japan (Y.M., T.I., H.T.). Neurosurgery Division, Department of Clinical Neurosciences, Faculty of Medicine, Geneva University Medical Center, Switzerland (R.G., P.B.).

Acknowledgments

Drs Mensing, Molenberg, van Dijk, Aalbers, Wermer, Juvela, Lindgren, Jääskeläinen, Koivisto, Yamazaki, Uyttenboogaart, Morita, Tominari, Arai, Nozaki, Murayama, Ishibashi, Takao, Gondar, Bijlenga, Rinkel, Greving and Ruigrok contributed to data collection. Dr Zuurbier searched the literature. Dr Rinkel, Ruigrok, Greving, and Zuurbier communicated with coauthors for individual patient data. Dr Zuurbier performed the data analysis under the supervision of Dr Ruigrok, Greving, and Rinkel. Dr Zuurbier generated the figures. Dr Zuurbier wrote the first draft of the article and all authors revised the article critically and approved the final version.

Sources of Funding

We acknowledge the support from the Netherlands Cardiovascular Research Initiative: An initiative with support of the Dutch Heart Foundation, CVON2015-08 ERASE (Optimal Early Recognition of Persons at High Risk of Aneurysmal Subarachnoid Hemorrhage). This project has received funding from the European Research Council (ERC) under the European Union's Horizon 2020 research and innovation program (grant agreement No. 852173). The Swiss study was performed within the framework of the AneuX project supported by SystemsX.ch, and evaluated by the Swiss National Science Foundation (2014/261).

Disclosures

None.

Supplemental Material

Figure S1
Table S1–S2

REFERENCES

1. Vlak MH, Algra A, Brandenburg R, Rinkel GJ. Prevalence of unruptured intracranial aneurysms, with emphasis on sex, age, comorbidity, country, and time period: a systematic review and meta-analysis. *Lancet Neurol*. 2011;10:626–636. doi: 10.1016/S1474-4422(11)70109-0
2. van Gijn J, Kerr RS, Rinkel GJ. Subarachnoid haemorrhage. *Lancet*. 2007;369:306–318. doi: 10.1016/S0140-6736(07)60153-6
3. de Rooij NK, Linn FH, van der Plas JA, Algra A, Rinkel GJ. Incidence of subarachnoid haemorrhage: a systematic review with emphasis on region, age, gender and time trends. *J Neurol Neurosurg Psychiatry*. 2007;78:1365–1372. doi: 10.1136/jnnp.2007.117655
4. Algra AM, Lindgren A, Vergouwen MDI, Greving JP, van der Schaaf IC, van Doormaal TPC, Rinkel GJE. Procedural clinical complications, case-fatality risks, and risk factors in endovascular and neurosurgical rreatment of unruptured intracranial aneurysms: a systematic review and meta-analysis. *JAMA Neurol*. 2019;76:282–293. doi: 10.1001/jamaneurol.2018.4165
5. Greving JP, Wermer MJ, Brown RD Jr, Morita A, Juvela S, Yonekura M, Ishibashi T, Torner JC, Nakayama T, Rinkel GJ, et al. Development of the PHASES score for prediction of risk of rupture of intracranial aneurysms: a pooled analysis of six prospective cohort studies. *Lancet Neurol*. 2014;13:59–66. doi: 10.1016/S1474-4422(13)70263-1
6. Wermer MJ, van der Schaaf IC, Algra A, Rinkel GJ. Risk of rupture of unruptured intracranial aneurysms in relation to patient and aneurysm characteristics: an updated meta-analysis. *Stroke*. 2007;38:1404–1410. doi: 10.1161/01.STR.0000260955.51401.cd
7. Moher D, Liberati A, Tetzlaff J, Altman DG; PRISMA Group. Preferred reporting items for systematic reviews and meta-analyses: the PRISMA statement. *PLoS Med*. 2009;6:e1000097. doi: 10.1371/journal.pmed.1000097
8. Stroup DF, Berlin JA, Morton SC, Olkin I, Williamson GD, Rennie D, Moher D, Becker BJ, Sipe TA, Thacker SB. Meta-analysis of observational studies in epidemiology: a proposal for reporting. Meta-analysis Of Observational Studies in Epidemiology (MOOSE) group. *JAMA*. 2000;283:2008–2012. doi: 10.1001/jama.283.15.2008
9. Matsumoto K, Oshino S, Sasaki M, Tsuruzono K, Taketsuna S, Yoshimine T. Incidence of growth and rupture of unruptured intracranial aneurysms followed by serial MRA. *Acta Neurochir (Wien)*. 2013;155:211–216. doi: 10.1007/s00701-012-1566-z
10. Güresir E, Vatter H, Schuss P, Platz J, Konczalla J, de Rochement Rdu M, Berkefeld J, Seifert V. Natural history of small unruptured anterior circulation aneurysms: a prospective cohort study. *Stroke*. 2013;44:3027–3031. doi: 10.1161/STROKEAHA.113.001107
11. Wiebers DO, Whisnant JP, Huston J 3rd, Meissner I, Brown RD Jr, Piepgras DG, Forbes GS, Thielen K, Nichols D, O'Fallon WM, et al; International Study of Unruptured Intracranial Aneurysms Investigators. Unruptured intracranial aneurysms: natural history, clinical outcome, and risks of surgical and endovascular treatment. *Lancet*. 2003;362:103–110. doi: 10.1016/s0140-6736(03)13860-3
12. Juvela S, Poussa K, Lehto H, Porras M. Natural history of unruptured intracranial aneurysms: a long-term follow-up study. *Stroke*. 2013;44:2414–2421. doi: 10.1161/STROKEAHA.113.001838
13. Mensing LA, Greving JP, Verhoeff TA, Rinkel GJE, Ruigrok YM. Comparison of rupture risk of intracranial aneurysms between familial and sporadic patients. *Stroke*. 2019;50:1380–1383. doi: 10.1161/STROKEAHA.118.023783
14. Morita A, Kirino T, Hashi K, Aoki N, Fukuhara S, Hashimoto N, et al; UCAS Japan Investigators. The natural course of unruptured cerebral aneurysms in a Japanese cohort. *N Engl J Med*. 2012;366:2474–2482. doi: 10.1056/NEJMoa1113260
15. Murayama Y, Takao H, Ishibashi T, Saguchi T, Ebara M, Yuki I, Arakawa H, Irie K, Urashima M, Molyneux AJ. Risk analysis of unruptured intracranial aneurysms: prospective 10-year cohort study. *Stroke*. 2016;47:365–371. doi: 10.1161/STROKEAHA.115.010698
16. Wermer MJ, van der Schaaf IC, Velthuis BK, Majoie CB, Albrecht KW, Rinkel GJ. Yield of short-term follow-up CT/MR angiography for small aneurysms detected at screening. *Stroke*. 2006;37:414–418. doi: 10.1161/01.STR.0000199077.06390.35
17. Molenberg R, Aalbers MW, Metzemaekers JDM, Mazuri A, Luijckx GJ, Groen RJM, Uyttenboogaart M, van Dijk JMC. Clinical relevance of short-term follow-up of unruptured intracranial aneurysms. *Neurosurg Focus*. 2019;47:E7. doi: 10.3171/2019.4.FOCUS1995
18. Sonobe M, Yamazaki T, Yonekura M, Kikuchi H. Small unruptured intracranial aneurysm verification study: SUAVe study, Japan. *Stroke*. 2010;41:1969–1977. doi: 10.1161/STROKEAHA.110.585059
19. Gondar R, Gautschi OP, Cuony J, Perren F, Jägersberg M, Corniola MV, Schatlo B, Molliqaj G, Morel S, Kulcsár Z, et al. Unruptured intracranial aneurysm follow-up and treatment after morphological change is safe: observational study and systematic review. *J Neurol Neurosurg Psychiatry*. 2016;87:1277–1282. doi: 10.1136/jnnp-2016-313584
20. Lindgren AE, Koivisto T, Björkman J, von Und Zu Fraunberg M, Helin K, Jääskeläinen JE, Frösen J. Irregular shape of intracranial aneurysm indicates rupture risk irrespective of size in a population-based cohort. *Stroke*. 2016;47:1219–1226. doi: 10.1161/STROKEAHA.115.012404
21. Grambsch PM, Therneau TM. Proportional hazards tests and diagnostics based on weighted residuals. *Biometrika*. 1994;81:515–526. doi: 10.1093/biomet/81.3.515
22. Kleinloog R, de Mul N, Verweij BH, Post JA, Rinkel GJE, Ruigrok YM. Risk factors for intracranial aneurysm rupture: a systematic review. *Neurosurgery*. 2018;82:431–440. doi: 10.1093/neuros/nyx238
23. Tominari S, Morita A, Ishibashi T, Yamazaki T, Takao H, Murayama Y, Sonobe M, Yonekura M, Saito N, Shiokawa Y, et al. Prediction model for 3-year rupture risk of unruptured cerebral aneurysms in japanese patients. *Ann Neurol*. 2015;77:1050–1059. doi: 10.1002/ana.24400
24. Algra AM, Klijn CJ, Helmerhorst FM, Algra A, Rinkel GJ. Female risk factors for subarachnoid hemorrhage: a systematic review. *Neurology*. 2012;79:1230–1236. doi: 10.1212/WNL.0b013e31826aace6
25. Lindekleiv H, Sandvei MS, Njølstad I, Løchen ML, Romundstad PR, Vatten L, Ingebrigtsen T, Vik A, Mathiesen EB. Sex differences in risk factors for aneurysmal subarachnoid hemorrhage: a cohort study. *Neurology*. 2011;76:637–643. doi: 10.1212/WNL.0b013e31820c30d3
26. Mehan WA Jr, Romero JM, Hirsch JA, Sabbag DJ, Gonzalez RG, Heit JJ, Schaefer PW. Unruptured intracranial aneurysms conservatively followed with serial CT angiography: could morphology and growth predict rupture? *J Neurointerv Surg*. 2014;6:761–766. doi: 10.1136/neurintsurg-2013-010944
27. Juvela S, Porras M, Poussa K. Natural history of unruptured intracranial aneurysms: probability of and risk factors for aneurysm rupture. *J Neurosurg*. 2000;93:379–387. doi: 10.3171/jns.2000.93.3.0379
28. Backes D, Vergouwen MD, Velthuis BK, van der Schaaf IC, Bor AS, Algra A, Rinkel GJ. Difference in aneurysm characteristics between ruptured and unruptured aneurysms in patients with multiple intracranial aneurysms. *Stroke*. 2014;45:1299–1303. doi: 10.1161/STROKEAHA.113.004421